

**ANALYSIS OF CLOUD AND CLOUD-TO-GROUND LIGHTNING IN
WINTER CONVECTION**

A Dissertation Presented to the Faculty of the Graduate School
University of Missouri-Columbia

In Partial Fulfillment for the Degree
Doctorate of Philosophy

by

Brian P. Pettegrew

Dr. Patrick S. Market, Dissertation Supervisor

May 2008

© Copyright by Brian Pettegrew 2008

All Rights Reserved

The undersigned, appointed by the dean of the Graduate School, have examined the dissertation entitled

ANALYSIS OF CLOUD AND CLOUD-TO-GROUND LIGHTNING IN
WINTER CONVECTION

presented by Brian P. Pettegrew,

a candidate for the degree of doctor of philosophy,

and hereby certify that, in their opinion, it is worthy of acceptance.

Associate Professor Patrick S. Market

Associate Professor Anthony R. Lupo

Assistant Professor Neil I. Fox

Professor John P. Dwyer

Mr. Ronald L. Holle

Acknowledgements

Most importantly, I would like to begin by thinking my wonderful wife for all the love and support during this trying time. Without her and possibly the love and support from our loving pet Azalea, I may not have been able to finish with as much as success.

To my parents who have always believed in my and have succumbed to the realization that all these years of hard work and education have paid off in the end.

To both of my sisters, your love and support have helped carry me through many years of toil and struggling striving for what I am about to achieve.

To my future niece/nephew, while we are not always present, we will be a constant in your life and may I forever be your "Uncle Doc."

I would like to thank all of my close friends. You have always been there for me in thick and in thin. All of you are an important part of life, here, and in the past. I will never forget you guys.

I would like to thank Charly Clendenning of the University of Missouri for all the work she has done for me to be able to finish this work in a timely manner and for also keeping me well versed on my music and comedies as well.

I would further like to thank Dr. Patrick Market and the rest of my committee for their insightful input into the research performed. Special thanks go to Mr. Ron Holle for his guidance and for aiding in the continual development of this research.

Contents

ACKNOWLEDGEMENTS	ii
LIST OF FIGURES	v
LIST OF TABLES.....	xvii
ABSTRACT	xviii
CHAPTER 1 INTRODUCTION	1
CHAPTER 2 LITERATURE REVIEW	4
2.1 LIGHTNING CHARACTERISTICS.....	4
2.1.1 <i>Generation of Lightning</i>	8
2.2 WINTER LIGHTNING.....	11
2.2.1 <i>Thundersnow</i>	14
CHAPTER 3 DATA AND METHODOLOGY	21
3.1 LIGHTNING DETECTION.....	21
3.2 ANALYSIS DATA.....	25
3.2.1 <i>RUC Model Resolutions</i>	25
3.2.2 <i>RUC Data Assimilation</i>	26
3.2.3 <i>RUC Dynamics and Physics</i>	27
3.2.4 <i>RUC Variables</i>	29
3.3 CASE DATA.....	30
3.4 SEPARATION ANALYSIS.....	31
3.5 COMPOSITE SOUNDING	34
CHAPTER 4 RESULTS.....	36
4.1 INDIVIDUAL STORM ANALYSES	36
4.1.1 <i>November 09-11, 2006</i>	38
4.1.2 <i>November 27-28, 2006</i>	42
4.1.3 <i>November 29 - December 01, 2006</i>	46
4.1.4 <i>December 18-22, 2006</i>	50
4.1.5 <i>December 28-31, 2006</i>	55
4.1.6 <i>January 12-15, 2007</i>	58
4.1.7 <i>January 20-22, 2007</i>	62
4.1.8 <i>January 30-31, 2007</i>	66
4.1.9 <i>February 12-14, 2007</i>	67
4.1.10 <i>February 23-25, 2006</i>	72

4.1.11	<i>February 28 - March 02, 2007</i>	76
4.1.12	<i>April 02-03, 2007</i>	79
4.1.13	<i>April 07-08, 2007</i>	83
4.1.14	<i>April 13-14, 2007</i>	87
4.2	COMBINED ANALYSIS	91
4.2.1	<i>Percent Occurrence</i>	91
4.2.2	<i>Cloud to CG Ratio and Distance</i>	93
4.2.3	<i>Diurnal Trends</i>	95
4.2.4	<i>Seasonal Trends</i>	96
4.2.5	<i>Spatial Trends</i>	100
CHAPTER 5 SOUNDING ANALYSIS		104
5.1	COMPOSITE SOUNDINGS	104
5.2	NORTHEAST COMPOSITE SOUNDINGS	106
5.3	NORTHWEST COMPOSITES	115
CHAPTER 6 THUNDERSNOW ANALYSIS		120
6.1	ANALYSIS OF 02 DECEMBER 2007	120
6.2	LIGHTNING CHARACTERISTICS	121
6.3	CASE STUDY	125
6.3.1	<i>Case Overview</i>	126
CHAPTER 7 WARM PRECIPITATION ANALYSIS		162
7.1	INTRODUCTION	162
7.2	LIGHTNING CHARACTERISTICS	163
7.3	CASE STUDY	166
7.3.1	<i>Case Overview</i>	166
CHAPTER 8 CONCLUSIONS		191
REFERENCES		198
VITA AUCTORIS		205

List of Figures

- Figure 3.1 Example map encompassing central U.S. representing domain from which lightning data was queried along with surface METAR observations. Dashed lines are 850-1000-mb thickness from 1290 gpm to 1310 gpm. Line represents rain-to-snow transition. 31
- Figure 4.1 Lightning map indicating negative and positive CG flashes ending at 2350 UTC 10 November 2006. Line indicates rain/freeze transition. All lightning above line are in subfreezing air. Lightning in this image produced from NLDN flash data in GEMPAK. 39
- Figure 4.2 Storm total lightning trend for both *a)* the total storm and *b)* the lightning associated with winter precipitation for 09 November 2006 through 11 November 2006. Time given in hours from the onset of lightning detected in winter precipitation. Date labeled every 12 hours in UTC. 41
- Figure 4.3 Line diagram showing the dominant occurrence of low amplitude negative CG strokes for lightning occurring in winter precipitation for thundersnow event on 10 November 2006. The x-axis is peak current in kA and the y-axis is the number of times a stroke of a given amplitude occurred. 42
- Figure 4.4 Lightning map indicating negative and positive CG flashes ending at 0800 UTC 28 November 2006. Line indicates rain/freeze transition. All lightning above and right of line are in subfreezing air. Lightning in this image produced from NLDN flash data in GEMPAK. 44
- Figure 4.5 Storm total lightning trend for both *a)* the total storm and *b)* the lightning associated with winter precipitation for 27 November 2006 through 29 November 2006. Time given in hours from the onset of lightning detected in winter precipitation. Date labeled every 12 hours in UTC. 45

Figure 4.6 Lightning map indicating negative and positive CG strokes and cloud flashes for one hour ending at 0700 UTC 01 December 2006. Line indicates rain/freeze transition. All lightning above and left of line are in subfreezing air..... 47

Figure 4.7 Storm total lightning trend for both *a)* the total storm and *b)* the lightning associated with winter precipitation for 29 November 2006 through 01 December 2006. Time given in hours from the onset of lightning detected in winter precipitation. Date labeled every 12 hours in UTC..... 48

Figure 4.8 Line diagram showing the dominant occurrence of low amplitude negative CG strokes for lightning occurring in winter precipitation for thundersnow event on 01 December 2006. The x-axis is peak current in kA and the y-axis is the number of times a stroke of a given amplitude occurred..... 49

Figure 4.9 Lightning map indicating negative and positive CG strokes and cloud flashes for one hour ending at 1625 UTC 19 December 2006. Line indicates rain/freeze transition. All lightning above and left of line are in subfreezing air..... 52

Figure 4.10 Storm total lightning trend for both *a)* the total storm and *b)* the lightning associated with winter precipitation for 19 December 2006 through 22 December 2006. Time given in hours from the onset of lightning detected in winter precipitation. Date labeled every 12 hours in UTC..... 53

Figure 4.11 Lightning map indicating negative and positive CG strokes and cloud flashes for one hour ending at 1900 UTC 29 December 2006. Line indicates rain/freeze transition. All lightning above line are in subfreezing air. 55

Figure 4.12 Storm total lightning trend for both *a)* the total storm and *b)* the lightning associated with winter precipitation for 29 December 2006 through 31 December 2006. Time given in hours from the onset of lightning detected in winter precipitation. Date labeled every 12 hours in UTC..... 57

Figure 4.13 Lightning map indicating negative and positive CG strokes and cloud flashes for one hour ending at 1535 UTC 13 January 2007. Line indicates rain/freeze transition. All lightning above and left of line are in subfreezing air. 59

Figure 4.14 Storm total lightning trend for both *a)* the total storm and *b)* the lightning associated with winter precipitation for 12 January 2007 through 14 January 2007. Time given in hours from the onset of lightning detected in winter precipitation. Date labeled every 12 hours in UTC..... 61

Figure 4.15 Lightning map indicating negative and positive CG strokes and cloud flashes for one hour ending at 1300 UTC 21 January 2007. Lightning enclosed in the circle represent lightning in subfreezing air..... 64

Figure 4.16 Storm total lightning trend for *a)* the total storm, *b)* the last 6-hrs of the total lightning, *c)* lightning associated with winter precipitation and *d)* the last 6-hrs of the lightning with winter precipitation for 19 January 2007 through 21 January 2007. Time given in hours from the onset of lightning detected in winter precipitation. Date labeled every 12 hours in UTC..... 65

Figure 4.17 Lightning map indicating single cloud flash for one hour of data ending at 1600 UTC 31 January 2007. Lightning enclosed in the circle represent lightning in subfreezing air..... 67

Figure 4.18 Storm total lightning trend for the total storm for 31 January 2007. Time given in hours from the onset of lightning detected in winter precipitation. Date labeled every 12 hours in UTC..... 68

Figure 4.19 Lightning map indicating negative and positive CG strokes and cloud flashes for one hour ending at 2300 UTC 12 February 2007. Line indicates rain/freeze transition. All lightning above line are in subfreezing air..... 69

Figure 4.20 Storm total lightning trend for both *a)* the total storm and *b)* the lightning associated with winter precipitation for 12 February 2007 through 14 February 2007. Time given in hours from the onset of lightning detected in winter precipitation. Date labeled every 12 hours in UTC..... 70

Figure 4.21 Lightning map indicating negative and positive CG strokes and cloud flashes taken at 0100 UTC 24 February 2007. Line indicates rain/freeze transition. All lightning above and right of line are in subfreezing air..... 73

Figure 4.22 Storm total lightning trend for both *a)* the total storm and *b)* the lightning associated with winter precipitation for 23 February 2007 through 25 February 2007. Time given in hours from the onset of lightning detected in winter precipitation. Date labeled every 12 hours in UTC..... 75

Figure 4.23 Lightning map indicating negative and positive CG strokes and cloud flashes for one hour ending at 0700 UTC 01 March 2007. Line indicates rain/freeze transition. All lightning above line are in subfreezing air. 77

Figure 4.24 Storm total lightning trend for both *a)* the total storm and *b)* the lightning associated with winter precipitation for 28 February 2007 through 02 March 2007. Time given in hours from the onset of lightning detected in winter precipitation. Date labeled every 12 hours in UTC. 78

Figure 4.25 Lightning map indicating negative and positive CG strokes and cloud flashes for one hour ending at 2130 UTC 03 April 2007. Lightning enclosed in the circle represent lightning in subfreezing air..... 80

Figure 4.26 Storm total lightning trend for both *a)* the total storm and *b)* the lightning associated with winter precipitation for 02 April 2007 through 04 April 2007. Time given in hours from the onset of lightning detected in winter precipitation. Date labeled every 12 hours in UTC. 82

Figure 4.27 Lightning map indicating negative and positive CG flashes ending at 1440 UTC 07 April 2007. Line indicates rain/freeze transition. All lightning above line are in subfreezing air. Lightning in this image produced from NLDN flash data in GEMPAK..... 84

Figure 4.28 Storm total lightning trend for both *a)* the total storm and *b)* the lightning associated with winter precipitation for 07 April 2007 through 08 April 2007. Time given in hours from the onset of lightning detected in winter precipitation. Date labeled every 12 hours in UTC. 85

Figure 4.29 Lightning map indicating negative and positive CG strokes and cloud flashes taken at 1500 UTC 13 April 2007. Line indicates rain/freeze transition. All lightning above and left of line are in subfreezing air. 88

Figure 4.30 Storm total lightning trend for both *a)* the total storm and *b)* the lightning associated with winter precipitation for 13 April 2007 through 14 April 2007. Time given in hours from the onset of lightning detected in winter precipitation. Date labeled every 12 hours in UTC. 89

Figure 4.31 24-hour trend of percent occurrence of lightning in winter precipitation. Y-axis represents the percentage while the x-axis is the time in hours UTC. 93

Figure 4.32 24-hour trend of Cloud to CG stroke ratio for storm total lightning (blue line) and winter lightning (yellow line). Trend types are labeled on right-hand side of graph. 94

Figure 4.33 24-hr lightning trend for both *a)* the storm total dataset and *b)* the lightning associated with winter precipitation for the winter season of 2006-2007. Time given in hours UTC. 97

Figure 4.34 Seasonal lightning trend for both *a)* the total storm dataset and *b)* the lightning associated with winter precipitation for the winter season 2006-2007. Dates are labeled by event occurrence..... 99

Figure 4.35 Map indicating monthly average location for winter lightning in the central U.S. Each red circle represents the latitude-longitude location of the average with the letter representing the month of the average. Green track connects average locations in order. 103

Figure 5.1 Full northeast composite (N=45) composited from RUC initial soundings at the latitude and longitude of most active lightning in winter precipitation. This consists of samples taken from all active lightning times occurring northeast of the cyclone. Solid red line is mean temperature, dashed red line is mean dewpoint, and wind barbs represent mean wind speeds in kts and median wind direction. Vertical Θ_e in yellow to the left of wind barbs..... 107

Figure 5.2 2000 to 0000 UTC northeast composite (N=8) composited from RUC initial soundings at the latitude and longitude of most active lightning in winter precipitation. Solid red line is mean temperature, dashed red line is mean dewpoint, and wind barbs represent mean wind speeds in kts and median wind direction. Vertical Θ_e in yellow to the left of wind barbs. 109

Figure 5.3 0000 to 0400 UTC northeast composite (N=12) composited from RUC initial soundings at the latitude and longitude of most active lightning in winter precipitation. Solid red line is mean temperature, dashed red line is mean dewpoint, and wind barbs represent mean wind speeds in kts and median wind direction. Vertical Θ_e in yellow to the left of wind barbs. 111

Figure 5.4 0400 UTC to 0800 UTC northeast composite (N=7) composited from RUC initial soundings at the latitude and longitude of most active lightning in winter precipitation. Solid red line is mean temperature, dashed red line is mean dewpoint, and wind barbs represent mean wind speeds in kts and median wind direction. Vertical Θ_e in yellow to the left of wind barbs. 113

Figure 5.5 Northwest composite (N=19 composited from RUC initial soundings at the latitude and longitude of most active lightning in winter precipitation. Solid red line is mean temperature, dashed red line is mean dewpoint, and wind barbs represent mean wind speeds in kts and median wind direction. Vertical Θ_e in yellow to the left of wind barbs..... 116

Figure 5.6 Comparison of height of -10° and -20°C isotherms for all derived northeast (NE) composites and the northwest (NW) composite. Composites are listed along the x-axis and height in km are along the y-axis. 118

Figure 6.1 Storm total lightning trend for both *a)* the total storm and *b)* the lightning associated with winter precipitation for 01 December 2007 through 02 December 2007. Time given in hours from the onset of lightning detected in winter precipitation. Date labeled every 12 hours in UTC. 124

Figure 6.2 Lightning map indicating negative and positive CG strokes and cloud flashes for one hour ending at 0200 UTC 02 December 2007. Sampled lightning circled in black..... 127

Figure 6.3 National Climate Data Center national base reflectivity radar mosaic valid at 0100 UTC on 02 December 2007. 128

Figure 6.4 GOES-12 IR imagery valid at 0115 UTC 02 December 2007. Cloud top temperatures are shaded in color with color scale representing every 10°C . Colder temperatures are represented by warmer colors. 128

Figure 6.5 RUC initial analysis at mean sea level pressure valid at 0100 UTC 02 December 2007. Sea level pressure contoured in black every 2 mb with 5400 gpm thickness line (500:1000-mb layer) plotted in blue. METAR decoded surface observations are plotted valid at the same time. 129

Figure 6.6 RUC initial analysis at 300 mb valid at 0100 UTC 02 December 2007. Geopotential height contoured every 60 gpm and isotachs in kts contoured every 10 kts above 50 kts and shaded. 130

Figure 6.7 RUC initial analysis at 500 mb valid at 0100 UTC 02 December 2007. Geopotential height contoured every 60 gpm and absolute vorticity contoured every $3 \times 10^{-5} \text{ s}^{-1}$ and shaded above $9 \times 10^{-5} \text{ s}^{-1}$ 131

Figure 6.8 RUC initial analysis at 700 mb valid at 0100 UTC 02 December 2007. Equivalent potential temperature contoured every 2 K and temperature advection contoured every $4 \times 10^{-5} \text{ K s}^{-1}$. Positive values of temperature advection are shaded in warm colors and negative values of temperature advection are shaded in cool colors occurring at this time. 133

Figure 6.9 RUC initial analysis at 850 mb valid at 0100 UTC 02 December 2007. Geopotential height contoured in black every 30 gpm and temperatures contoured in red dashed every 10°C . Relative humidity contoured and shaded every 10% above 70%. 134

Figure 6.10 RUC initial analysis at 900 mb valid at 0100 UTC 02 December 2007. Height contoured in black every 30 gpm and temperature advection contoured every $4 \times 10^{-5} \text{ K s}^{-1}$. Positive values are shaded in warm colors and negative values are shaded in cool colors. 135

Figure 6.11 Stability profile valid at 0100 UTC 02 December 2007. Left panel is 3-dimensional equivalent potential vorticity. Shaded contours represent values of 0.25 PVU and less. The right panel is the σ^2 growth-rate parameter shaded for values above 0.1 h^{-2} 135

Figure 6.12 0100 UTC December 2, 2007 sounding. Solid red line is temperature, dashed red line is dewpoint, and wind barbs represent wind speeds in kts and wind direction. Vertical Θ_e in yellow to the left of wind barbs. 137

Figure 6.13 Lightning map indicating negative and positive CG strokes and cloud flashes for one hour ending at 0800 UTC 02 December 2007. Sampled lightning strokes circled in black. 139

Figure 6.14 National Climate Data Center national base reflectivity radar mosaic valid at 0800 UTC on 02 December 2007. 140

Figure 6.15 GOES-12 IR imagery valid at 0815 UTC 02 December 2007. Cloud top temperatures are shaded in color with color scale representing every 10°C . Colder temperatures are represented by warmer colors. 140

Figure 6.16 RUC initial analysis at mean sea level pressure valid at 0800 UTC 02 December 2007. Sea level pressure contoured in black every 2 mb with 5400 gpm thickness line (500:1000-mb layer) plotted in blue. METAR decoded surface observations are plotted valid at the same time. 141

Figure 6.17 RUC initial analysis at 300 mb valid at 0800 UTC 02 December 2007. Geopotential height contoured every 60 gpm and isotachs in kts contoured every 10 kts above 50 kts and shaded. 142

Figure 6.18 RUC initial analysis at 500 mb valid at 0800 UTC 02 December 2007. Geopotential height contoured every 60 gpm and absolute vorticity contoured every $3 \times 10^{-5} \text{ s}^{-1}$ and shaded above $9 \times 10^{-5} \text{ s}^{-1}$ 143

Figure 6.19 RUC initial analysis at 700 mb valid at 0800 UTC 02 December 2007. Equivalent potential temperature contoured every 2 K and temperature advection contoured every $4 \times 10^{-5} \text{ K s}^{-1}$. Positive values of temperature advection are shaded in warm colors and negative values of temperature advection are shaded in cool colors occurring at this time. 144

Figure 6.20 RUC initial analysis at 850 mb valid at 0800 UTC 02 December 2007. Geopotential height contoured in black every 30 gpm and temperatures contoured in red dashed every 10°C . Relative humidity contoured and shaded every 10% above 70%. 145

Figure 6.21 RUC initial analysis at 900 mb valid at 0800 UTC 02 December 2007. Geopotential height contoured in black every 30 gpm and temperature advection contoured every $4 \times 10^{-5} \text{ K s}^{-1}$. Positive values of temperature advection are shaded in warm colors and negative values of temperature advection are shaded in cool colors. 145

Figure 6.22 Stability profile valid at 0800 UTC 02 December 2007. Left panel is 3-dimensional equivalent potential vorticity. Shaded contours represent values of 0.25 PVU and less. The right panel is the σ^2 growth-rate parameter shaded for values above 0.1 h^{-2} 146

Figure 6.23 0800 UTC December 2, 2007 sounding. Solid red line is temperature, dashed red line is dewpoint, and wind barbs represent wind speeds in kts and wind direction. Vertical Θ_e in yellow to the left of wind barbs. 147

Figure 6.24 Lightning map indicating negative and positive CG strokes and cloud flashes for one hour ending at 1800 UTC 02 December 2007. Sampled lightning stroke circled in black.....	149
Figure 6.25 National Climate Data Center national base reflectivity radar mosaic valid at 1800 UTC on 02 December 2007.	150
Figure 6.26 GOES-12 IR imagery valid at 1815 UTC 02 December 2007. Cloud top temperatures are shaded in color with color scale representing every 10°C. Colder temperatures are represented by warmer colors.....	150
Figure 6.27 RUC initial analysis at mean sea level pressure valid at 1800 UTC 02 December 2007. Sea level pressure contoured in black every 2 mb with 5400 gpm thickness line (500:1000-mb layer) plotted in blue. METAR decoded surface observations are plotted valid at the same time.	151
Figure 6.28 RUC initial analysis at 300 mb valid at 1800 UTC 02 December 2007. Geopotential height contoured every 60 gpm and isotachs in kts contoured every 10 kts above 50 kts and shaded.	152
Figure 6.29 RUC initial analysis at 500 mb valid at 1800 UTC 02 December 2007. Geopotential height contoured every 60 gpm and absolute vorticity contoured every $3 \times 10^{-5} \text{ s}^{-1}$ and shaded above $9 \times 10^{-5} \text{ s}^{-1}$	153
Figure 6.30 RUC initial analysis at 700 mb valid at 1800 UTC 02 December 2007. Equivalent potential temperature contoured every 2 K and temperature advection contoured every $4 \times 10^{-5} \text{ K s}^{-1}$. Positive values of temperature advection are shaded in warm colors and negative values of temperature advection are shaded in cool colors occurring at this time.....	154
Figure 6.31 RUC initial analysis at 850 mb valid at 1800 UTC 02 December 2007. Geopotential height contoured in black every 30 gpm and temperatures contoured in red dashed every 10°C. Relative humidity contoured and shaded every 10% above 70%.	155
Figure 6.32 RUC initial analysis at 900 mb valid at 1800 UTC 02 December 2007. Geopotential height contoured in black every 30 gpm and temperature advection contoured every $4 \times 10^{-5} \text{ K s}^{-1}$. Positive values of temperature advection are shaded in warm colors and negative values of temperature advection are shaded in cool colors.	156

Figure 6.33 Stability profile valid at 1800 UTC 02 December 2007. Left panel is 3-dimensional equivalent potential vorticity. Shaded contours represent values of 0.25 PVU and less. The right panel is the σ^2 growth-rate parameter shaded for values above 0.1 h^{-2} 156

Figure 6.34 1800 UTC December 2, 2007 sounding. CAPE is shaded in color. Solid red line is temperature, dashed red line is dewpoint, and wind barbs represent wind speeds in kts and wind direction. Vertical Θ_e in yellow to the left of wind barbs. 158

Figure 7.1 Storm total lightning trend for 12-13 October 2007. Time given in hours from the onset of lightning detected. Date labeled every 12 hours in UTC. 164

Figure 7.2 Lightning map indicating negative and positive CG strokes and cloud flashes for one hour ending at 1200 UTC 12 October 2007. 167

Figure 7.3 National Climate Data Center national base reflectivity radar mosaic valid at 1200 UTC on 12 October 2007. 168

Figure 7.4 GOES-12 IR imagery valid at 1215 UTC 12 October 2007. Cloud top temperatures are shaded in color with color scale representing every 10°C . Colder temperatures are represented by warmer colors. 169

Figure 7.5 RUC initial analysis at mean sea level pressure valid at 1200 UTC 12 October 2007. Sea level pressure contoured in black every 2 mb with 5400 gpm thickness line (500:1000-mb layer) plotted in blue. METAR decoded surface observations are plotted valid at the same time. 170

Figure 7.6 RUC initial analysis at 300 mb valid at 1200 UTC 12 October 2007. Geopotential height contoured every 60 gpm and isotachs in kts contoured every 10 kts above 50 kts and shaded. 171

Figure 7.7 RUC initial analysis at 500 mb valid at 1200 UTC 12 October 2007. Geopotential height contoured every 60 gpm and absolute vorticity contoured every $3 \times 10^{-5} \text{ s}^{-1}$ and shaded above $9 \times 10^{-5} \text{ s}^{-1}$ 172

Figure 7.8 RUC initial analysis at 700 mb valid at 1200 UTC 12 October 2007. Equivalent potential temperature contoured every 2 K and temperature advection contoured every $4 \times 10^{-5} \text{ K s}^{-1}$. Positive values of temperature advection are shaded in warm colors and negative values of temperature advection are shaded in cool colors. 173

Figure 7.9 RUC initial analysis at 850 mb valid at 1200 UTC 12 October 2007. Geopotential height contoured in black every 30 gpm and temperatures contoured in red dashed every 10°C . Relative humidity contoured and shaded every 10% above 70%. 173

Figure 7.10 RUC initial analysis at 900 mb valid at 1200 UTC 12 October 2007. Geopotential height contoured in black every 30 gpm and temperature advection contoured every $4 \times 10^{-5} \text{ K s}^{-1}$. Positive values of temperature advection are shaded in warm colors and negative values of temperature advection are shaded in cool colors. 175

Figure 7.11 1200 UTC October 12, 2007 sounding. Solid red line is temperature, dashed red line is dewpoint, and wind barbs represent wind speeds in kts and wind direction. CAPE is shaded. Vertical Θ_e in yellow to the left of wind barbs..... 176

Figure 7.12 Lightning map indicating negative and positive CG strokes and cloud flashes for one hour ending at 1200 UTC 13 October 2007. 178

Figure 7.13 National Climate Data Center national base reflectivity radar mosaic valid at 1200 UTC on 13 October 2007. 179

Figure 7.14 GOES-12 IR imagery valid at 1215 UTC 13 October 2007. Cloud top temperatures are shaded in color with color scale representing every 10°C . Colder temperatures are represented by warmer colors. 180

Figure 7.15 RUC initial analysis at mean sea level pressure valid at 1200 UTC 13 October 2007. Sea level pressure contoured in black every 2 mb with 5400 gpm thickness line (500:1000-mb layer) plotted in blue. METAR decoded surface observations are plotted valid at the same time. 181

Figure 7.16 RUC initial analysis at 300 mb valid at 1200 UTC 13 October 2007. Geopotential height contoured every 60 gpm and isotachs in kts contoured every 10 kts above 50 kts and shaded. 181

Figure 7.17 RUC initial analysis at 500 mb valid at 1200 UTC 13 October 2007. Geopotential height contoured every 60 gpm and absolute vorticity contoured every $3 \times 10^{-5} \text{ s}^{-1}$ and shaded above $9 \times 10^{-5} \text{ s}^{-1}$ 183

Figure 7.18 RUC initial analysis at 700 mb valid at 1200 UTC 13 October 2007. Equivalent potential temperature contoured every 2 K and temperature advection contoured every $4 \times 10^{-5} \text{ K s}^{-1}$. Positive values of temperature advection are shaded in warm colors and negative values of temperature advection are shaded in cool colors occurring at this time..... 184

Figure 7.19 RUC initial analysis at 850 mb valid at 1200 UTC 13 October 2007. Geopotential height contoured in black every 30 gpm and temperatures contoured in red dashed every 10°C . Relative humidity contoured and shaded every 10% above 70%. 185

Figure 7.20 RUC initial analysis at 900 mb valid at 1200 UTC 13 October 2007. Geopotential height contoured in black every 30 gpm and temperature advection contoured every $4 \times 10^{-5} \text{ K s}^{-1}$. Positive values of temperature advection are shaded in warm colors and negative values of temperature advection are shaded in cool colors. 185

Figure 7.21 RUC initial sounding valid at 1200 UTC October 13, 2007 near Topeka, KS. Solid red line is temperature, dashed red line is dewpoint, and wind barbs represent wind speeds in kts and wind direction. CIN shaded in blue. Vertical Θ_e in yellow to the left of wind barbs. 186

Figure 7.22 Comparison of height of -10° and -20°C isotherms for all derived northeast (NE) composites and the northwest (NW) composite along with the thundersnow and warm precipitation case study. Events are listed along the x-axis and height in km are along the y-axis. 187

List of Tables

Table 3.1 The dates of each individual case represented in this paper for analysis during the 2006-2007 winter season, extending from October to April. There are fourteen total events for this winter in which thundersnow in the central U.S. was observed.	30
Table 4.1 Lightning totals for each individual storm during the 2006-2007 winter season including storm totals and totals with winter precipitation.	37

ANALYSIS OF CLOUD AND CLOUD-TO-GROUND LIGHTNING IN WINTER CONVECTION

Brian Pettegrew

Dr. Patrick Market, Dissertation Supervisor

Abstract

The combination of the full suite of cloud-to-ground (CG) and cloud stroke data is used to observe lightning in precipitation events involving winter precipitation. In particular, we employ data for the winter season of 2006 to 2007, which is defined as October through April, for winter events that generated the weather phenomenon known as thundersnow, or convective snow. There were a total of 44,122 lightning strokes associated with winter precipitation in 14 events involving the occurrence of thundersnow. This total made up only 1.4% of all lightning observed in these events. Cloud flashes made up 31.4% of the observed lightning in winter precipitation. Furthermore, 92.0% of the observed CG strokes were found to have a negative polarity. Storm total histograms consistently showed the dominance of lower amplitude negative strokes (between -20 and -30 kA) in each storm. The lightning in winter precipitation maintained a cloud-to-CG ratio of 0.46 (or 1 cloud to 2.2 CG strokes) throughout the season. Analysis of diurnal trends in the winter lightning showed a tendency for greater activity between 0000 UTC and 0400 UTC. Using Rapid Update Cycle (RUC) initial fields, composite soundings were generated for areas of greatest (or exact) observed lightning location, showing a similarity to previous work done on proximity soundings in thundersnow events. A comparison to an elevated warm precipitation event shows similarity in the vertical profiles. However, the diurnal characteristics of the lightning show no similarity as do synoptic and mesoscale environments surrounding the event.

Chapter 1 Introduction

Until the last decade, little work had been done to analyze the characteristics and stability associated with convective snow, or thundersnow, events across the central U.S. The most important aspect of this research is the knowledge that may be passed to operational meteorologists in order to quickly notify and/or warn the public of impending hazardous conditions. According to Crowe et al. (2006), there is a distinct correlation between the location of the highest snow total in a storm with the occurrence of lightning and coincident surface observation. However, the correlations are not exact, thus, indicating that while a number of times the highest snow totals may be associated with lightning occurrence; this is not always the case. In this instance, the occurrence of thundersnow may represent a hazard associated with the rate of snowfall. Heavy snowfall not only accumulates quickly on cool surfaces making it difficult for road crews to keep the roads clear, but for those few still on the roads, it

creates near blinding conditions making navigation nearly impossible. Additionally, these hazards do not relate to only thundersnow, but all types of frozen precipitation, including, but not limited to, sleet, graupel, freezing rain, ice pellets, and snow pellets. Further hazards may arise from associated heavy winds.

While all thundersnow is considered convective snow, not all convective snow is thundersnow. This is based on the assertion that in order to precipitate there must be some associated vertical motions. The difference lies in the amount of vertical motion in the precipitating cloud, and whether or not the vertical motions and associated stability characteristics are enough to generate lightning in a cloud.

The goal of this research is twofold. The first goal is to study the characteristics and trends of lightning, both cloud and cloud-to-ground, using Vaisala, Inc.'s National Lightning Detection Network (NLDN) data. From this effort, an initial climatology of lightning in winter precipitation may be established on the basis of thundersnow occurrence. The second goal is to use this lightning data to establish localized vertical profiles using initial mesoscale model fields. By observing these fields, a mean profile for the occurrence of lightning in winter precipitation may be developed. Further, these characteristics, trends, and mean profiles are compared to elevated convective

events in both a warm precipitation event and a convective snow event outside of the parent dataset.

From this comparison, the purpose of this research is to assess the use of the full suite of lightning data provided in addition to gaining a physical understanding of a convective snow event using the trend of this data. Additionally, the purpose is to develop a mean profile characteristic of convection capable of producing lightning in winter precipitation.

Two main tasks are identified to fulfill the purpose of this study.

These analyses will seek to:

- Analyze the trends and characteristics of lightning in winter precipitation based on observed convective snow events.
- Create a mean profile of the localized environment producing lightning and compare it to elevated convective events with lightning in both warm precipitation and frozen precipitation.

Chapter 2 Literature Review

2.1 Lightning Characteristics

Lightning characteristics in weather events across the continental United States have been studied extensively in the last decade using Vaisala's National Lightning Detection Network (NLDN: Orville 1991; 1994; Zajac and Rutledge 2001; Carey and Rutledge 2003) and the North America Lightning Detection Network (NALDN: Orville et al. 2002). Most of these studies, however, either focus on the climatological aspect of cloud-to-ground (CG) lightning characteristics over a number of years or by specific weather type (Carey and Rutledge 2003). Orville (1994) identified a latitudinal dependence on the polarity of lightning, showing that the percentage of positive flashes increases with increasing latitude. He analyzed over 46 million flashes over the continental United States (CONUS) between 1989 and 1991 using flash data from

the NLDN. The positive flashes made up 3.66% of the total, varying spatially from 1.6% to over 25%. These values tended to increase from south to north showing the latitudinal dependence of percent of positive flashes. In terms of positive flash density (the number of flashes per square kilometer per minute), the maximum was over Florida while a second maximum occurred over the Midwest. He also indicated diurnal tendencies in flash rate and percent positive flashes, but Reap and MacGorman (1989) attributed them to dissipating mesoscale convective systems over the central plains.

Reap and MacGorman (1989) observed climatological characteristics of CG lightning over Kansas and Oklahoma by the National Severe Storm Laboratory (NSSL) including seasonal, diurnal, and spatial variations for the summers of 1985-1986. For the season, 4.3% were observed positive flashes to ground with monthly peaks of 9.2% in April and 2.6% in August. A lag in peak positive flash occurrence was identified, which the authors say probably reflected the dominance of positive flashes in dissipating storms (Orville et al. 1983; Fuquay 1982; Rutledge and MacGorman 1988; Rust 1986). The overall diurnal trend of the analyzed CG flashes showed a tendency for activity to occur between 4 and 10 hours past local noon (6 hours behind UTC). The variation in signal strength indicated that higher peak currents in negative flashes tend to occur at night and in the early morning hours, while the higher positive peak

flash currents tended to occur during the afternoon hours (Reap and MacGorman 1989). No relationship between terrain elevation and lightning density was observed. Concurrently, correlations to atmospheric variables such as wind shear and freezing height were found to be less significant than boundary-layer fields such as boundary-layer moisture convergence with regards to thunderstorm formation and resulting lightning. However this may be different during other seasons. Further, a correspondence between lightning intensity and radar echo intensity was identified.

Further relationships between lightning and radar reflectivity were made by Peterson et al. (1996) during tropical convection, comparing CG lightning data from remote magnetic direction finders. They found that lightning in deep tropical convection is characterized with cells that reach 30 dBZ above the height of the -10°C isotherm. The descent of hydrometeors around that reflectivity was correlated with peaks in CG lightning activity. The diurnal cycle of lightning in these instances was correlated with atmospheric variables determined from mobile radiosonde data and local precipitation observations. Particularly, the peak in lightning activity was found to have a weak positive correlation with the presence of convective available potential energy (CAPE), while maintaining a strong correlation with wet-bulb potential temperature. The

frequency of lightning exhibited sensitivity to changes in mixed-layer wet-bulb potential temperature.

Orville et al. (2002) revisited the NLDN for the years 1998-2000 using a combination of the NLDN and the Canadian lightning network, the combined network referred to as the NALDN. The authors analyzed all identified ground flashes, positive and negative, the percentage of positive lightning, positive and negative peak currents, and positive and negative multiplicities. The percent of positive lightning flashes occurring was on average 8.9% for the 3-year study. This, of course, varied geographically for the continent. Values of typically less than 10% occurred most frequently in the western and eastern U.S., while values of 10-15% were found in the Midwest with steadily increasing values towards the U.S./Canada border where values were close to 20%. Median peak currents for positive flashes were 15.3 kA, but when flashes of less than 10 kA are eliminated from the data set, the median peak current went up to 19.8 kA. The median peak current for all negative flashes was 16.5 kA. It was found that across North America, peak currents decreased from lower to higher latitudes.

Carey and Rutledge (2003) performed a study from the Kansas/Colorado border to Minnesota of CG lightning in severe and nonsevere storms during the warm seasons of 1989-1998. One of their primary findings is the higher percentage of positive flashes making contact with the ground in

severe as opposed to nonsevere storms. Also, median peak currents for positive flashes were higher in severe as opposed to nonsevere while median peak currents for negative flashes were lower for severe storms. The authors found spatial differences in properties of lightning producing severe storms where severe storms in different regions of the central U.S. had different positive CG percentages, lower positive peak currents and higher negative peak currents associated with the peak large hail and tornado activities that occurred.

2.1.1 Generation of Lightning

Lightning in thunderstorms is dependent largely on the charge structure in the cloud. Benjamin Franklin was the first to establish the existence of at least negative charge in a thunderstorm (MacGorman and Rust 1998). The original dipole structure suggested as being in electrified thunderclouds (positive charge existing above negative charge) was identified by Wilson (1916, 1920, 1929). Measurements from Simpson and Robinson (1941) found that two charge structures were insufficient to generate the necessary separation for lightning to occur, thus introducing the positively charged screening layer creating a tripole structure in convective clouds. This was confirmed in research from Marshall and Winn (1982) and Marshall and Rust (1991). Thus, today's accepted structure of a thundercloud maintains a dipole/tripole structure with an upper mixed-

charge screening layer above the cloud top. MacGorman and Rust (1998) stated that typical characteristics of a charged cloud include negative charge dominant in the lower cloud typically within a temperature range of -10° to -25°C , positive charge above the negative charge ($<1\text{km}$), a small screening layer at the top and bottom boundaries of the cloud a few hundred meters thick, and positive charge is usually carried below the cloud in precipitation.

Clouds usually can gain charge through one of two methods. These are inductive and non-inductive methods. Inductive mechanisms are defined as those requiring an electric field to induce charge on the surface of hydrometeors (MacGorman and Rust 1998). This inductive reasoning relies on hydrometeor polarity and polarity of cloud matter. The ambient electric field in the atmosphere, thus, creates a polar field on these hydrometeors and cloud particles. Some of the charge transfer is from rebounding particles as the hydrometeors fall from the cloud. The noninductive method refers to any charging mechanism that does not require hydrometeors to gain charge from the ambient electric field. One such mechanism is the graupel-ice mechanism. This refers to the effects of temperature and physical state on a charged hydrometeor. Warmer, liquid hydrometeors, found in the lower portion of the clouds, typically have a negative charge, while frozen hydrometeors, such as graupel, typically have a positive charge (Hobbs 1974). The noninductive methods also include

charges due to melting ice and graupel particles and supercooled water droplets. While research had not shown that one mechanism alone was enough to create sufficient charge for lightning to occur, researchers were leaning towards a combination of the two methods (MacGorman and Rust 1998). However, it appears, today, that non-inductive mechanisms are considered to be more primary.

There are only two primary types of lightning. One is the cloud flash and the other is the cloud-to-ground flash. Cloud flashes, according to MacGorman and Rust (1998), consist of several varieties of flashes. These types include intracloud flashes (those that are confined to the inside of the cloud), cloud-to-air flashes, and cloud-to-cloud flashes, which can be confused with intracloud flashes especially when more than one storm cell is present. There is also the air discharge that does not make contact with ground but has visible channels propagating into the air. The second type of lightning is, as stated above, the cloud-to-ground lightning, which is any stroke or flash that makes contact with the ground. The most common of these lightning is the downward propagating negative leader (Berger 1977).

2.2 *Winter Lightning*

Previous research on lightning in winter precipitation has been done primarily on the mountainous coasts of Japan (Taniguchi et al. 1982; Brook et al. 1982; Michimoto 1993), while few studies of lightning with winter precipitation have been done over the central U.S. (e.g., Trapp et al. 2001; Holle and Watson 1996). Part of the difficulty with *in situ* studies in this region has been the flat terrain and strong winds creating blizzard conditions, with cloud particles and precipitation particles blowing around significantly (MacGorman and Rust 1998). Such conditions would create difficulty with capturing a local microphysical profile. The current work seeks to gain an understanding of the thundersnow environment using lightning data along with assessing the value of cloud lightning detection in the NLDN in storms involving winter precipitation. Recent research in thundersnow in the United States has aroused new interest in lightning characteristics in a specific weather event. Previous studies of this phenomenon include Holle et al. (1998) who examined surface observations at or below freezing in the presence of thunder and lightning. The focus was not specifically on the occurrence of thundersnow, but on the presence of thunder and lightning reported at first order surface stations that were at or near freezing temperatures. The authors found in storms between 0°C and 10°C that rain was the most common form of precipitation while heavy snow was most common for

reports below 0°C. This climatology, of sorts, provided a ground base for studies of thunder near freezing temperatures, which they found occurred most often in the central U.S. Secondary maxima occurred at or near the Great Lakes region, and a few reports were in the high plains and eastern Rocky Mountains. More significantly, they found evidence that precipitation may be heavier in areas of coincident reports of thunder and/or lightning.

Most research on winter lightning has occurred along the mountainous coasts of Japan. Taniguchi et al. (1982) studied the charge distribution in active winter clouds. The authors suggest that the common frequency of positive lightning flashes in winter thunderstorms were closely related to low cloud height and strong vertical wind shear. Using electric-charge sondes lifted into the clouds with balloons in December of 1978 and 1979, vertical charge structure was monitored in the convective clouds. They found that positive fields were identified predominantly in the lower regions of the cloud while the upper cloud contained mostly negative electric fields. They also note that while growing snow usually contains a positive charge, those that are evaporating have a negative charge.

Brook et al. (1982) analyzed lightning flashes from eight winter thunderstorms in Hokuriku, Japan in an attempt to identify and confirm the charge structure in these storms. Based on balloon observations in these storms,

the dipole structure was consistent with the high observed horizontal winds. Of the 63 lightning flashes observed in these eight storms, 26 lowered positive charge to ground. They note that it is unusual to see lightning produced in low top, highly sheared environments, but in these storms, this was the case. As a result of the findings, a strong correlation of positive CG lightning flashes was found with increasing shear with height, suggesting that the occurrence of positive lightning in these storms was a result of the strong vertical wind shear, in a way that the shear helps create such a horizontal displacement in the electric charge regions of the cloud that an initiating positive streamer will continue to ground instead of passing through a negatively charged region. They also suggest that positive lightning strokes to ground should appear at a threshold shear value of $1.5 \text{ m s}^{-1} \text{ km}^{-1}$. Michimoto (1993) studied winter thunderclouds using radar data with Constant Altitude Plan Position Indicator (CAPPI). In these cases he discovered that lightning was favorable when the 30 dBZ echo top developed higher than the -20°C isotherm. He also found that the altitude of the -10°C isotherm was important. When the altitude of the -10°C isotherm was greater than 1.8 km, the clouds exhibited greater lightning activity. When the altitude was between 1.4 and 1.8 km, there was little to no lightning activity, and below 1.4 km, there were no discharges whatsoever indicating the significance of the vertical thermal structure in a winter cloud.

Moore and Idone (1999) presented a study on CG lightning at low surface temperatures in order to find a lower temperature limit based on currently used lightning detection systems at that time. Using six winters (December through February) of data from 1988-89 through 1993-94, they identified hundreds of lightning events occurring at or below 32°F, consisting of only a few flashes per storm. They found that the number of storms and flashes decreased as surface temperatures decreased. During those seasons, of all the flashes recorded by the NLDN, they found only 0.55% to occur below 32°F, 0.045% occurred at or below 13°F and a meager 0.00079% occurred below 0°F. They found, for the winter seasons of 1988-89 through 1993-94, that the greatest amounts of lightning in freezing surface air were geographically distributed in a line from New England through the Great Plains with some of the coldest surface temperatures being observed with lightning flashes in the Great Plains.

2.2.1 Thundersnow

Curran and Pearson (1971) were among the first to study the physical parameters of thunderstorms with snow by examining proximity soundings. At the time, there was no pre-existing literature on the occurrence of thunderstorms with snow, or commonly, thundersnow. Their dataset included three years of surface observations reporting thunder, snow, or thundersnow. Only 76

observations were found to have both thunder and snow in the same report out of 114,924 reporting snow and 5,834 reporting thunder without snow. These surface observations were further filtered by eliminating those that did not fall within +/- 3 hours or 90 nautical miles of a radiosonde launch time and site respectively. This left only 13 radiosonde stations. The mean proximity sounding was characterized by a deep layer above the inversion with relative humidities of 90% or above. The inversion layer itself is approximately 81 mb deep. Further, the mean sounding is moist adiabatic in the mid-levels with minimal changes in Θ_e . Stability indices showed little correlation, however, as the authors noted that most of these flights occurred during ongoing convection.

This paper was followed up by Market et al. (2006) with a larger dataset and more statistical analyses. Market et al. (2006) studied surface observations from 1961-1990, comparing both thundersnow proximity soundings to non-thundering snow proximity soundings. Their primary finding was the noticeable decrease in static stability in events where thundersnow was observed. Further, the most unstable parcel in these events was found 30-50 mb above the frontal inversion and significant drying was in the column about 100 mb above the most unstable parcel. The composite temperature at the level of the most unstable parcel was found to be at -8.7°C , which is thermodynamically favorable for the existence of supercooled water. Moreover, the composite

height of the -10°C level was found to be 2959 m (2.9 km), which, according to Michimoto (1993), favors the production of lightning in a cloud. However, there is no convective available potential energy (CAPE) present in the composite soundings. Van Den Broeke et al. (2005) showed that elevated storms needed at least 100 J kg^{-1} of CAPE for the production of lightning. The authors also suggested that the ideal physical conditions in elevated convection for the generation of lightning is sufficient instability in the mixed-phase region of the cloud, a lifting condensation level warmer than -10°C and an equilibrium level colder than -20°C (MacGorman and Rust 1998).

Colman (1990a) studied elevated thunderstorms across the contiguous U.S. with positive CAPE. His initial study was a climatology of these events over a 4-year period creating a composite analysis on elevated thunderstorms. Subjectively eliminated were those storms that had their roots in the boundary layer. He found that the primary location of elevated convection occurred northeast of the associated low pressure center and north of the warm frontal boundary, which was confirmed further by Market et al. (2002) in the location of elevated convective snowfall. In these instances, the boundary layer was found to be stable, using 850 mb as representative of the boundary layer. Further, these instances of convection northeast of the parent cyclone, more often than not, were found in a strong baroclinic region under the influence of the left exit

region of the 300-mb jet. One of the most notable differences between elevated storms and surface-based convective storms was the amount of CAPE. Elevated convection was found to be most common temporally in early April and September. Most convection occurring during the winter months of December through February is elevated. During this time, elevated convection is found most often spatially across the mid-Mississippi River Valley north from the Gulf of Mexico coast. Case studies from elevated storms during the spring revealed that during elevated convection, the associated convective instability diminishes quickly while convection persists above the frontal inversion. One such mechanism that could explain such phenomena is the presence of symmetric instability occurring in a strongly baroclinic environment (Colman 1990b).

One of the earlier case studies involving the occurrence of frozen precipitation and lightning in the central U.S. was documented by Holle and Watson (1996). They studied two storms from January of 1994 that affected parts of Kansas, Oklahoma, Missouri, and Arkansas. In addition to meteorological observations available at the time, they also used NLDN data, which, at the time, the NLDN was equipped with magnetic direction finders (Krider et al. 1976, 1980; Holle and Lopez 1993). The first storm subsequently lowered 27 CG flashes to ground in subfreezing air recorded at the surface. In this case, it was found that 59% of these flashes carried a positive charge, which was found to be much

higher than the 4% found by Orville (1994). In the second case, there were 2417 identified CG flashes in total, which were scattered similarly to the first case. 25 of those flashes occurred in subfreezing air, of which 52% were found in subfreezing air. Further, it was found that the location of lightning in subfreezing air was coincident with regions of diagnosed conditional symmetric instability (CSI). Although several flashes were identified, no surface observations ever reported thunder. Fields of 850-mb temperature advection and 850-500-mb differential vorticity had similar magnitudes in regions of lightning occurrence in both cases as well. In both cases, radar echoes grew from weak to moderate within a few hours with high echo tops, which better indicated where lightning occurred than reflectivity.

Market et al. (2002) extended this work by creating a 30-year climatology of thundersnow, and dividing it spatially and temporally over the U.S. during the winter season, which was defined as October through April. This was performed as a first step in analyzing the synoptic and dynamic characteristics of a snowstorm with thunder. This climatology used only synoptic reports taken every three hours that included the occurrence of thunder with snow. As a result, they found the maximum occurrence of thundersnow events, over the 30-year period of 1961-1990, centered in the Rocky Mountains over Utah and extending into Idaho, Nevada, Wyoming, Colorado and south into the higher

elevations of Arizona, which have not been studied. A smaller maximum occurred over the central plains, mostly occurring in the high plains of western Nebraska and Kansas. An even smaller maximum occurred over the Great Lakes. The frequency of occurrence tended to decrease with decreasing latitude toward the Gulf of Mexico. Looking at the monthly distribution, it was found that thundersnow was more likely to occur in March with a smaller peak in November and December. With reference to the intensity of the thundersnow that occurred, Market et al. (2002) found that reports of light thundersnow tended to be most common with heavy and moderate to divide the rest of the cases. When separated into event type, cyclone events were most common of the seven determined types, although several of the authors' event types could be organized into one or more other event types. Finally, the authors typified surface conditions for a thundersnow producing storm. These reports consisted of overcast skies, northerly breeze, surface temperatures around 30°F (-1.1°C) and dewpoint temperatures 2-3°F cooler.

Other research on thundersnow has taken place, though, primarily over regions of greater mesoscale influence, such as lake-effect and orographically enhanced snowfall. Schultz (1999) examined lake effect snowstorms in Utah and New York with and without the occurrence of thundersnow. Unlike research by Market et al. (2006), Schultz (1999) focused on storms that involve lower-

tropospheric convection, as opposed to elevated convection. 49 events were used for the Great Salt Lake area, 28 primarily from Carpenter (1993), 16 from Steenburgh et al. (2000) and five additional events from the climatology of Holle et al. (1998). 26 lake-effect storms were used for the New York case. Surface temperatures common to Great Salt Lake lake-effect snow ranged from -7° to 10°C with the warmer temperatures more associated with lightning reports. For the western New York cases, reports were taken from Buffalo, New York. The typical range of surface temperatures for lake-effect snowstorms were greater than in Utah with temperatures ranging from -15°C to 1°C . More importantly, convective parameters such as CAPE were found to be a non-factor in lightning and non-lightning events. Results of the lower-tropospheric temperature data for the snowstorms showed that surface temperatures were more important, statistically, in forecasting lightning in lake-effect snowstorms than are parameters such as CAPE and dewpoint depressions.

Chapter 3 Data and Methodology

Lightning stroke data were taken from local archives of Vaisala's NLDN data feed. Vaisala, Inc. implemented recent software updates (Cummins et al. 2006) to adjust the threshold frequency of observed lightning in order to minimize the number of false positive cloud-to-ground strokes and flashes and identify them instead as cloud flashes. A collaboration between Vaisala, Inc. and the University of Missouri was started in order to use the cloud lightning data to analyze not only the feasibility of the product but also the storm characteristics of convective snowfall using lightning data.

3.1 Lightning Detection

Lightning detection originated from technology from the 1920's with the implementation of a cathode-ray direction finder by Watson-Watt and Herd (1926). The technology employed loop antennas tuned to a very low frequency

(VLF) around 10 kHz that detect the magnetic field that is generated when lightning makes contact with ground (Krider et al. 1976). The early direction finder output an azimuth on an x-y oscilloscope with the resulting vector pointing in the direction of the discharge. A location was found from two or more direction finders detecting the same discharge. Krider et al. (1976) presented a version of the magnetic direction finder utilizing only the peak magnetic waveform for accurate direction finding. The waveform only lasts for a few microseconds. For this particular setup, the direction finders that detected lightning discharges from 10 to 100 km away had errors of 1° to 2°.

According to Cummins et al. (1998), the NLDN more recently employs a combined system of magnetic direction finding (MDF) and a time-of-arrival (TOA) technique. This method computes return stroke locations by calculating polynomial equations governing the intersection of at least two hyperbolas. The hyperbolas are determined based on the time-of-arrival from the location of the return stroke to the detection system. MDF systems were used in combination to specify an initial interval for finding the roots of the polynomial equations (Peterson et al. 1996).

The upgraded technology of the sensors includes the grouping for flash data and flash multiplicity. A spatial and clustering algorithm is used to identify lightning flashes. After the first stroke is detected, any additional strokes

identified within 10 km of the first stroke, and within 500 ms, are considered part of one flash. The multiplicity limitation is 15 strokes. The detection efficiency for the entire network is determined by the individual sensor detection efficiency, the number of sensors and the sensor baselines. Regional tests at NASA Kennedy Space Center, Florida found location accuracy to be within 2 to 4 km, although recent studies have found median locations to be within 200 to 300 m (Ward et al. 2008). The median location reporting error of the NLDN is about 500 m. Further implementations had been made since 1998 to limit the amount of ground noise detected when contact with the ground is made by lightning discharges (Cummins et al. 2006) including better filtering of low amplitude positive returns which is discussed in the next section.

Biagi et al. (2007), in a study of the NLDN in Arizona, Texas, and Oklahoma, reported a detection efficiency of ~71% for cloud-to-ground (CG) strokes and >90% for CG flashes during four field campaigns from 2003 to 2004. During this study, the best observed detection efficiency was found in Arizona at 93% with first stroke detection efficiency of 76%. The values for Texas and Oklahoma were 92% and 86% respectively. Overall, the detection efficiency for negative first strokes (92%) was better than positive detected first strokes producing a ground contact (81%). Further, based on these studies, it was found that the median error in location was 424 m in Arizona while only 282 m in Texas

and Oklahoma, much lower than the observed 500 m from Cummins et al. (1998), which may have been a function of NLDN detector spacing. The detection efficiency of the cloud lightning in the NLDN varies between 10 and 20%. In previous studies (Orville et al. 2002), low amplitude (<10 kA) positive CG flashes were eliminated from datasets and deemed to be cloud flashes. Biagi et al. (2007) divided the data set into CG type and peak current values. It was found that 1.4-7% of identified positive CG lightning with peak currents less than 10 kA were verified as CG strokes, with those remaining probably being cloud flashes. Further, 4.7 to 26% of identified CG strokes with peak currents between 10 and 20 kA were confirmed, and strokes with peak currents above 20 kA were found to make contact with the surface 67-95% of the time. Detected negative CG strokes were confirmed for peak currents of 10 kA or less 50-87% of the time. Designating low amplitude positive strokes as cloud flashes is not necessary for this study since the implementation of a frequency threshold was added to perform this task (Cummins et al. 2006). It should be noted that the latitude and longitude data represented in the NLDN for CG strokes indicates the point where the lightning strikes the ground and not where it originates in the cloud, which could be several kilometers away. The detection of cloud flashes is more complicated since there is no contact with ground. The detection efficiency of cloud flashes, however, is only on the order of 10-20% (Nicholas Demetriades,

personal communication). Furthermore, it is commonplace, with the NLDN, to find cloud flashes located within close proximity to CG strokes (Murphy et al. 2007).

3.2 Analysis Data

Rapid Update Cycle (RUC) initial field analyses were used for synoptic scale features primarily with some meso- α and meso- β diagnostic variables for a few of the well documented cases. The RUC is well established in the operational community as a means of high-resolution analysis and short-term forecasting (Benjamin et al. 2004a, b). The 40-km RUC initial field was used specifically for diagnostic variables using smoothing to accommodate geostrophic assumptions in the synoptic analysis as suggested by Barnes et al. (1996). Currently the 40-km version is fully archived with all initializations and forecast hours. These archives are provided via the Cooperative Program for Operational Meteorology, Education, and Training (COMET).

3.2.1 RUC Model Resolutions

The RUC model was chosen because of its ability to assimilate data at a high frequency and because it has fine vertical and horizontal resolution. The RUC uses primarily an isentropic (Θ) coordinate field for its vertical resolution. For near-surface resolution in the vertical it uses sigma (σ) coordinates. The

hybrid σ - Θ coordinate field allows for a better depiction of systems aloft with the ability of Θ coordinates to handle the location and intensity of frontal boundaries and also tropopause undulations. The use of σ coordinates also provides a more homogenous view of observations than quasi-horizontal surfaces. In total, the vertical coordinates of the 40-km RUC-2 are divided into 40 levels. Layer thicknesses vary based on terrain features (Benjamin 1998). The horizontal features include 17,063 grid points on a 151 x 113 grid. This covers about 50 percent more area than its RUC-1 predecessor, including more areas off the coastlines to help improve short-term forecasting affected by land and sea processes. Included in the finer horizontal resolutions is the depiction of terrain features. The RUC uses a "slope envelope" topography. In slope envelope topography, the terrain standard deviation is calculated with respect to a plane fit to the topography in each grid box (Benjamin et al. 1998).

3.2.2 RUC Data Assimilation

Some of the data the RUC is able to assimilate during its analysis include Velocity-Azimuth Display (VAD) wind profiles, land and ship buoy reports, aircraft reports (ascending and descending), GOES precipitable water retrievals, GOES high-density cloud-drift winds, and reconnaissance tropical storm dropwindsonde data (Kim and Benjamin 2001; Benjamin et al. 1998). The RUC

model is built in with a quality control "buddy check" system that flags suspicious observations during data assimilation. By subtracting the known anomaly from a previous forecast, the quality control sensitivity is increased to actual assimilation errors. Some of the profiles that are controlled in such a manner are bird and insect contamination from VAD wind profiles and profiler winds (Benjamin et al. 1998).

3.2.3 RUC Dynamics and Physics

The RUC model incorporates several physical, dynamical processes to derive certain prognostic variables. The more impressive of the physical features of this model are the explicit cloud and moisture processes. The RUC uses similar microphysics to the Penn State mesoscale model MM5 identifying the five hydrometeor species of cloud water, rain water, snow, ice, and graupel and the prediction of ice particle concentration (Reisner et al. 1998). In addition to the moisture processes, the RUC also uses the MM5 radiation package (Grell et al. 1994). This scheme has separate components for both longwave and shortwave radiative processes. It also takes into account the earth's rotation about the sun. The RUC further includes algorithms to include possible turbulent mixing in the boundary layer. Surface layer mixing follows a three-layer scheme to calculate

the total kinetic energy near the surface and energy maxima aloft, specifically near frontal zones and other like disturbances.

The RUC uses the Grell (1993) cumulus parameterization scheme. This scheme was originally developed as a simple cumulus parameterization to avoid first-order errors (Grell et al. 1994). There are three main parts to this convective scheme; they are the dynamic control, the feedback, and the static control. The dynamic control is defined as the effects of the environment on the convection. This helps to determine location and strength of the convection. This control, using stability closures, assumes observed changes in available buoyant energy, or positive areas of convective energy. It also uses a Kuo (1965) type scheme in relating convective activity to total moisture convergence at a grid point. The feedback describes the effects of the convection on the environment, handling and distributing the heating and drying of the atmosphere. Similar to the dynamic control, the feedback uses a stabilizing approach (Kuo 1974) where the convection tends to adjust the atmosphere into a moist neutral state. Thus, the feedback is largely dependent on differences of temperature and moisture between the environment and the cloud (Grell 1993; Grell and Devenyi 2001). The effects that convection has on the surrounding environment include subsidence and detrainment of cool dry air, which occurs from the expansion, cooling, and subsequent sinking of a parcel out of a convective environment,

especially in most warm-season heavy rain events. Also, the RUC is more concerned with the location of where the overall magnitude of the cloud mass is influenced rather than where the latent heat release occurs. (Grell 1993). The static control in this convective parameterization controls the properties of the updraft and downdraft which includes the dynamics of entraining or detraining air. This control assumes a cloud rises and falls instantly without a steady-state stage. In addition, cloud properties are mixed horizontally with the subsided environment instead of being made dependent on precipitation efficiency and shear (Grell 1993). Note, also, that in the Grell scheme, no cloud water is assumed to exist, but it all is converted into rain (Grell et al. 1994).

3.2.4 RUC Variables

The RUC model diagnoses several key variables. These fields that are not pertinent to this research, but do go so far as to show the depth and abilities of the RUC model. Such variables include the diagnosis of sub-grid scale precipitation, snow accumulation, snow depth, categorical precipitation types, convective measures, such as CAPE, CIN, lifted index, best lifted index, and helicity, and soil moisture levels. The more valuable diagnosed fields include relative humidity, specific humidity, temperature, dewpoint, and precipitation accumulation. The 40-km RUC also includes an algorithm to assimilate

precipitable water data from GOES precipitable water observations (Benjamin et al. 1998).

3.3 Case Data

Fourteen cases were analyzed for the winter season (October through April; Table 3.1). These cases were all storms producing moderate to heavy precipitation both in the warm sector of the cyclone and in the subfreezing air, where winter precipitation fell. Table 3.1 shows the dates of the storms analyzed.

Table 3.1 The dates of each individual case represented in this paper for analysis during the 2006-2007 winter season, extending from October to April. There are fourteen total events for this winter in which thundersnow in the central U.S. was observed.

Storm Dates	
2006	2007
09-11 November	12-15 January
27-28 November	20-22 January
29 November - 02 December	30-31 January
18-22 December	12-14 February
28-31 December	23-25 February
	28 February - 02 March
	01-03 April
	07-08 April
	13-14 April

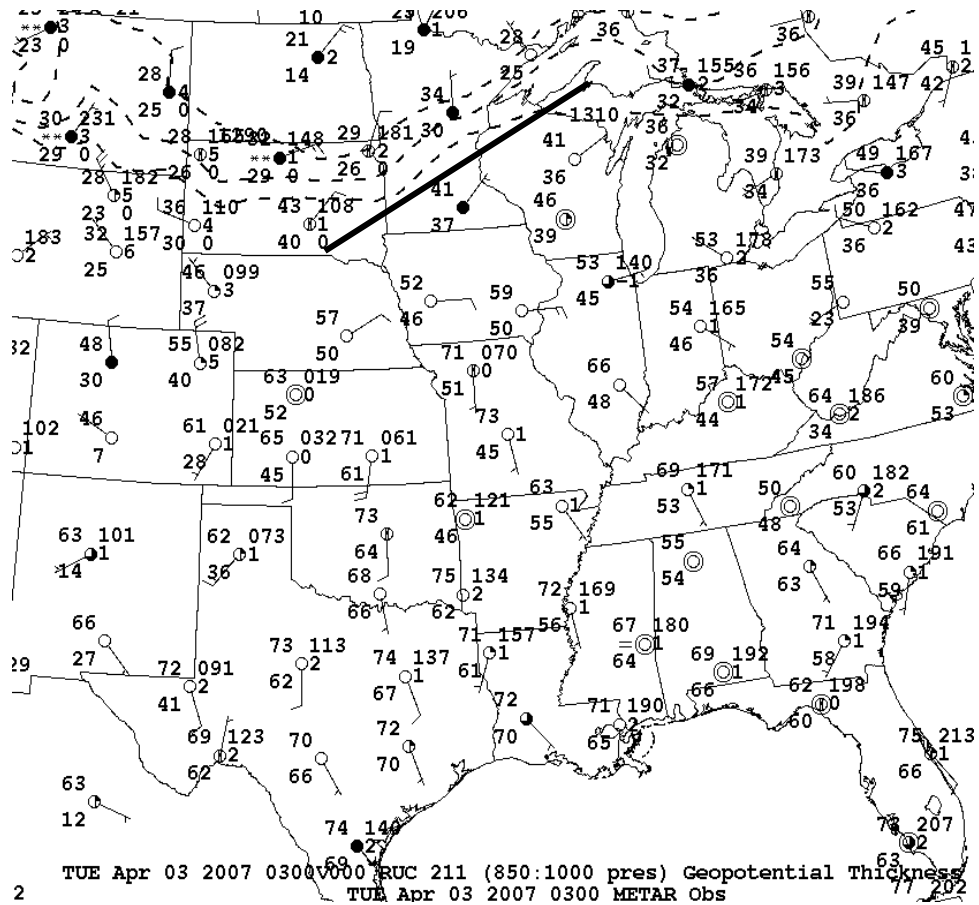


Figure 3.1 Example map encompassing central U.S. representing domain from which lightning data was queried along with surface METAR observations. Dashed lines are 850-1000-mb thickness from 1290 gpm to 1310 gpm. Line represents rain-to-snow transition.

3.4 Separation Analysis

For each of the fourteen cases, lightning data were queried for a region encompassing the central U.S. (longitude 114 W to longitude 79 W and latitude 26 N to latitude 49 N: Figure 3.1) and separated into cloud and CG events. Using the surface METAR reports and 40-km Rapid Update Cycle (RUC2) analysis of 850-1000-mb thickness, a rain-snow transition line was determined. The

standard rain-to-snow transition line in this partial thickness regime is taken as 1290 geopotential meters (gpm).

However, mixed-phase precipitation such as sleet, ice pellets, and freezing rain can occur at thicknesses greater than 1290 gpm. For this reason, thickness was plotted as high as 1310 gpm at a 10-gpm interval and plotted with surface METAR reports at matching times every 4 hours. From this approach, a line is fixed with two endpoints, each having a longitude and latitude point, indicating a transition line representative of the 4-hour period. The slope of the line was calculated given the coordinates for these endpoints. We employed a simple linear equation of the classic form:

$$y = mx + b$$

Where m is the slope, x is a point in the x direction, which is represented by a change in the longitude between the western endpoint and the longitude of any given lightning event detected, and b is the y -intercept given by the latitude on the western endpoint of the line. Solving for y gives the latitude of the line at any given longitude of a detected lightning event, thus by comparing the latitude of the line to the latitude of the detected lightning, those that occur in cold air as opposed to warm air can be separated. Given the large numbers of lightning data used in this, the linear method was employed to help simplify the process.

Lightning trends were determined in each case based on both the total lightning from the storm and from lightning determined to be associated with frozen precipitation. A percent occurrence of each type of lightning (e.g. negative CG, positive CG, and cloud) was also calculated in each case along with a cloud to CG ratio. It should be noted that cloud to CG ratio values will not apply exactly to other lightning research as this work is done using individual stroke data as opposed to flash data. The average multiplicity for a lightning flash is about 2-3 strokes per flash in the U.S. Further, both average and median locations for each storm were taken for each 4-hr subset, daily, and monthly. This will help not only to gain knowledge of lightning characteristics in storms with frozen precipitation but also serve as a determination of the value of cloud lightning detection by Vaisala's NLDN. Also, a seasonal trend was developed for the entirety of the season, both with the total dataset and the winter dataset. This was further divided into the individual lightning types. This trend was created on the principle that this was not a sufficient dataset to create such a trend, but it still could be useful for further analysis as more seasons are analyzed in a similar context.

Groupings were formed in each winter dataset that had been observed at the same time to the tenth of a second. While the NLDN can make observations up to a thousandth of a second, the groupings were only matched to the tenth for

simplification. These pairings needed to possess both a cloud flash and a CG stroke and be located within at least 0.5° longitude and latitude from each other. The average distance between cloud flashes and CG strokes were then determined. Ideal pairings consisted of one CG stroke and one cloud flash at the same time, but of course, this is not the case in some of these cases, particularly those that exhibited some stronger tendency to lightning activity. The observation associated with this is that cloud flashes and CG strokes occur within close proximity to each other, according to NLDN observations (Murphy et al. 2007).

3.5 Composite Sounding

Each case and case subset was further analyzed for its physical characteristics using model initial soundings from the RUC model. The 4-hr subsets were observed for lightning activity, in particular, the most active hour within these subsets. A model initial time was taken from this approach, along with a latitude and longitude location of the most active lightning associated with frozen precipitation. The location was determined from the average location for all lightning detected in winter precipitation within that single, most active hour. In the General Meteorological Package (GEMPAK) display software, the RUC model displays a data point vertically every 50 mb from 50

mb down to the surface. Further, the RUC initial fields were plotted in plan view to determine the reference location of the sounding to be taken, whether it be geographically northeast (NE) or northwest (NW) of the subsequent surface cyclone, following the procedure employed by Market et al. (2006). Employing Brown's (1993) feature preserving techniques for composite soundings, the most unstable lifted parcel level (MULPL), the top of the inversion layer, the height (pressure and height in meters) of the -10°C isotherm, and the height (pressure and height in meters) of the -20°C isotherm were determined for compositing. The mean of these sounding features and each vertical level every 50 mb (i.e. 850, 800, 750, 700, etc...) were determined. From these data, a sounding profile was produced using the RAOB 5.7 sounding analysis software. For the NE cases, there were 45 soundings to composite while there were only 19 for NW cases. Given the dominance of NE thundersnow events for this particular season, the NE cases were further subdivided into three 4-hour segments, the four hours prior to the most active lightning (N=7), the four hours during the most active lightning (N=12), and the four hours after the most active lightning occurred (N=8). Caution is given to results given the smaller dataset.

Chapter 4 Results

4.1 Individual Storm Analyses

The following chapter provides a detailed analysis of each individual storm analyzed during the 2006-2007 winter season. Table 4.1 shows the lightning count total for both the entire storm and the portion of the storm with winter precipitation. This is further divided into lightning types (i.e. cloud or CG) as well. However, there is no significant correlation between the amount of lightning observed and the intensity and snowfall total observed with each storm (Iskendarian 1998). Each case will be discussed separately in chronological order starting with the events in 2006. The beginning and end time of each event was rounded to the nearest hour of the first and last thundersnow observation in the central U.S. domain.

Table 4.1 Lightning totals for each storm during the 2006-2007 winter season including storm totals and totals with winter precipitation.

Dates	Total	CG	Cloud	Winter	CG	Cloud
09-11 Nov 2006	316466	198735	117731	48	31	17
27-28 Nov 2006	66049	48601	17448	3004	2182	822
29 Nov-02 Dec 2006	85852	56873	28968	7329	4360	2980
18-22 Dec 2006	112868	79342	33526	12982	9625	3357
28-31 Dec 2006	497546	297840	199706	1801	1290	511
12-15 Jan 2007	53375	35914	17461	2177	1472	705
20-22 Jan 2007	23	12	11	6	0	6
30-31 Jan 2007	650	398	252	1	0	1
12-14 Feb 2007	248097	164195	83902	18	11	7
23-25 Feb 2007	253272	155253	98019	706	373	322
28 Feb-02 Mar 2007	334847	233617	101230	6552	3944	2568
02-03 Apr 2007	730609	495805	234804	2	1	1
07-08 Apr 2007	12052	10249	1803	2241	1907	334
13-14 Apr 2007	473920	293453	180467	7413	5172	2234
Total	3185829	1969186	1115397	44280	30368	13865

When the term “lightning events” is used, it is describing the combination of both cloud flashes and CG strokes. The term “cloud flashes” is used when describing only cloud lightning. Since stroke data is being used, the term “stroke” will only be used when referring to CG strokes that are detected, with both negative and positive polarity.

4.1.1 November 09-11, 2006

This date marked the first occurrence of thundersnow in the Midwestern U.S. for the winter season. An early fall clipper, defined by a surface low moving quasi-zonally across the southern Canadian provinces and the northern U.S., moved across the Dakotas and into Minnesota and Wisconsin and eventually occluded over the Great Lakes. The first observation of thundersnow with this particular event occurred at 0700 UTC on 10 November 2006 and continued until the last observation reported near 0600 UTC on 11 November 2006. Some lightning from this event are shown in Figure 4.1.

During the 40 hours that thundersnow was reported in the central U.S., there was a total of 316,466 lightning events across the U.S. (Table 4.1). Among this total, 62.8% were CG strokes and the remaining 37.2% were cloud flashes. According to Uman (2001), however, there are, on average, about 10 cloud flashes for every one CG flash, although recent studies are indicating a ratio closer to 5:1. This ratio, of course, does not apply fully to this work since stroke data is being used. Using an average multiplicity of 2-3 strokes per CG flash, it can be assumed that there are about 1.7-2.5 cloud flashes for every one CG lightning stroke. 96.3% of the CG strokes had a negative polarity while only 3.7% were positive strokes.

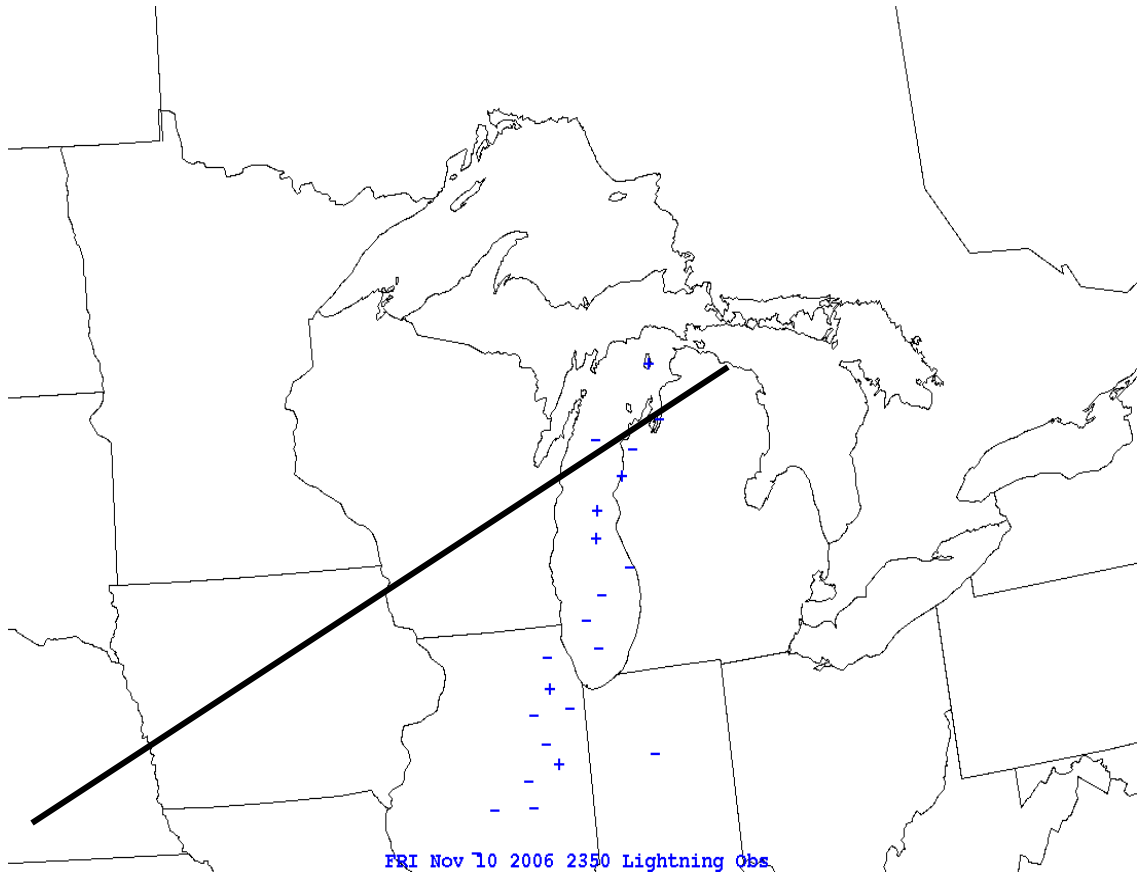


Figure 4.1 Lightning map indicating negative and positive CG flashes ending at 2350 UTC 10 November 2006. Line indicates rain/freeze transition. All lightning above line are in subfreezing air. Lightning in this image produced from NLDN flash data in GEMPAK.

Of all the lightning events observed, only 48, or 0.015%, were found in subfreezing air in the central U.S. Of those 48 lightning events found in freezing air, 35.4% were cloud flashes, while 64.6% were CG strokes. Of the CG strokes, 74.2% were negative CG strokes and 25.8% were positive. The lightning over the central U.S. came at an average rate of 87.9 min^{-1} , while the average rate for lightning associated with frozen precipitation was 0.022 min^{-1} .

The maximum lightning for the total storm was between 0000 UTC and 0400 UTC on 11 November 2006, which had a total of 182,516 lightning events (Fig. 4.2a). This was associated with an event rate of about 760 min⁻¹. Only 0.007%, or 13, dominated by 11 CG strokes, was found associated with winter precipitation at this time. The maximum time in lightning associated with winter precipitation occurred during the storm (Fig. 4.2b). This time occurred 4 hours previous to the overall storm total maximum, occurring between 2000 UTC on 10 November 2006 and 0000 UTC on 11 November 2006. In this duration there were 29 events found associated with winter precipitation, of which 55.0% were CG strokes and 45.0% were cloud flashes. This time had an event rate of 0.12 min⁻¹. Negative CG strokes consisted of 69% of all CG strokes and 31% were positive. Figure 4.3 shows the dominance of negative CG strokes in the winter lightning, which contrasts with the findings of Hobbs (1974), Brook et al. (1982) and MacGorman and Rust (1998) where they found a bias towards positive polarity in winter lightning off the coast of Japan. The majority of the negative CG strokes were between 0 and 20 kA. Note that Biagi et al. (2007) found that up to 80% of low amplitude negative strokes in the NLDN were most likely CG strokes.

To summarize, this event was the first observed thundersnow of the season in the Midwest. Much of the lightning in winter precipitation was found

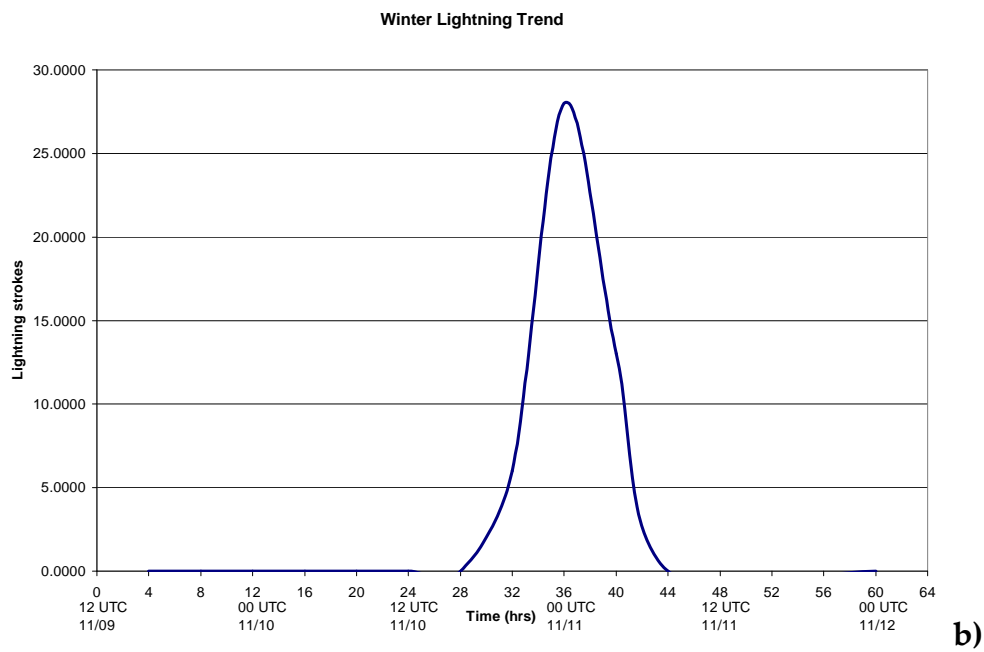
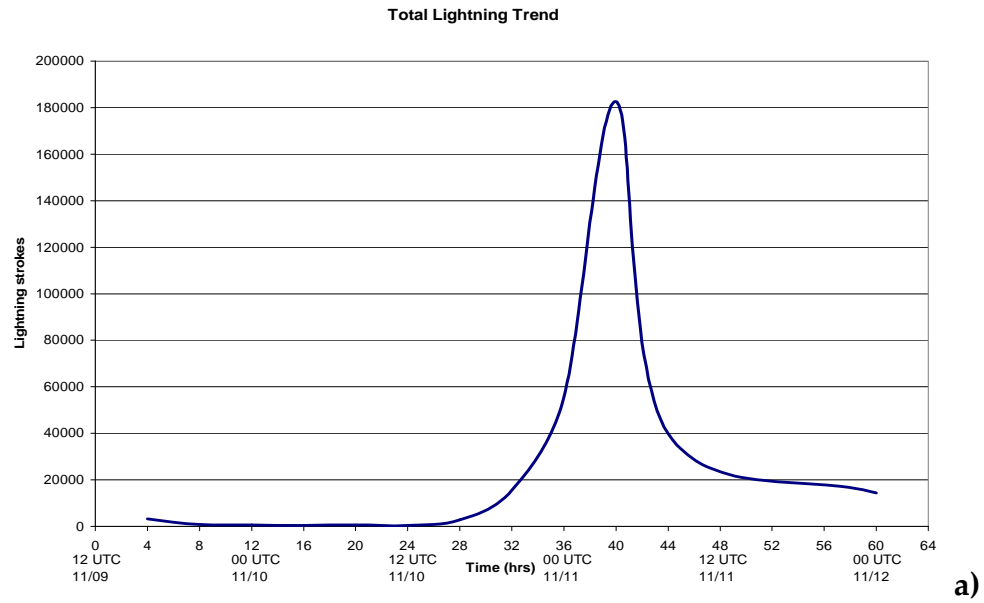


Figure 4.2 Storm total lightning trend for both *a)* the total storm and *b)* the lightning associated with winter precipitation for 09 November 2006 through 11 November 2006. Time given in hours from the onset of lightning detected in winter precipitation. Date labeled every 12 hours in UTC.

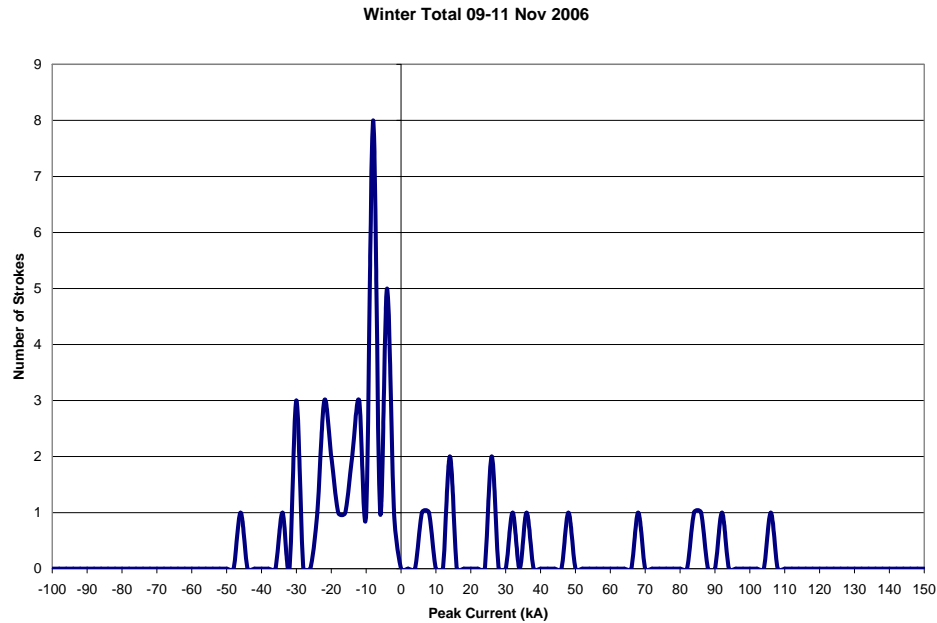


Figure 4.3 Line diagram showing the dominant occurrence of low amplitude negative CG strokes for lightning occurring in winter precipitation for thundersnow event on 10 November 2006. The x-axis is peak current in kA and the y-axis is the number of times a stroke of a given amplitude occurred.

along the northern states of the central U.S. Further, the amount of lightning in winter precipitation was not significant compared to all lightning occurring with this storm. This case also provided the first insight into the percent occurrence of individual lightning types including cloud flashes. It will be shown, that these percentages are close to the full seasonal average for percent occurrence with both CG strokes and cloud flashes.

4.1.2 November 27-28, 2006

The second case of the season was a weak shortwave system that again clipped the north-central U.S. Overall, this system produced significantly fewer

lightning events, but larger numbers of them occurred with winter precipitation. This case began in the early hours of 27 November 2006 and stretched across the Northern Plains for 48 hours. The first thundersnow report occurred near 0000 UTC 27 November 2006 and the last one at 1600 UTC 28 November 2006. While thundersnow continued again on 29 November 2006, the occurrence of thundersnow is from a separate system and thus is analyzed separately. Figure 4.4 shows five-minute lightning ending at 0800 UTC on 28 November.

Again, the lightning totals for this event are shown in Table 4.1. This clipper system produced 66,049 observed lightning events. From this total, 26.4% were cloud flashes with the remaining 73.6% being CG strokes. Of the CG total, 97.3% were negative CG strokes with the other 2.7% being positive CG strokes.

However, of the total, 3399, or 5.1%, were found associated with winter precipitation in the central U.S. This total consisted of 71.1% CG strokes and 28.9% cloud flashes. The CG strokes consisted of 89.2% negative CG strokes and 10.8% positive CG strokes. The average event rate for lightning over the central U.S. during this event was 21.2 min^{-1} while the average stroke rate for lightning associated with winter precipitation over the central U.S. was 1.1 min^{-1} .

The maximum time of lightning occurrence during this event occurred between 0800 UTC and 1200 UTC on 28 November 2006 (Fig. 4.5a). This time

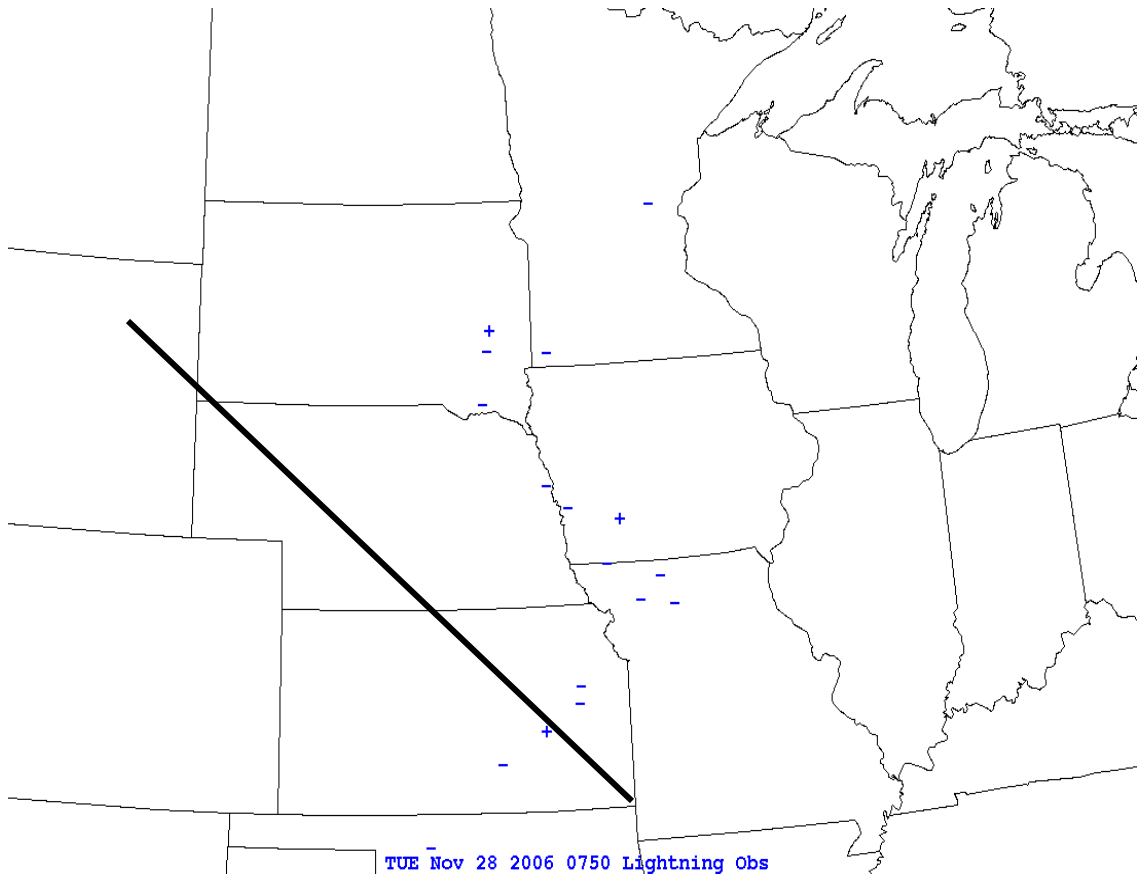


Figure 4.4 Lightning map indicating negative and positive CG flashes ending at 0800 UTC 28 November 2006. Line indicates rain/freeze transition. All lightning above and right of line are in subfreezing air. Lightning in this image produced from NLDN flash data in GEMPAK.

consisted of 43.2% of all lightning, at an average event rate of 119 min^{-1} . As with the previous system, the maximum in lightning associated with winter precipitation occurred in the four hours previous to the overall lightning maximum, between 0400 UTC and 0800 UTC on 28 November (Fig. 4.5b). During this 4-hr subset, there were 2992 events, at an average rate of 12.5 min^{-1} , observed to be associated with winter precipitation, which consisted of 88.0% of all lightning found in winter lightning. Of this, 27.4% were cloud flashes and

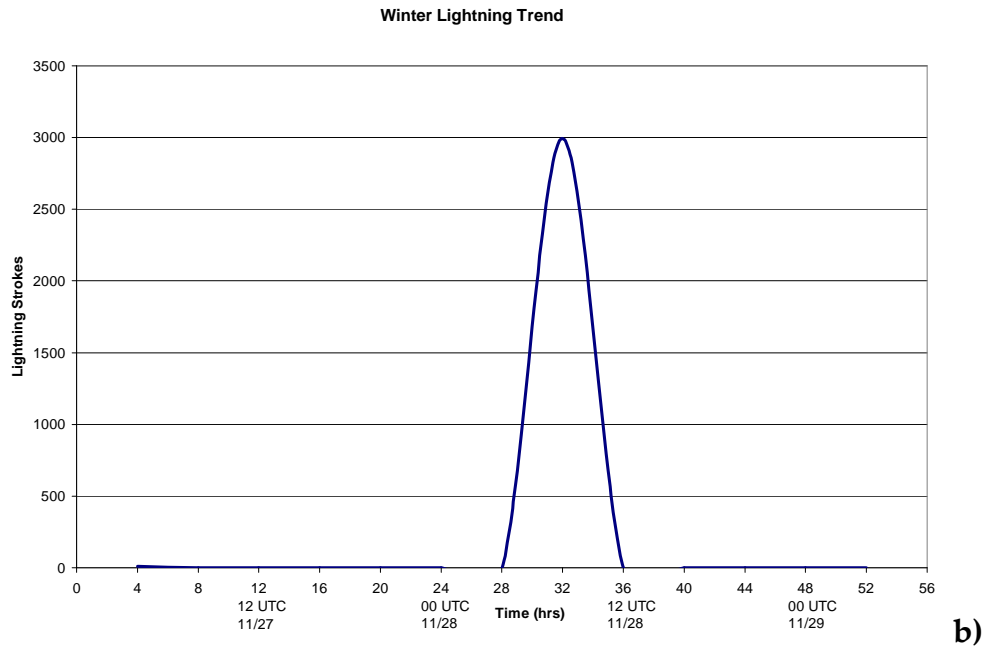
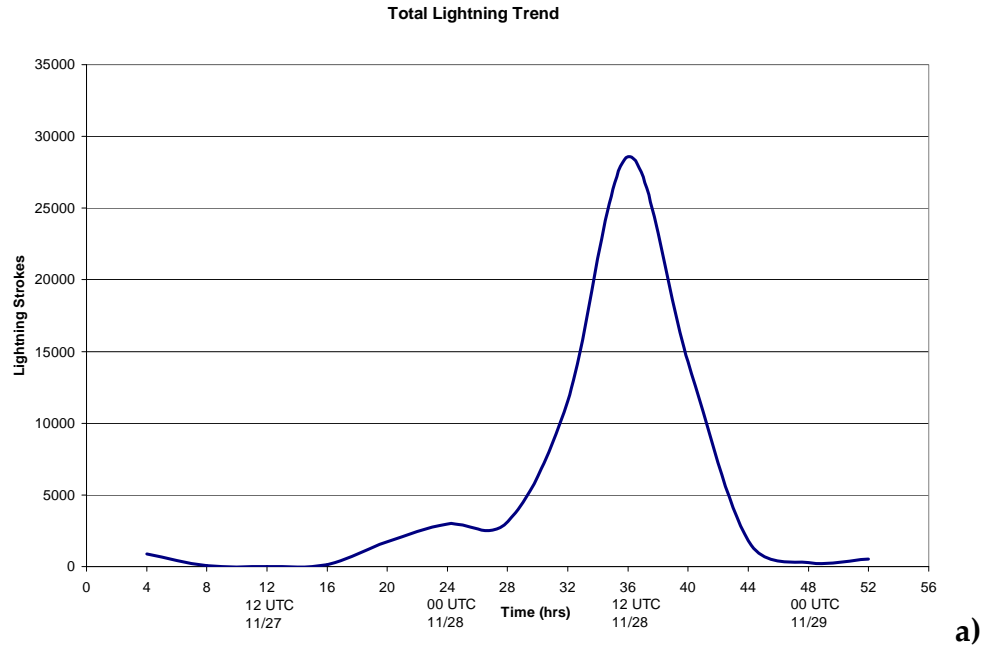


Figure 4.5 Storm total lightning trend for both a) the total storm and b) the lightning associated with winter precipitation for 27 November 2006 through 29 November 2006. Time given in hours from the onset of lightning detected in winter precipitation. Date labeled every 12 hours in UTC.

72.6% were CG strokes. Of the CG strokes, 88.9% were negative and 11.1% were positive.

This case was very similar to the first case in terms of percentages, albeit slightly lower. Further, these systems were very similar, but overall this storm had slightly more lightning in frozen precipitation.

4.1.3 November 29 - December 01, 2006

This storm began during the day of 29 November 2006 and lasted through 01 December 2006. Significant lightning with frozen precipitation began at 1900 UTC on 29 November and lasted until the last thundersnow report was observed near 1200 UTC on 01 December. Throughout the duration of the storm, the NLDN observed 85,852 total lightning events in the central U.S. Of the storm total lightning events, 33.7% were cloud flashes and 66.3% were CG strokes. Of the CG strokes, 94.6% were negative while the remaining 5.4% were positive. For the total storm, positive strokes made up 3.5% of all the strokes.

When separated by temperature at the surface, 7329 lightning events, or 8.5% of the storm total, were found to occur in surface temperatures at or below freezing and associated with winter precipitation (Fig. 4.6). Of those, 40.7% were cloud flashes and 59.3% were CG strokes, in which 91.2% of the CG strokes were negative CG strokes and 8.8% were positive. Positive CG strokes made up 5.2%

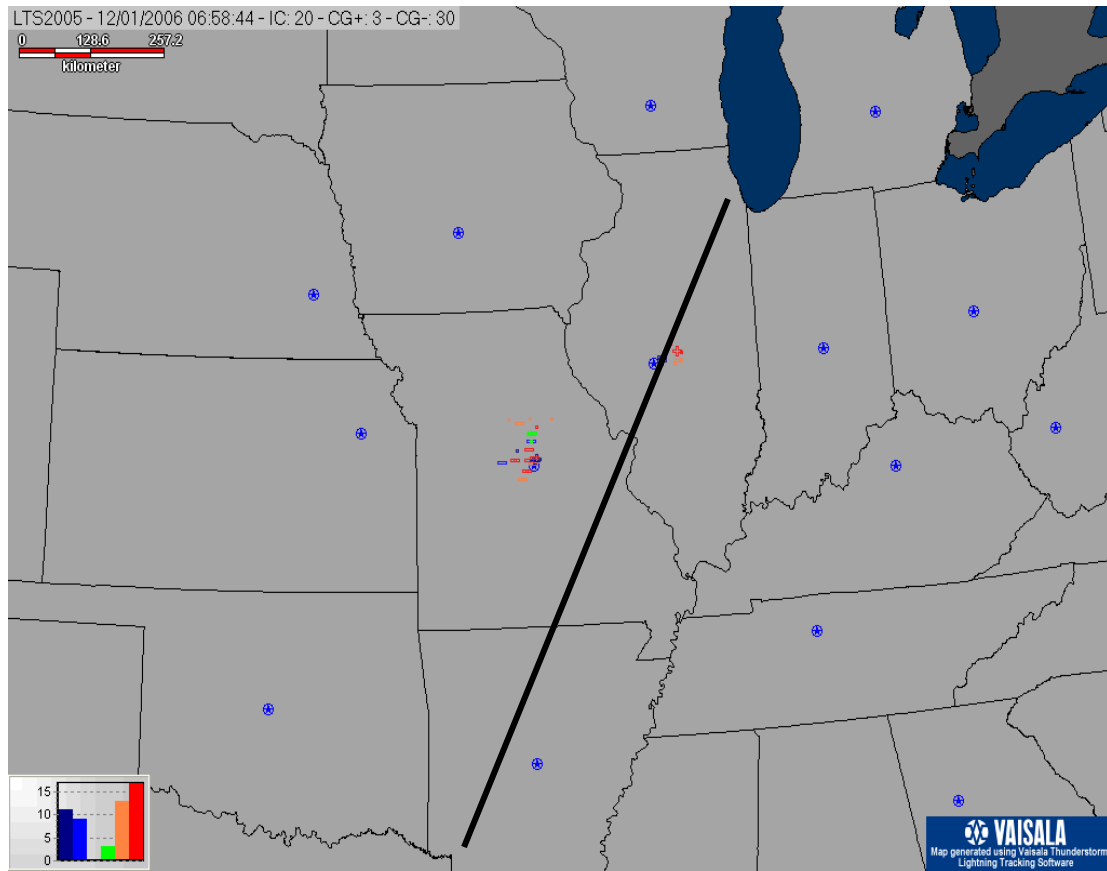


Figure 4.6 Lightning map indicating negative and positive CG strokes and cloud flashes for one hour ending at 0700 UTC 01 December 2006. Line indicates rain/freeze transition. All lightning above and left of line are in subfreezing air.

of the total lightning events with winter precipitation. On average, this storm displayed lightning event rates of 35 min^{-1} with a rate of 3 min^{-1} in the winter precipitation.

The maximum lightning times for this storm occurred between 0000 UTC and 0400 UTC on 30 November 2006 with a total of 34,126 total events (Fig. 4.7a), of which 2030 events were associated with winter precipitation (Fig. 4.7b). Of

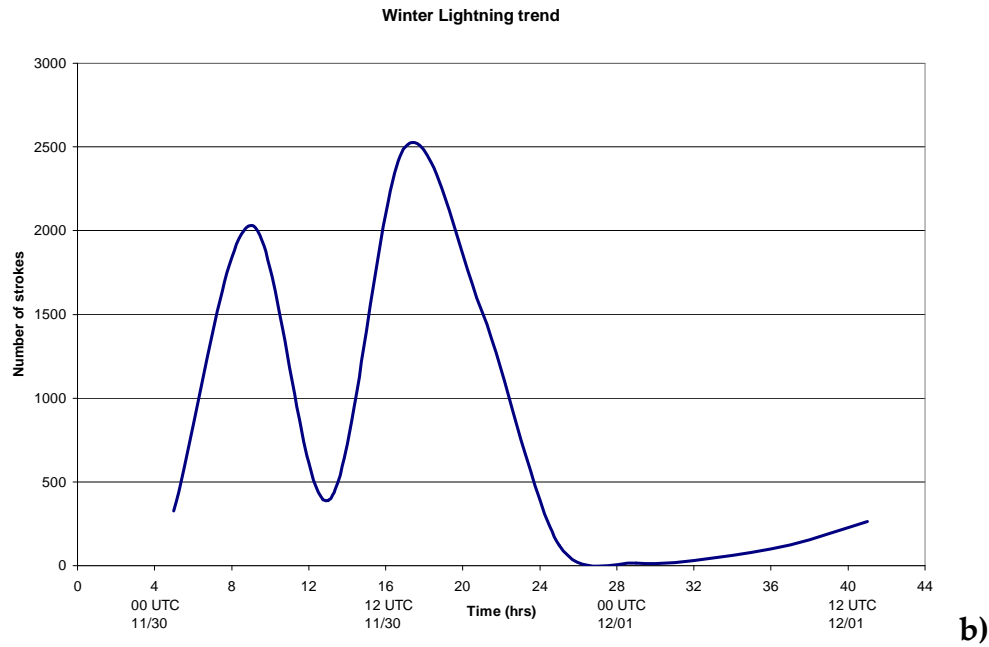
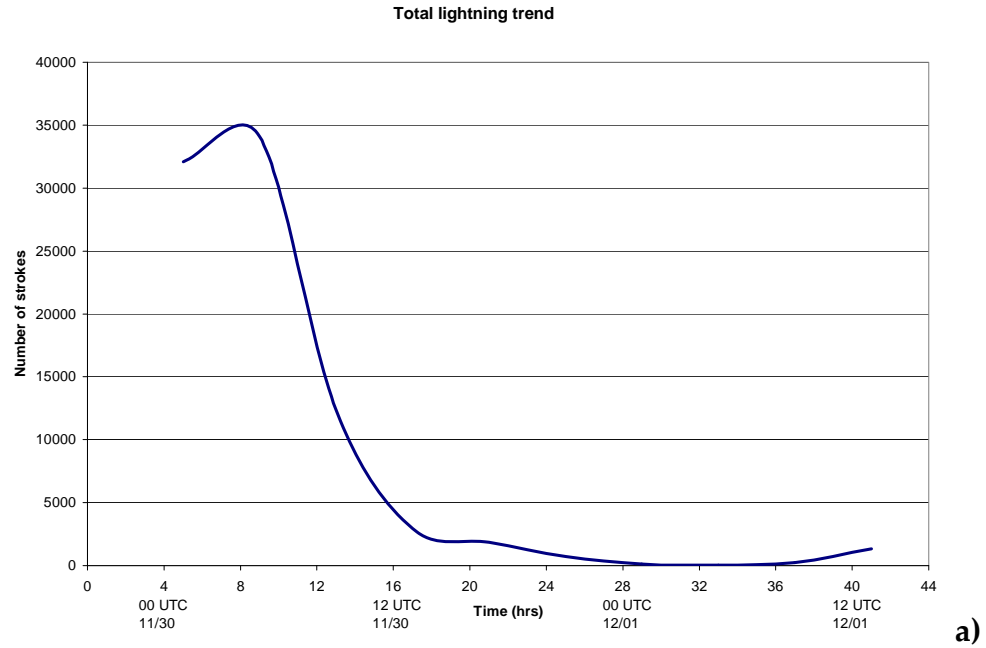


Figure 4.7 Storm total lightning trend for both *a*) the total storm and *b*) the lightning associated with winter precipitation for 29 November 2006 through 01 December 2006. Time given in hours from the onset of lightning detected in winter precipitation. Date labeled every 12 hours in UTC.

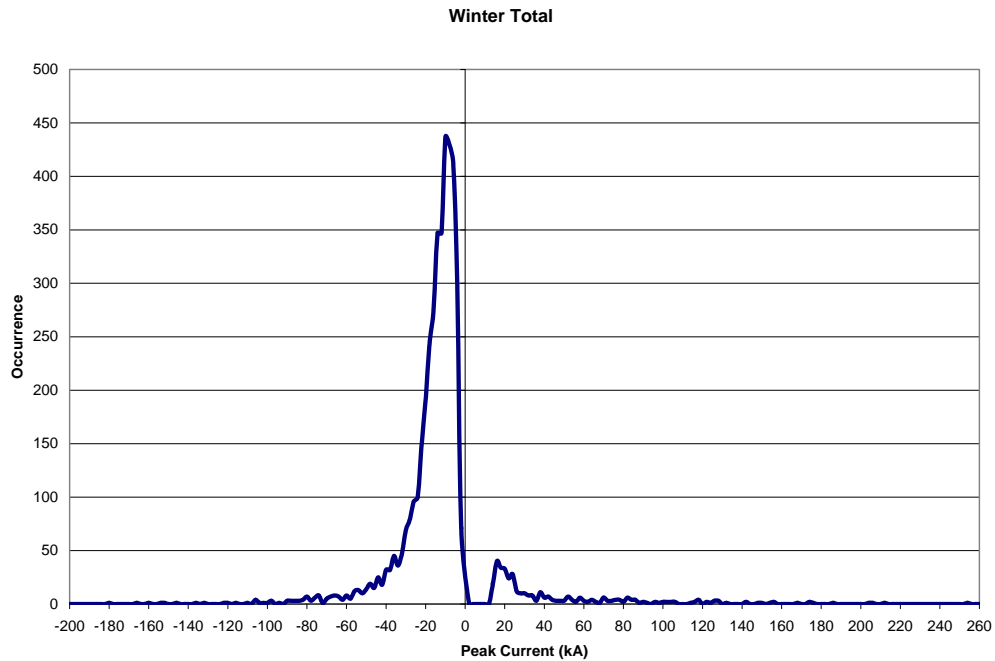


Figure 4.8 Line diagram showing the dominant occurrence of low amplitude negative CG strokes for lightning occurring in winter precipitation for thundersnow event on 01 December 2006. The x-axis is peak current in kA and the y-axis is the number of times a stroke of a given amplitude occurred.

this winter total, 57.6% were CG strokes along with 42.4% cloud flashes. The event rate at this time was 142 min^{-1} for the total storm and 8.5 min^{-1} for those in winter precipitation. The maximum for lightning associated with winter precipitation was between 0800 UTC and 1200 UTC on 30 November with a total of 2497 events, of which 58.1% were CG strokes and 41.9% were cloud flashes, resulting in an event rate of 10 min^{-1} . Figure 4.7a,b shows the lightning trend both for the total storm and for lightning events associated with winter precipitation. Notice the diurnal trend in the winter lightning with maximums near dusk and dawn. While this does not appear in the overall storm total trend,

it appears in the local trend for lightning in winter precipitation for this particular storm. There has been little mention of morning maxima in precipitation and no mention of a morning peak in lightning associated with elevated convection. Also note the tail in the trends towards the event. These are representative of the deepening of the storm as it exits the central U.S. domain.

Similarly to the previous storms analyzed, there is a significant dominance of negatively polar lightning associated with the winter precipitation (Fig. 4.8). The dominant range of peak current again is between 0 and 20 kA.

In summary, this event marked the first significant snow storm producing lightning in the central U.S. for this winter season. In this case, there was a higher percentage of lightning that occurred in winter precipitation than the previous events. Further, given the intensity of this storm, there were markedly fewer lightning events observed than the previous winter storms.

4.1.4 December 18-22, 2006

This event marked the second intense, thundersnow producing cyclone across the central U.S. The first thundersnow observation was reported near 1000 UTC on 19 December 2006 and continued through the central U.S. ending near 1800 UTC on 22 December. The deepening of this storm produced many

lightning events extending from the Texas panhandle and up through Oklahoma, going slightly farther south than the storm immediately before. For the 92-hour event, there was a total of 112,868 observed lightning events in the central U.S. Of this total, 29.7% were cloud flashes while 70.3% were CG strokes. From the CG strokes, 92.3% were negative and 7.7% were positive. An example map of the storm is shown in Figure 4.9. The lightning shown is for one hour of this event ending at 1625 UTC on 19 December 2006.

For the event, 12,982, or 11.5% of the total, lightning events were found associated with winter precipitation. 25.9% of this total was cloud flashes with the other 74.1% being CG strokes. Of the CG strokes, 93.4% were negative and only 6.6% were positive. The average event rate for lightning across the central U.S. was 20.4 min^{-1} . The average event rate for those occurring with winter precipitation was 2.4 min^{-1} .

There were two maximum times in the storm total lightning. The first, and smaller, maxima (Fig 4.10a) occurred between 0000 UTC and 0400 UTC on 20 December 2006 with a gradual increase in lightning occurrence. There were 7890 lightning events, of which 33.2% were cloud flashes and 66.8% were CG strokes. This resulted in an average event rate of 32.8 min^{-1} . 93.4% of the CG strokes were negative while 6.6% were positive. This maximum coincided with the primary maximum in lightning associated with winter precipitation (Fig.

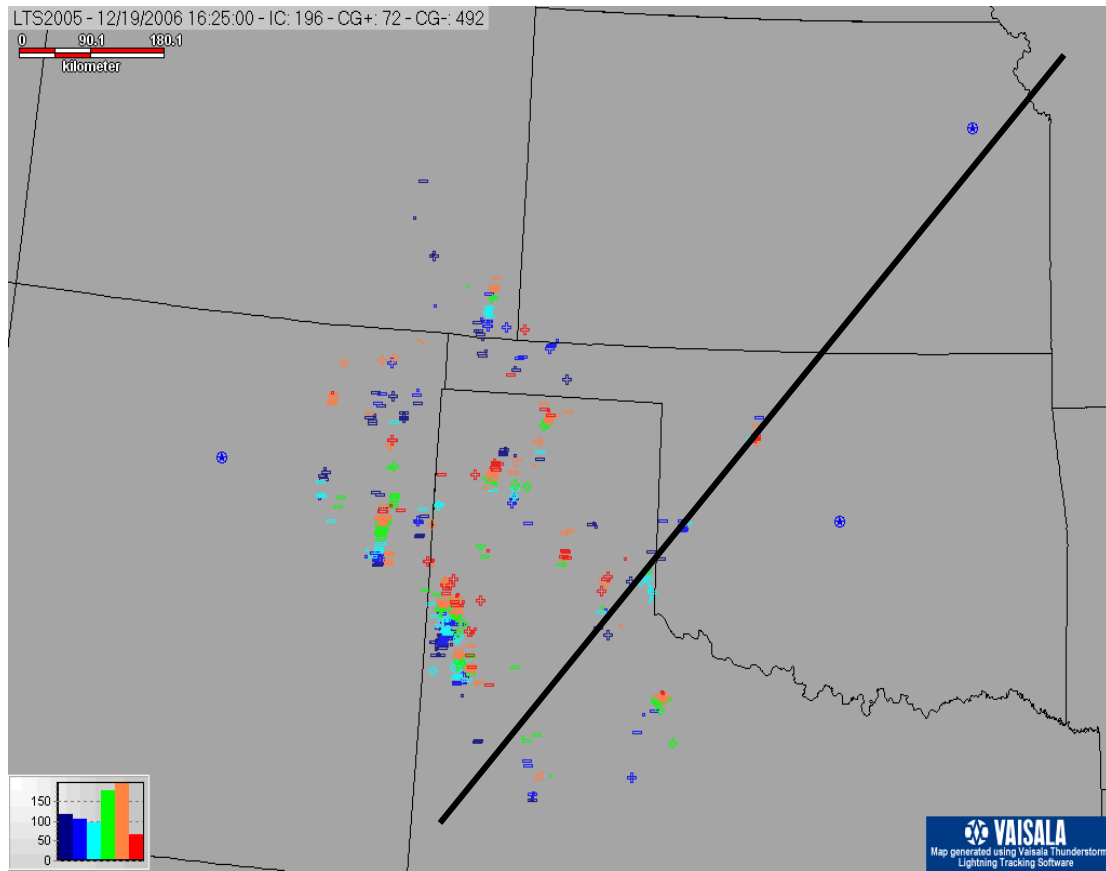
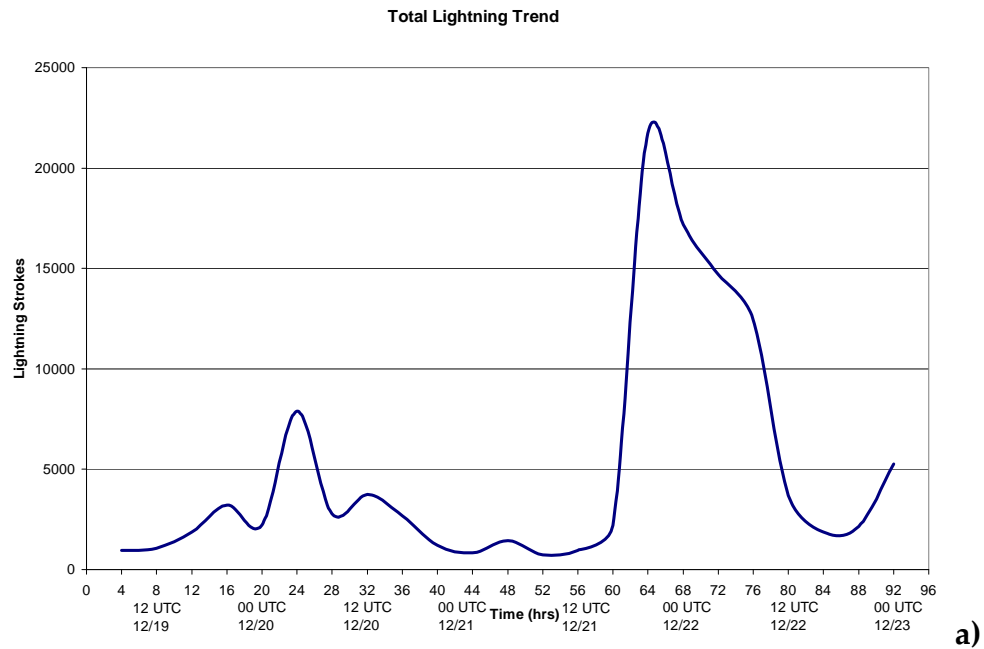


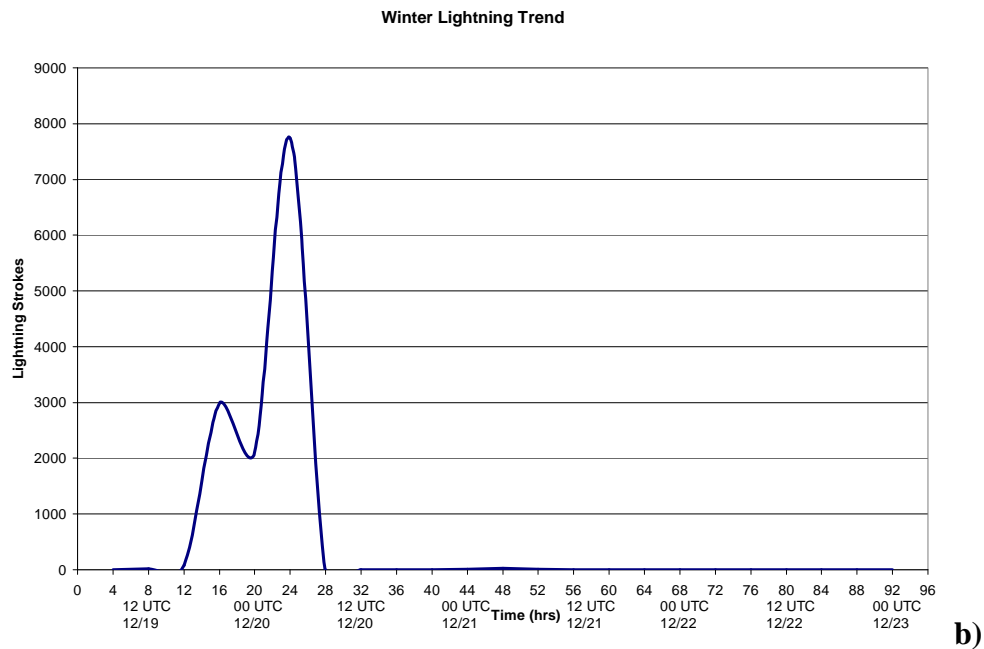
Figure 4.9 Lightning map indicating negative and positive CG strokes and cloud flashes for one hour ending at 1625 UTC 19 December 2006. Line indicates rain/freeze transition. All lightning above and left of line are in subfreezing air.

4.10b). In this same four-hour subset, 7742 events were found to occur in regions of winter precipitation. This made up 98.1% of the total observed lightning events at this time. 33.0% of the winter lightning events during this time were cloud flashes and 67.0% were CG strokes, of which 93.8% were negative CG strokes. This had an average event rate of 32.2 min⁻¹.

The second maximum time for the total lightning occurred later in the storm between 1600 UTC and 2000 UTC on 21 December. This maximum far



a)



b)

Figure 4.10 Storm total lightning trend for both a) the total storm and b) the lightning associated with winter precipitation for 19 December 2006 through 22 December 2006. Time given in hours from the onset of lightning detected in winter precipitation. Date labeled every 12 hours in UTC.

outweighed the first maximum with a total of 21,742 lightning events during this four-hour time. This total consisted of 38.6% cloud flashes and 61.4% CG strokes at a rate 90.6 min^{-1} . The CG total consisted of 96.5% negative strokes and 3.5% positive strokes. There was no lightning found associated with winter precipitation during this time while the total lightning events gradually decreased towards the end of the storm. The last maximum in lightning events with winter precipitation occurred between 0000 UTC and 0400 UTC 21 December with only 25 observed lightning events found.

To summarize, this storm had multiple maximum occurrences of lightning separated by a 24-hour period. However, only one of those times exhibited lightning in winter precipitation, which at this time, made up a majority of the lightning during this time. This is different from the previous storms due to the nature of the storm to have multiple storm total peaks, but most importantly, this shows a difference in the percentage of lightning occurring in winter precipitation with respect to the storm total lightning at this time. Other than this, the percentages of cloud flashes and CG stroke occurrence remained similar.

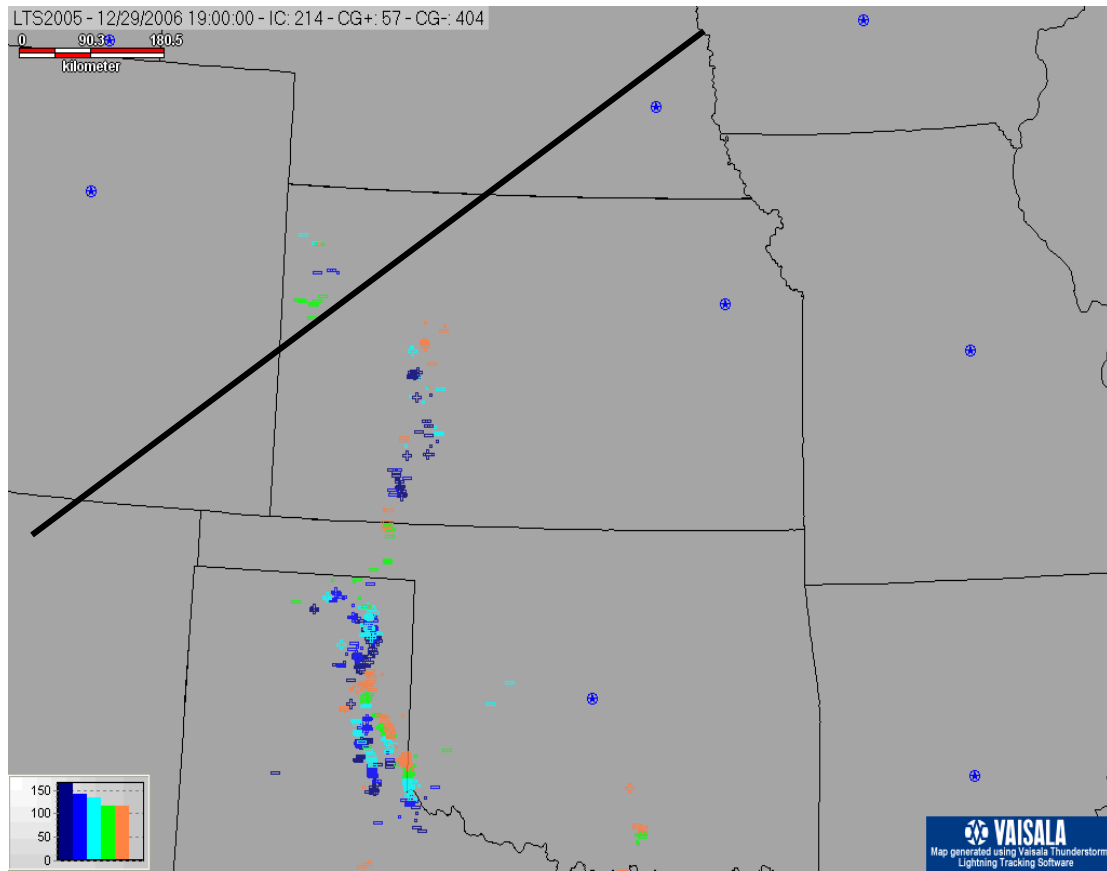


Figure 4.11 Lightning map indicating negative and positive CG strokes and cloud flashes for one hour ending at 1900 UTC 29 December 2006. Line indicates rain/freeze transition. All lightning above line are in subfreezing air.

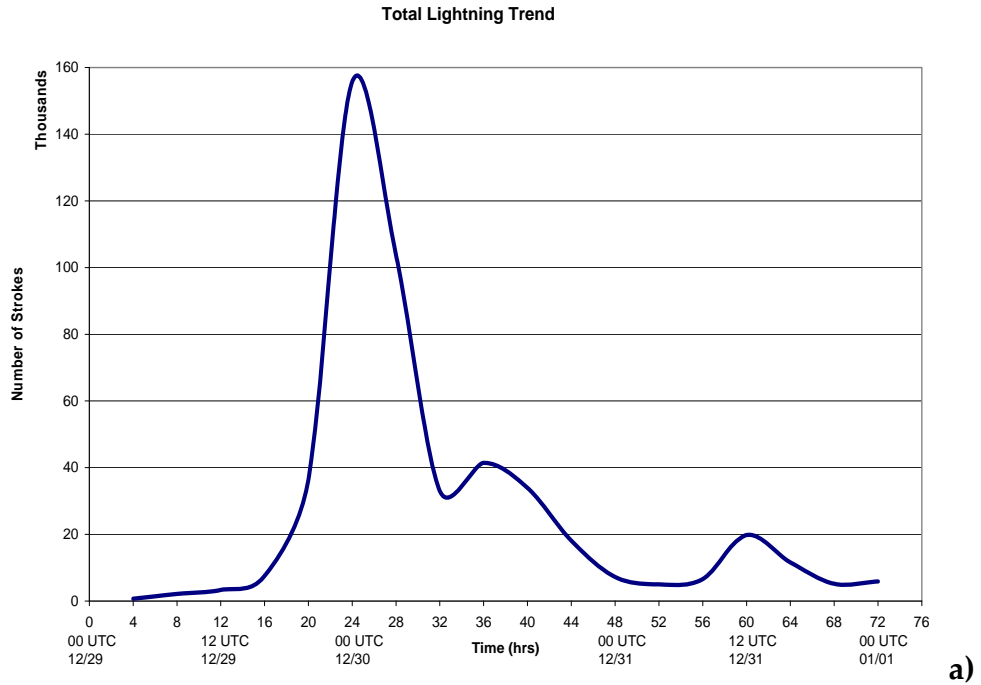
4.1.5 December 28-31, 2006

This storm occurred between 0000 UTC on 29 December 2006 and 2200 UTC on 31 December 2006. This cyclone event lasted for 72 hours with much of the lightning occurring towards the south over the Texas and Oklahoma panhandle regions. The result of this storm was a storm total accumulation of 497,546 lightning events. Of this total, 40% were cloud flashes and 60% were CG strokes. Only 6% of the CG strokes had positive polarity and a positive to storm

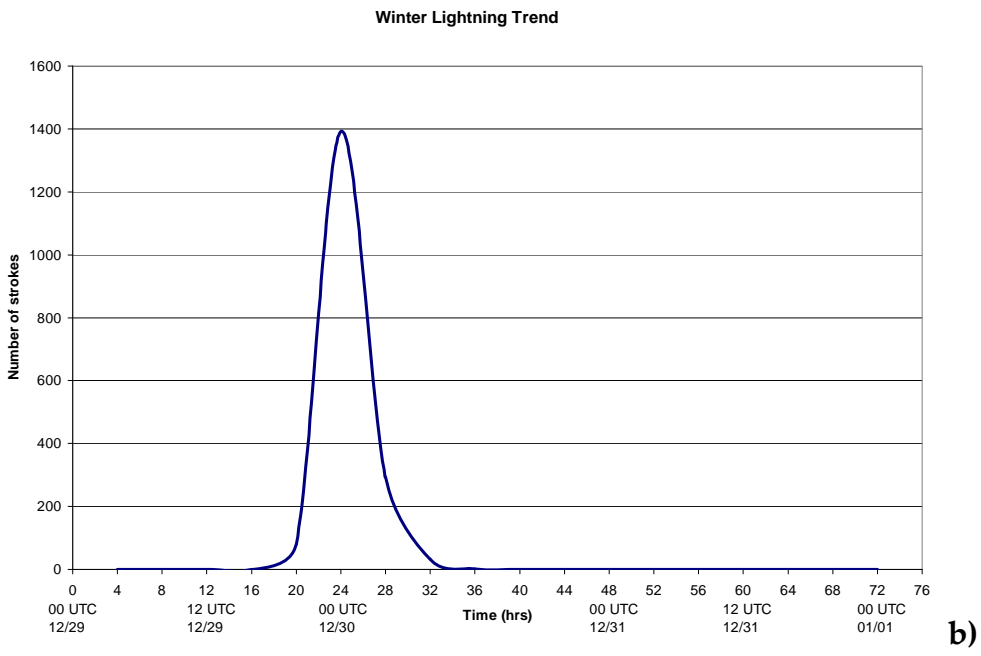
total lightning ratio of 3.5%. A total of 1801 lightning events (0.4% of total) were associated with winter precipitation in this storm, of which 28% were cloud flashes and 72% were CG strokes. Positive strokes made up 9.4% of all lightning events in subfreezing temperatures in the central U.S. The total average event rate for the storm total lightning was 115 min^{-1} with the event rate in winter precipitation only at 0.5 min^{-1} . Figure 4.11 shows lightning from Kansas to Texas at 1900 UTC on 29 December 2006.

The maximum time of lightning occurrence for the entire storm and winter lightning was between 2000 UTC 29 December and 0000 UTC 30 December when 155,769 total events were detected at a rate of 649 min^{-1} and 1392, or 0.9% of the total, were associated with winter precipitation at a rate of 6 min^{-1} . Of this total, only 27% were cloud flashes and 73% were CG strokes. Figure 4.12a,b shows the trend for this storm. A slight diurnal maximum appears in the storm total trend, while only one maximum occurs in the winter lightning trend, but matches a time of day associated with diurnal trends in the previous storm's analysis. Much like the previous events, this storm was dominated by the instance of low amplitude negative CG strokes (not shown).

In summary, this storm had a very high storm total amount of lightning, but unlike the previous storms, a very small percentage of them occurred in



a)



b)

Figure 4.12 Storm total lightning trend for both a) the total storm and b) the lightning associated with winter precipitation for 29 December 2006 through 31 December 2006. Time given in hours from the onset of lightning detected in winter precipitation. Date labeled every 12 hours in UTC.

winter precipitation. The previous storms exhibited percentages from 5% to 11%. The first storm of the season was an exception with a percentage of only 0.015%. This storm maintained a percentage of lightning in winter percentage of only 0.4%. Also, the storm total lightning trend showed a second maximum in lightning occurrence, but only one maximum of winter lightning occurred. The large numbers of storm total lightning with such a small percentage of lightning occurring in winter precipitation further supports the idea that the amount of lightning in an entire system and intensity of the storm does not necessarily correlate with the amount of lightning in winter precipitation and the amount of winter precipitation that falls.

4.1.6 January 12-15, 2007

This storm was a weak event that more than likely resulted from upslope flow in the Panhandles Region of Oklahoma and Texas. (Fig. 4.13) The first thundersnow report associated with this event was observed at 2200 UTC 12 January 2007 and lasted until the last thundersnow report in the central U.S. at 0000 UTC 15 January 2007. The lightning analyzed for this event covered 56 hours of lightning in the central U.S.

The NLDN observed 53,375 lightning events associated with this storm. This resulted in an average event rate of 17.1 min^{-1} . Of this total, 32.7% were

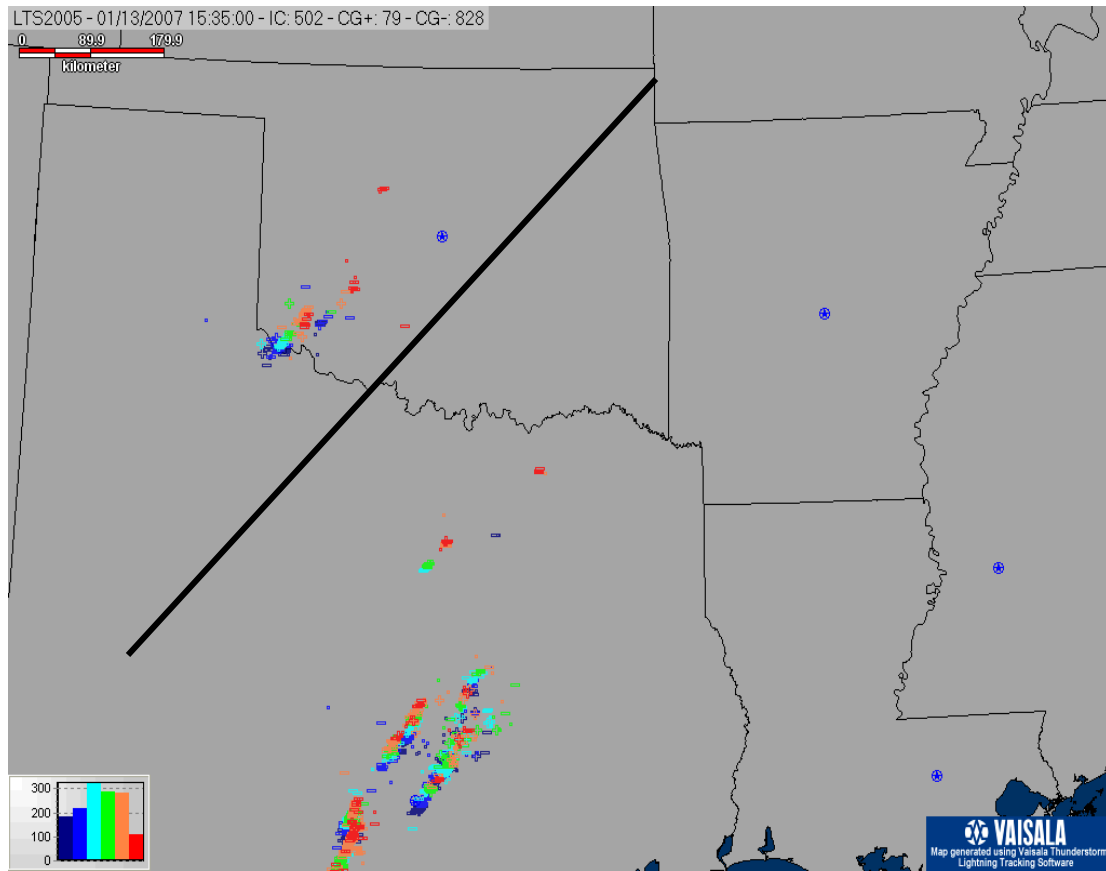


Figure 4.13 Lightning map indicating negative and positive CG strokes and cloud flashes for one hour ending at 1535 UTC 13 January 2007. Line indicates rain/freeze transition. All lightning above and left of line are in subfreezing air.

cloud flashes and 67.3% were CG strokes. Among this CG total, 92.6% were negative CG strokes and 7.4% were positive.

The lightning events associated with winter precipitation for this event totaled only 2177. This was only 4.1% of the storm total lightning. Among these, 32.4% were cloud flashes and 67.6% were CG strokes. Of the CG strokes, 92.6% were found to be negative with only 7.4% positive. The total lightning events associated with winter precipitation came at an average event rate of 0.7 min⁻¹.

Two maximums in the total lightning trend occurred during the course of the event in the central U.S. (Fig. 4.14a). The first was a small, less significant maximum occurring between 1200 UTC and 1600 UTC on 13 January 2007. This smaller maximum had a total of 4851 lightning events in a four-hour time span at an average event rate of 20.2 min^{-1} , of which 35.0% were cloud flashes and 65.0% were CG strokes. 91.2% of the observed CG strokes were negative and 8.8% were positive. Lightning events associated with winter precipitation at this time were part of a broader peak that began between 0400 and 0800 UTC on 13 January and lasted through the subset between 1600 and 2000 UTC on 13 January (Fig. 4.12b). Between 1200 and 1600 UTC there were 392 lightning events found in winter precipitation, of which 34.7% were cloud flashes and 65.3% were CG strokes. Of those CG strokes, 92.6% were negative CG strokes and 7.4% were positive CG strokes. The true maximum in lightning during winter precipitation occurred between 0400 and 0800 UTC 13 January at the beginning of the broad peak period (Fig. 4.14b). During this time there were 518 total lightning events found associated with winter precipitation, which was 41.4% of the total lightning at that time. Of the lightning associated with winter precipitation, 27.6% were cloud flashes and 72.4% were CG strokes. Of the CG strokes, 98.4% were negative CG strokes and 1.6% were positive strokes. The second maximum in total lightning, and largest maximum, occurred between 0000 and 0400 UTC

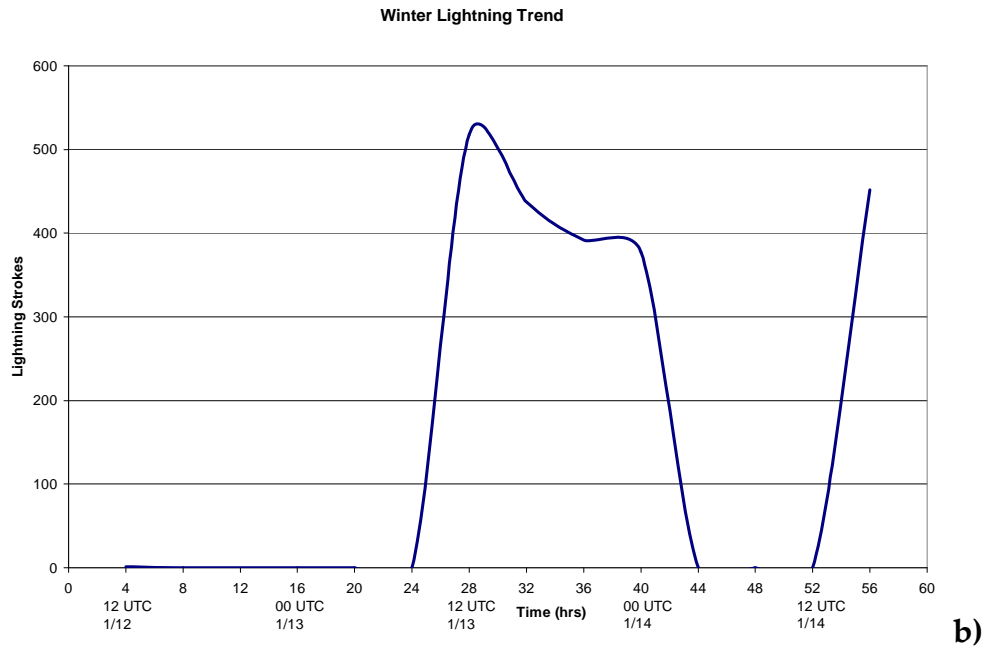
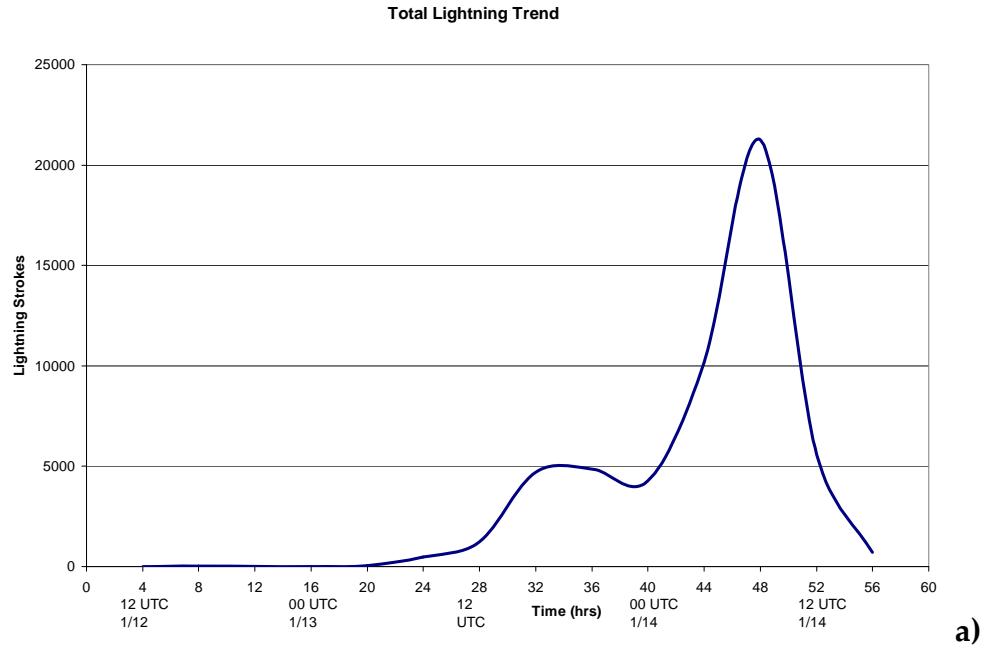


Figure 4.14 Storm total lightning trend for both a) the total storm and b) the lightning associated with winter precipitation for 12 January 2007 through 14 January 2007. Time given in hours from the onset of lightning detected in winter precipitation. Date labeled every 12 hours in UTC.

14 January with a total of 21,263 lightning events during this time. This total contained 31.7% cloud flashes and 68.3% CG strokes, of which 92.6% were negative and 7.4% positive.

This last maximum, so far displaced from the primary activity (Fig. 4.12b) in lightning associated with winter precipitation, could be indicative of cyclone intensification over the Appalachian Mountains as the storm exits the central U.S. At that location, the bulk of the precipitation became prefrontal and most winter precipitation was lifted north beyond the Great Lakes into Canada.

In summary, this storm exhibited many similar percentages with respect to lightning type. What is unique about this storm is the elongated elevated occurrence of lightning associated with winter precipitation lasting continually, most as a result of orographic upslope in the Texas and Oklahoma panhandles, for up to 20 hours during the course of this event. Another unique trait, specifically during initial peak in winter lightning, was the high percentage of occurrence of lightning in winter precipitation (41.4%) with respect to the storm total at that time. Only the 27-28 November 2006 storm had a higher percentage.

4.1.7 January 20-22, 2007

This case was an example of a weak low producing few lightning events as the system moved across the central U.S. Throughout the elongated event,

spanning 60 hours, only 226 total lightning events were observed at an average rate of 0.06 min^{-1} . Of this total, 35.4% were cloud flashes and 64.6% were CG strokes. Of those CG strokes, 71.2% were negative strokes and 28.8% were positive strokes. However, the first thundersnow observation occurred at 0000 UTC 21 January while the last observation was near 1800 UTC 21 January. During the 18 hours of thundersnow, only 23 lightning events were observed at an average rate of 0.19 min^{-1} . Of this total, 47.8% were cloud flashes and 52.2% were CG strokes, of which 50% were negative strokes and 50% were positive strokes. Figure 4.15 shows one of the more active times of this storm with a single cluster of cloud flashes located in eastern Iowa.

During the course of the event, only 6 lightning events were observed in winter precipitation. Specifically, these occurred between 1200 and 1600 UTC 21 January towards the end of the event over the central U.S. All of these observed lightning events were cloud flashes while no CG strokes were observed. This is the first of two events in this dataset where this occurred.

At the beginning of the event, before thundersnow was observed, there were two primary maximums in the total lightning between 1200 and 1600 UTC 19 January and again between 0000 and 0400 UTC 20 January (Fig. 4.16a). The first maximum, observed during the morning hours, had only 25 observed lightning events where 44.0% were cloud flashes and 56.0% were CG strokes, of

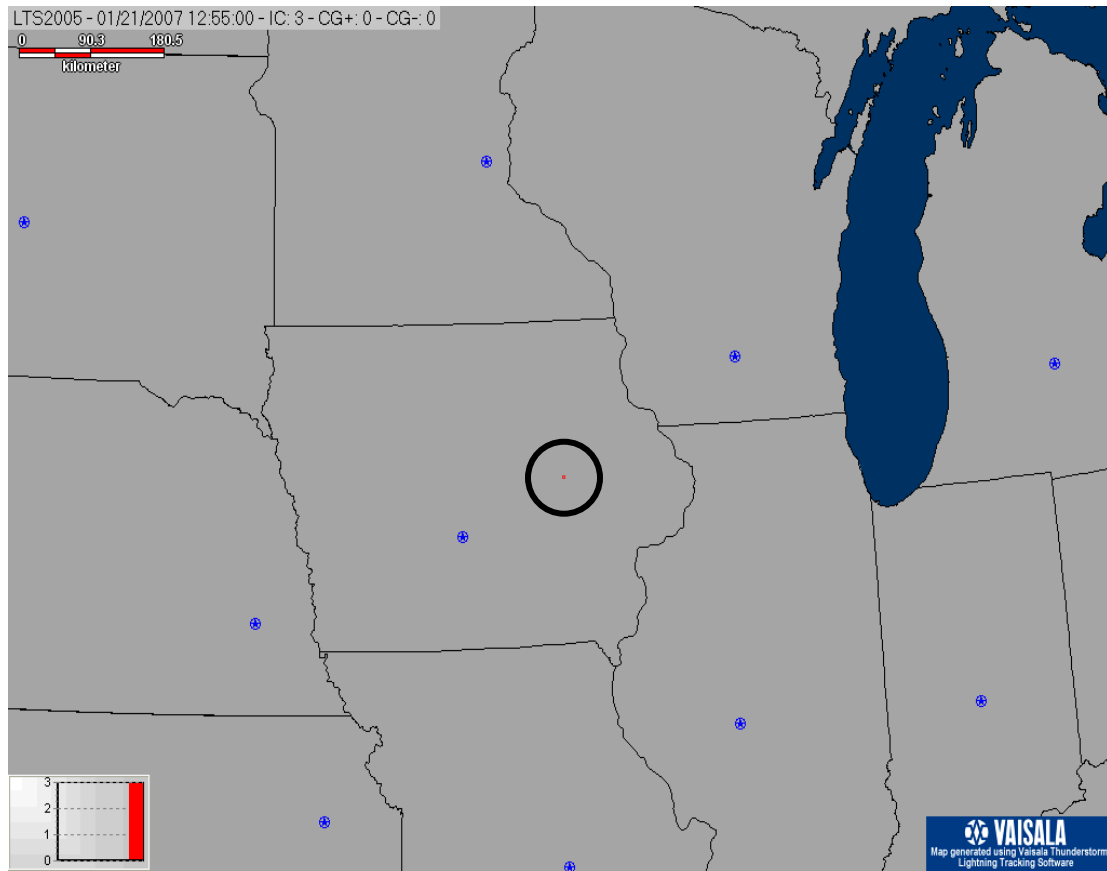


Figure 4.15 Lightning map indicating negative and positive CG strokes and cloud flashes for one hour ending at 1300 UTC 21 January 2007. Lightning enclosed in the circle represent lightning in subfreezing air.

which 57.1% were negative CG strokes. The second maximum, occurring in the late afternoon, had a maximum of 79 observed lightning events where 29.1% were cloud flashes and 70.9% were CG strokes. Of these CG strokes, 73.2% were negative and 26.8% were positive. Figure 4.16a shows a tail at the end of the event similar that that of 01 December 2006 indicative of the system deepening as it exits the central U.S. However, Figure 4.14b shows that the tail end of this was where all the lightning in winter precipitation occurred. Figures 4.16c,d zoom in

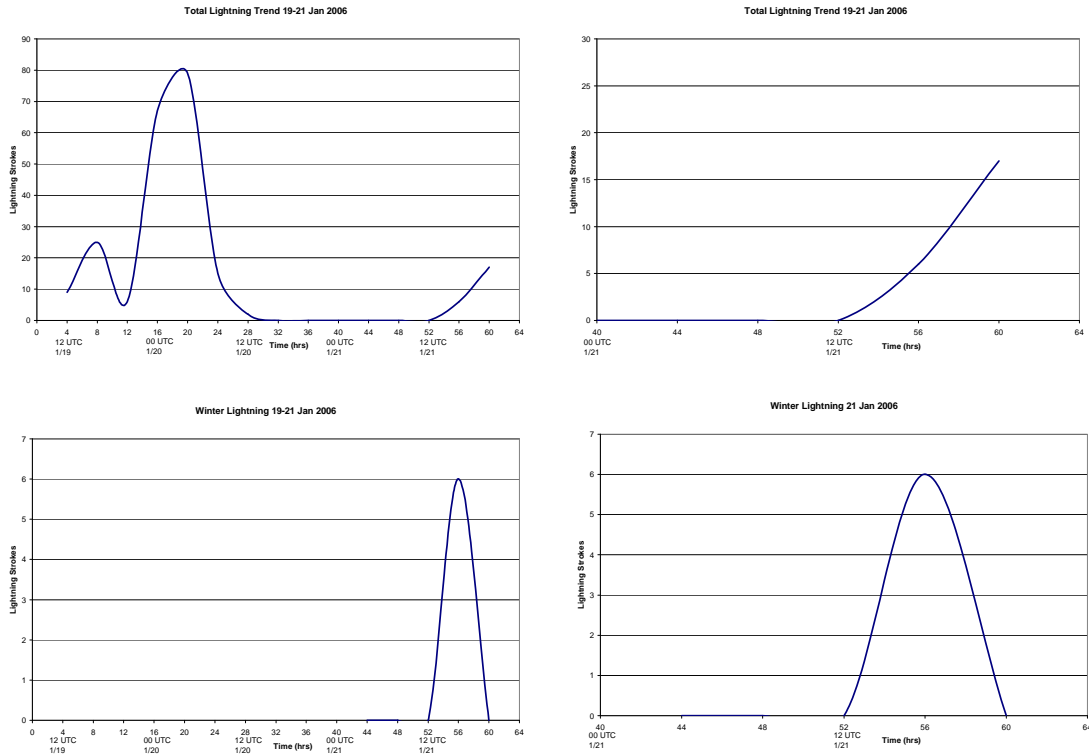


Figure 4.16 Storm total lightning trend for a) the total storm, b) the last 6-hrs of the total lightning, c) lightning associated with winter precipitation and d) the last 6-hrs of the lightning with winter precipitation for 19 January 2007 through 21 January 2007. Time given in hours from the onset of lightning detected in winter precipitation. Date labeled every 12 hours in UTC.

on the 4-hour period towards the end where this occurred. Storm total lightning events maximized towards the end of the period with 17 lightning events occurring between 1600 and 2000 UTC 21 January. This was four hours previous to the maximum of winter lightning events (Fig. 4.16c,d).

In summary, this case was unique in that very few lightning events were observed associated with winter precipitation. Specifically, the lightning found was only cloud flashes. Similar to the storm intensification on 01 December where lightning increased as the storm exited the domain, this storm exhibited

its only winter lightning northwest of the cyclone as it intensified and exited the central U.S.

4.1.8 January 30-31, 2007

This case was miniscule compared to other cases examined here and was also relatively short, given that the first thundersnow observation occurred approximately at 1200 UTC 31 January with the last one 12 hours later. During this brief event, only 650 lightning events were observed. Of these events, 38.8% were cloud flashes and 61.2% were CG strokes. Of those CG strokes, 91.5% were negative CG strokes and 8.5% were positive CG strokes. The single observed lightning event associated with winter precipitation (Fig. 4.17) occurred near the beginning of the event between 1200 and 1600 UTC 31 January, which was also the peak in total lightning at the time, which saw 327 total lightning events (Fig. 4.18). The single lightning event in winter precipitation made up only 0.31% of the total and was identified as a cloud flash. The total lightning declined between 1600 and 2000 UTC 31 January and peaked again, but no more lightning was observed associated with winter precipitation.

In summary, this was a small event with a single cloud flash observed in southern Oklahoma. This was the only lightning found associated with winter precipitation. This storm falls in line with the previous event where there were

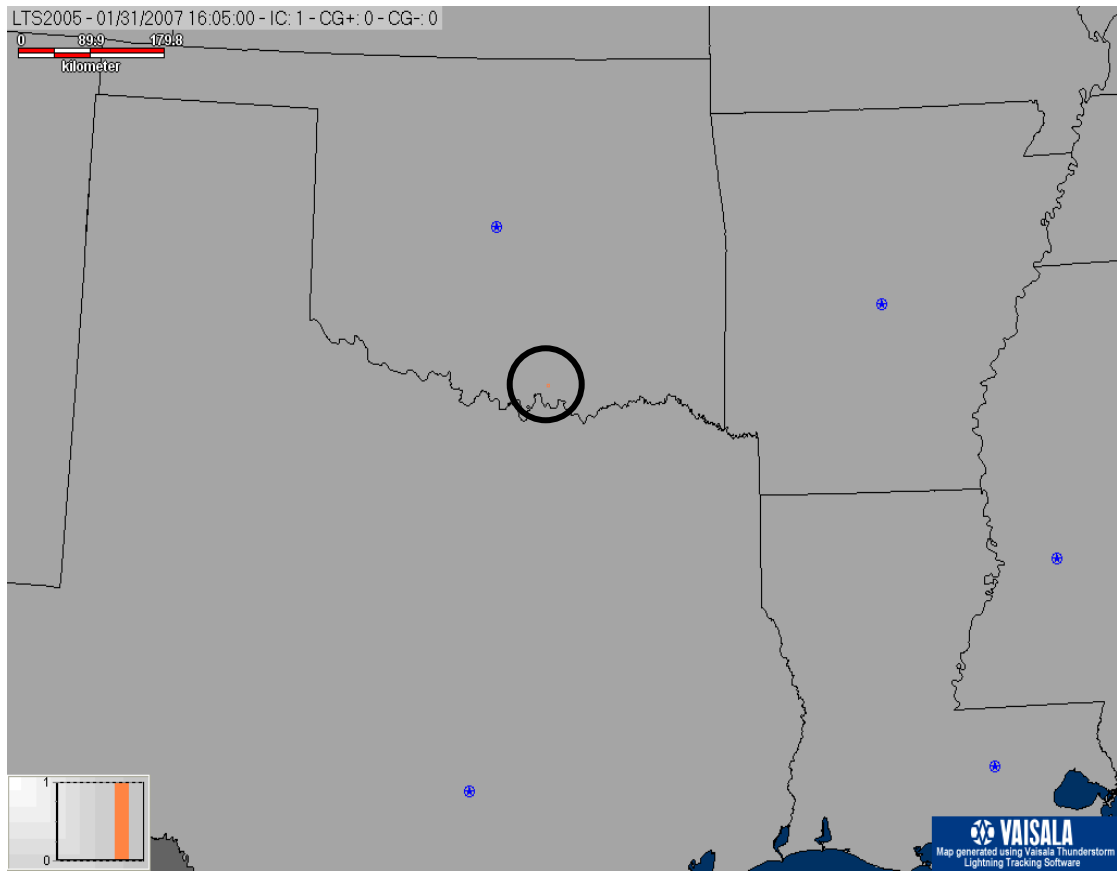


Figure 4.17 Lightning map indicating single cloud flash for one hour of data ending at 1600 UTC 31 January 2007. Lightning enclosed in the circle represent lightning in subfreezing air.

very few lightning events observed in the central U.S. Figure 4.18 shows that the lightning maximized as the system entered into the central U.S., minimized as it moved across the central plains and then intensified again as lightning increased exiting the central U.S.

4.1.9 February 12-14, 2007

This was a rather robust case compared to those events beginning the 2007 year with snow and lightning occurring along the Midwest. Figure 4.19 shows

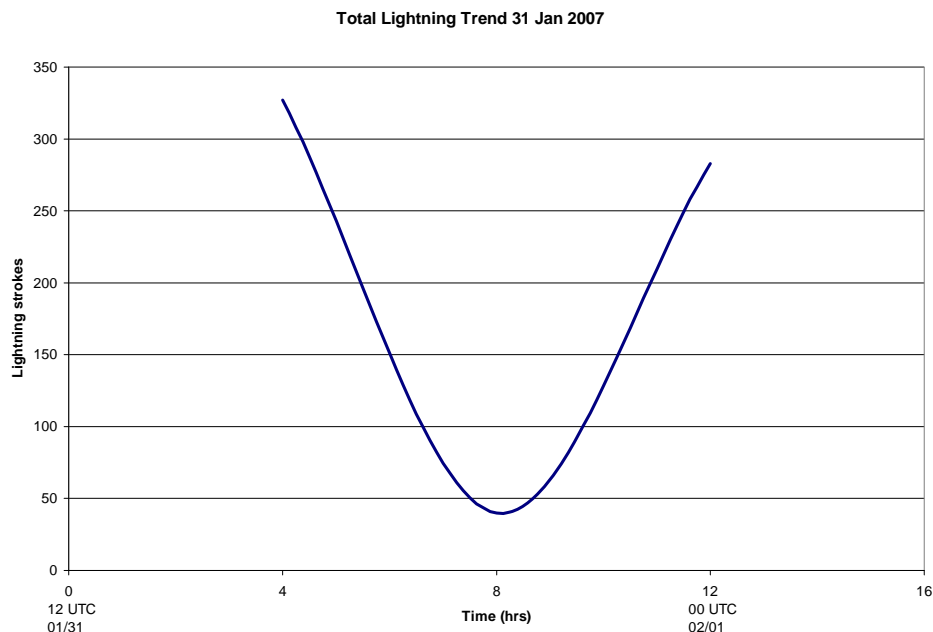


Figure 4.18 Storm total lightning trend for the total storm for 31 January 2007. Time given in hours from the onset of lightning detected in winter precipitation. Date labeled every 12 hours in UTC.

CG lightning associated with winter precipitation in central Kansas during the beginning of the event. There was a gradual increase in the number of lightning events, maximize, then a slow dissipation, following the pattern of a storm’s lifecycle (Fig. 4.20a). Thundersnow in this case was observed close to the beginning of the event near 1200 UTC 12 February and ended by 0400 UTC 14 February. The total lightning count for the entire storm system through the central U.S. was 248,097 events. Of this total, 33.8% were cloud flashes and 66.2% were CG strokes, of which 93.6% were negative CG strokes and 6.4% were positive CG strokes. These lightning events came at an average rate of 94.0 min⁻¹.

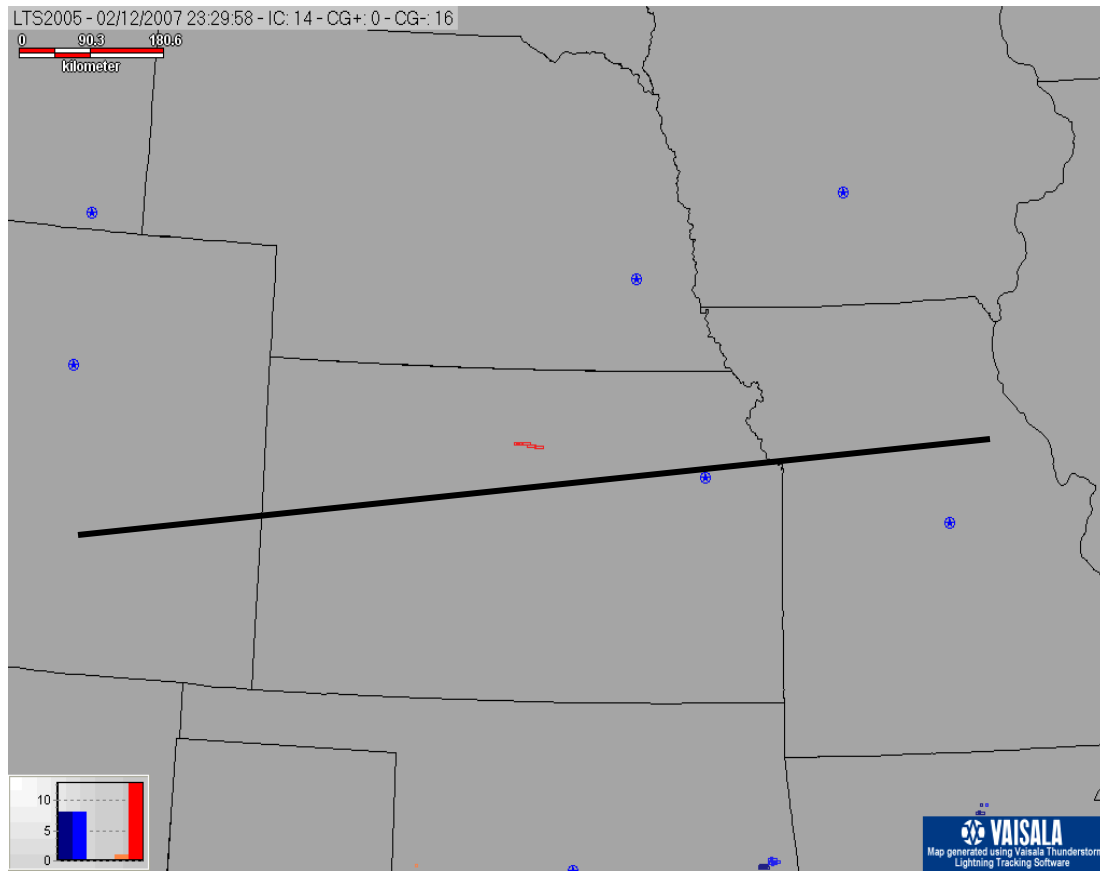


Figure 4.19 Lightning map indicating negative and positive CG strokes and cloud flashes for one hour ending at 2300 UTC 12 February 2007. Line indicates rain/freeze transition. All lightning above line are in subfreezing air.

However, there were only 18 lightning events found associated with winter precipitation, which was only 0.007% of the total lightning. Of these events found in winter precipitation, 38.9% were cloud flashes and 61.1% were CG strokes. In this instance, all observed CG strokes were negative. The average rate of lightning in winter precipitation was 0.007 min^{-1} .

While several smaller maximums occurred in the total lightning trend (Fig. 4.20a), the absolute maximum of the event in total lightning occurred

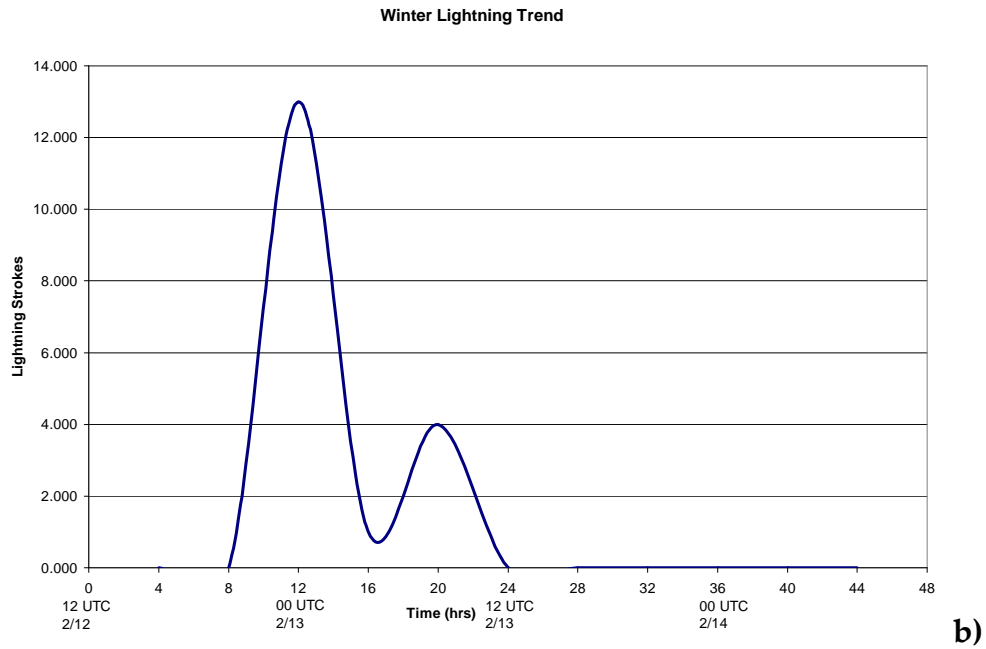
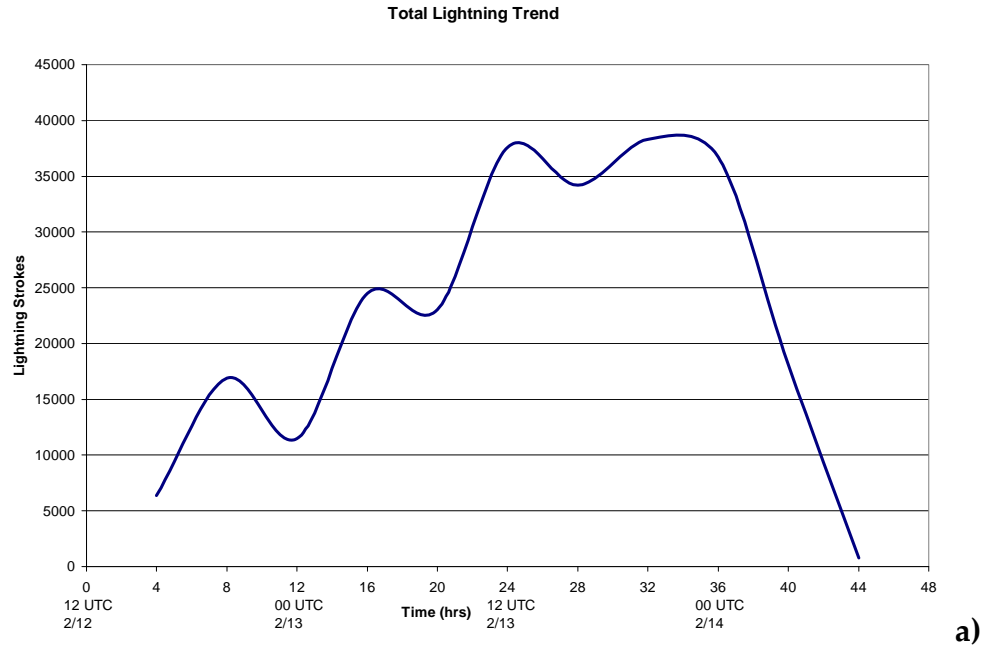


Figure 4.20 Storm total lightning trend for both a) the total storm and b) the lightning associated with winter precipitation for 12 February 2007 through 14 February 2007. Time given in hours from the onset of lightning detected in winter precipitation. Date labeled every 12 hours in UTC.

between 1600 and 2000 UTC 13 February. During this time, there were a total of 38,297 observed lightning events, of which 28.2% were cloud flashes and 71.8% were CG strokes. Of the CG strokes, 95.4% were negative CG strokes and 4.6% were positive CG strokes. However, the maximum in lightning associated with winter precipitation occurred between 2000 UTC 12 February and 0000 UTC 13 February, in which a total of 13 lightning events were found (Fig. 4.20b). This made up 0.11% of the storm total lightning at this same time. Of these 13 events, 6, or 46.2% were cloud flashes and 7, or 53.8%, were CG strokes. All 7 observed CG strokes at this time were negative.

The time of maximum lightning associated with winter precipitation came during the first small decrease in the total occurrence of lightning associated with this event before maximizing again in the next four hours at 24,484 lightning events, of which only 1 event was found to associated with winter precipitation. Following another slight decrease in total lightning events between 0400 and 0800 UTC 13 February, lightning associated with winter precipitation increased again slightly to a total of 4 lightning events, all of which were observed negative CG strokes.

This storm displayed similarities to storms early in the winter season by producing several lightning events during the entirety of its lifecycle. Very few of these lightning events actually occurred in winter precipitation. Unlike some

of the storms in which winter lightning was found to be scarce, with the occurrence of one lightning type, this storm had an even mix of cloud flashes and CG strokes. Given the small amounts of lightning found in winter precipitation, the percent occurrence of both types might be slightly skewed higher than what has been typically found to this point, but given greater numbers of lightning in this event, percentages might tend to change.

4.1.10 February 23-25, 2006

This fairly intense cyclogenetic event across the central plains and through the Mississippi River Valley region brought fairly heavy snow totals to the central plains and blizzard like conditions in the wake of the passing surface low through areas such as Nebraska, Iowa, and Missouri. Figure 4.21 reveals a swath of lightning extending across Iowa associated with a band of snow at the time. Similar to its predecessor between 12 and 14 February, this event showed few small maximums as the lightning totals trended upward to one peak before the storm dissipated and exited the central U.S. The first thundersnow report with this system was at 1800 UTC 23 February and the last thundersnow observation was near 1200 UTC 25 February. During the course of this analysis, there was no lightning in the domain, according to the NLDN, beyond 0800 UTC 25 February, so analysis was not performed beyond this time. For the 44-hour long event, a

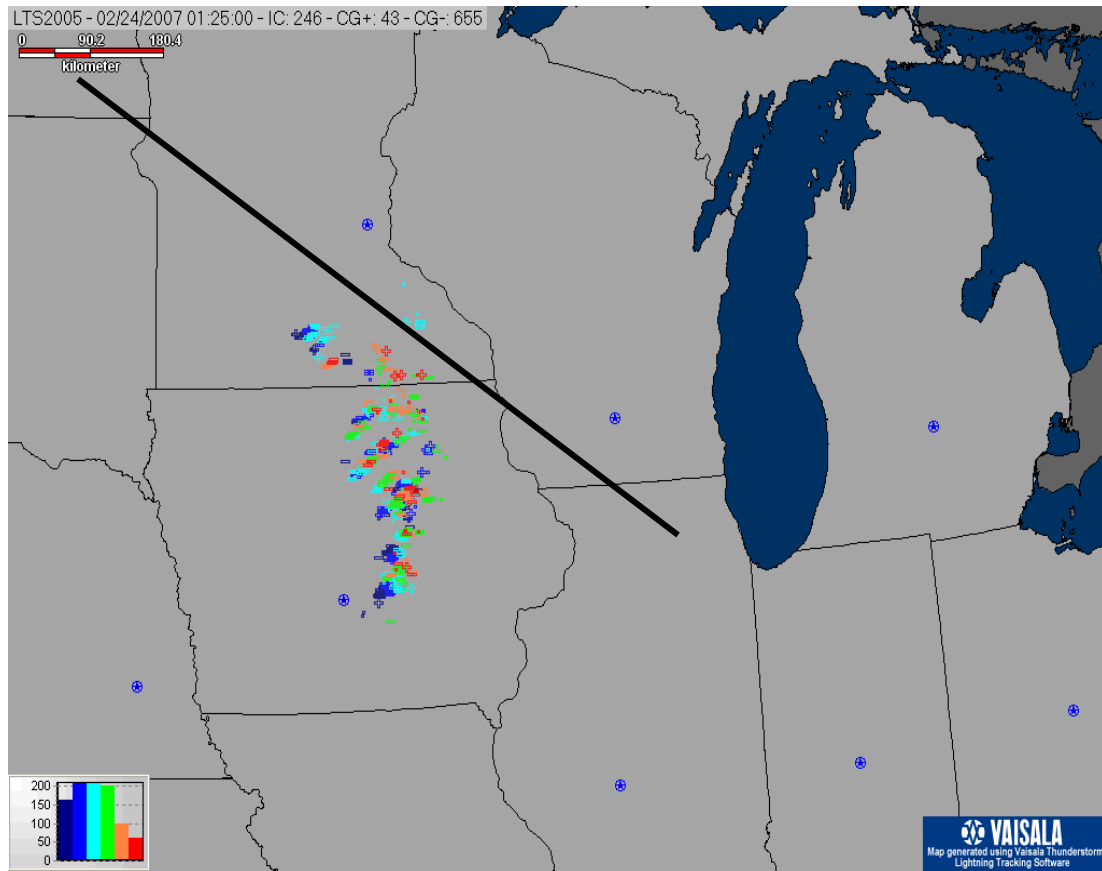


Figure 4.21 Lightning map indicating negative and positive CG strokes and cloud flashes taken at 0100 UTC 24 February 2007. Line indicates rain/freeze transition. All lightning above and right of line are in subfreezing air.

total of 253,272 lightning events were observed at an average rate of 95.9 min⁻¹.

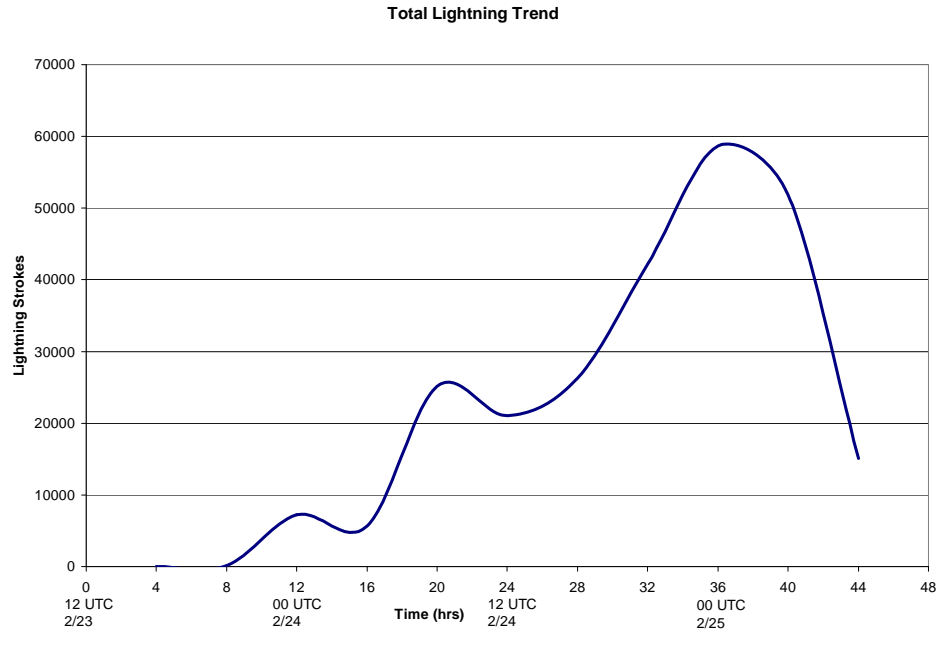
Of this total, 38.7% were cloud flashes and 61.3% were CG strokes. Of the CG strokes, 93.8% were negative and 6.2% were positive.

A total of 708 lightning events were found to be associated with winter precipitation for this event at an average rate of 0.27 min⁻¹. This only accounted for 0.28% of the total lightning observed with this system in the central U.S. Of

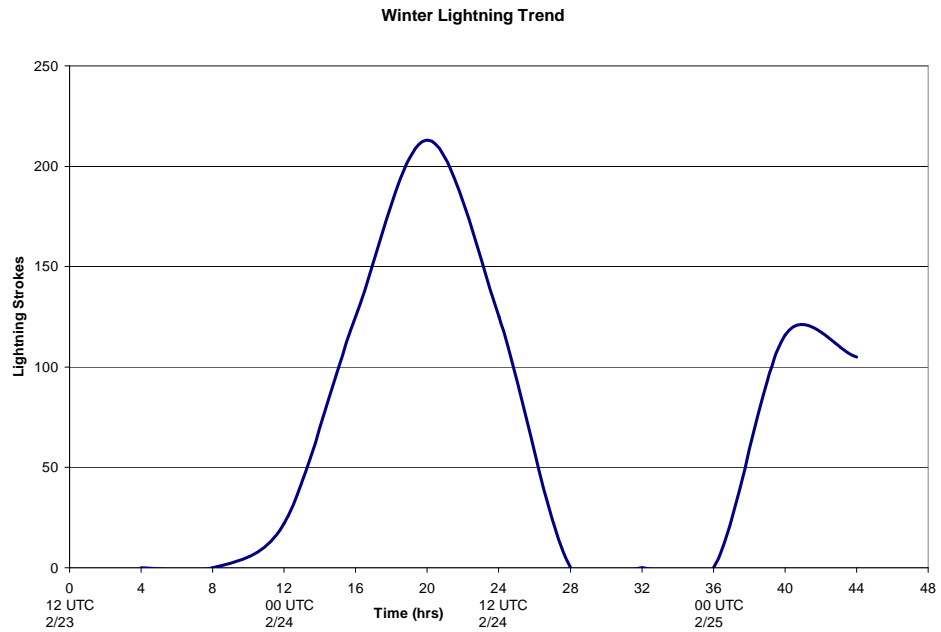
these winter events, 45.5% were cloud flashes and 54.5% were CG strokes, of which 80.7% were negative CG strokes and 19.3% were positive.

As stated previously, there are a few smaller maximums, but an overall increase in lightning event occurrence during the life cycle of the storm (Fig. 4.22a). The peak occurred between 2000 UTC 24 February and 0000 UTC 25 February with a total of 58,677 lightning events during those four hours. Cloud flashes made up 40.6% of the total and 59.4% were CG strokes. Of those CG strokes, 93.7% were negative CG strokes with 6.3% positive CG strokes. The maximum for lightning associated with winter precipitation occurred between 0400 and 0800 UTC 24 February (Fig. 4.22b), associated with a smaller maximum in the storm total lightning. There was a storm total of 25,148 observed lightning events during that time with 213 of those, or 0.86%, being associated with winter precipitation. Among this winter lighting peak, 48.4% were cloud flashes and 51.6% were CG strokes. Of these CG strokes, 89.8% were negative CG strokes and 10.2% were positive.

In summary, this was a well-defined convective snow event with obvious lightning associated with winter precipitation. Further, this storm fit the assumption that the more snow that falls is correlated with the higher number of lightning events observed. Also, the percent positive lightning was uncharacteristically high with this event, compared to previous events. This fits



a)



b)

Figure 4.22 Storm total lightning trend for both a) the total storm and b) the lightning associated with winter precipitation for 23 February 2007 through 25 February 2007. Time given in hours from the onset of lightning detected in winter precipitation. Date labeled every 12 hours in UTC.

the assumption, that while winter events may not be dominated by positive CG lightning, the relative percentage of positive CG lightning may still increase due to its association with winter precipitation.

4.1.11 February 28 - March 02, 2007

This event followed, very similarly, in the footsteps of the event from 23-25 February 2007. Similar to its predecessor, this event was a case of west-to-east cyclogenesis producing heavy snow totals in the Midwest along with several lightning events associated with snowfall. Further, this system produced severe blizzard conditions in much of Iowa, Minnesota and Wisconsin. Figure 4.23 shows lightning associated with this storm oriented in several bands that were associated with snowfall. This event began near 1800 UTC 28 February 2007 and ended by 0400 UTC 02 March 2007. The duration of this storm lasted about 44 hrs across the central U.S. and produced a storm total of 334,847 lightning events, with an average event rate of 127 min⁻¹. The total consisted of 30.0% cloud flashes and 70.0% CG strokes. Positive CG strokes made up 4.5% of all CG strokes and 3.2% of the storm total lightning.

Lightning events in winter precipitation made up only 2.0%, or 6552 events, of the storm total lightning. The event rate in winter precipitation was 2.5 min⁻¹. Cloud flashes in winter precipitation made up 39.0% of the winter total

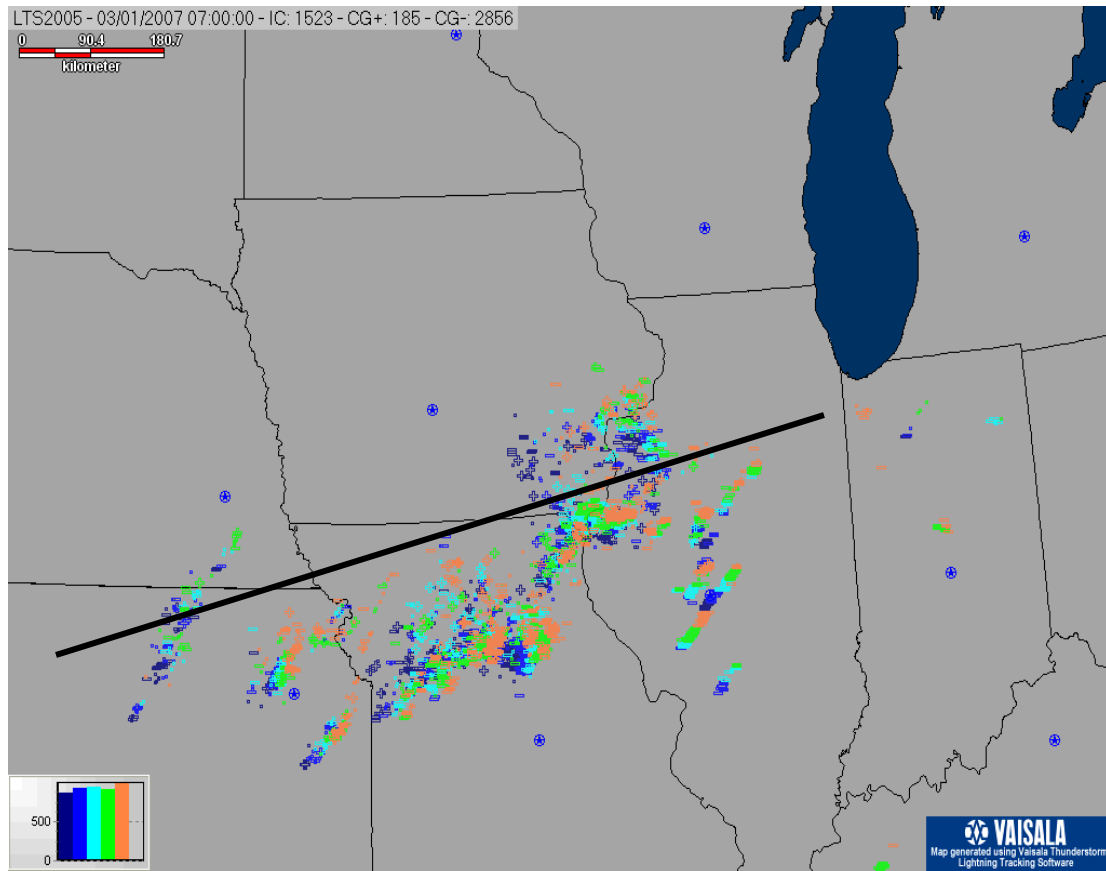


Figure 4.23 Lightning map indicating negative and positive CG strokes and cloud flashes for one hour ending at 0700 UTC 01 March 2007. Line indicates rain/freeze transition. All lightning above line are in subfreezing air.

and the 61.0% were CG strokes. Positive strokes made up 14% of the CG total associated with winter precipitation, but only 5.0% of all winter lightning total (cloud and CG). The maximum in lightning activity for the entire storm occurred between 0800 and 1200 UTC on 01 March with 75,706 events at a rate of 315 min⁻¹ (Fig. 4.24a) while the maximum for lightning in winter precipitation occurred between 0400 and 0800 UTC on 01 March with a total of 2733 events at a rate of 11 min⁻¹. A secondary maximum in winter lightning occurred between 2000 UTC

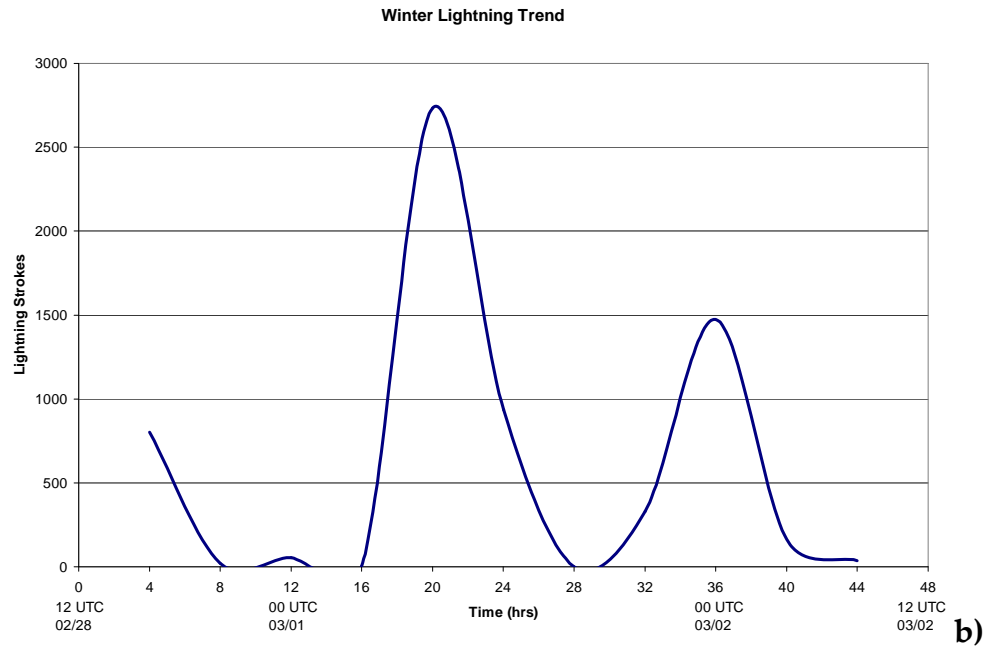
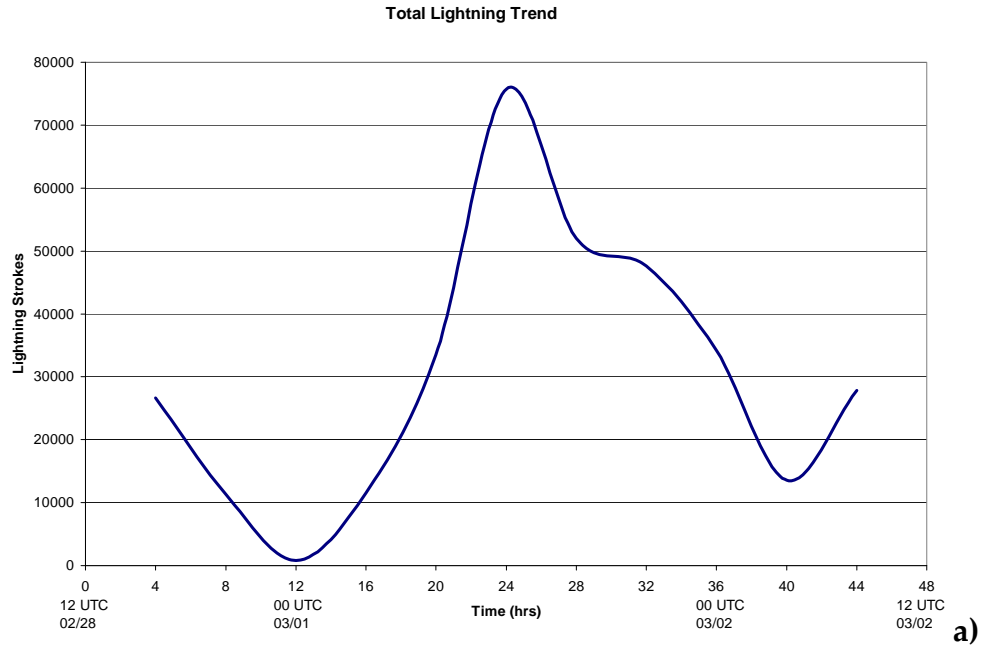


Figure 4.24 Storm total lightning trend for both a) the total storm and b) the lightning associated with winter precipitation for 28 February 2007 through 02 March 2007. Time given in hours from the onset of lightning detected in winter precipitation. Date labeled every 12 hours in UTC.

01 March and 0000 UTC 02 March (Fig. 4.24b). This maximum in lightning in winter precipitation coincided with the gradual decline in total lightning activity. A total of 1474 lightning events were observed during this time in association with winter precipitation, which made up 4.3% of the storm total lightning. Again, this storm showed a tendency to be dominated by negatively polarized lightning strokes in winter precipitation, similar to that of the previous storms.

In summary, this storm continued almost entirely along the same path as the storm immediately previous with much of the same effects. Similarities continue to arise with the increased amount of lightning totals in winter precipitation correlated to the increased amounts of snow that fell. Further, this storm followed a distinct diurnal pattern seen most notably in the event on 01 December 2006. The percent positive occurrence in this storm was decreased, more similar to amounts previously seen in the winter season. The average percent occurrence of cloud and CG lightning also seemed to correlate well with seasonal averages thus far.

4.1.12 April 02-03, 2007

This event continued a sequence of spring time cyclones across the central U.S., however there were fewer incidences of snow and other winter precipitation. Large numbers of lightning events were observed through the life

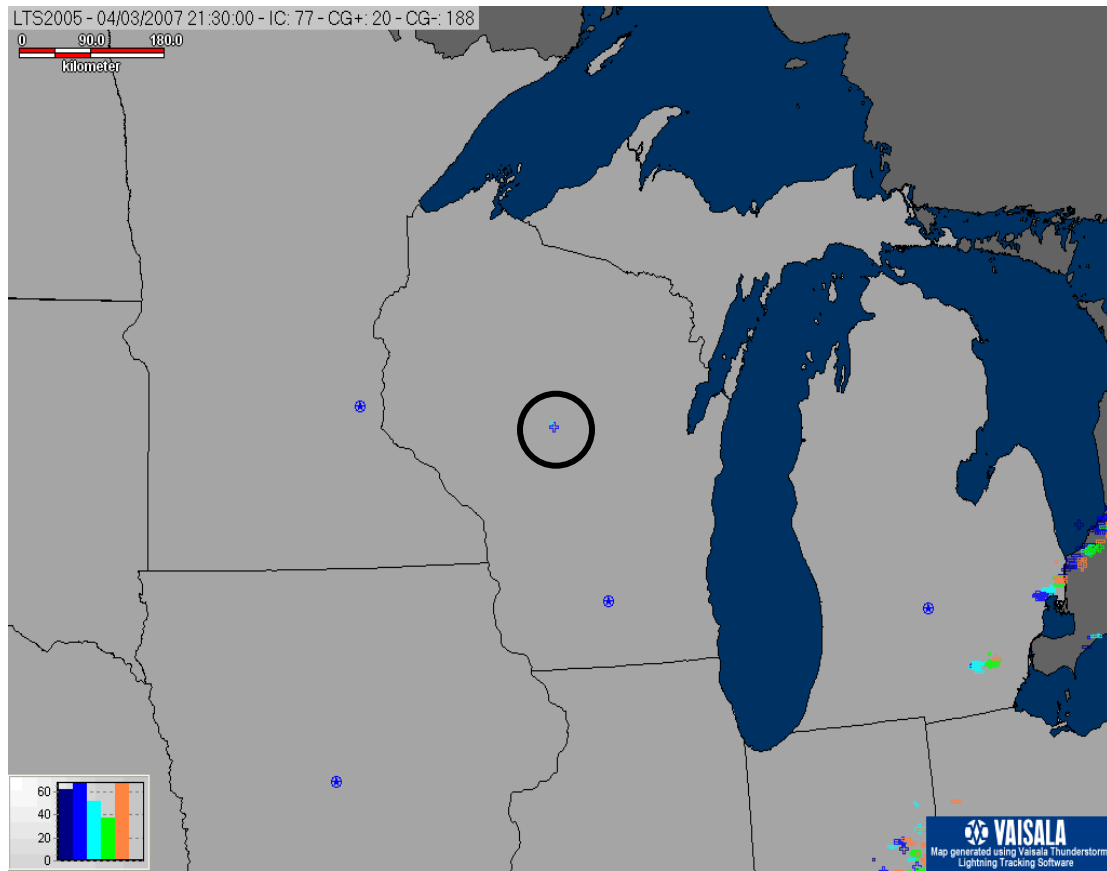


Figure 4.25 Lightning map indicating negative and positive CG strokes and cloud flashes for one hour ending at 2130 UTC 03 April 2007. Lightning enclosed in the circle represent lightning in subfreezing air.

cycle of the total system, while few events occurred behind freezing air, and most that did occurred in high elevations in the Rocky Mountains and are thus eliminated from the dataset. Lightning that did occur in the central U.S. associated with winter precipitation tended to occur in a line from Indiana up into Michigan (Fig. 4.25)

Figure 4.26a shows the general trend of lightning for this event occurred at 2000 UTC on 02 April and moved off the east coast near 0000 UTC 05 April.

Thundersnow first occurred on 01 April at higher elevations, but did not occur in the central U.S. until 02 April. The last thundersnow observation was by 1200 UTC 04 April as the storm began to dissipate over the central U.S. and move east. The total lightning count for the event over the central U.S. was 730,843 at an average event rate of 202.9 min⁻¹. The high numbers of lightning events seem more evident of a strongly convective synoptic scale system in the spring time. Of this total, 32.1% were cloud flashes and 67.9% were CG strokes. Of the CG strokes, 96.1% were negative and 3.9% were positive.

Only two lightning events were associated with winter precipitation in the central U.S., occurring between 2000 UTC 03 April and 0000 UTC 04 April (Fig 4.26b). One was identified as a cloud flash and the other was observed as a CG stroke. There were a few other lightning events in regions associated with winter precipitation and subfreezing air, but were scattered and located in the Rocky Mountains. These two lightning events were coincident with the maximum in storm total lightning activity. Between 2000 UTC 03 April and 0000 UTC 04 April, 148,860 total lightning events were observed at an event rate of 620 min⁻¹. This total was composed of 39.1% cloud flashes and 60.9% CG strokes. Of the CG strokes, 96.0% were negative CG strokes and 4.0% were positive CG strokes.

In summary, this event represented the single most active system analyzed in terms of storm total lightning count, but was by far the least active

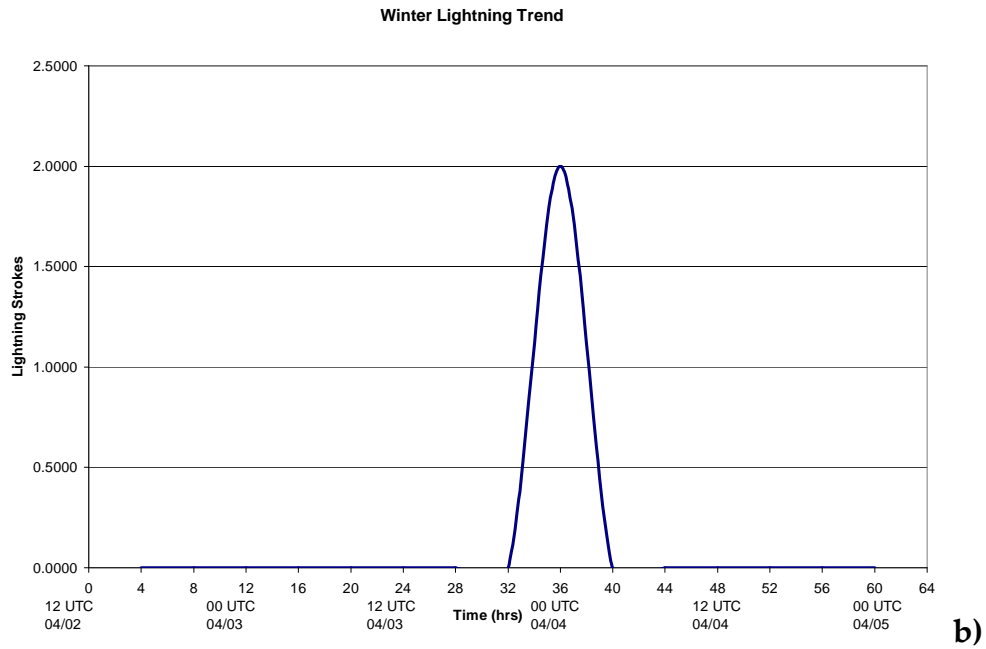
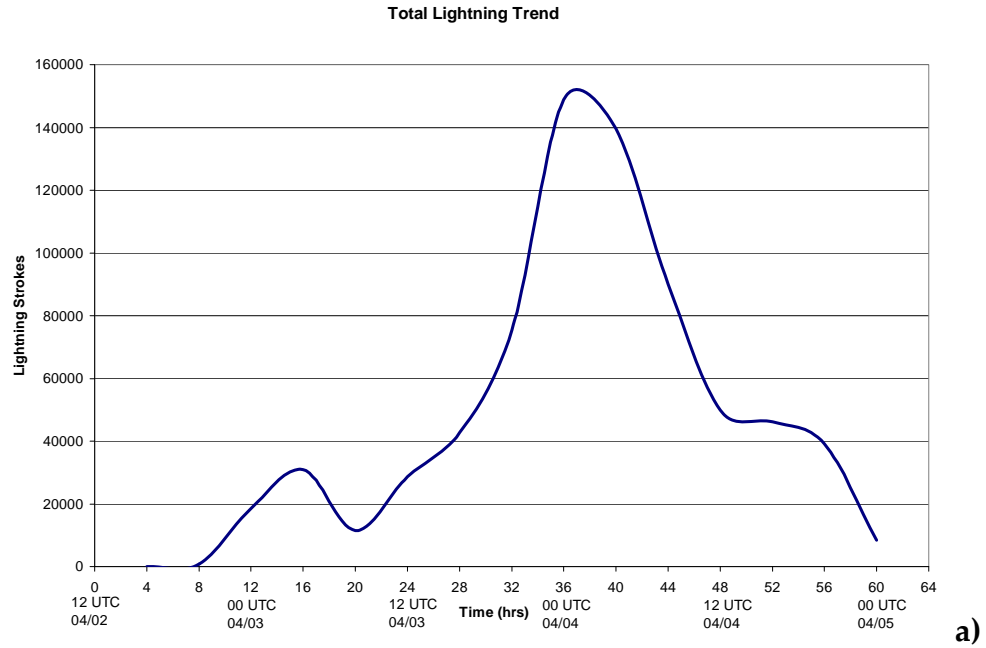


Figure 4.26 Storm total lightning trend for both a) the total storm and b) the lightning associated with winter precipitation for 02 April 2007 through 04 April 2007. Time given in hours from the onset of lightning detected in winter precipitation. Date labeled every 12 hours in UTC.

with only two lightning events found in winter precipitation. While this type of storm has occurred previous in this dataset, it shows that lightning in winter precipitation can be minimal and isolated.

4.1.13 April 07-08, 2007

This case circled out of the southwest U.S. and dropped snow, mostly in higher elevations of the central plains. This could be attributed to some upslope flow occurring over the panhandle of Texas and into eastern New Mexico. There was also convective activity along the east coast and the west coast as well, but those data were not included in order to focus on the storm in the central U.S. The bulk of lightning activity associated with this storm was located from through western Texas and towards the Rocky Mountains (Fig. 4.27). The first thundersnow observation was at 0000 UTC 07 April and the last observation was at 0600 UTC 08 April. This short, 30-hour storm produced a total of 12,052 observed lightning events at an average event rate of 6.3 min^{-1} . Of this, 15.0% were cloud flashes and 85.0% were CG strokes. Of the CG strokes, 96.0% were negative CG strokes and 4.0% were positive.

Throughout the storm, a total of 2241 lightning events were found associated with winter precipitation, which is 18.6% of the storm total, at an average event rate of 1.2 min^{-1} . This was by far the highest overall percentage of

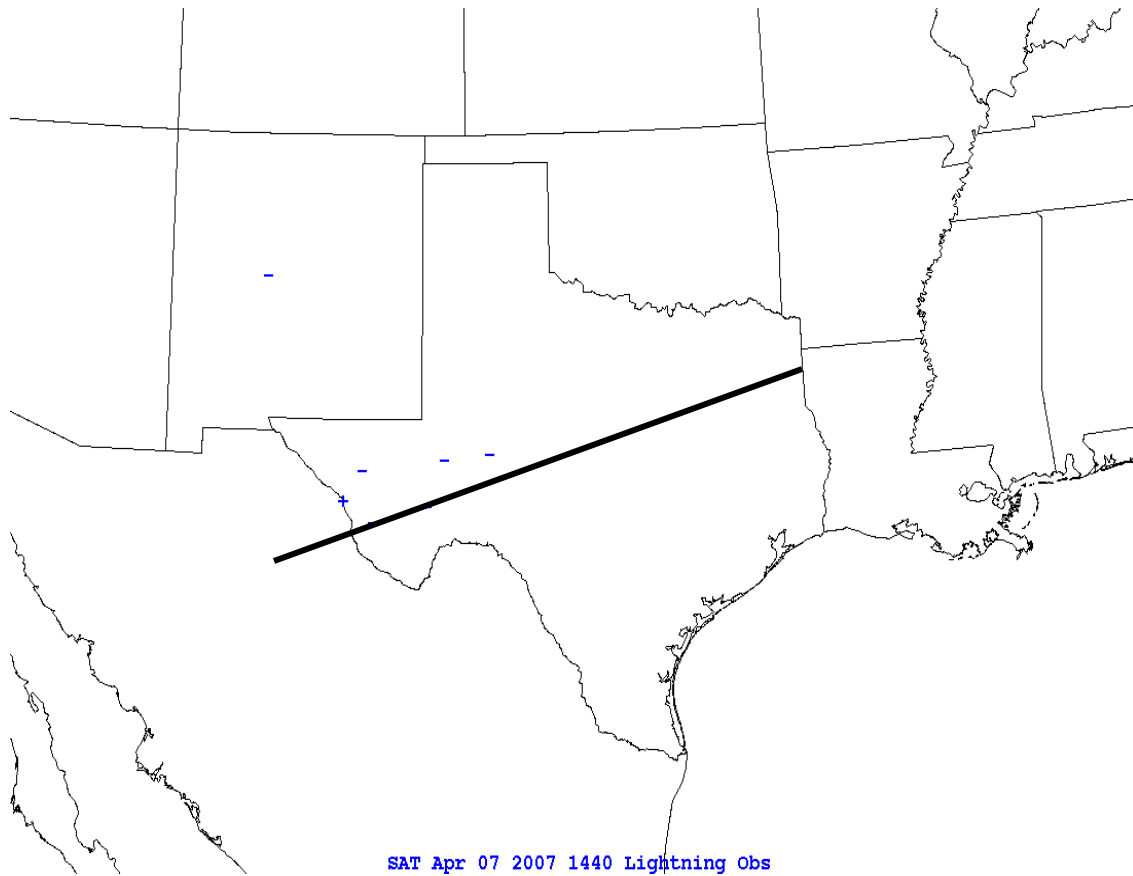


Figure 4.27 Lightning map indicating negative and positive CG flashes ending at 1440 UTC 07 April 2007. Line indicates rain/freeze transition. All lightning above line are in subfreezing air. Lightning in this image produced from NLDN flash data in GEMPAK.

lightning associated with winter precipitation found with respect to the storm total count of lightning events. Of these, 15.0% were cloud flashes and 85.0% were CG strokes. Of these, 97.2% were negative CG strokes and 2.8% were positive CG strokes.

According to Figure 4.28a, the storm total lightning was maximizing at the time when the first thundersnow observation was made between 0000 and 0400 UTC 07 April with a total of 3391 observed lightning events. This anomalous

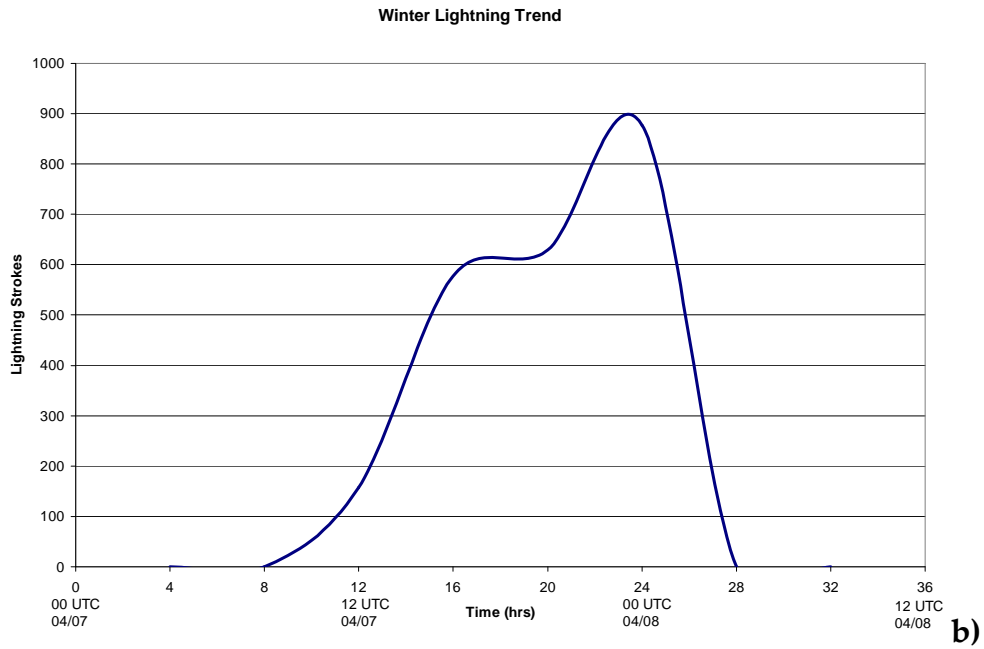
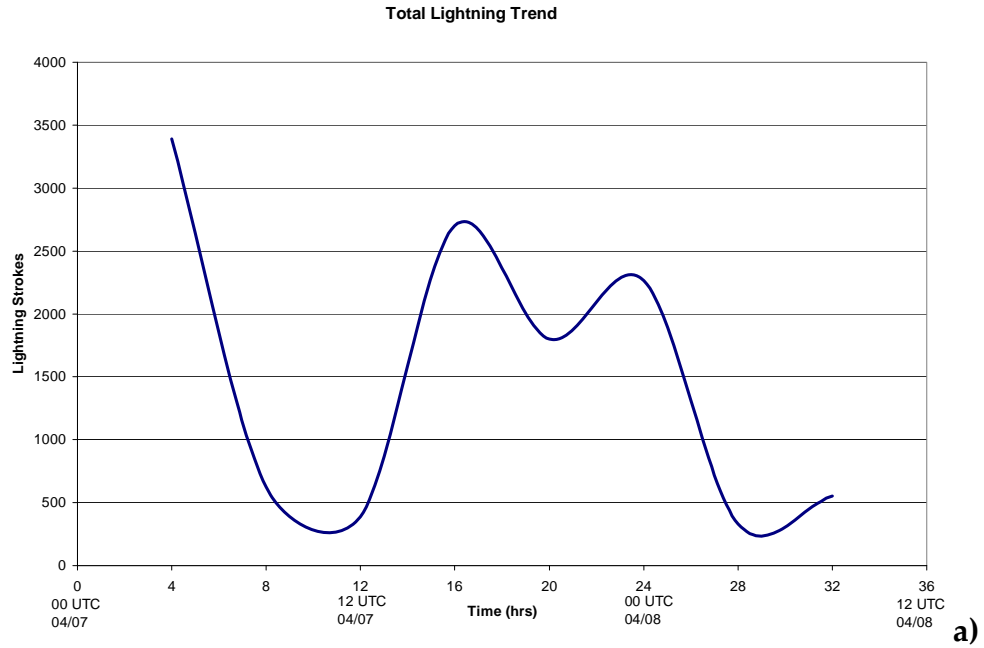


Figure 4.28 Storm total lightning trend for both a) the total storm and b) the lightning associated with winter precipitation for 07 April 2007 through 08 April 2007. Time given in hours from the onset of lightning detected in winter precipitation. Date labeled every 12 hours in UTC.

maximum appears incomplete due to the nature of the storm intensifying as it enters into the central U.S. domain. Of these, 9.8% were cloud flashes and 90.2% were CG strokes. Two more maximums in storm total lightning occurred during the course of the event. One occurred between 1200 and 1600 UTC 07 April. The second occurred between 2000 UTC 07 April and 0000 UTC 08 April. Both times were coincident with maximums in lightning events associated with winter precipitation (Fig. 4.28b). The first maximum was coincident with the storm total maximum between 1200 and 1600 UTC 07 April. During this time, 577 lightning events were found to be associated with winter precipitation, which was 21.4% of the total lightning at that time. This had an average event rate of 2.4 min^{-1} . Of these, 12.5% were cloud flashes and 87.5% were CG strokes. Of the CG strokes, 98.6% were negative CG strokes and 1.4% were positive CG strokes. While the storm total lightning declined into the second maximum, the lightning associated with winter precipitation was observed to gradually increase between 2000 UTC 07 April and 0000 UTC 08 April. 877 lightning events were found to be associated with winter precipitation during this time making up 38.7% of the total observed lightning for the same time. Of these winter lightning events, 17.4% were cloud flashes and 82.6% were CG strokes, of which 97.4% were negative CG strokes and 2.6% were positive strokes. The peak time for winter lightning had an average event rate of 3.6 min^{-1} .

To summarize, this storm had a fairly high percent occurrence of lightning associated with winter precipitation relative to the entire storm total and not just a single time frame, but this storm also exhibited a relatively low percent occurrence of cloud flashes with respect to the dataset up to this point. This also exhibited a fairly low percentage of positive CG strokes relative to the dataset.

4.1.14 April 13-14, 2007

This was the final event of the winter season, as defined in Chapter 3, which saw thundersnow observed in the central U.S. While thundersnow is typically seen beyond the middle of April, it is usually located over the higher elevations of the Rocky Mountains. This event was an isolated closed low over the foothills of New Mexico and into Texas. The first thundersnow observation occurred at 0600 UTC 13 April while the last one was observed near 1200 UTC 14 April. This storm generated a total of 473,920 lightning events. Of this total, 38.1% were cloud flashes and 61.9% were CG strokes. Of the CG strokes, 95.7% were negative CG strokes while only 4.3% were positive CG strokes. Figure 4.29 shows lightning activity over the Texas panhandle with the bands north of the transition line associated with winter precipitation.

Only 1.6% of the total, or 7413 total lightning events, were found to be associated with winter precipitation. Of this total, 30.1% were cloud flashes and

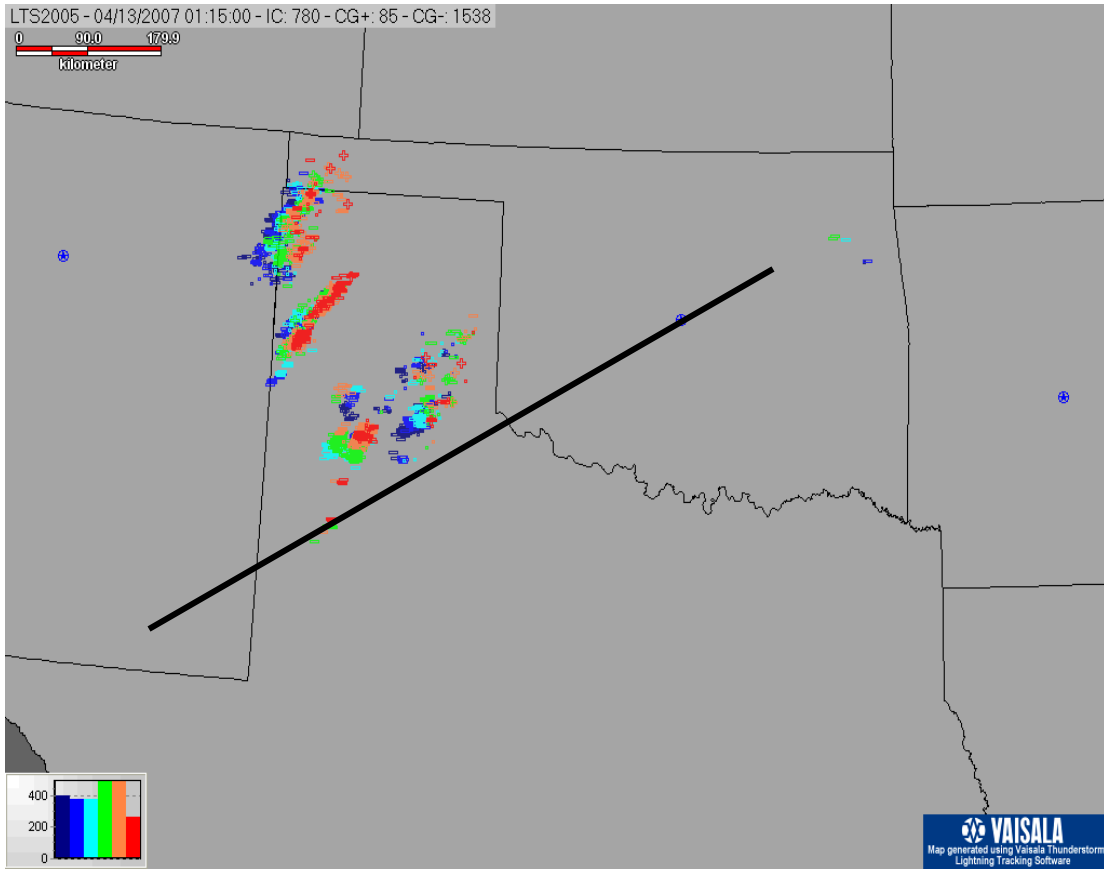


Figure 4.29 Lightning map indicating negative and positive CG strokes and cloud flashes taken at 1500 UTC 13 April 2007. Line indicates rain/freeze transition. All lightning above and left of line are in subfreezing air.

69.9% were CG strokes. Of the CG strokes, 95.5% were negative CG strokes and 4.5% were positive CG strokes.

The maximum in lightning associated with winter precipitation occurred at the beginning of the period when the storm total lightning was at a minimum (Fig. 4.30a). The irregular trend line for lightning in winter precipitation is indicative of lightning entering the domain at this time. There are more lightning events associated with winter precipitation occurring before this, but

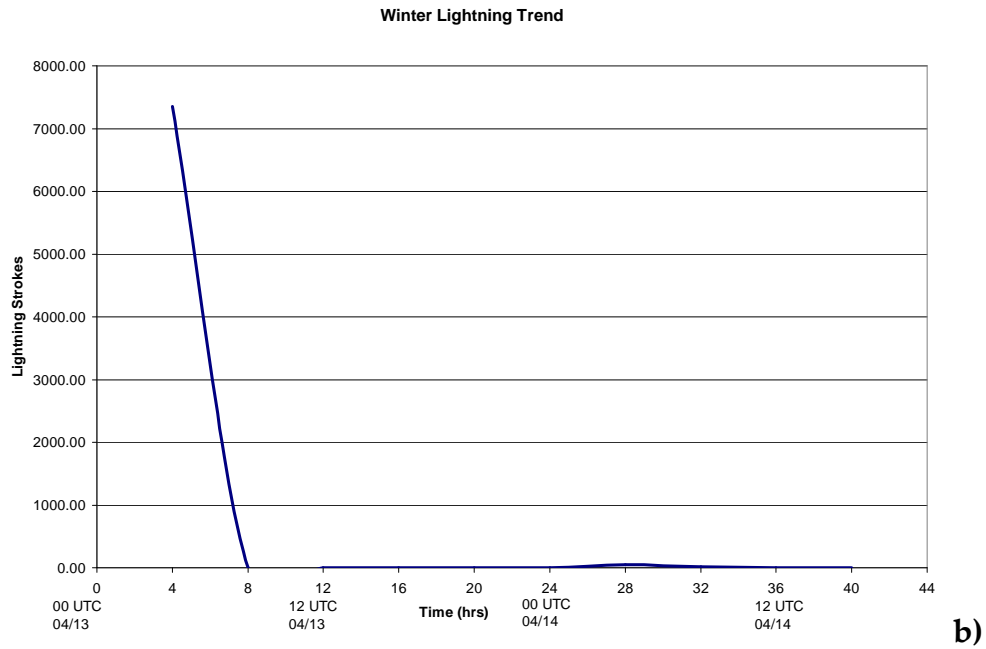
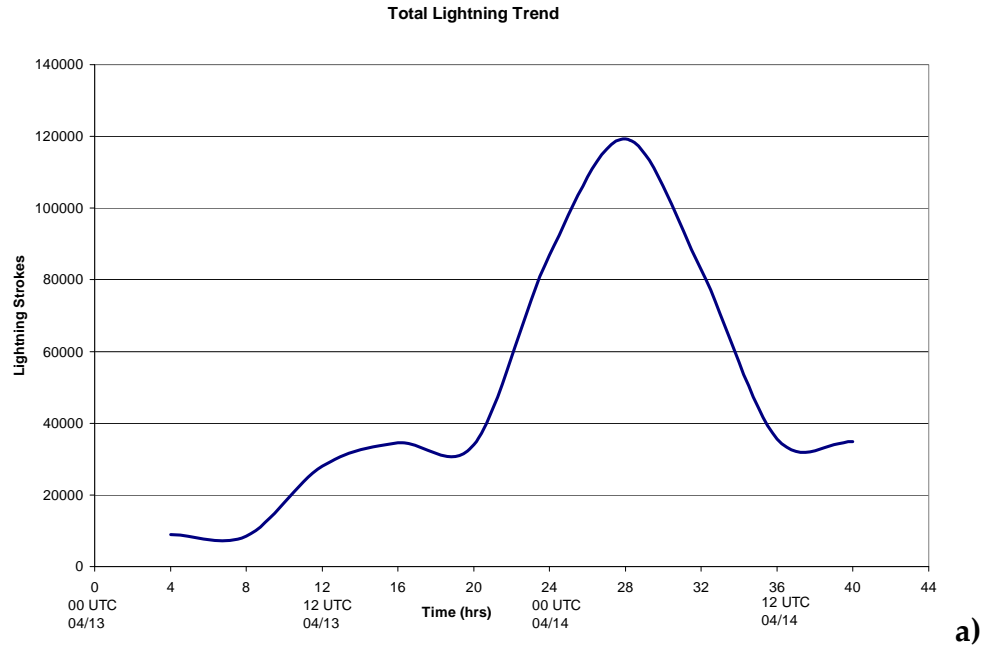


Figure 4.30 Storm total lightning trend for both a) the total storm and b) the lightning associated with winter precipitation for 13 April 2007 through 14 April 2007. Time given in hours from the onset of lightning detected in winter precipitation. Date labeled every 12 hours in UTC.

they occurred at higher elevations and were eliminated from the dataset. This minimum in storm total lightning occurred at the beginning of the period between 0000 and 0400 UTC 13 April with a total of 8992 lightning events, of which 81.8%, or 7351 lightning events, were found associated with winter precipitation (Fig. 4.30b). Of the lightning associated with winter precipitation, 30.2% were cloud flashes and 69.8% were CG strokes, of which 95.5% were negative CG strokes and 4.5% were positive CG strokes. The maximum time in storm total lightning occurred between 0000 and 0400 UTC on 14 April, with a total of 119,292 lightning events. This was coincident with a small maximum in lightning associated with winter precipitation. There were 45 lightning events, 0.04% of the storm total at that time. 15.6% of these were cloud flashes and 84.4% were CG strokes, of which 92.1% were negative CG strokes and 7.9% were positive CG strokes.

In summary, this event was rather anomalous having occurred so late in the winter season. However, this represented another event where a very small percentage was found associated with winter precipitation and the amount of lightning was not representative of the snow/winter precipitation that occurred.

4.2 *Combined Analysis*

4.2.1 **Percent Occurrence**

The values of the fourteen individual storms were combined by compositing the lightning data for each 4-hour segment with the times of the day. Thus, all lightning occurring between 0000 and 0400 UTC for a given storm was composited with lightning from all other storms for the same diurnal period. The result was an overall 24-hour trend for the entire season. The fourteen-storm total lightning event count was 3,185,829. In this, 35.0% were cloud flashes and 65.0% were CG strokes. Of all of the CG strokes, 95.1% were negative CG strokes with only 4.9% being positive CG strokes. Out of the total dataset, positive CG strokes made up 3.2% on average. The storm total lightning events were observed at an average event rate of 76.6 min⁻¹. Only 1.4%, or 44,280 events, of these storms' total count occurred in regions containing winter precipitation, of which 31.3% were cloud flashes and 68.7% were CG strokes. Of the CG strokes, 92.0% were negative CG strokes with 8.0% being positive CG strokes.

With regard to the entire dataset of lightning in winter precipitation, positive CG strokes accounted for 5.5% of the total (this includes all CG and cloud flashes in winter precipitation). The percentage of positive lightning events was well under the average (~11%) found by Orville (1994). Further, the

percentage of positive lightning in winter precipitation is contrary to Hobbs (1974) and MacGorman and Rust (1998) who state that since ice particles typically attain a positive charge in a winter cloud, a lightning event in a winter cloud might lower positive charge to the surface. Other work by Holle and Watson (1996) found a convective winter storm that lowered up to 59% positive lightning events associated with winter precipitation. However, Orville and Huffines (2001) found that the monthly mean percentage of positive lightning from 1989-1998 peaked at about 17% in December and gradually decreased into the spring. There is considerable speculation that since ice particles in a cloud tend to gain a positive charge that it will more likely lower a positive charge to ground, thus assuming that lightning in winter precipitation should be dominated by positive CG lightning. The NLDN climatology from Orville and Huffines (2001) would suggest that lightning in the continental U.S. during the winter season is still pre-dominantly negative, but the percent occurrence of positive lightning does increase. This appears to be the case for these events, excluding cloud flashes, as the majority of charges lowered to ground were low amplitude negative CG strokes.

The percentage of lightning that made up the dataset of lightning activity associated with winter precipitation fluctuated within the divided 4-hr subsets. While the average percentage for the entire season was about 1.4%, the highest

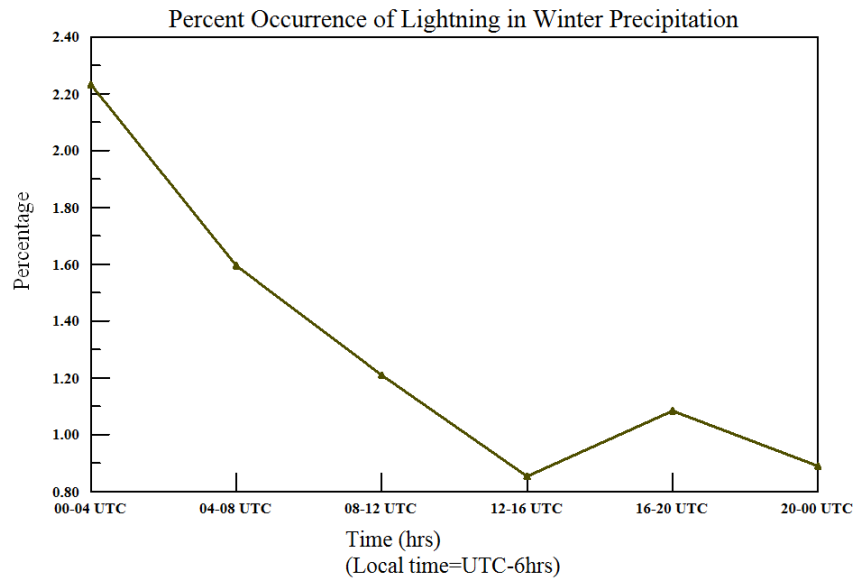


Figure 4.31 24-hour trend of percent occurrence of lightning in winter precipitation. Y-axis represents the percentage while the x-axis is the time in hours UTC.

percentage of 2.2%, occurred during the hours, typically, from 0000 to 0400 UTC. This higher percentage of winter lightning coincided not only with the maximum time for storm total lightning activity, but also the maximum time for lightning activity coincident with winter precipitation. This percentage gradually decreased during the daytime and reached a minimum of 0.8% twice in the 24-hour period, one being between 1200 and 1600 UTC and the other between 2000 and 0000 UTC (Fig. 4.31).

4.2.2 Cloud to CG Ratio and Distance

The cloud:CG ratio for all lightning in these storms is on average about 0.53. Remember, the detection efficiency for cloud flashes is about 10-20% and

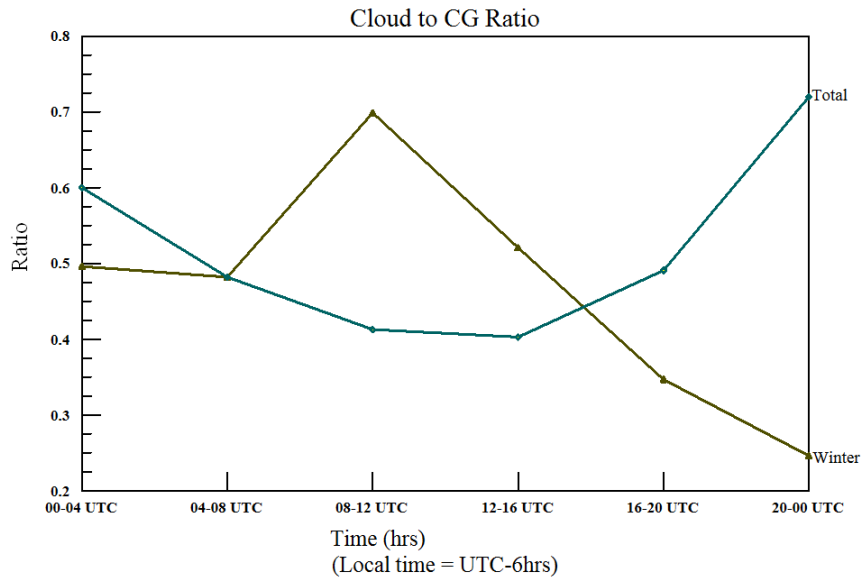


Figure 4.32 24-hour trend of Cloud to CG stroke ratio for storm total lightning (blue line) and winter lightning (yellow line). Trend types are labeled on right-hand side of graph.

this dataset utilizes individual stroke data as opposed to the more commonly used flash data. When divided into the 4-hour subsets, the ratio ranges from its highest at 0.72 at 0000 to 0400 UTC to 0.40 during the minimum in lightning activity (1200 to 2000 UTC; Fig. 4.32). The minimum occurs during the morning hours when daytime stability is at its highest before any heating occurs. The cloud:CG ratio for those lightning events associated with winter precipitation is on average about 0.46. When divided into the 4-hour subsets, the ratio is a minimum of 0.25 during the late afternoon to early evening (2000 to 0000 UTC) when lightning activity begins to steadily increase. However, the cloud lightning activity continues to decrease until after 0000 UTC when it begins to increase again and then maximizes at 0400 UTC along with the CG lightning. The

maximum ratio of 0.70 occurs during the morning hours in the central U.S. (0800 to 1200 UTC). This is seen with the decrease of the occurrence of CG lightning and continuously observed cloud lightning. It can be inferred from these ratios that cloud lightning observations become more important for lightning in winter precipitation especially during a time of day that displays minimum lightning activity.

Further analysis performed between cloud flashes and CG strokes were to attempt to quantify the observed distance between observed cloud flashes and CG strokes occurring at the same time in the same storm (Murphy et al. 2007). It was found that on average, cloud flashes and CG strokes occurred within approximately 0.74 km from each other. This value varied from as close as 0.25 km to as much as 1.75 km.

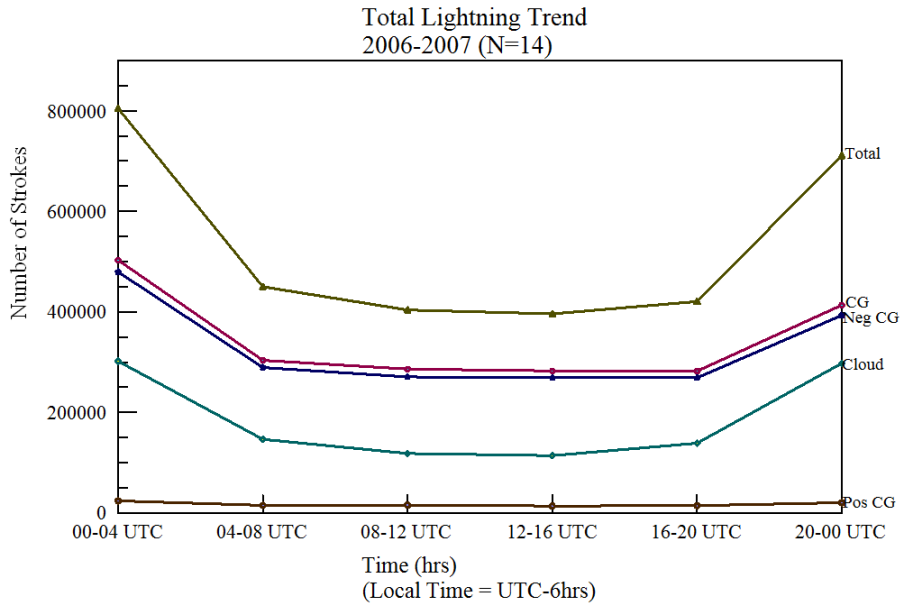
4.2.3 Diurnal Trends

When the data are composited with the individual times of day, a more coherent trend appears for wintertime cyclone events. Figure 4.33a shows the 24-hour lightning trends for the combined storm dataset, along with the 24-hour lightning trend in winter precipitation in Figure 4.33b. The storm total lightning trend for this winter season shows a decrease in occurrence of all lightning types from 10:00 P.M. to 2:00 A.M. local time (0400 to 0800 UTC) with a flat trend until

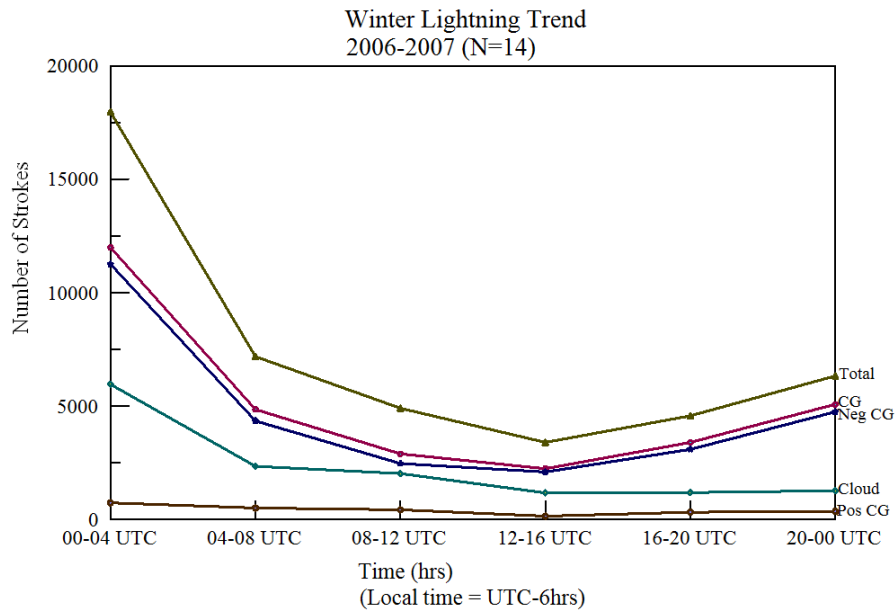
late in the afternoon. The overall trend begins to increase again near 2:00 P.M. local time (2000 UTC) with the number of events increasing until it reaches its maximum from 6:00 to 10:00 P.M. (0000 to 0400 UTC). Orville (1994) identified overall diurnal trends in the high plains for yearly climatologies of the overall lightning detection network, partly due to the increase in mesoscale convective system (MCS) activity during the summer months. The 24-hour trend for positive storm total CG lightning in Figure 4.31a is fairly steady with minimal change. However, this is not the case for lightning events associated with frozen precipitation (Fig. 4.31b). The 24-hour trend of lightning associated with winter precipitation shows a much more defined diurnal pattern with a maximum temporally similar to that of the storm total lightning, between 0000 and 0400 UTC. Instead of a steady average, the lightning events associated with winter precipitation minimizes in the afternoon near 12:00 pm (1800 UTC). This trend is evident with all of the observed lightning types found in winter precipitation. There are few positive CG strokes giving the appearance that it appears non-existent.

4.2.4 Seasonal Trends

While little emphasis can be placed on the seasonal trend of lightning occurrence given only one year of data, a trend was formed to gain knowledge of



a)

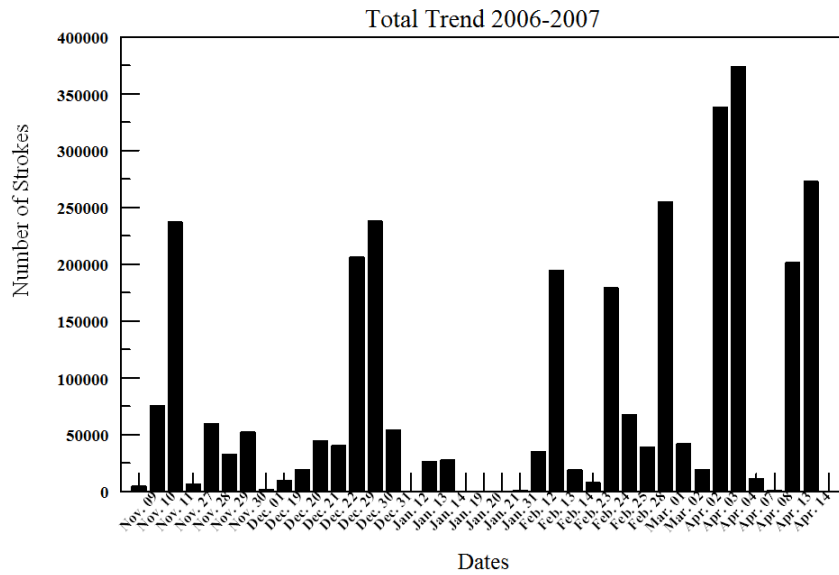


b)

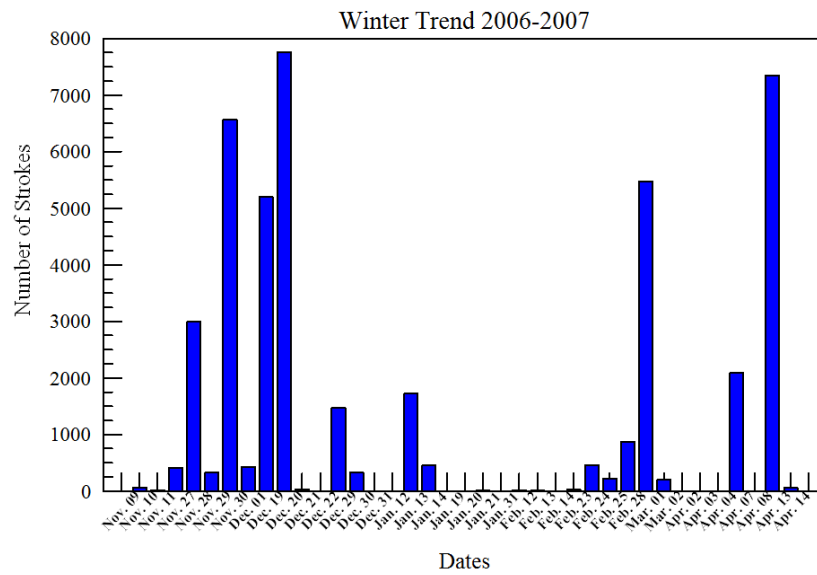
Figure 4.33 24-hr lightning trend for both a) the storm total dataset and b) the lightning associated with winter precipitation for the winter season of 2006-2007. Time given in hours UTC.

how the winter season of 2006-2007 performed. For this season, the overall trend, only including the fourteen observed thundersnow events, showed a general tendency for increased storm total lightning activity through the course of the winter season (October through April; Fig. 4.34a). Accordingly, this also shows that lightning activity reaches a maximum in November and December, particularly towards the end of the month and the beginning of January. While declining in through the primary winter months (January and February), storm total lightning activity again maximizes during the beginning of March into April. This is attributed to more active spring weather associated with less winter precipitation as demonstrated in sections 4.1.12 through 4.1.14.

The trend in lightning associated with winter precipitation, however, is much different with a fairly linear trend only to slightly decrease towards the end of the winter season due to decreased winter precipitation (Fig. 4.34b). This does not follow the findings of Market et al. (2002) in which occurrence of thundersnow tends to increase through the season. However, the occurrence of thundersnow may also not gage the actual number of observed lightning events associated with winter precipitation well. The early and late winter maxima are similar to Market et al. (2002).



a)



b)

Figure 4.34 Seasonal lightning trend for both a) the total storm dataset and b) the lightning associated with winter precipitation for the winter season 2006-2007. Dates are labeled by event occurrence.

4.2.5 Spatial Trends

Further, the trends were analyzed spatially. The average location of lightning coincident with winter precipitation was found for each day of occurrence and averaged for each month. October was not included. The first thundersnow event for the winter season did not occur until 09-10 November. However, no significant lightning event with associated winter precipitation occurred during the month of October, thus was not analyzed with this dataset.

Additionally, there is no correlation between the amount of lightning found in winter precipitation and the intensity of the storm itself. One would assume that in a more intense system (i.e. greater pressure and/or height falls) more lightning might occur. Iskenderian (1988) showed that, in the context of precipitation maxima, the deepening of cyclones do not always correlate with the maximum precipitation.

According to Figure 4.33, the mean location for winter lightning in November and February was located in southern Iowa. This, however, does not mean that all events necessarily occurred directly over this region. Individual events for November ranged from southern Minnesota and Wisconsin, through Iowa and into Kansas and Missouri. This average appears reasonable given the seasonal transition that occurs, when polar, sub-freezing temperatures begin to move southward in events that affect the Upper Plains. The average location

shifts southwest towards southwest Kansas and the Oklahoma panhandle through December, which could be associated with further southerly transport of polar air in coincidence with a more dynamic beginning of the winter season. This average location is also associated with more frequent occurrence of leeside cyclogenesis in the New Mexico and Colorado Front Range of the Rocky Mountains that generate significant precipitation events. The average location does not shift much and moves into central Oklahoma by January. This location may be associated with the combination of the southward transport of polar air and subtropical moisture from the south in the depth of the winter season. The average location for the month of February shifts back to southern Iowa. February represents the calendar end of the winter season in the central U.S. with fewer winter precipitation events. During the beginning of this transition, the cold air begins to retreat to the north. The average location in March shifts north to southern Wisconsin and may represent the seasonal shift from winter to spring in the central U.S. Weather events during this time are dominated by deeper, more intense cyclones with cold air staying further north. The intensity of these storms is greater due to the tighter temperature gradient existing between freezing and non-freezing air. Finally, the average location for April is shifted to south central Kansas. This particular one-year dataset appears to be unusual. The events for April for the 2006-2007 winter season involved mostly

closed off lows over the southwest U.S. that generated winter precipitation and lightning over the Texas and Oklahoma panhandles. If average monthly locations for lightning associated with winter precipitation were analyzed for further years in the future, one might expect the average location for April to shift slowly back to the north. Further, given the different annual and decadal cycles on a much larger scale, one might expect the locations to vary northward as more data is added.

In summary, section 4.2 looked at the combined lightning data for all thundersnow events during the winter season of 2006-2007. These data were analyzed for the percent occurrence of lightning in winter precipitation and individual lightning types. Further, these lightning data revealed different temporal and spatial trends. It was shown for this winter season that lightning in thundersnow producing storms and lightning occurring in winter precipitation from the same storms generally occurred more frequently between the hours of 0000 and 0400 UTC. Further, it was found for this dataset that cloud flash lightning appeared important for observing lightning in winter precipitation particularly in the hours of 1200 to 1600 UTC when the lightning is at a minimum. Finally, the average locations for the occurrence of lightning in winter precipitation formed a coherent trend, although these locations may not be fully representative of exact locations, but they did follow a seasonal pattern.

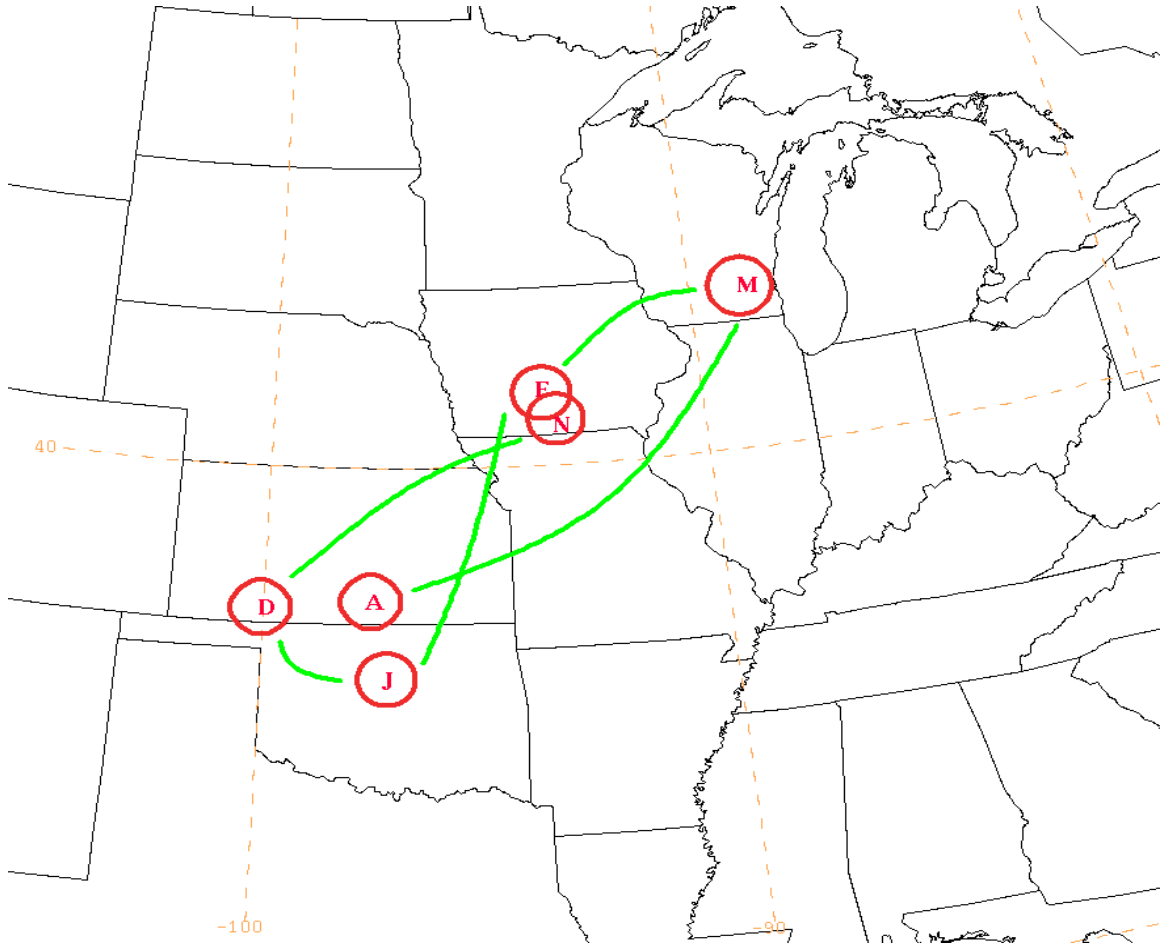


Figure 4.35 Map indicating monthly average location for winter lightning in the central U.S. Each red circle represents the latitude-longitude location of the average with the letter representing the month of the average. Green track connects average locations in order.

Chapter 5 Sounding Analysis

5.1 Composite Soundings

The following chapter will discuss the composite sounding analysis related to the lightning analysis in chapter 4. This analysis was performed in order to view the local environment directly related to the observation of CG strokes and cloud flashes. Market et al. (2006) performed a composite sounding analysis using proximity soundings from thundersnow observations on either the northeast or northwest side of the parent cyclone. The following sounding analysis will attempt to reveal the physical characteristics of the local environment relating to the direct detection of lightning events in the context of a thundersnow event. Further, it will attempt to add to and further validate previous work done (i.e. Schultz 1999 and Market et al. 2006).

As described in Chapter 3, the composite soundings are composed of RUC initial sounding features from an average (in some cases sole) location of most active lightning in regions of winter precipitation during a single 4-hour subset. For example, the maximum occurrence in lightning in winter precipitation during the 30 November-02 December 2006 winter storm was between 0800 and 1200 UTC. From the lightning occurring in that time, the hour of most active occurrence was determined and an average location for that time was taken. This resulted in small local regions of winter lightning with which to take a mean location and sample sounding from. Further, the location(s) was analyzed in plan view for its geographic orientation with respect to the location of the center of the surface low. In contrast to papers by Market et al. (2002, 2006), a majority of the lightning events for this season were found to occur northeast (NE) of the cyclone center. In total, there were 45 4-hour subsets when sample soundings were derived. Some subsets were divided and composites created separately for their timing significance, although the division significantly decreases the number of samples (i.e. NE lightning events occurring strictly between 2000 and 0000 UTC). There were only 19 northwest (NW) cases of the analyzed 4-hr subsets that occurred in 5 of the thundersnow events. These composite soundings were analyzed using RAOB 5.7 software. These composites further made use of Brown's (1993) feature preserving compositing method, more

specifically preserving the heights and pressure levels of the -10°C and -20°C isotherms. These were found and inserted into the composite data for reference to a lightning favoring profile. It should be noted, especially in the NE composites, the surface is located at a mean sea level pressure of 1000 mb. In most instances, the cyclones did not reach below 1000 mb, especially NE of the center. The surface for the NW composites indeed is lower than the NE as a result of sea level pressure reduction after passage of the parent low.

5.2 Northeast Composite Soundings

The NE composite sounding (Fig. 5.1) was warmer than the NW composite sounding. The top of the inversion layer was located just below 800 mb in this profile. The top of the inversion represented the necessary warm nose in these instances to produce at least some form of frozen precipitation. In this composite for this season, the temperature at the top of the inversion was 2.7°C . The profile between the top of the inversion down to 950 mb represents a stable isothermal layer. Above the inversion, the temperature profile is moist-neutral up to approximately 500 mb. The tropopause level is at about 250 mb. Veering in the wind pattern in the lowest 200 mb (up to about 800 mb) indicates warm air advection below 800 mb and then winds become fairly linear with little directional shear. This is supported by the curvature of the hodograph inset on

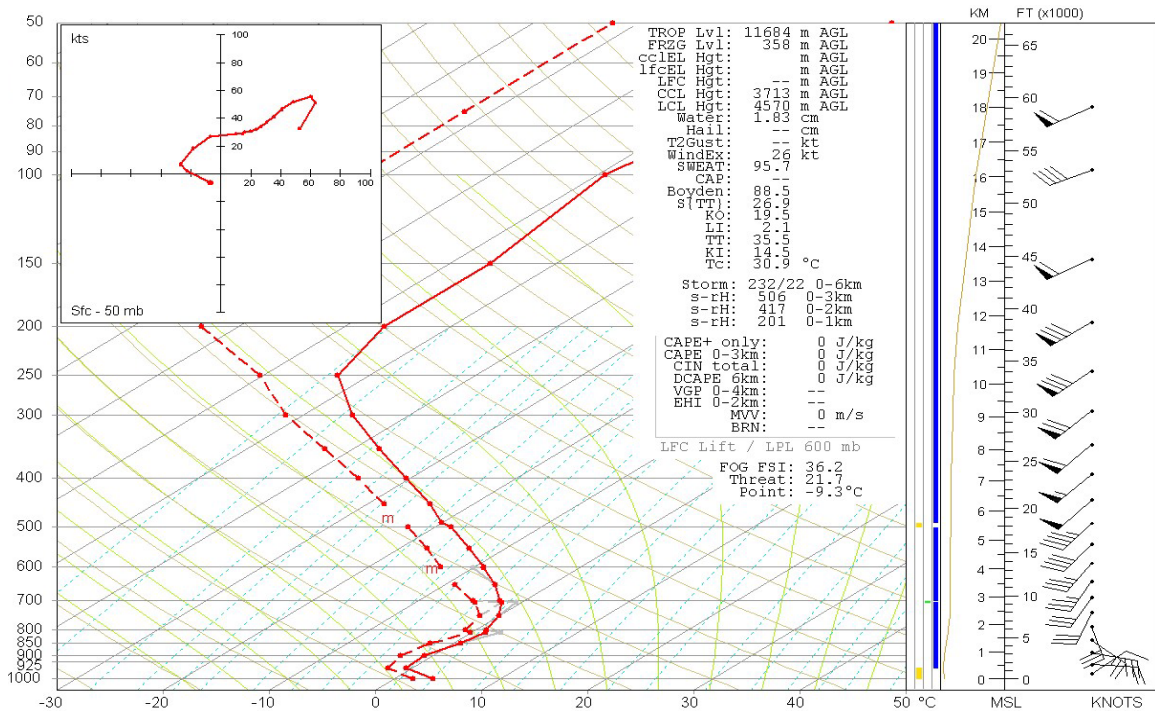


Figure 5.1 Full northeast composite (N=45) composited from RUC initial soundings at the latitude and longitude of most active lightning in winter precipitation. This consists of samples taken from all active lightning times occurring northeast of the cyclone. Solid red line is mean temperature, dashed red line is mean dewpoint, and wind barbs represent mean wind speeds in kts and median wind direction. Vertical Θ_e in yellow to the left of wind barbs.

Figure 5.1. There is little speed shear represented in the vertical also with winds near the surface at near 20 kts (10.3 m s^{-1}) increasing to 40 kts (20.6 m s^{-1}) by 550 mb and an 80 kts (41.1 m s^{-1}) jet above 300 mb. In terms of instability parameters, there is no CAPE when lifting (from) the most unstable parcel. In this case, the most unstable parcel originated at 600 mb. However, this composite had a lifted index (LI) of 2.1, which reveals some weak potential instability, as revealed by vertical equivalent potential temperature (Θ_e) profile in Figure 5.1, and is considered statistically significant according to Market et al. (2006).

In this composite, the -10°C isotherm was at 600 mb and a height of 4175 m (4.2 km). This average height is well above the 1.8 km recommended by Michimoto (1993). In this composite, this isothermal height was above the frontal inversion and at the most unstable lifted parcel level (MULPL) well within the moist-neutral layer between 800 and 600 mb. The level of the MULPL at or below the -10°C isotherm has been correlated to instability profiles most often associated with those of convective winter precipitation events. Following MacGorman and Rust (1998), the best region of mixed-phase particles, including graupel and supercooled water droplets, occurs typically between -10°C and -20°C . For this reason, the level and height of the -20°C isotherm were preserved for this profile as well. On average, the pressure height of this isotherm was 490 mb, or 5745 m (5.7 km), which is well above the moist-neutral layer.

The composites were further divided into three representative 4-hour segments. These divided composites were derived using the diurnal trends determined in section 4.2.3. and included the 4 hours prior to the maximum lightning activity (2000 to 0000 UTC), the 4 hours during the maximum lightning activity (0000 to 0400 UTC), and the 4 hours immediately following the maximum lightning activity (0400 to 0800 UTC). These are discussed in the order given. Despite the small dataset of soundings, Brown's (1993) feature preserving methods were again employed to remain consistent with compositing methods.

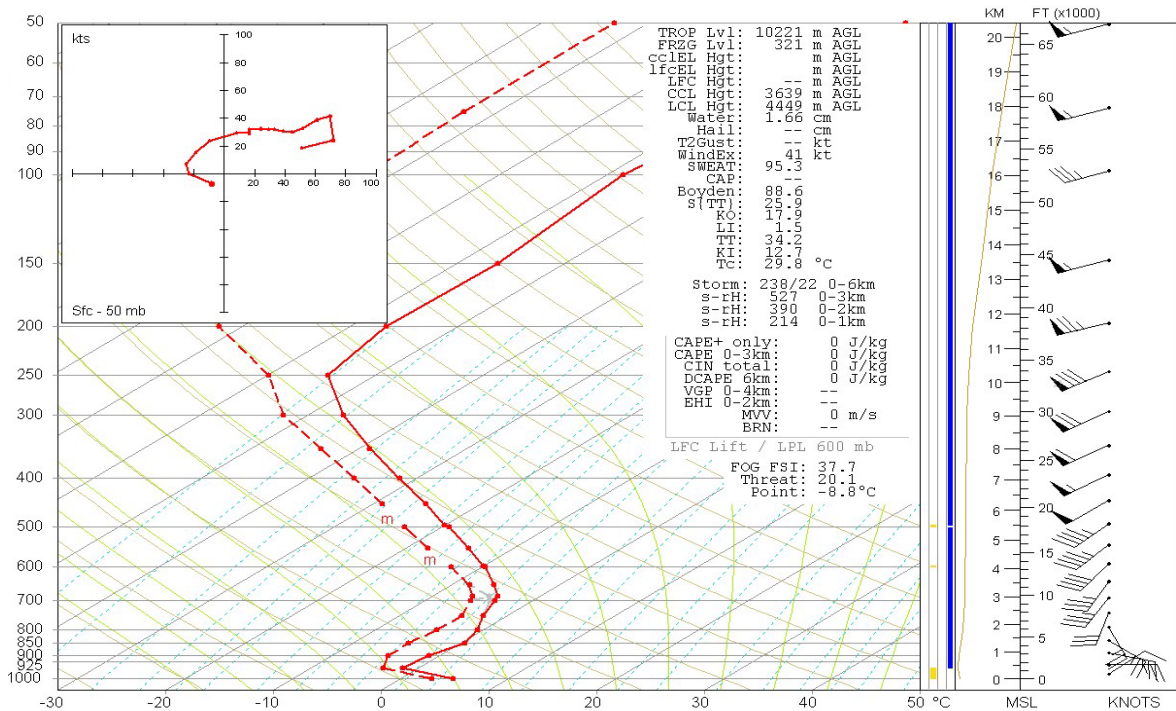


Figure 5.2 2000 to 0000 UTC northeast composite (N=8) composited from RUC initial soundings at the latitude and longitude of most active lightning in winter precipitation. Solid red line is mean temperature, dashed red line is mean dewpoint, and wind barbs represent mean wind speeds in kts and median wind direction. Vertical Θ_e in yellow to the left of wind barbs.

The first divided composite encompasses the 4 hours previous to the most active lightning (2000 to 0000 UTC). 8 sample soundings taken from 2000 and 0000 UTC were used to calculate this composite sounding (Fig. 5.2). This composite sounding was the coldest NE composite. The top of the inversion layer for this profile is 850 mb at a temperature of 0.5°C. Below the inversion layer, the profile follows the 0°C isotherm to 950 mb. Above the inversion, the profile continues to be potentially stable between 850 and 700 mb where the lapse rate lies between that of the dry adiabat and moist adiabat. This is shown

in Figure 5.2 with the Θ_e profile increasing with height through this layer. Above 700 mb, the profile turns moist-neutral up to 450 mb. The MULPL, as analyzed by RAOB, is at 600 mb, which is at the level of the -10°C isotherm, 597 mb, or 4206 m (4.2 km). Again, the winds veer from a mean wind speed of 20 kts at 950 mb from the northeast to 40 kts at 600 mb from the west. Similar to the full NE composite, this profile has no CAPE. However, the LI, 1.5, is actually lower than the full NE composite, suggesting some weak instability and a decrease in stability during this time. The decrease does not hold for all stability parameters. Such parameters as Total totals (TT) and the K-index (KI) were slightly below or similar to those of the full NE composite. The TT for the full NE composite was 35.5 as opposed to 34.2 from 2000 to 0000 UTC. The KI was the same, 13.1 and 13.2, respectively between the full NE composite and the 2000 to 0000 UTC composite. However, according to Market et al. (2006), most stability parameters were found to be uncorrelated to the occurrence of thundersnow.

According to the diurnal trend determined in section 4.2.3, the most active time of lightning in winter precipitation occurred between 0000 and 0400 UTC. The top of the frontal inversion in this case was again at 800 mb (Fig. 5.3). This profile is still colder than the full NE composite profile and slightly warmer at the top of the inversion than 4 hours earlier (2000 to 0000 UTC). Temperatures near the top of the inversion in this case are near 1°C . Temperatures at the

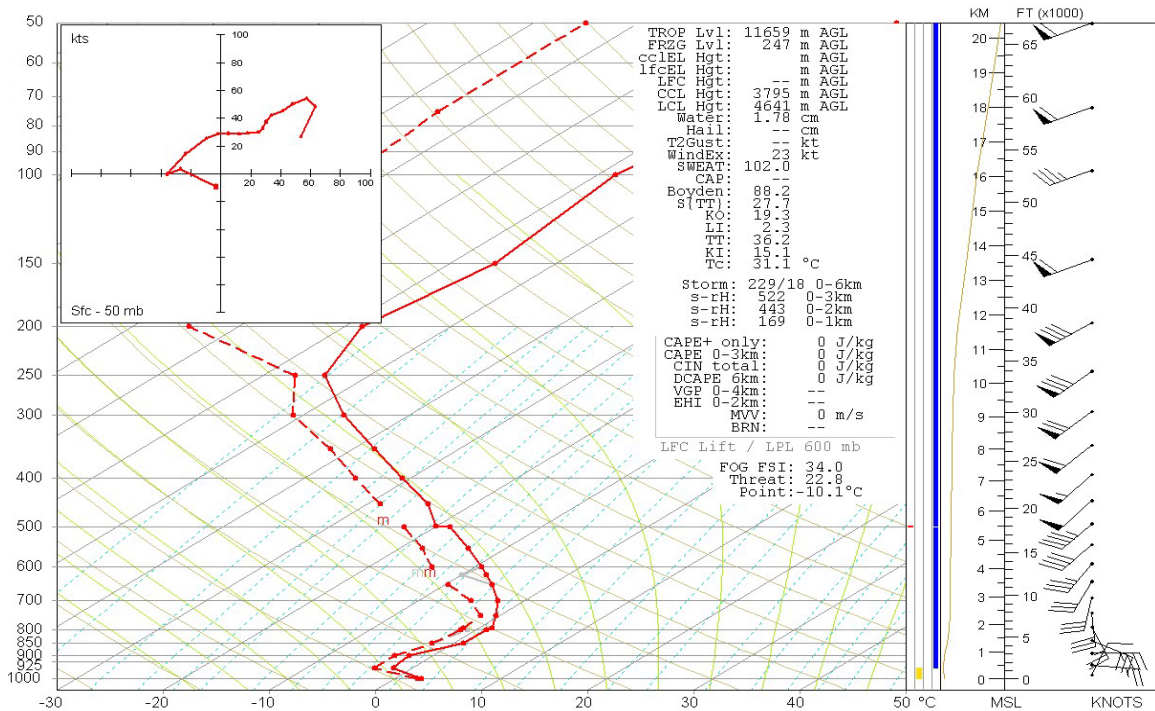


Figure 5.3 0000 to 0400 UTC northeast composite (N=12) composited from RUC initial soundings at the latitude and longitude of most active lightning in winter precipitation. Solid red line is mean temperature, dashed red line is mean dewpoint, and wind barbs represent mean wind speeds in kts and median wind direction. Vertical Θ_e in yellow to the left of wind barbs.

ground (1000 mb) are between 1° and 2°C during this time. Again, there is no elevated CAPE present in this sounding. Without any smoothing, there existed a shallow layer above the frontal inversion where CAPE is present, but this was deemed a function of feature preservation along with a small dataset. The height and level of this -10°C isotherm is at 3864 m (3.9 km) and 621 mb respectively. Compared to the other NE composites, this height is closest to the surface. In the composites up to this point, the -10°C level resided above 4.0 km and pressure levels at or below 600 mb. Above this level, the profile remains near moist-

neutral up to the tropopause. The -20°C isotherm in this profile resides at 5603 m (5.6 km) and 500 mb. Again, the -20°C isotherm during the most active lightning resides lower in this profile, but is not statistically significant. More wind shear exists in this profile as well, going from 10 kts from 20° to 35 kts from 90° 100 mb above the surface. While mean wind speeds do not tend to increase significantly above 900 mb, the direction continues to veer from a median wind direction of 90° to 200° at the MULPL. Noting this region of greatest shear is important as the greatest wind shear resides in a region above the -10°C isotherm where mixed-phase precipitation particles are considered at their greatest for lightning production. Brooks et al. (1982) stated that wind shear may play a significant role in lightning generation. Further instability parameters such as TT and KI are also at their greatest at this time at 36.2 and 15.1, respectively. An LI of 2.3 was found in this profile to add to the convective nature of this profile.

Finally, a composite sounding of the 4 hours following the most active lightning from 0400 to 0800 UTC was created (Fig. 5.4). This 4-hour time was again determined by data provided from section 4.2.3. However, this profile has the fewest soundings included in the composite (N=7). This profile showed a decrease in instability. The top of the inversion was still present, but not as nearly pronounced with less steep lapse rates below the inversion layer. The top of the inversion layer was at 825 mb for this profile, lower than the top of the

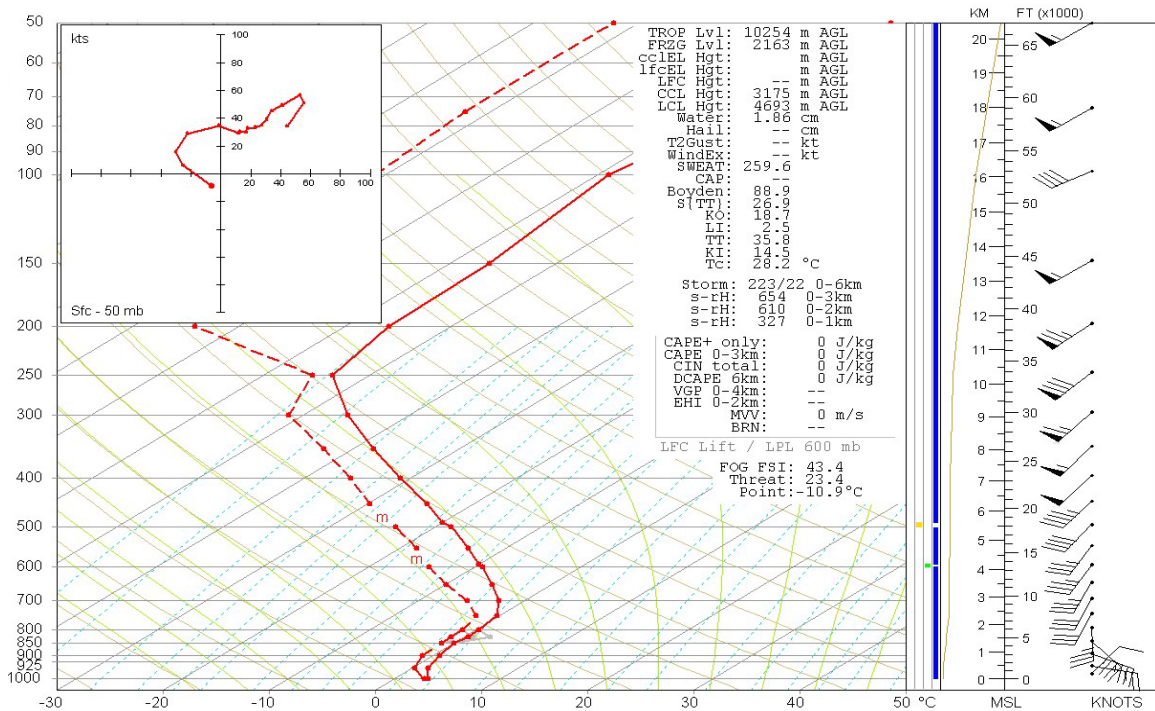


Figure 5.4 0400 UTC to 0800 UTC northeast composite (N=7) composited from RUC initial soundings at the latitude and longitude of most active lightning in winter precipitation. Solid red line is mean temperature, dashed red line is mean dewpoint, and wind barbs represent mean wind speeds in kts and median wind direction. Vertical Θ_e in yellow to the left of wind barbs.

inversion for the full NE composite and the other subset composites. However, this time is also the warmest of the composites with an isothermal layer below the inversion near the 0°C isotherm and slightly above. Above the inversion, the profile is moist-neutral up to 450 mb and is drier above 700 mb. The MULPL in this composite is at 600 mb, well above the saturated air, making conditions less capable of lightning generation. No potential instability is present in this profile as shown by the Θ_e profile to the right of the sounding in Figure 5.4. The wind veers from a mean wind speed of 10 kts from a median wind direction of 36° at

the surface to 26 kts and 104° aloft at 950 mb. The wind speeds slowly increase with altitude and continue to veer to 200° at the 750 mb. No CAPE or DCAPE is present in this profile. However, other stability parameters are still greater at this time than with the full NE composite and the 4 hours previous to the greatest lightning activity. These include an LI value of 2.5, a TT value of 35.8 and a KI of 14.5 showing a tendency for stability (instability) to increase (decrease) as the tendency for lightning occurrence decreases.

In summary, the suite of NE composite soundings showed a resemblance to one another. The full NE composite showed a resemblance to soundings derived from Market et al. (2006) with similar values in the statistical range of accepted instability parameters for thundersnow occurrence. In terms of the depth of the inversion layer, both the full NE composite and the 0000 to 0400 UTC composite soundings were similar with a deeper inversion (1000 to 800 mb) while the 2000 to 0000 UTC and 0400 to 0800 UTC composites both had a more shallow inversion layer (1000 to 900mb). Stability parameters such as LI, TT, and KI did not vary much among the composites, but did tend to indicate more instability in the full NE and 0000 to 0400 UTC composites (increased TT and KI along with decreased LI). In terms of the -10° to -20°C isothermal layer, the depth is similar. The only outstanding difference is the proximity of the -10°C isotherm to the surface. This isotherm was its lowest in the 0000 to 0400 UTC

composite, which represented the 4-hour segment where lightning was more active in winter precipitation, although still higher than those heights found in Market et al. (2006). These values will be compared further to the full NW composites in the following section.

5.3 Northwest Composites

The northwest (NW) composite is conceptually colder than the NE composite. This profile is completely below freezing (0°C) in the column, indicative of a snowfall event. Snow is a more common occurrence on the NW side of a cyclone where the cold air begins to occur behind the typically associated cold frontal boundary (i.e. Martin 1998a, 1998b). The sounding profile for the NW cases (Fig. 5.5) looks similar to the subset composite from 0400 to 0800 UTC NE composite. As opposed to the NE composite, it should be pointed out that the profiles for the NW cases did not reach 1000 mb, so the surface in this instance is at 950 mb. This is most likely due to the subsequent pressure fall at this time, such that 1000 mb would not exist in a model initial field. Using the feature preserving compositing, a slight warm nose (still below 0°C) indicative of the top of an inversion layer exists at 800 mb. The MULPL for this profile was found further aloft than in any of the NE composites at 550 mb. The NW composite is more saturated than any of the NE composites and is so up to 700

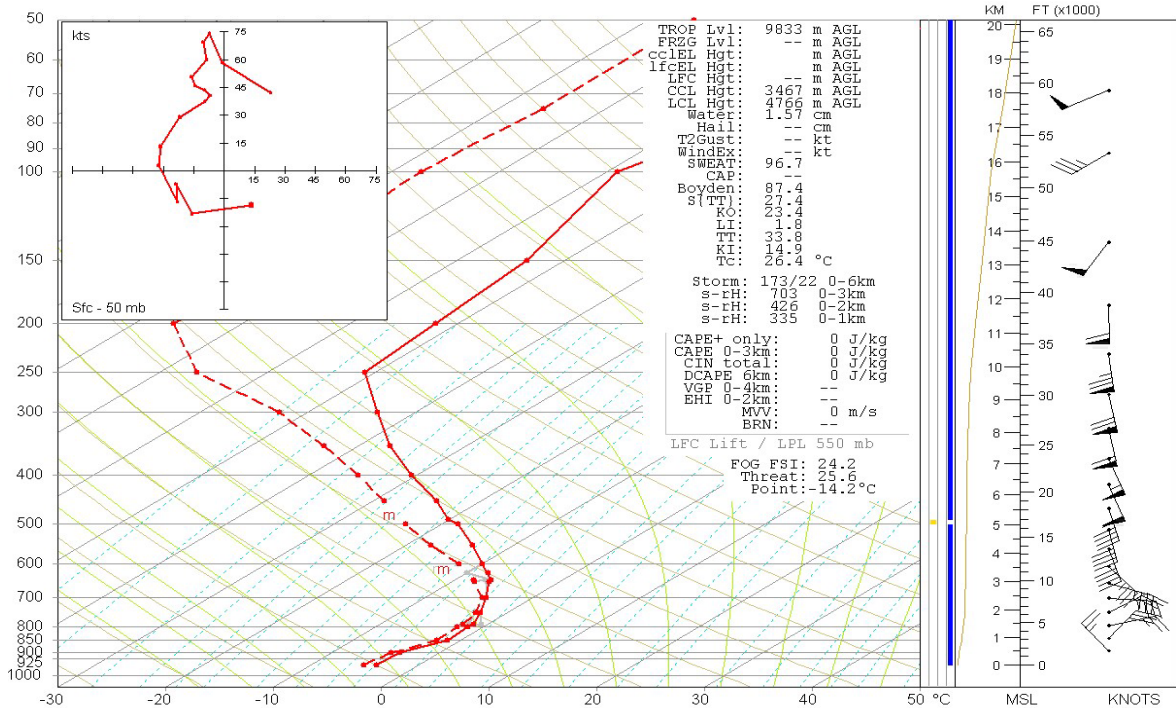


Figure 5.5 Northwest composite (N=19 composited from RUC initial soundings at the latitude and longitude of most active lightning in winter precipitation). Solid red line is mean temperature, dashed red line is mean dewpoint, and wind barbs represent mean wind speeds in kts and median wind direction. Vertical Θ_c in yellow to the left of wind barbs.

mb where the profile becomes drier. Near the surface, the temperature profile is nearly isothermal between 800 and 900 mb. Below 800 mb, the profile cools more quickly to indicate a stable atmosphere, probably in the vicinity of the frontal boundary. Above the inversion, the sounding shows a moist-neutral profile up to 500 mb where it becomes stable again and decreases more steadily up to the tropopause. There is considerably less wind shear for the NW composite than that of the NE composite. Mean wind speeds near the surface for this profile are about 23 kts from a median direction of 49° backing to 324° at 900 mb. Unlike the

NE composites, the wind backs in the lowest 300 mb (up to 600 mb) where the profile becomes less saturated. Above this, the wind begins to veer slightly indicative of a small warming layer above a layer of cooling closer to the surface. The -10°C isotherm in this profile is at 623 mb or 3942 m (3.9 km). Compared to the NE composite this is closer to the surface where it was located 4.2 km above the surface. This pressure level and height, however, are very similar to those found in the NE composite from 0000 to 0400 UTC, which is the period of most active lightning. Thus, as a whole, the NW composite appears more conducive to lightning generation based on the thermal profile alone when compared to events that were observed on the NE side of the cyclone. In terms of the -20°C isotherm, similar circumstances are found, where the height and pressure level are more closely correlated to the 0000 to 0400 UTC NE composite. In terms of stability parameters, the TT for the NW composite was slightly lower than the NE cases at 33.8 and a slightly higher KI at 14.9. This composite had an LI of 1.8, lower than the full NE composite (2.1), further indicating that weak potential instability present as supported by the vertical Θ_e profile in Figure 5.5.

In summary, the NE and NW composite soundings bear some similarities and contradictions. The similarities involve mostly the elevated moist-neutral atmosphere above the frontal inversion along with weak potential instability and similar stability parameters. However, while the TT is higher in the NE

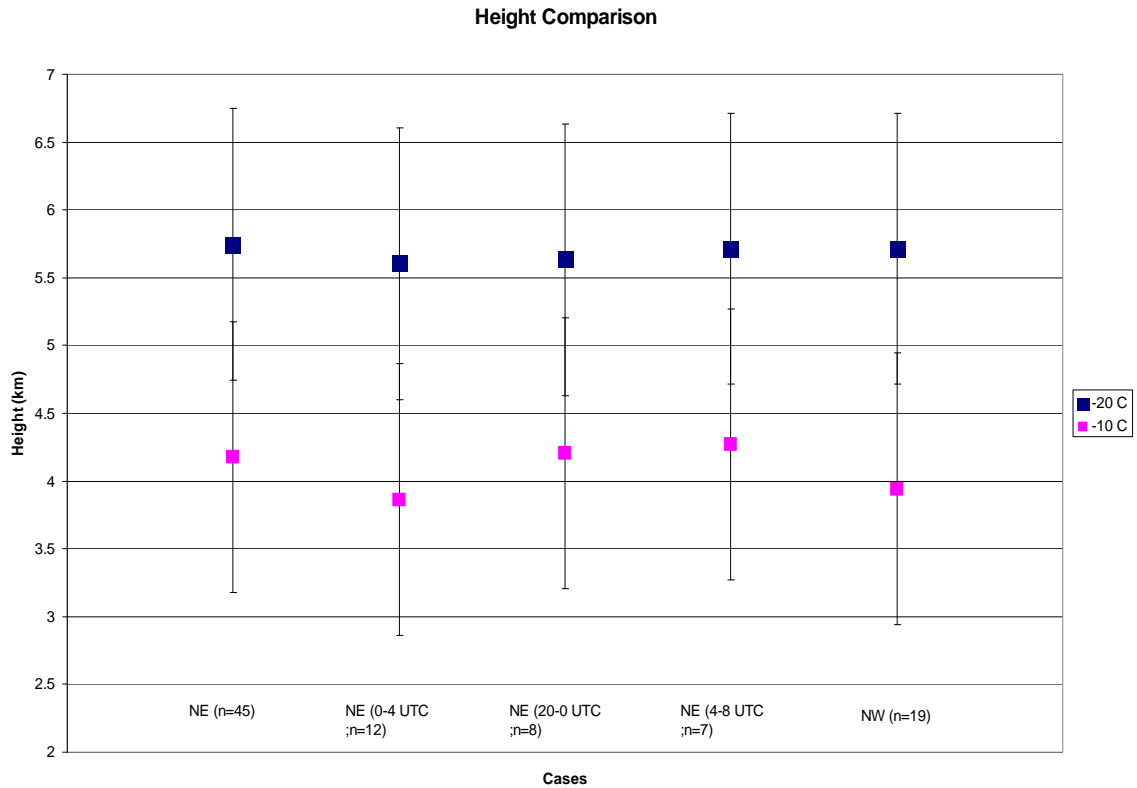


Figure 5.6 Comparison of height of -10° and -20°C isotherms for all derived northeast (NE) composites and the northwest (NW) composite. Composites are listed along the x-axis and height in km are along the y-axis.

composite, the KI is higher in the NW composite. When broken down into its individual 4-hour subsets, the NE composite begins to show some similarity to the NW composite, including the profile for the period of greatest lightning activity from 0000 to 0400 UTC. Among the similarities are the height and pressure level of the -10°C isotherm, located 3.8 to 3.9 km above ground level respectively and between 600 and 650 mb. This similarity also exists with the -20°C isotherm. Figure 5.6 shows a comparison of the various isothermal height differences. Case studies of two different events will be performed in the

following chapters comparing and contrasting lightning characteristics and vertical sounding profiles for an elevated convective event with warm precipitation and an observed thundersnow event from the 2007 and 2008 winter season.

Chapter 6 Thundersnow Analysis

6.1 Analysis of 02 December 2007

The following chapter describes both the lightning characteristics and synoptic and mesoscale features associated with a thundersnow event. The particular date chosen encompassed the day of 02 December 2007. This date occurred outside of the analyzed winter season. The reason for studying a storm outside of the dataset is to obtain knowledge from data that has not been analyzed. Further, there have been some attempts to correlate lightning activity and heavy winter precipitation with cold cloud top temperatures (i.e. Goodman et al. 1988 and Hanna et al. 2008). According to Magano and Lee (1966), the preferred temperature region for growth of snow crystals and habits are between 0°C and -40°C where the best vapor supply for growth are present and also where supercooled water droplets continue to exist. Satellite data will be

presented in the following cases for regions of lightning occurrence in winter precipitation to gain some idea of what kind of cloud-top temperatures can be expected in a winter convective event. Finally, the resultant sounding will be presented to compare to those composites formed in chapter 5. For section 6.2, the same lightning terminology as in chapter 4 will be used.

6.2 Lightning Characteristics

This event appeared weak compared to some of the winter weather events from the 2006-2007 winter season. However, this event has some similarities to its counterparts from a season earlier. Figure 6.1a,b shows the lightning trend for this event for both the storm total lightning in the central U.S. and the lightning only associated with winter precipitation. While this situation did not involve a deep surface low (< 1008 mb), enough lift and forcing were present to generate convection. The trends in lightning associated with winter precipitation showed a strong similarity to cases analyzed from the 2006-2007 winter season, particularly the 12-hour diurnal trend.

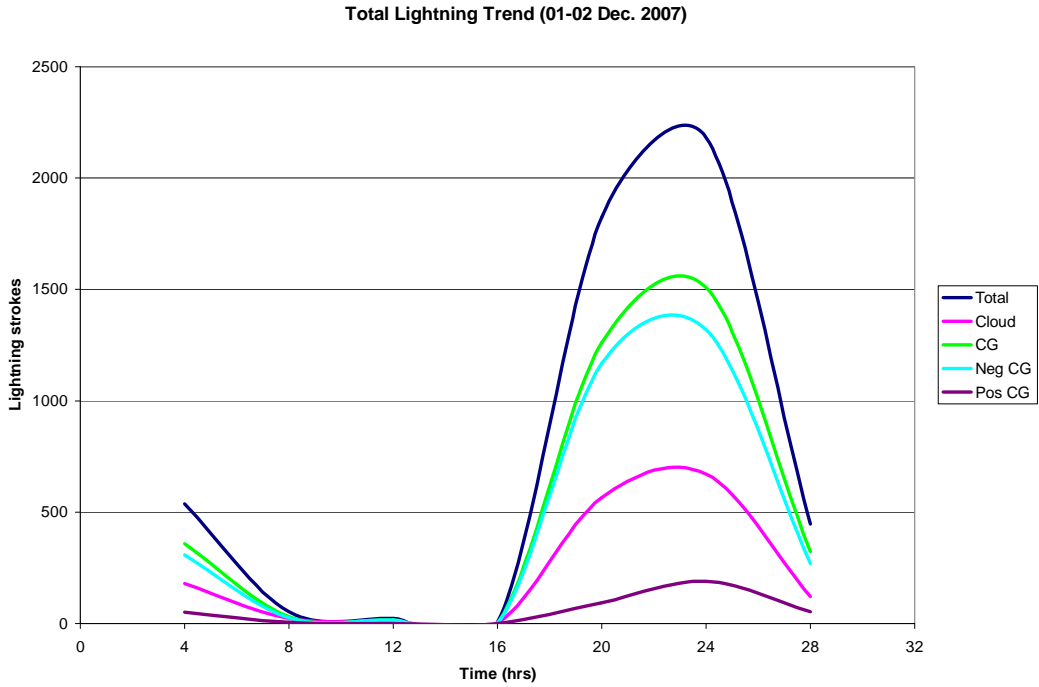
During this brief event, covering only 28 hours from 2000 UTC on 01 December until 0000 UTC 03 December, there were only 5071 observed lightning events in the central U.S. (Fig. 6.1a). Of this total, 31.0% were cloud flashes and 69.0% were CG strokes, of which 88.8% were negative CG strokes. The

combined average from the 2006-2007 winter season for cloud flashes was 35.0%, only slightly higher than this case. The storm total lightning was observed in this case at an average event rate of 3.0 min^{-1} . The maximum time for storm total lightning in this event occurred between 1600 and 2000 UTC on 02 December. During that time, 2181 lightning events were observed. Of this total, 31.0% were cloud flashes and 69.0% were CG strokes. Of the CG strokes, 87.5% were negative CG strokes. The lightning during this time was observed at an average event rate of 9.1 min^{-1} . The total cloud-to-CG ratio observed in this event was 0.59.

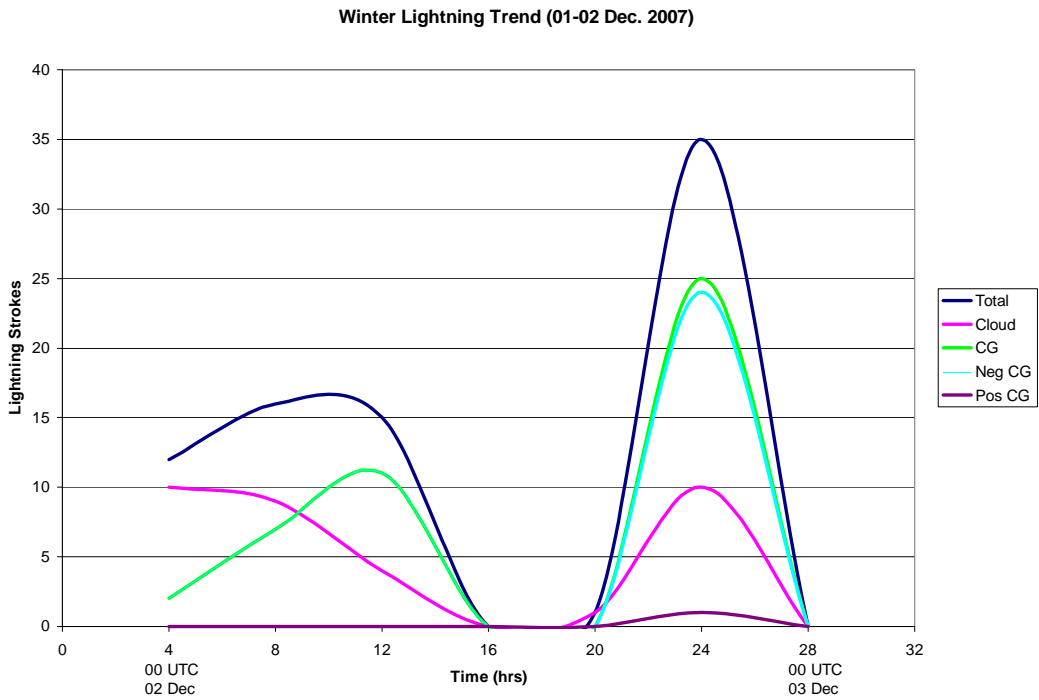
For this event, only 1.6%, or 79 lightning events, of the storm total were found to occur in regions of frozen precipitation (Fig. 6.1b). This is only slightly higher than the average value found for the entire winter season of 2006-2007 of 1.4%. Of these lightning events in winter precipitation, 43.0% were cloud flashes and 57.0% were CG strokes. Of those CG strokes, 97.7% were negative CG strokes. The lightning events found in winter precipitation were observed at an average event rate of 0.05 min^{-1} . Compared to the season averages described in section 4.2, the percentage of cloud flashes was higher than the average 31.3%. Also, the percentage of negative CG strokes among all CG strokes was also higher than the average of 92.0% found. The maximum times were similar to the overall 24-hour trend displayed as the 2006-2007 average for lightning in winter

precipitation. The first maximum in winter lightning occurred between 0000 and 0400 UTC 02 December with a total of 16 observed lightning events. Of those 56.3%, or 9 events, were cloud flashes, higher than the storm total 43.0%. Only 7 of those events were CG strokes. In this case, all observed CG strokes were negative. These events were observed at an average event rate of 0.07 min^{-1} . This time was the maximum time for cloud flashes. While the observed storm total lightning events were slightly less between 0400 and 0800 UTC time frame, the number of CG strokes increased. The percentage of cloud flashes in this time frame is nearly half of the percentage from the previous 4-hour subset where winter lightning was maximized. This smaller percentage remains constant through the remainder of the event. The cloud-to-CG ratio for this maximum time is 1.3, or slightly more than 1 cloud flash to every 1 CG stroke, which falls to 0.37, or 1 cloud flash to almost 3 observed CG strokes, at the CG maximum 4 hours later.

The other maximum time occurred between 2000 UTC on 02 December and 0000 UTC on 03 December, when 35 lightning events associated with winter precipitation were observed. Of those, 28.6% were cloud flashes with the other 71.4% CG strokes. Of those CG strokes, 96.0% were negative CG strokes. The lightning events at this time were observed at an average event rate of 0.15 min^{-1} . The percentage of cloud flashes during this 4-hour subset is closer to the average



a)



b)

Figure 6.1 Storm total lightning trend for both a) the total storm and b) the lightning associated with winter precipitation for 01 December 2007 through 02 December 2007. Time given in hours from the onset of lightning detected in winter precipitation. Date labeled every 12 hours in UTC.

percentage found for cloud flashes in winter lightning from the 2006-2007 winter season.

6.3 Case Study

A synoptic and mesoscale case study including model initial soundings of the most active lightning times and locations for this event were analyzed for a comparison to composite analyses for the 2006-2007 winter season. There were three observed maximum times for lightning analyzed in this section. The first time (0100 UTC) represents a maximum in cloud flashes in winter precipitation, the second time (0800 UTC) represents a maximum in total lightning associated with winter precipitation, dominated by CG strokes, and the third and final time (1800 UTC) represents the overall maximum time for lightning in winter precipitation. Each time will be introduced by radar and satellite imagery of the observed precipitation followed by a synoptic and mesoscale analysis of the event. The subsequent sounding will be presented following the synoptic analysis and then compared back to composite soundings observed in Chapter 5.

6.3.1 Case Overview

6.3.1.1 0100 UTC 02 December 2007

There were three lightning maxima of interest in this case. The first maximum represented a maximum in cloud flash occurrence (Fig. 6.1b) at 0100 UTC on 02 December. The location of this peak occurred at 43.7° N and -87.8° W, north of Milwaukee, Wisconsin along the shore of Lake Michigan (Fig. 6.2).

Figure 6.3 shows this location near a dry intrusion. Composite base reflectivity at this location shows echo returns greater than or equal to 35 dBZ. While this location would normally be associated with lake enhanced convection, a look at the sounding, discussed later, reveals that winds 100 mb above the surface appear more dynamically linked to the synoptic scale situation than the mesoscale influences of lake enhanced snowfall. This association is made so as not to mislead, since the focus of the study is on thundersnow events in the Midwest away from lake enhanced convection.

The GOES-12 IR imagery at this time demonstrates the broad spectrum of synoptic influence in this event. Looking at cloud top temperatures (Fig. 6.4), one can see that temperatures are cool with respect to typically shallow cloud-tops in traditional winter events. At this time, notice the region of temperatures

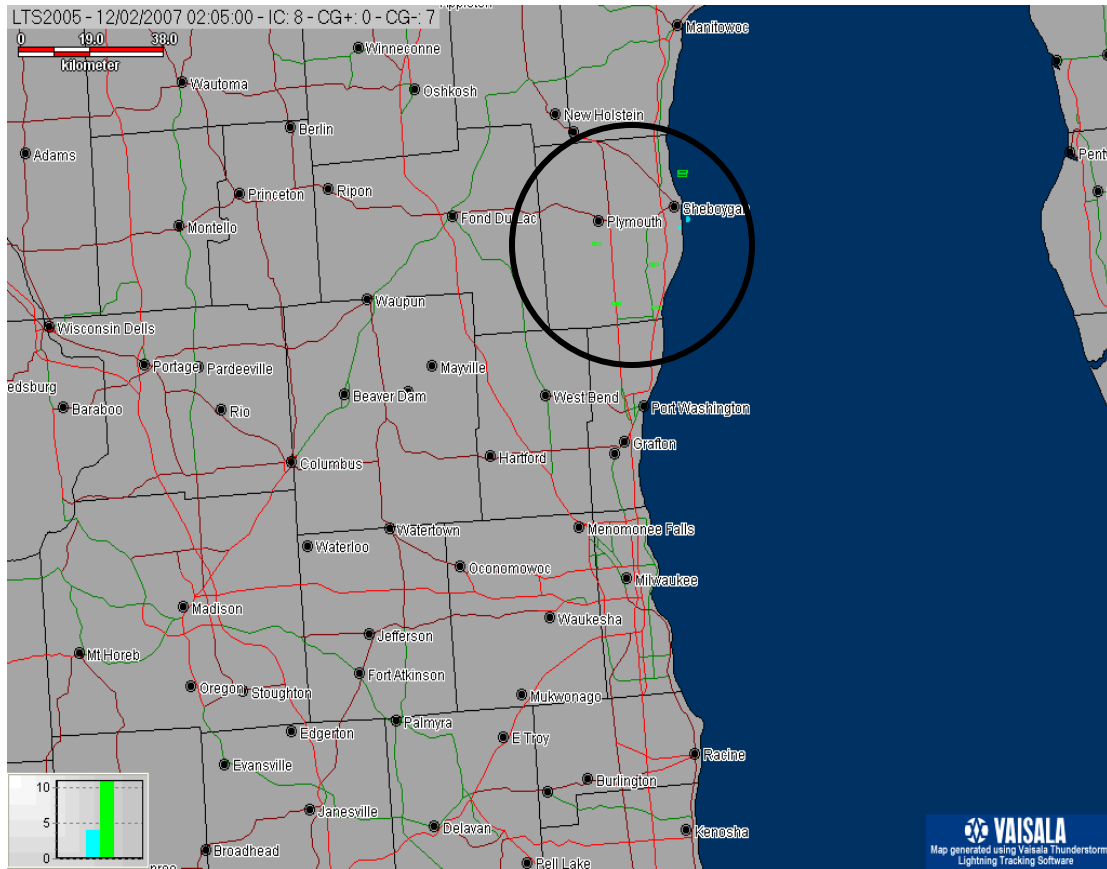


Figure 6.2 Lightning map indicating negative and positive CG strokes and cloud flashes for one hour ending at 0200 UTC 02 December 2007. Sampled lightning circled in black.

at -50°C over east central Wisconsin where lightning and winter precipitation is occurring (Fig. 6.2).

The following section will provide a synoptic and mesoscale analysis of the atmosphere at this time. The surface analysis at this time shows a 998 mb low centered over western Kansas into Iowa northeast of the parent low (Fig. 6.5). Surface temperatures in this region are below freezing with the temperature in northern Illinois at 31°F . The 5400-gpm thickness line, however, is located in northern Wisconsin.

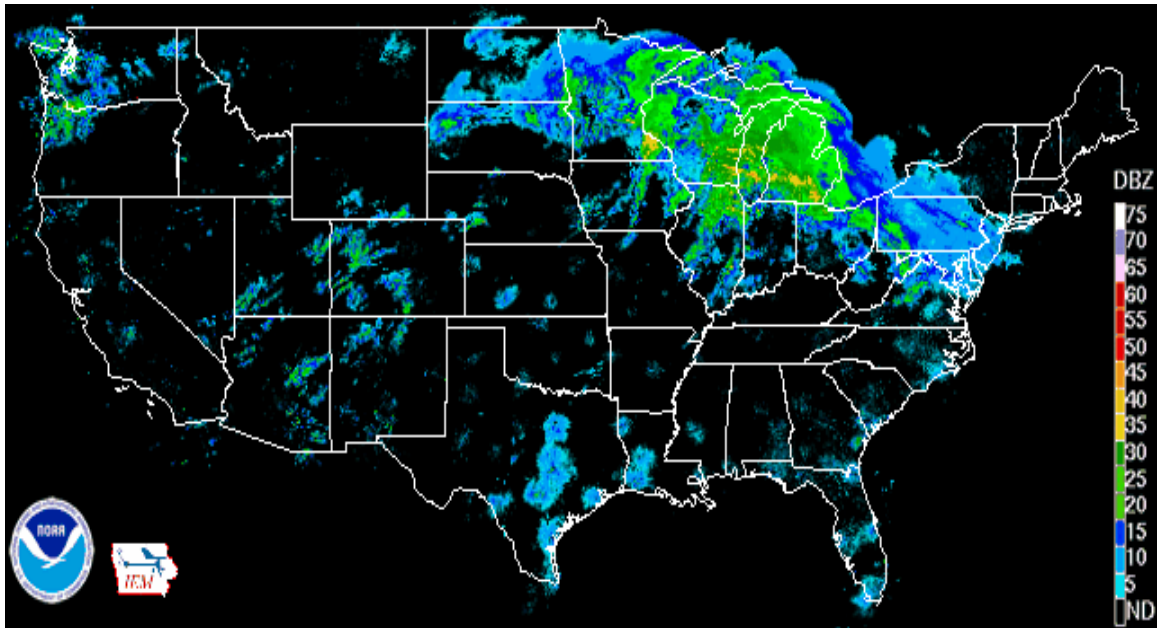


Figure 6.3 National Climate Data Center national base reflectivity radar mosaic valid at 0100 UTC on 02 December 2007.

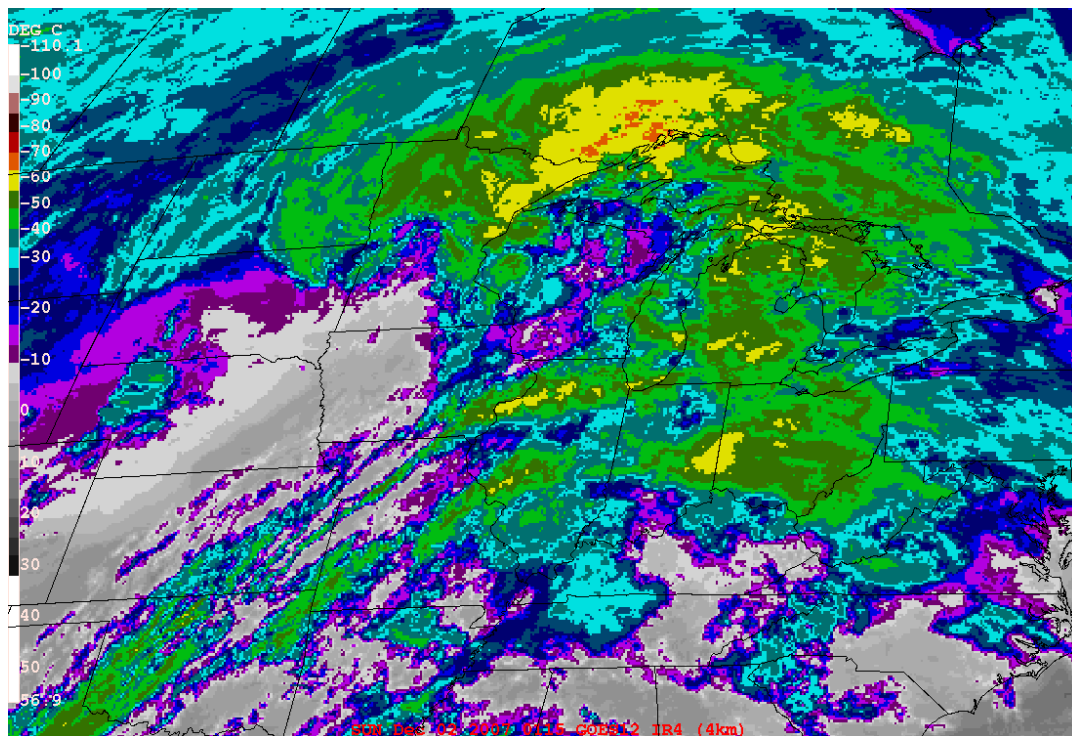


Figure 6.4 GOES-12 IR imagery valid at 0115 UTC 02 December 2007. Cloud top temperatures are shaded in color with color scale representing every 10°C. Colder temperatures are represented by warmer colors.

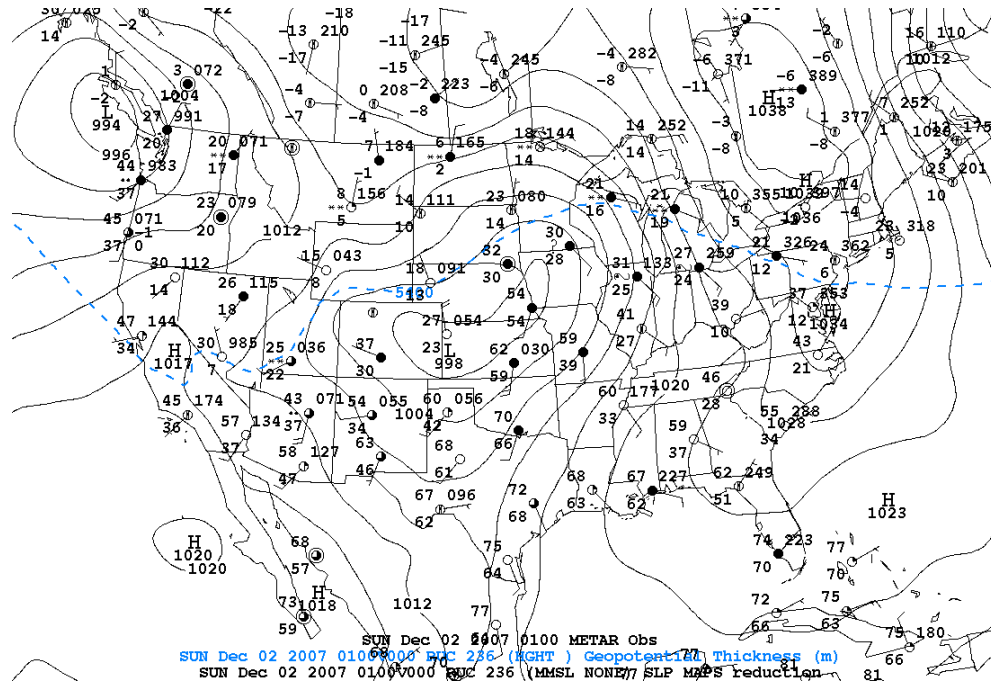


Figure 6.5 RUC initial analysis at mean sea level pressure valid at 0100 UTC 02 December 2007. Sea level pressure contoured in black every 2 mb with 5400 gpm thickness line (500:1000-mb layer) plotted in blue. METAR decoded surface observations are plotted valid at the same time.

Figure 6.6 shows this location coupled between two jet cores at 300 mb where the primary activity is occurring in the right entrance region of a 100-kt polar jet from Ontario, Canada through Hudson Bay and into the Atlantic Ocean. Indeed, maximum wind divergence values at this time are $\geq 3 \times 10^{-5} \text{ s}^{-1}$ over much of southern Wisconsin (not shown). The entrance region is coupled with the left exit region of another 100 kt jet streak from the southwest U.S. Coincidentally, the upstream location in Minnesota is enclosed by a circulation with absolute vorticity values of at least $9 \times 10^{-5} \text{ s}^{-1}$ at 500 mb (Fig. 6.7). The maximum vorticity is located in east central Minnesota at $27 \times 10^{-5} \text{ s}^{-1}$.

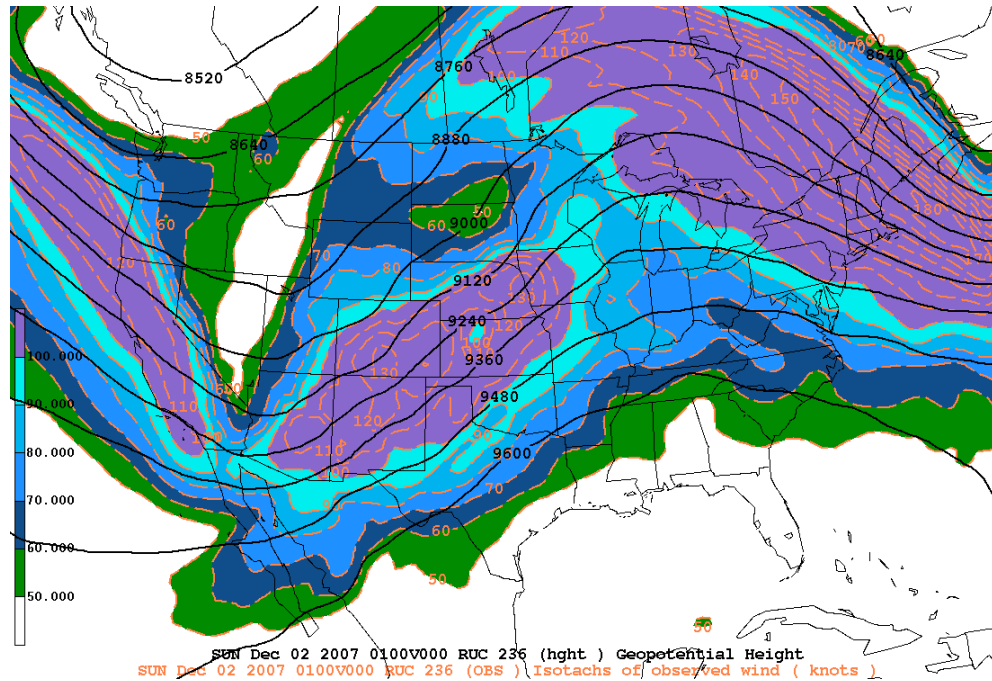


Figure 6.6 RUC initial analysis at 300 mb valid at 0100 UTC 02 December 2007. Geopotential height contoured every 60 gpm and isotachs in kts contoured every 10 kts above 50 kts and shaded.

The 700-mb (Fig. 6.8) Θ_e plot shows a maximum just to the south of the lightning associated with winter precipitation in Figure 6.2 with a small enclosed region of mid-level cold air advection. The region of active winter lightning, though, is dominated by warm air advection at 700 mb with values near $2.4 \times 10^{-4} \text{ K s}^{-1}$.

The 850-mb analysis (Fig. 6.9) shows a closed low over Minnesota and extending into Colorado with the center analyzed over southwestern Minnesota and a trough axis through Wisconsin along an elevated warm frontal boundary. Notice the weak thermal ridge at 850 mb building into Lake Michigan providing

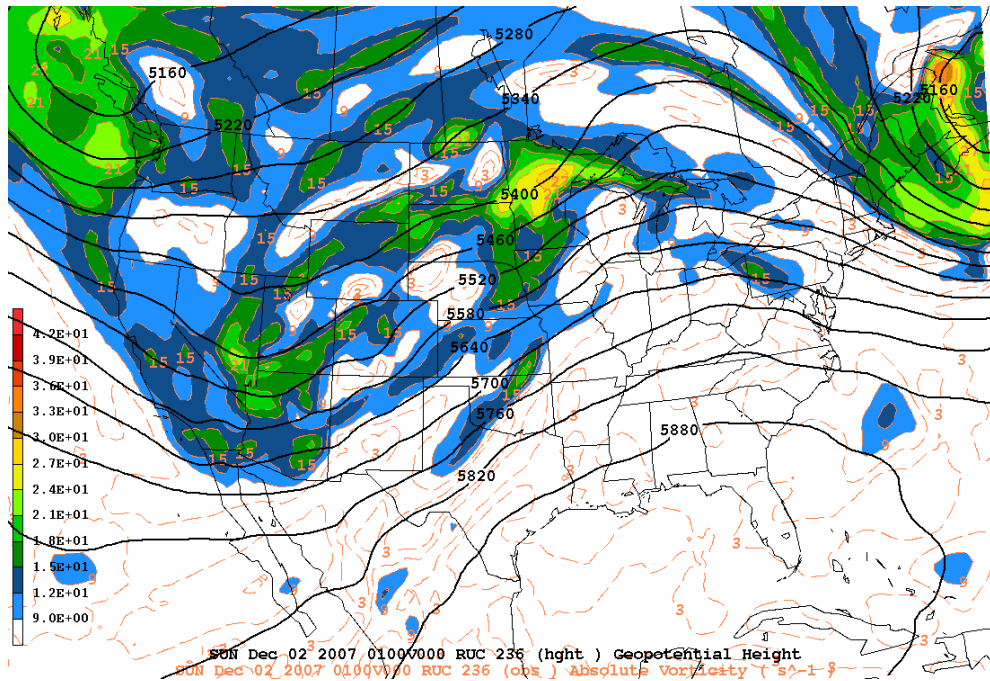


Figure 6.7 RUC initial analysis at 500 mb valid at 0100 UTC 02 December 2007. Geopotential height contoured every 60 gpm and absolute vorticity contoured every $3 \times 10^{-5} \text{ s}^{-1}$ and shaded above $9 \times 10^{-5} \text{ s}^{-1}$.

further thermal instability. Further notice the moisture gradient located along this axis, particularly in east central Wisconsin where the winter lightning in Figure 6.2 is maximized at this time. The winter lightning is under a relative humidity of $>90\%$ at this time at 850 and 700 mb. Drier air at 850 mb is located within 50 km while drier air aloft at 700 mb is located between 300 and 325 km from the winter lightning. The dry air proximity appears to be a result of a dry slot associated with a dry conveyor belt of ascending warm air. This warm air ascension would help to destabilize elevated levels of the atmosphere (above 850 mb) creating essential vertical or slantwise motion to gain enough charge

separation to generate lightning. This will further be confirmed in the sounding, which is nearly saturated through the column. It can be inferred that the most active lightning lay on the moist side of the gradient between 850 and 700 mb.

The 900-mb analysis (Fig. 6.10) shows a similar picture with the low centered over southwestern Minnesota and a trough axis extending eastward through Wisconsin and the Great Lakes. The region is fully dominated by warm air advection in the lower levels (at least $2.4 \times 10^{-4} \text{ K s}^{-1}$). Cold air advection is present to the north most likely associated with a trough of warm air aloft (TROWAL) structure. This is a result of descending cold, dry enclosing a layer of elevated warm air (Martin 1998a,b). The most active winter lightning from Figure 6.2 is downstream of the TROWAL in this case.

Figure 6.11 helps to establish the presence of elevated instability in this system. The left panel of Figure 6.11 shows the three-dimensional equivalent potential vorticity (EPV) at 700 mb (McCann 1995). Three dimensional EPV is commonly used as a determinant for elevated instability associated with conditional symmetric instability (CSI) commonly associated with slantwise convection. The units for EPV are potential vorticity units (PVU; $10^{-7} \text{ K m}^2 \text{ kg}^{-1} \text{ s}^{-1}$). The presence of negative values of EPV in the middle troposphere indicates a potentially unstable atmosphere that can be released in the presence of a

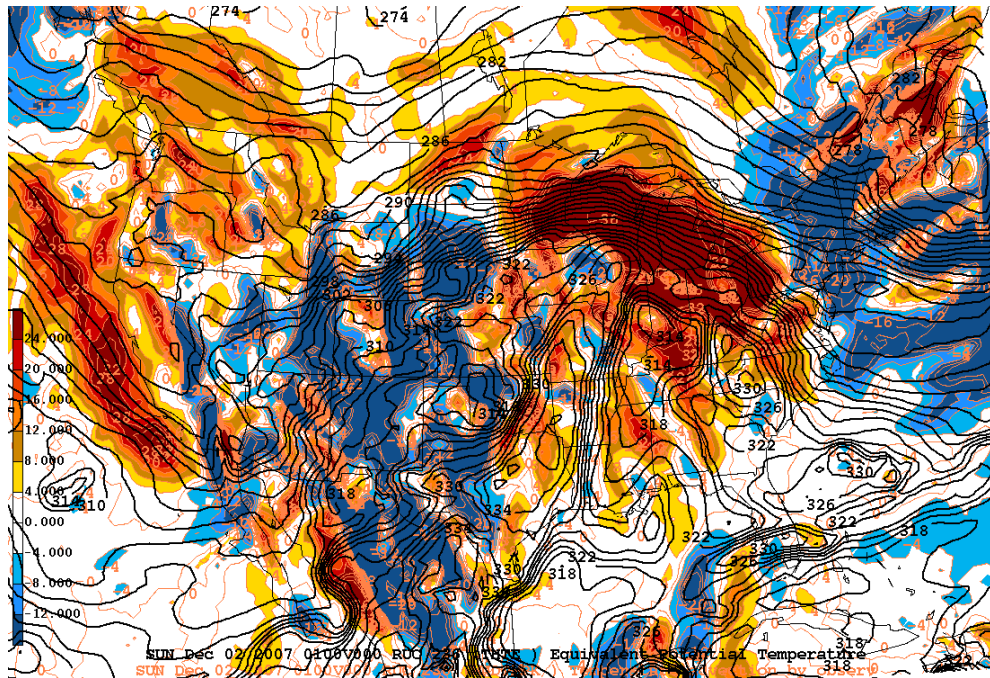


Figure 6.8 RUC initial analysis at 700 mb valid at 0100 UTC 02 December 2007. Equivalent potential temperature contoured every 2 K and temperature advection contoured every 4×10^{-5} K s⁻¹. Positive values of temperature advection are shaded in warm colors and negative values of temperature advection are shaded in cool colors occurring at this time.

forcing mechanism. During this time, there is a narrow band of negative values of EPV (≤ -0.25 PVU) just to the south of the active winter lightning from Figure 6.2. Some lightning was further observed in this region (not shown). A strong gradient to slightly positive values (≤ 0.25 PVU) exists where our sample of active winter lightning is located. On the right side is the sigma squared (σ^2) growth rate parameter (Bennetts and Hoskins 1979, Bennetts and Sharp 1982) used to assess the instability of a storm in terms of the formation of mesoscale precipitation bands. It has been found (Melick et al. 2007) that a positive value of at least 0.2 h^{-2} represents a higher probability of forming mesoscale precipitation

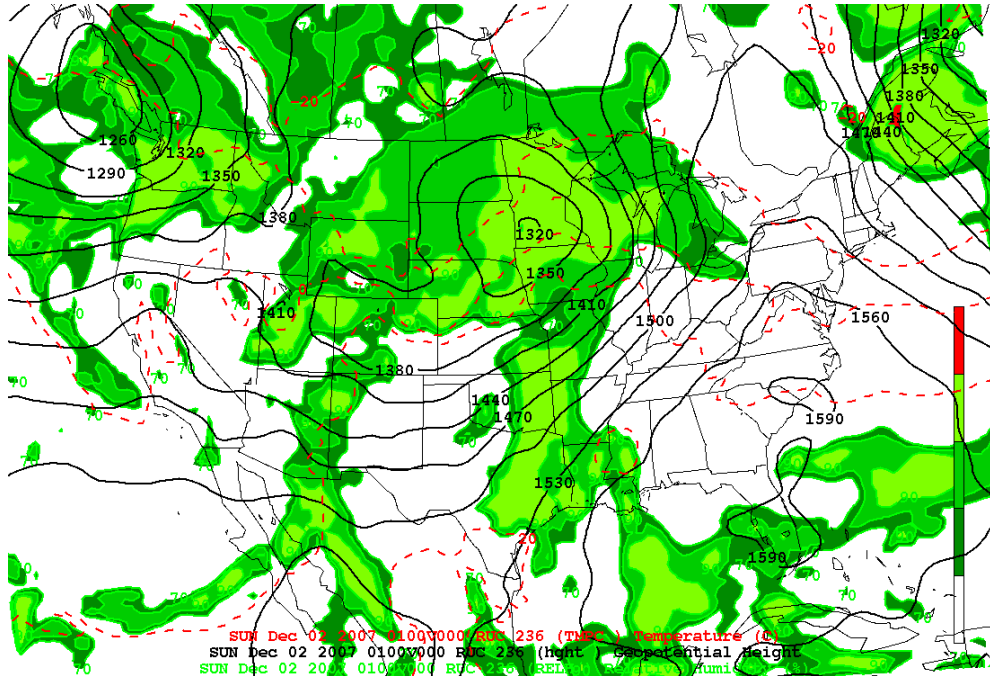


Figure 6.9 RUC initial analysis at 850 mb valid at 0100 UTC 02 December 2007. Geopotential height contoured in black every 30 gpm and temperatures contoured in red dashed every 10°C. Relative humidity contoured and shaded every 10% above 70%.

bands. The right side of Figure 6.11 shows contoured regions of greater than 0.1 h^{-2} centered over the Wisconsin-Illinois border coincident with where the greatest EPV reduction zone exists. Slightly west of the winter lightning (Fig. 6.2), values are still slightly positive. However, the winter lightning is mostly occurring in the gradient.

The resultant sounding from this synoptic and mesoscale situation is shown in Figure 6.12. The sounding, valid at 0100 02 December, is located at the grid point encompassing the winter lightning in Figure 6.2. The sounding shows

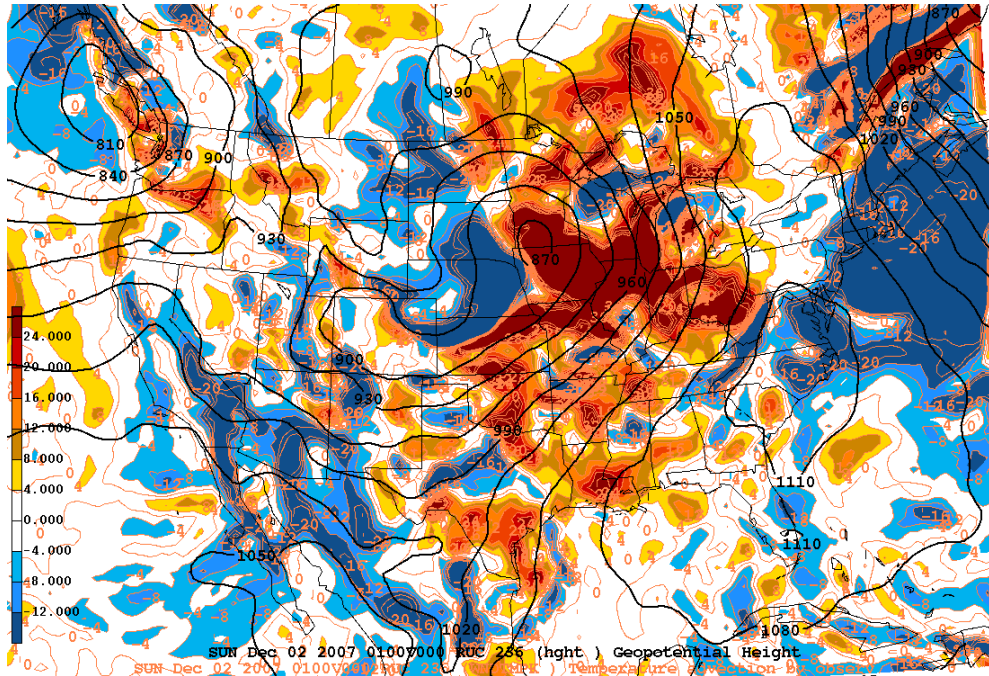


Figure 6.10 RUC initial analysis at 900 mb valid at 0100 UTC 02 December 2007. Height contoured in black every 30 gpm and temperature advection contoured every $4 \times 10^{-5} \text{ K s}^{-1}$. Positive values are shaded in warm colors and negative values are shaded in cool colors.

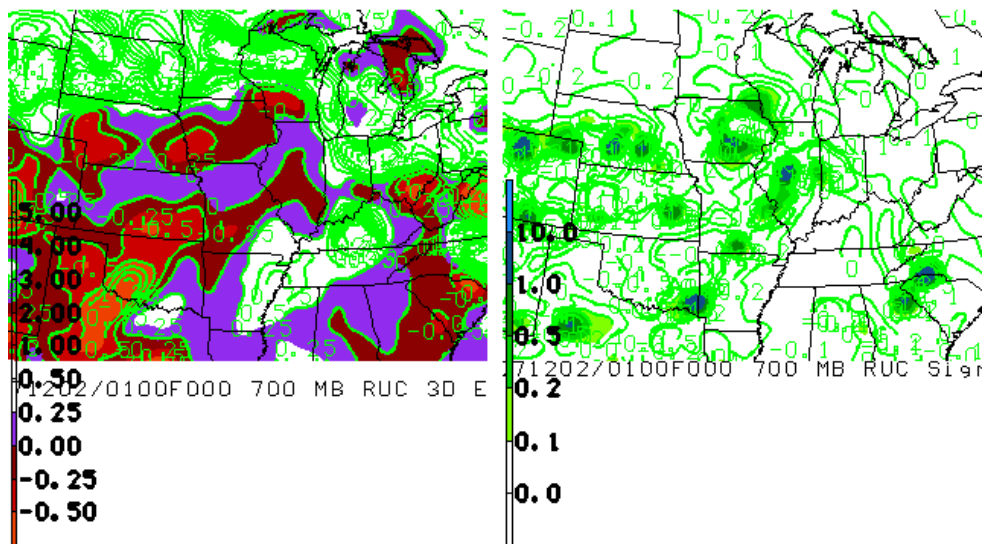


Figure 6.11 Stability profile valid at 0100 UTC 02 December 2007. Left panel is 3-dimensional equivalent potential vorticity. Shaded contours represent values of 0.25 PVU and less. The right panel is the σ^2 growth-rate parameter shaded for values above 0.1 h^{-2} .

a nearly saturated profile extending almost entirely up the column from the surface to 400 mb. A steep frontal inversion is located from just above the surface, at 900 mb, to its warmest point at 700 mb. The atmosphere remains completely below 0°C through the profile, fully supportive of snowfall. Looking at the increasing Θ_e profile with height (Fig. 6.12), the sounding becomes potential stable above the frontal inversion up to 550 mb, which is analyzed as the most unstable parcel. Above 550 mb, the profile becomes moist adiabatic. The overall profile is similar to the full NE and NW composite soundings, presented in sections 5.2 and 5.3 respectively, with the steep frontal inversion and moist adiabatic profile above. Although this lightning is NE of the low, the sounding is most similar to the NW composite where the MULPL was more elevated at 550 mb. However, it differs in that this profile remains saturated almost entirely up to the tropopause whereas the composite images typically dry out above 700 mb. The most unstable parcel level (550 mb) is located above that of the NE composite soundings, which is at 600 mb and at 650 mb for the NE composite in the 0000 to 0400 UTC time frame. The height of the -10°C isotherm in this sounding is 5.5 km (at 500 mb). While the height of the -10°C isotherm in this sounding is much higher than is found in the composites, it fits the stability profile in that it is located above the MULPL. Smith et al. (2005) found that in cases of convective snowfall, the MULPL was typically located below the -10°C

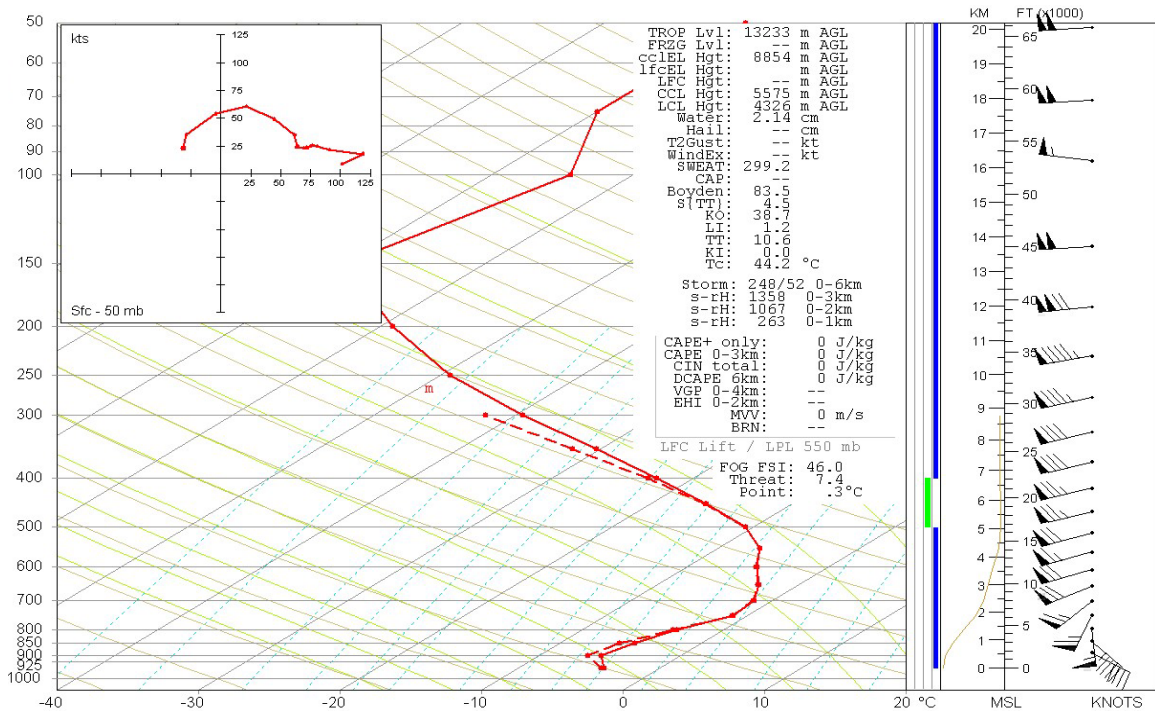


Figure 6.12 0100 UTC December 2, 2007 sounding. Solid red line is temperature, dashed red line is dewpoint, and wind barbs represent wind speeds in kts and wind direction. Vertical Θ_e in yellow to the left of wind barbs.

isotherm. The -20°C isotherm, or the top of the best mixed-phase region, is at 7.0 km, higher than any of the composite analyses. The top of this layer in the warm season soundings are also found at 7.0 km. Additional stability parameters such as TT and KI are fairly low with values of 10.6 and 0.0 respectively. The LI for this sounding (found above the MULPL of 550 mb) is 1.2. The low stability values indicate that the best instability at this time resided well into the upper troposphere and the interaction leading to lightning may have been in the lower

to mid-troposphere, most likely within the steep frontal inversion where ample forcing was expected to reside.

6.3.1.2 0800 UTC 02 December 2007

The second maximum in lightning associated with winter lightning, according to Figure 6.1b, is at 0800 UTC on 02 December. This time represents a second winter lightning peak, more specifically a local maximum in CG strokes. This region was located in northern Michigan at this time at 45.0° N and -83.9° W (Fig. 6.13). Figure 6.14 shows the NCDC national base reflectivity mosaic valid at 0800 UTC. The imagery shows a radar echo of greater than 30 dBZ located over northern Michigan. While this region is located near the Great Lakes region, the lower level winds shown later indicates a southerly flow over land into this region. This system is also quite dynamically active, so the mesoscale influence of the lake can be ignored.

GOES-12 IR imagery (Fig. 6.15) shows little in the way of convective precipitation occurring at this time in this region. A small region with colder cloud tops appear in this region, but with a cloud top temperature of -20°C , warmer than the cloud top temperature from 0100 UTC.

The following presents the synoptic and mesoscale situation of this winter lightning (Fig. 6.13). The active winter lightning in focus is located in northern

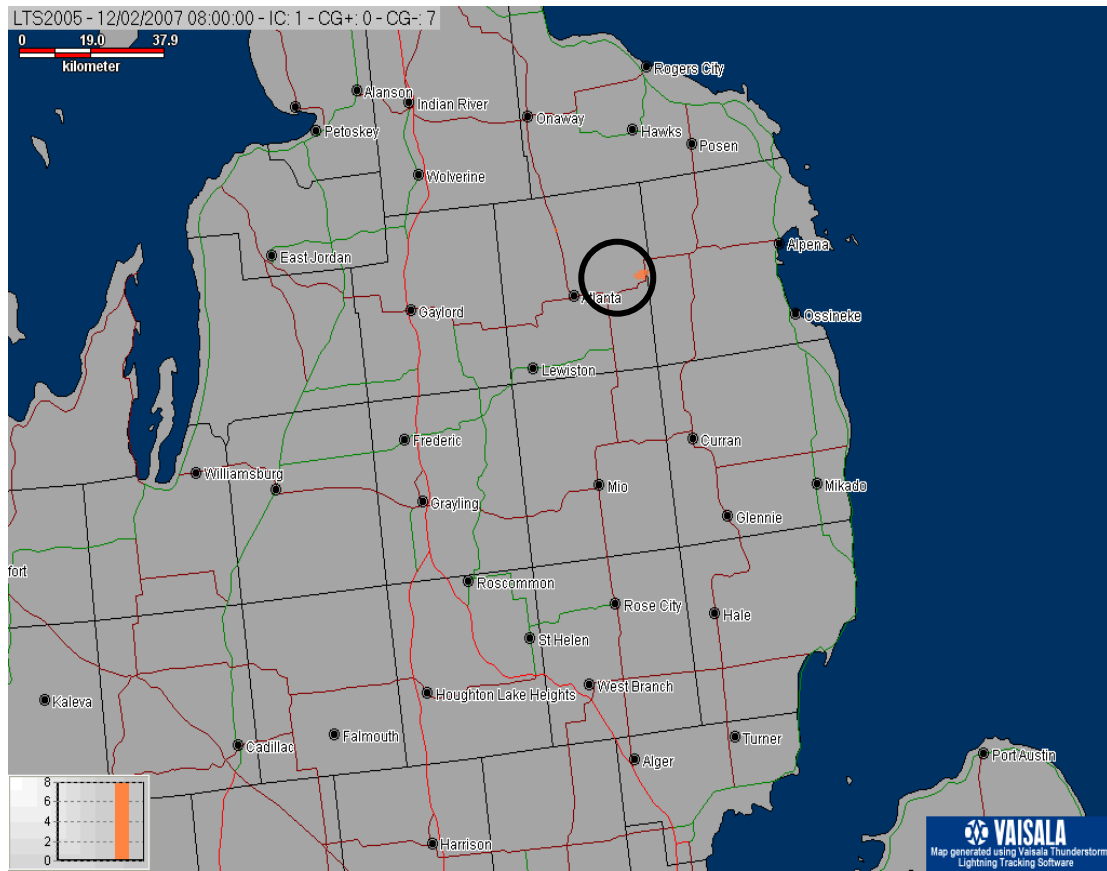


Figure 6.13 Lightning map indicating negative and positive CG strokes and cloud flashes for one hour ending at 0800 UTC 02 December 2007. Sampled lightning strokes circled in black.

Michigan, northeast of the parent surface low. The low is centered over southeastern Minnesota at 1004 mb with a broad 1008 mb contour extending from Minnesota and Wisconsin southwest into Kansas and Oklahoma. Surface temperatures (Fig. 6.16) range from -2.2°C (28°F) in northern Michigan to -1.1°C (30°F) in northern Ohio. According to the surface analysis, the region from Figure 6.13 indicating lightning in winter precipitation is again northeast of the low in a strong southerly flow due to the tightened pressure gradient.

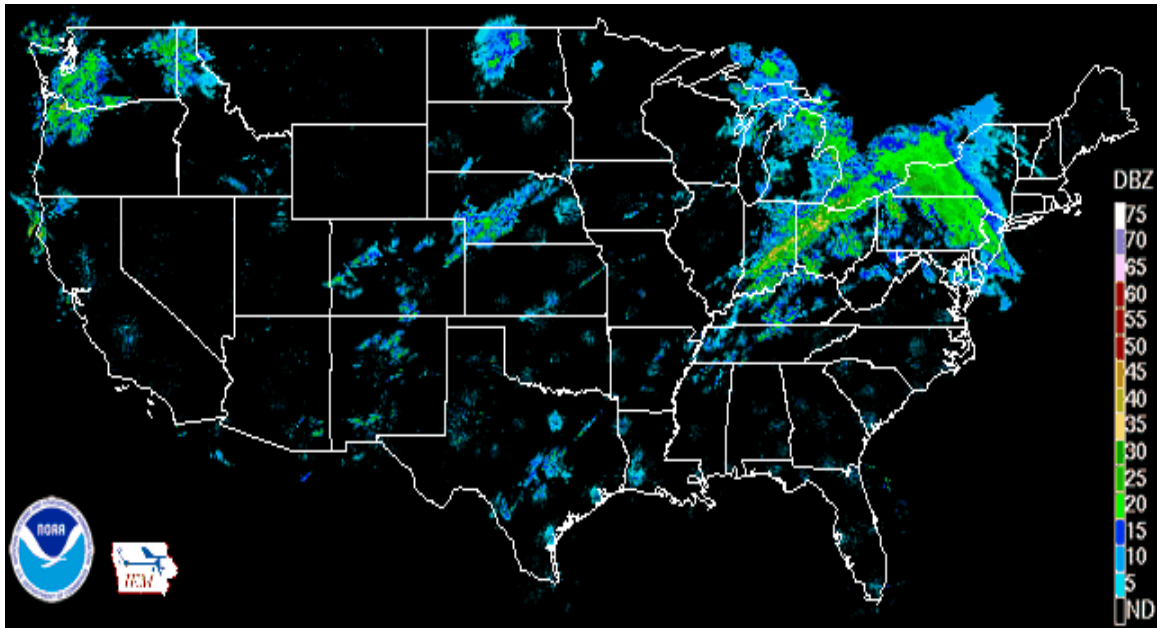


Figure 6.14 National Climate Data Center national base reflectivity radar mosaic valid at 0800 UTC on 02 December 2007.

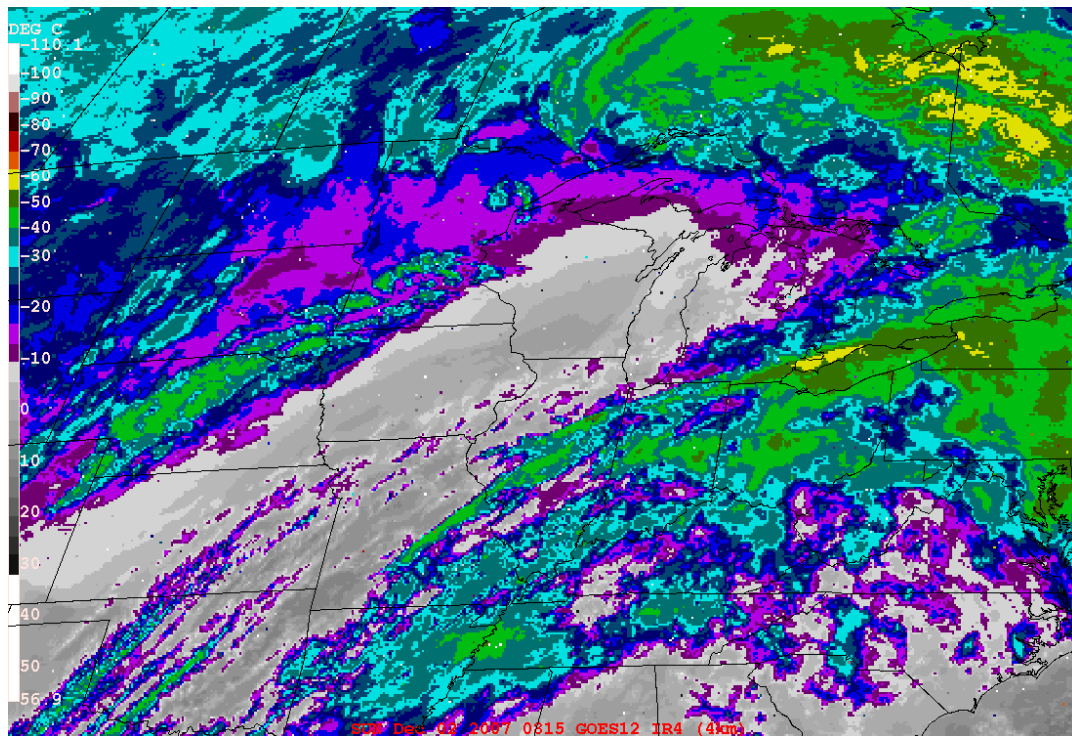


Figure 6.15 GOES-12 IR imagery valid at 0815 UTC 02 December 2007. Cloud top temperatures are shaded in color with color scale representing every 10°C. Colder temperatures are represented by warmer colors.

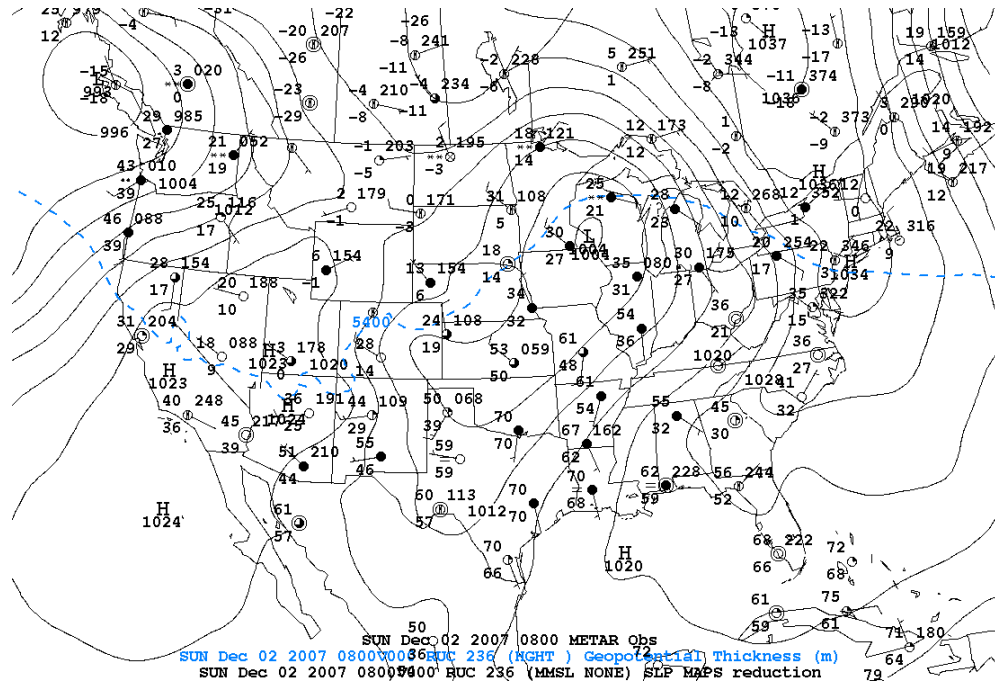


Figure 6.16 RUC initial analysis at mean sea level pressure valid at 0800 UTC 02 December 2007. Sea level pressure contoured in black every 2 mb with 5400 gpm thickness line (500:1000-mb layer) plotted in blue. METAR decoded surface observations are plotted valid at the same time.

A previously coupled jet stream has broadened to a 110-kt jet streak extending from Oklahoma northeastward towards Michigan and into Canada (Fig. 6.17). A wind divergence of $\leq 1 \times 10^{-5} \text{ s}^{-1}$ exists at this location, but is within 100 km of values $\geq 3 \times 10^{-5} \text{ s}^{-1}$ (not shown).

Similar to 0100 UTC, the region in northern Michigan where lightning is occurring (Fig. 6.13) is enclosed by a circulation of absolute vorticity with values of at least $9 \times 10^{-5} \text{ s}^{-1}$ (Fig. 6.18). Vorticity extends along the 500-mb shortwave axis with values of $15 \times 10^{-5} \text{ s}^{-1}$ to the maximum vorticity at the base of the shortwave at $33 \times 10^{-5} \text{ s}^{-1}$.

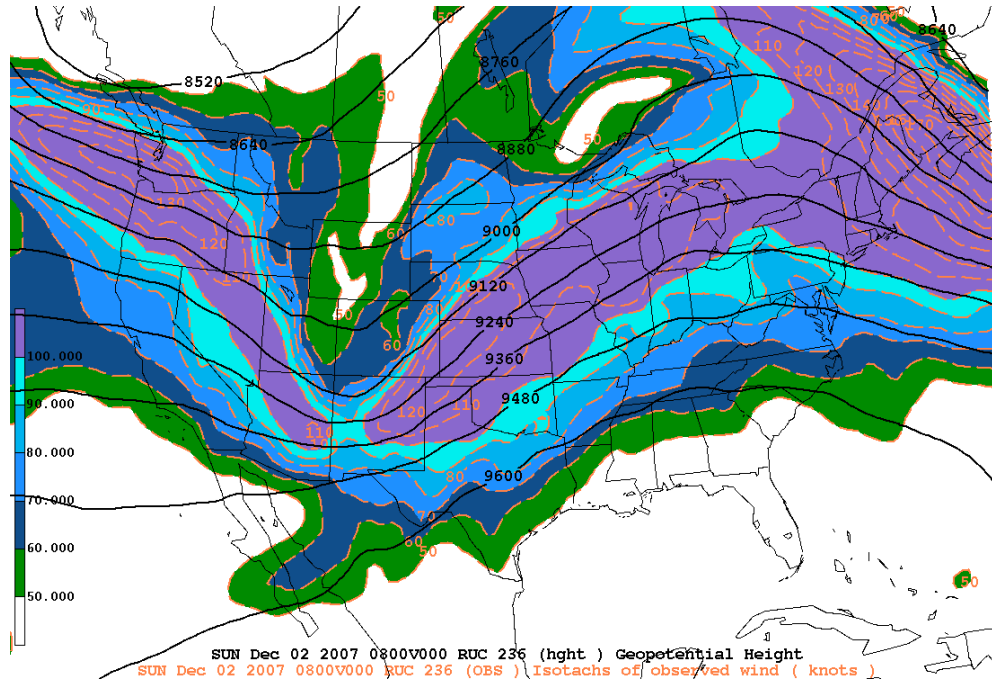


Figure 6.17 RUC initial analysis at 300 mb valid at 0800 UTC 02 December 2007. Geopotential height contoured every 60 gpm and isotachs in kts contoured every 10 kts above 50 kts and shaded.

Figure 6.19 shows the region under the influence of fairly strong warm air advection in the middle troposphere with values greater than $3.0 \times 10^{-4} \text{K s}^{-1}$. Further, northern Michigan is under a 700-mb Θ_e gradient that extends southwest and around Lake Superior. Θ_e maxima are present to the south in Indiana and ridging occurs into Wisconsin and northeast into Michigan. The ridging into Wisconsin appears to be the beginning of the TROWAL circulation. The strong mid-level warm air advection immediately to the north of this Θ_e ridge would represent a warm conveyor belt.

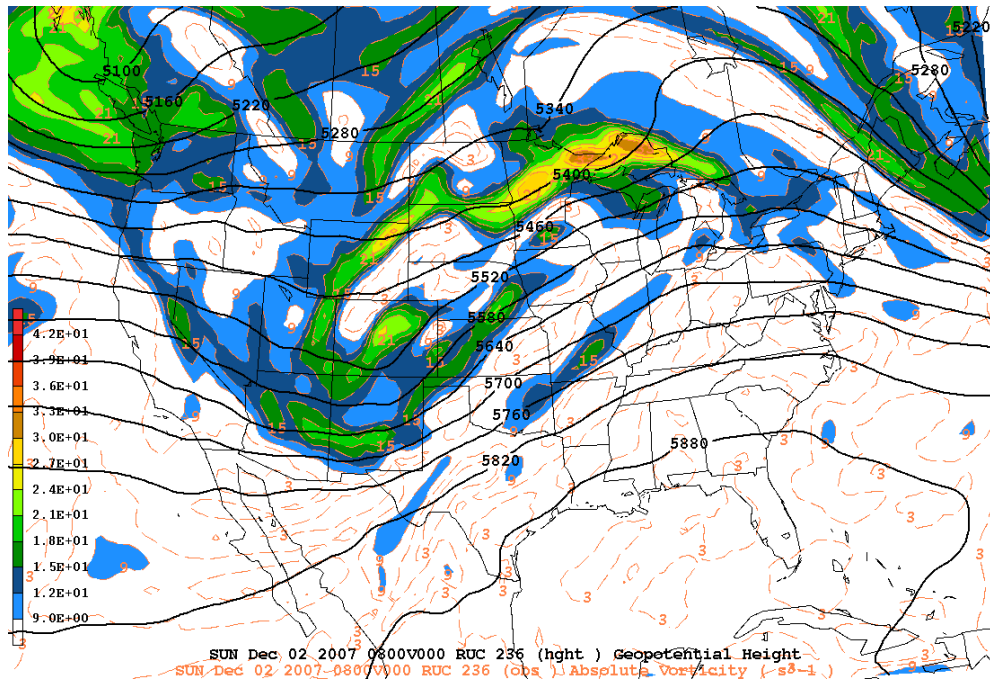


Figure 6.18 RUC initial analysis at 500 mb valid at 0800 UTC 02 December 2007. Geopotential height contoured every 60 gpm and absolute vorticity contoured every $3 \times 10^{-5} \text{ s}^{-1}$ and shaded above $9 \times 10^{-5} \text{ s}^{-1}$.

The center of the closed low at 850 mb (Fig. 6.20) is over western Wisconsin by this time just upstream from a small thermal ridge extending into eastern Wisconsin. Another small thermal ridge is further downstream extending from north central Ohio across Lake Erie and into Canada. The location of active lightning (Fig. 6.13) is in the thermal trough between these ridges. Of particular interest is the location of the active lightning with respect to the moisture gradient. The lightning is found in RH greater than 90% at 850 and 700 mb, but is only about 200 km from RH < 70% at 850 mb and between 400 and 450 km from RH < 70% at 700 mb indicating proximity to dry air, assumed to be

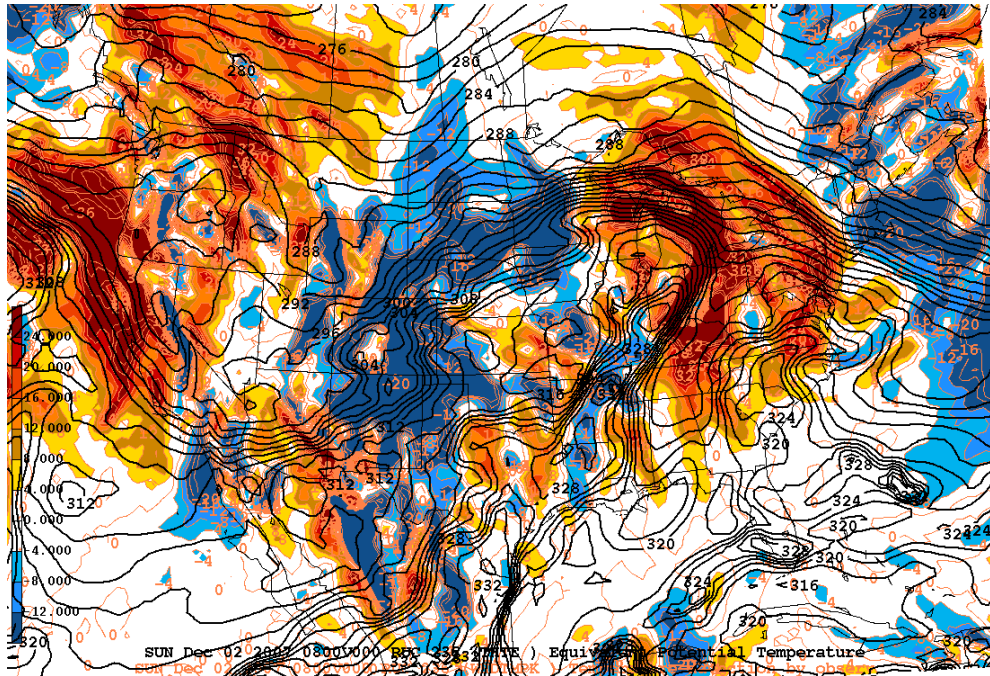


Figure 6.19 RUC initial analysis at 700 mb valid at 0800 UTC 02 December 2007. Equivalent potential temperature contoured every 2 K and temperature advection contoured every $4 \times 10^{-5} \text{ K s}^{-1}$. Positive values of temperature advection are shaded in warm colors and negative values of temperature advection are shaded in cool colors occurring at this time.

the associated dry slot. The rapid drying occurs in northern Michigan and east central and southeast Michigan

The 900-mb closed low is collocated with the 850-mb low over western Wisconsin (Fig. 6.21). The region is dominated by warm air advection with values of greater than $2.4 \times 10^{-4} \text{ K s}^{-1}$. However, a couplet with cold air advection is present just to the north and east of this region indicating that potential temperatures have already reached their maximum and the cyclone is likely beginning its decay (Market et al. 2004).

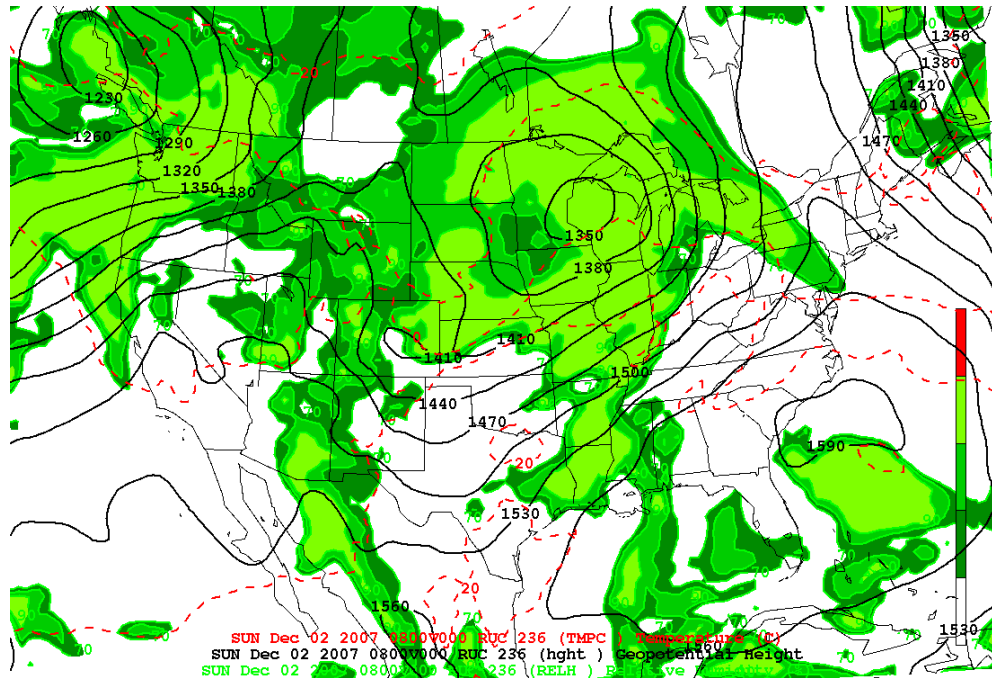


Figure 6.20 RUC initial analysis at 850 mb valid at 0800 UTC 02 December 2007. Geopotential height contoured in black every 30 gpm and temperatures contoured in red dashed every 10°C. Relative humidity contoured and shaded every 10% above 70%.

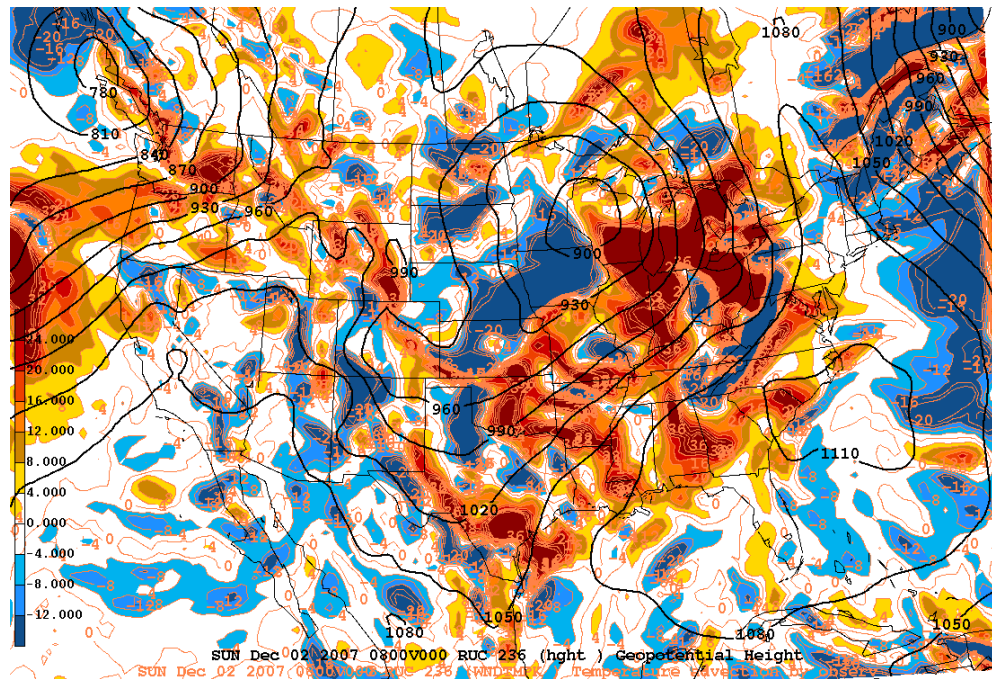


Figure 6.21 RUC initial analysis at 900 mb valid at 0800 UTC 02 December 2007. Geopotential height contoured in black every 30 gpm and temperature advection contoured every $4 \times 10^{-5} \text{ K s}^{-1}$. Positive values of temperature advection are shaded in warm colors and negative values of temperature advection are shaded in cool colors.

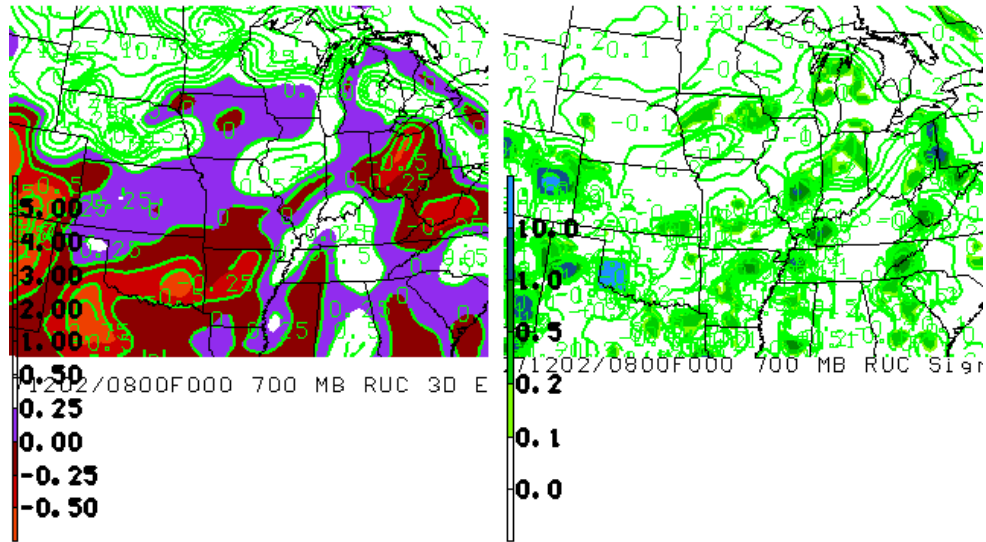


Figure 6.22 Stability profile valid at 0800 UTC 02 December 2007. Left panel is 3-dimensional equivalent potential vorticity. Shaded contours represent values of 0.25 PVU and less. The right panel is the σ^2 growth-rate parameter shaded for values above 0.1 h^{-2} .

Figure 6.22 shows a swath of slightly positive values of EPV (between 0 and 0.25 PVU) through central Michigan with a gradient towards more positive values ($\geq 0.25 \text{ PVU}$) eastward. The winter lightning location (Fig. 6.13) at this time lies within the gradient of increasing values. On the right, σ^2 values of $> 0.1 \text{ h}^{-2}$ are present just to the west of the winter lightning in northern Michigan with values between 0 and 0.1 h^{-2} .

The resultant sounding at this time (Fig. 6.23) has a shallow frontal inversion extending from 800 mb to 700 mb. The increasing Θ_e from 700 mb up to 550 mb reveals a potentially stable layer (Fig. 6.23). 550 mb is the diagnosed MULPL for this sounding. The sounding is saturated from the bottom of the frontal inversion at 800 mb to just above the MULPL at 500 mb. Again, this is a

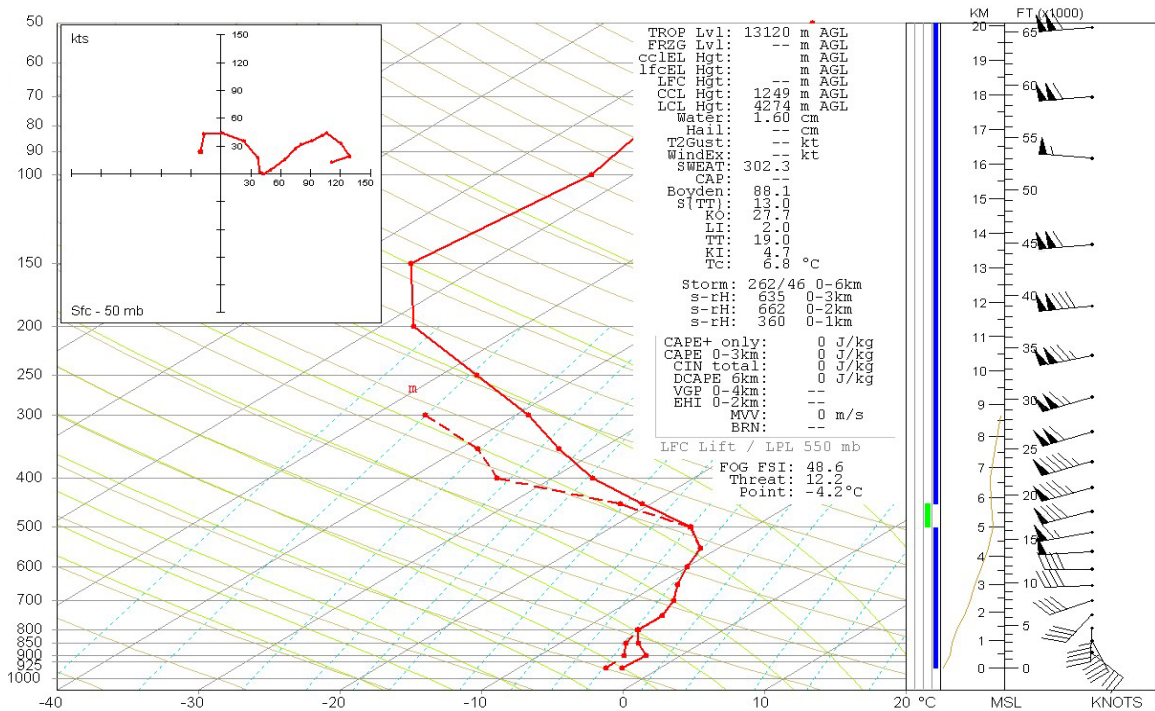


Figure 6.23 0800 UTC December 2, 2007 sounding. Solid red line is temperature, dashed red line is dewpoint, and wind barbs represent wind speeds in kts and wind direction. Vertical Θ_e in yellow to the left of wind barbs.

fairly elevated event. Given the synoptic situation, height falls in this region are such that 500 mb is relatively closer to the ground. Further, there is no potential instability. Stability parameters for this time indicate a slightly more unstable environment, with a TT and a KI of 19.0 and 4.7 respectively. The LI for this profile was slightly higher at 2.0. No CAPE was present in this profile. The greatest shear in this sounding occurred in the lowest 2 km of the troposphere as winds veered from 138° at 31 kts at the surface to 270° at 42 kts at 650 mb. While a significant amount of speed shear is not present, the veering is representative of warm air advection into the lower levels of the troposphere, similar to an

elevated event. The height of the -10°C isotherm for this profile is considerably lower than the 5.0 km in the 0100 UTC sounding, at 4.2 km above ground level. In pressure space, the height of this isotherm is just at 600 mb. This isotherm in the NE composite sounding in section 5.2 is at 4.0 km. The -20°C isotherm in this sounding is located at 6.3 km above the ground, again below the sounding valid from 0100 UTC and slightly above the composite sounding at 5.7 km.

6.3.1.3 1800 UTC 02 December 2007

The final most active period of the winter lightning and the most active portion of the entire storm, according to Figure 6.1b, is at 1800 UTC on 02 December 2007. This time period also matched the most active period for the entire storm, including those lightning events observed in warm air as well. During this time, there were 35 lightning events found in winter precipitation, 10 of those being cloud flashes and the other 25 were CG strokes. 24 of those CG strokes had a negative polarity. The overall distribution of lightning events in winter precipitation showed the maximum occurrence between 0000 and 0400 UTC, which was not the case in this particular situation. The average location for this lightning activity occurred at 42.6° N and -88.9° W , between Milwaukee, Wisconsin, and Chicago, Illinois (Fig. 6.24). Figure 6.25 shows the NCDC national base reflectivity radar mosaic valid at 1800 UTC 02 December indicating

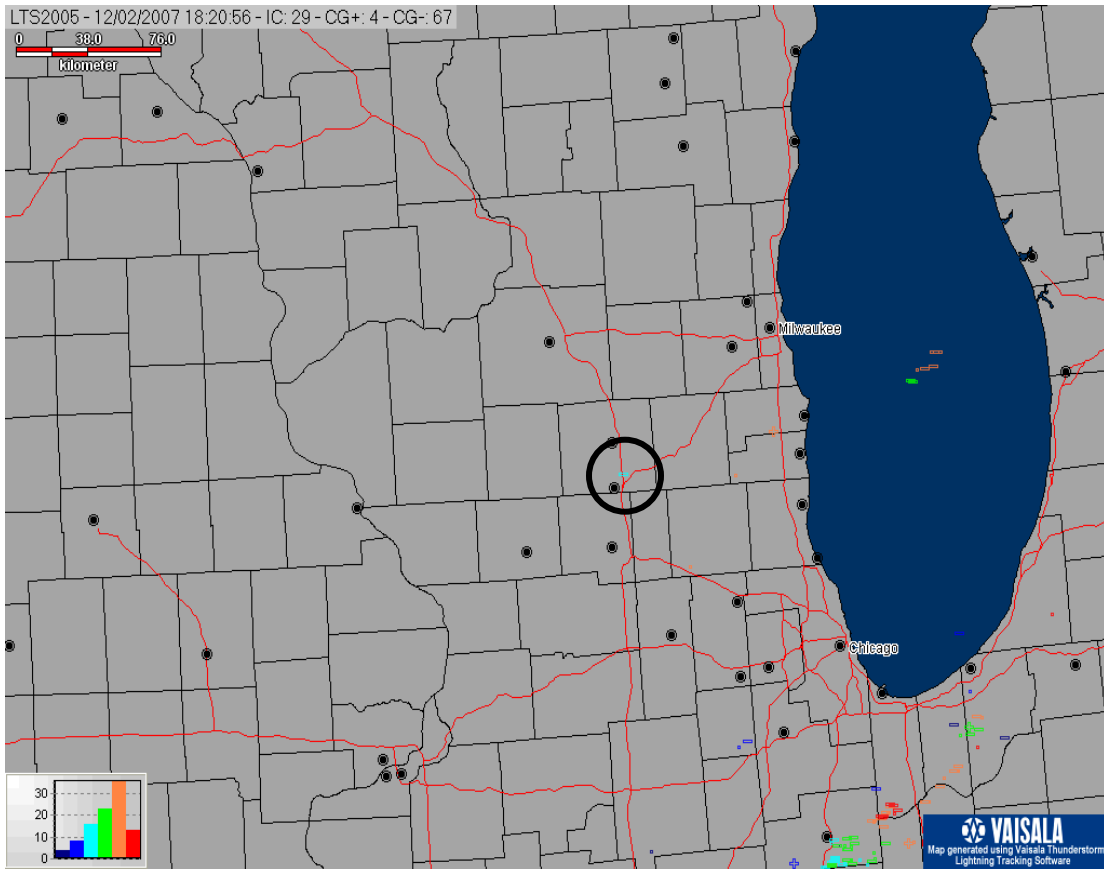


Figure 6.24 Lightning map indicating negative and positive CG strokes and cloud flashes for one hour ending at 1800 UTC 02 December 2007. Sampled lightning stroke circled in black.

a band of precipitation falling in this region with reflectivity values of greater than 25 dBZ. GOES-12 IR imagery (Fig. 6.26) indeed supports some type of convection over this region. Further, the IR reveals an area of cloud top temperatures below -50°C . Also, this area of cold cloud top temperatures is an isolated region of convection as will be determined by regions of synoptic forcing and gradients of advection in the lower and mid-troposphere and moisture.

During this time, the center of the surface low was found over Lake Michigan with the trough axis extending down through Illinois, Missouri,

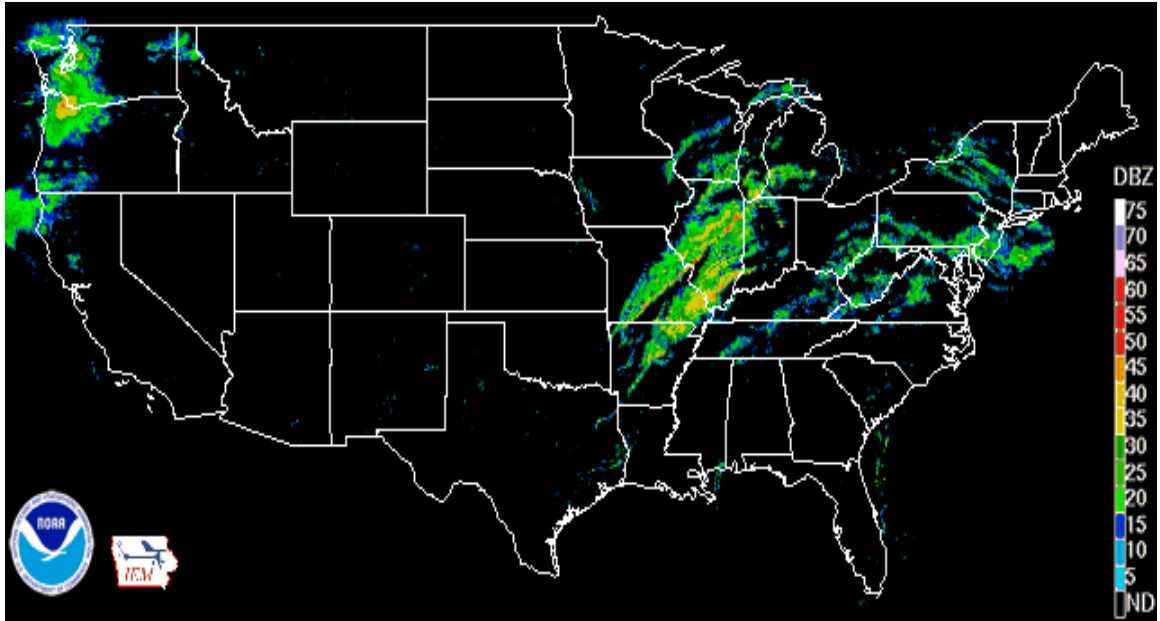


Figure 6.25 National Climate Data Center national base reflectivity radar mosaic valid at 1800 UTC on 02 December 2007.

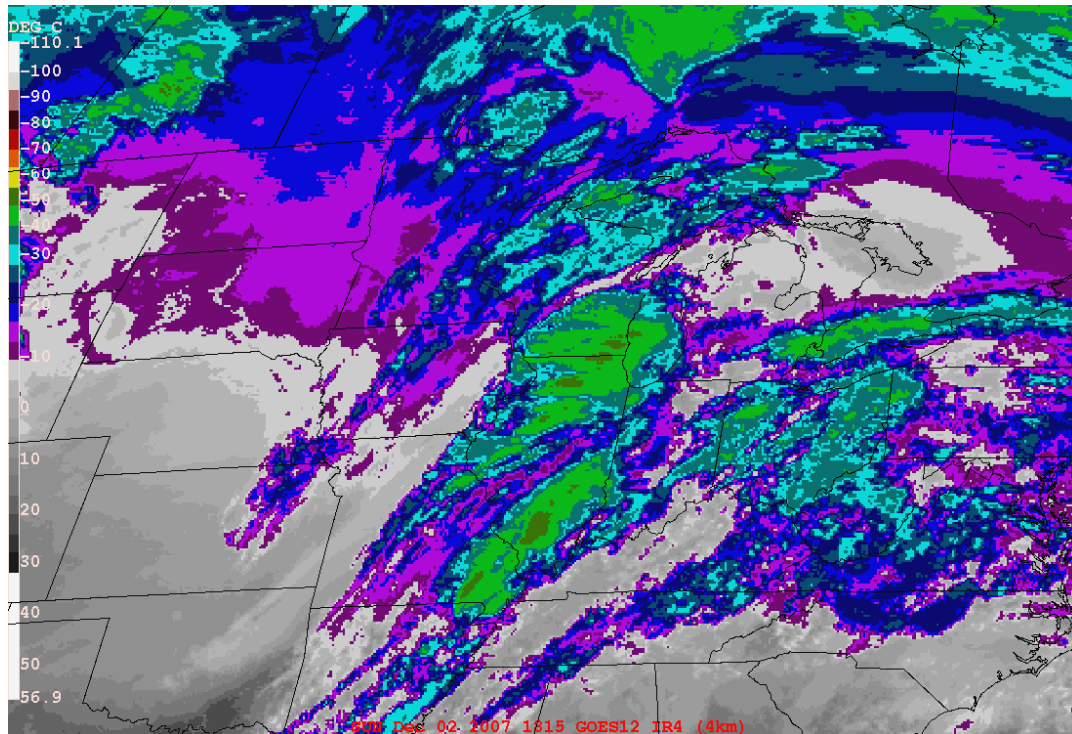


Figure 6.26 GOES-12 IR imagery valid at 1815 UTC 02 December 2007. Cloud top temperatures are shaded in color with color scale representing every 10°C. Colder temperatures are represented by warmer colors.

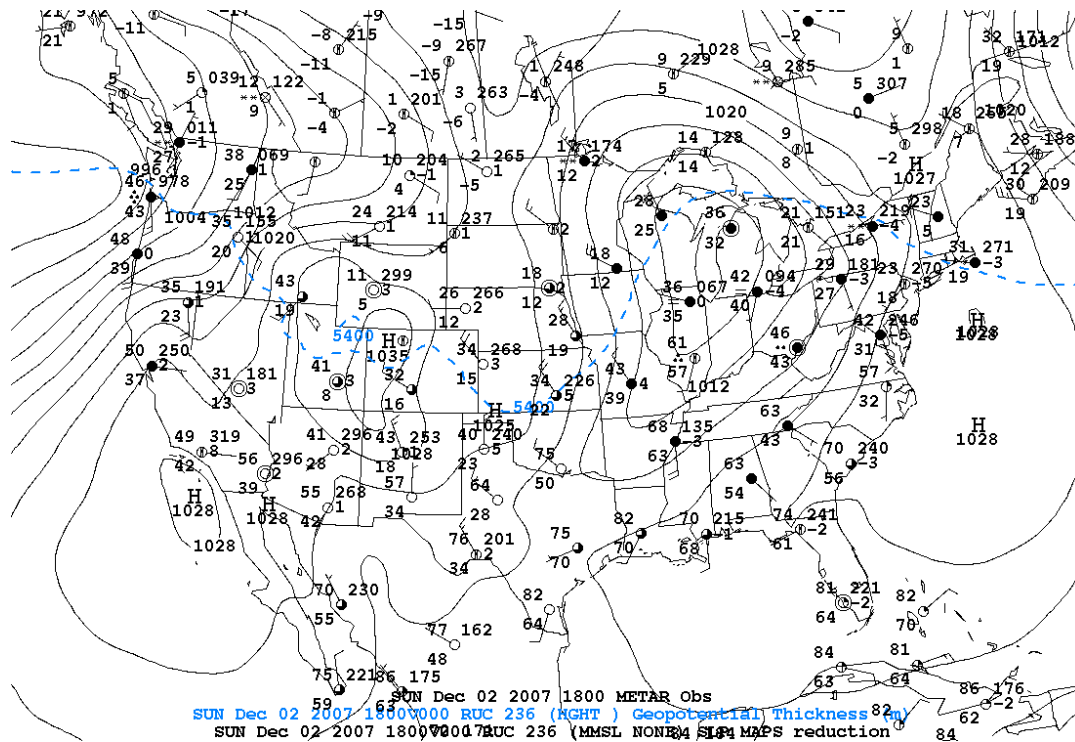


Figure 6.27 RUC initial analysis at mean sea level pressure valid at 1800 UTC 02 December 2007. Sea level pressure contoured in black every 2 mb with 5400 gpm thickness line (500:1000-mb layer) plotted in blue. METAR decoded surface observations are plotted valid at the same time.

Arkansas and Texas (Fig. 6.27). Looking at the 500:1000 mb thickness line, the thermal ridge in the presence of the warm and cold fronts has increased slightly with temperatures in Chicago, Illinois at 2.2°C (36°F). The preferred location for lightning at this time was located just north of Chicago, Illinois, and just to the south of Milwaukee, Wisconsin. Temperatures in northern Michigan have risen due to the warm frontal passage by this time with temperatures also at 36°F. With the surface low centered over Lake Michigan and the winter lightning

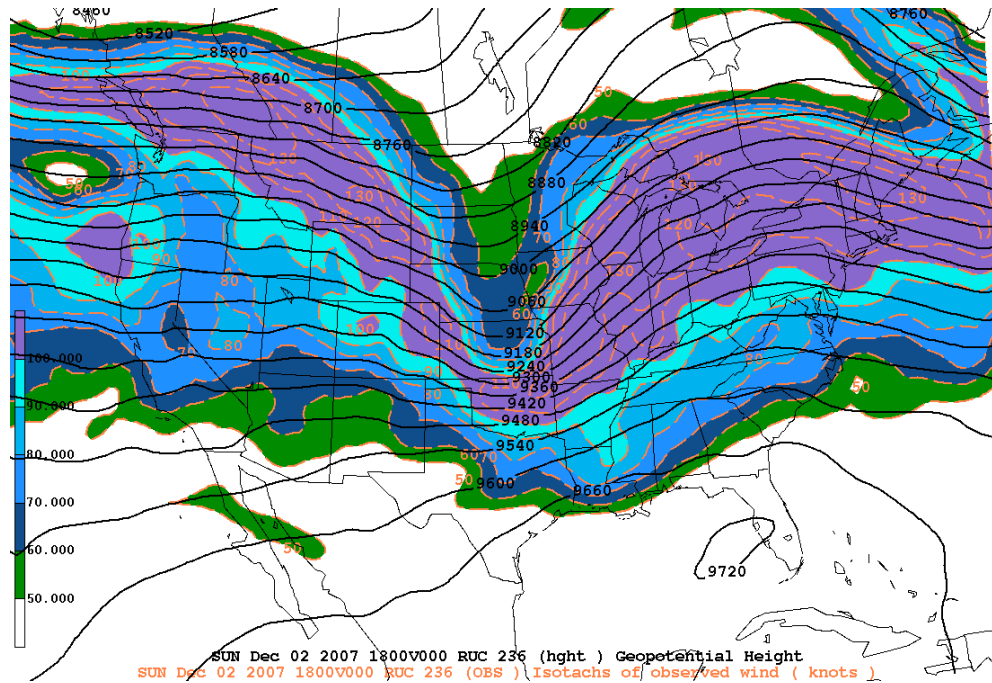


Figure 6.28 RUC initial analysis at 300 mb valid at 1800 UTC 02 December 2007. Geopotential height contoured every 60 gpm and isotachs in kts contoured every 10 kts above 50 kts and shaded.

occurring in Wisconsin (Fig. 6.24), this would be identified as a northwest case given the preferred lightning's location related to the center of the parent low.

Figure 6.28 shows an analyzed 300-mb jet streak of 120 kts extending from Missouri to the Great Lakes. This location at the Illinois and Wisconsin border is indeed under a gradient of mass divergence aloft between values of $1 \times 10^{-5} \text{ s}^{-1}$ and $\geq 3 \times 10^{-5} \text{ s}^{-1}$ (not shown). The RUC initial analysis also indicates the presence of a tightened 130-kt jet streak in southern Wisconsin and northern Illinois, closely associated with the presence of lightning in winter precipitation at this time.

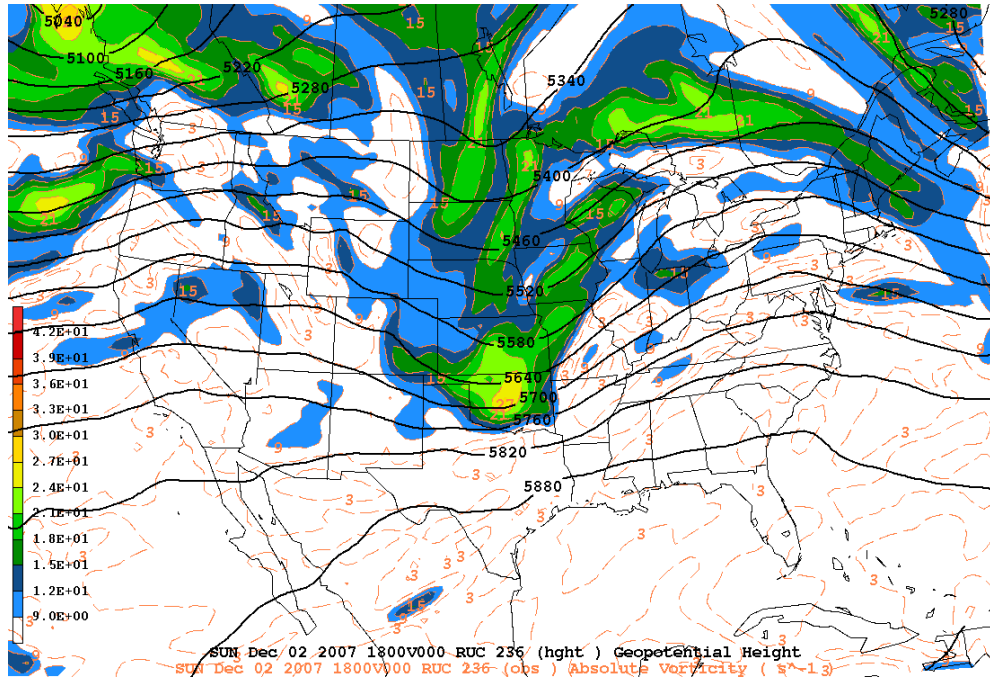


Figure 6.29 RUC initial analysis at 500 mb valid at 1800 UTC 02 December 2007. Geopotential height contoured every 60 gpm and absolute vorticity contoured every $3 \times 10^{-5} \text{ s}^{-1}$ and shaded above $9 \times 10^{-5} \text{ s}^{-1}$.

The 500-mb analysis (Fig. 6.29) shows this region enclosed by a circulation of absolute vorticity with values of at least $9 \times 10^{-5} \text{ s}^{-1}$. More than one vorticity maximum is analyzed at this time, but the primary trough axis runs along the border of North and South Dakota and Minnesota through Nebraska and into Kansas and Oklahoma. While the vorticity maximum is near the base of the trough in warmer air, there is an increasing vorticity maximum just upstream of the winter lightning (Fig. 6.24) with values of $18 \times 10^{-5} \text{ s}^{-1}$ providing dynamic forcing.

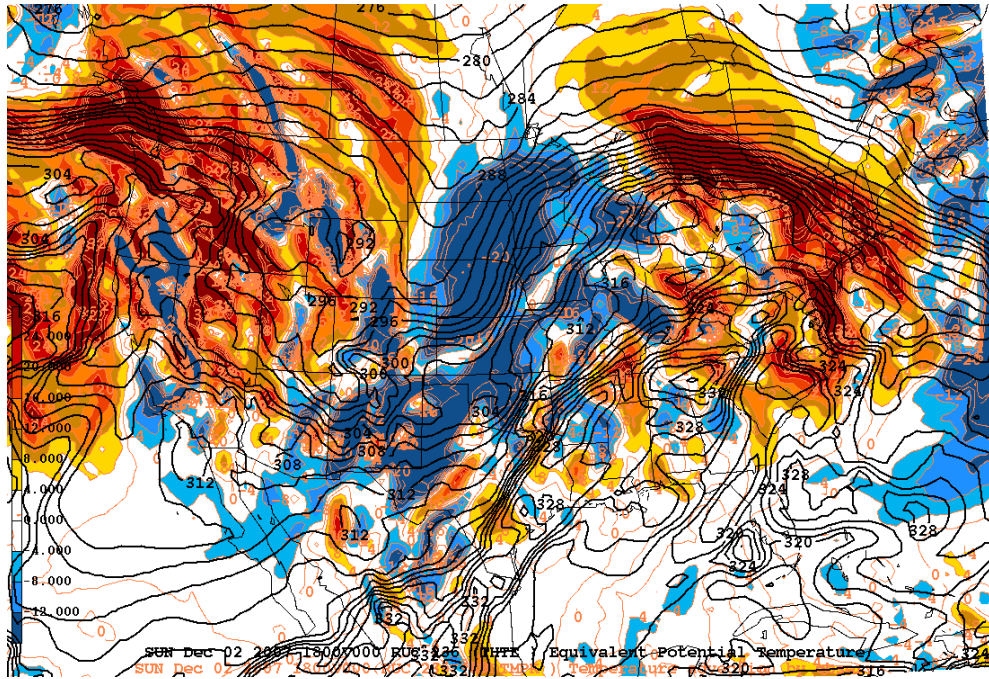


Figure 6.30 RUC initial analysis at 700 mb valid at 1800 UTC 02 December 2007. Equivalent potential temperature contoured every 2 K and temperature advection contoured every $4 \times 10^{-5} \text{ K s}^{-1}$. Positive values of temperature advection are shaded in warm colors and negative values of temperature advection are shaded in cool colors occurring at this time.

The 700-mb analysis (Fig. 6.30) shows a Θ_e maximum (316 K) over northern Illinois in the vicinity of the winter lightning. There is also a small region of mid-level warm air advection at $8.0 \times 10^{-5} \text{ K s}^{-1}$ enclosed by strong cold air advection to the north and south of $2.0 \times 10^{-4} \text{ K s}^{-1}$.

The 850-mb low (Fig. 6.31) is centered over the upper peninsula of Michigan with a thermal ridge axis extending from Illinois into Wisconsin and northern Minnesota. The RH is between 80% and 90%, but with a dry slot starting to approach from the west. A region of RH less than 70% encompasses the tri-state region of Iowa, Illinois, and Wisconsin. Westerly winds at this time

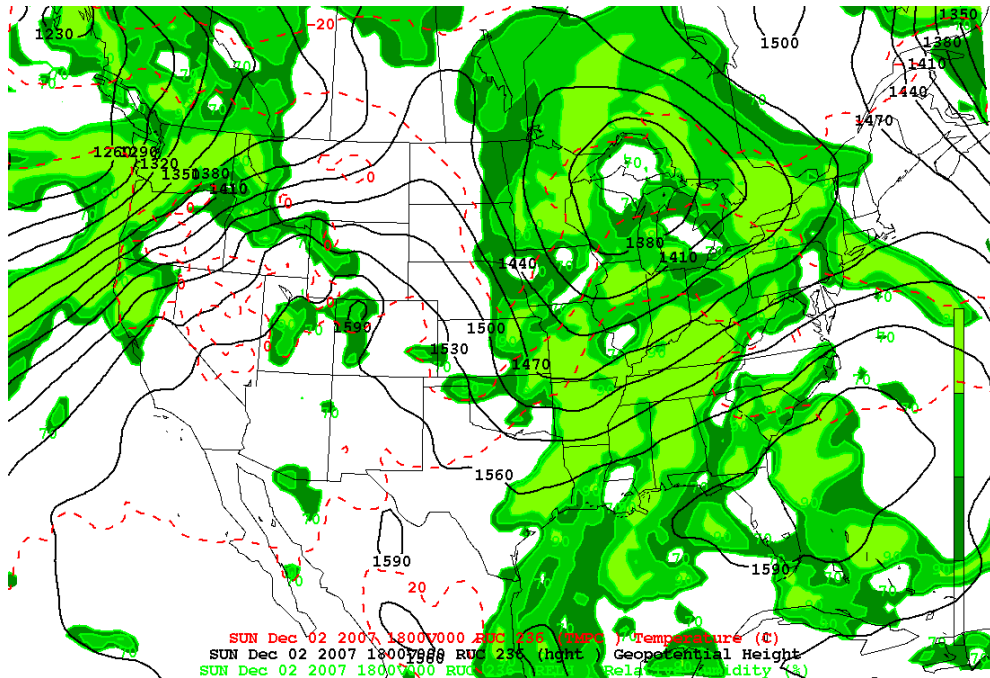


Figure 6.31 RUC initial analysis at 850 mb valid at 1800 UTC 02 December 2007. Geopotential height contoured in black every 30 gpm and temperatures contoured in red dashed every 10°C. Relative humidity contoured and shaded every 10% above 70%.

aid in the transport of dry air at this time. While the air is not fully saturated, the grid point is located within 10-15 km of RH greater than 90% and near 100 km from RH < 70%. Further, it is between 200 and 225 km from RH < 70% at 700 mb (not shown). The proximity of dry air intrusion at this time and at the previous times, displaying a maximum in winter precipitation in this storm, reveal an environment where winter lightning may be enhanced.

The regional warm air advection is not as prevalent at 900 mb (Fig. 6.32) with only a small area of it directly to the south of the lightning at a rate of $8.0 \times 10^{-5} \text{ K s}^{-1}$. Cold air advection from the west dominates the region. The lightning,

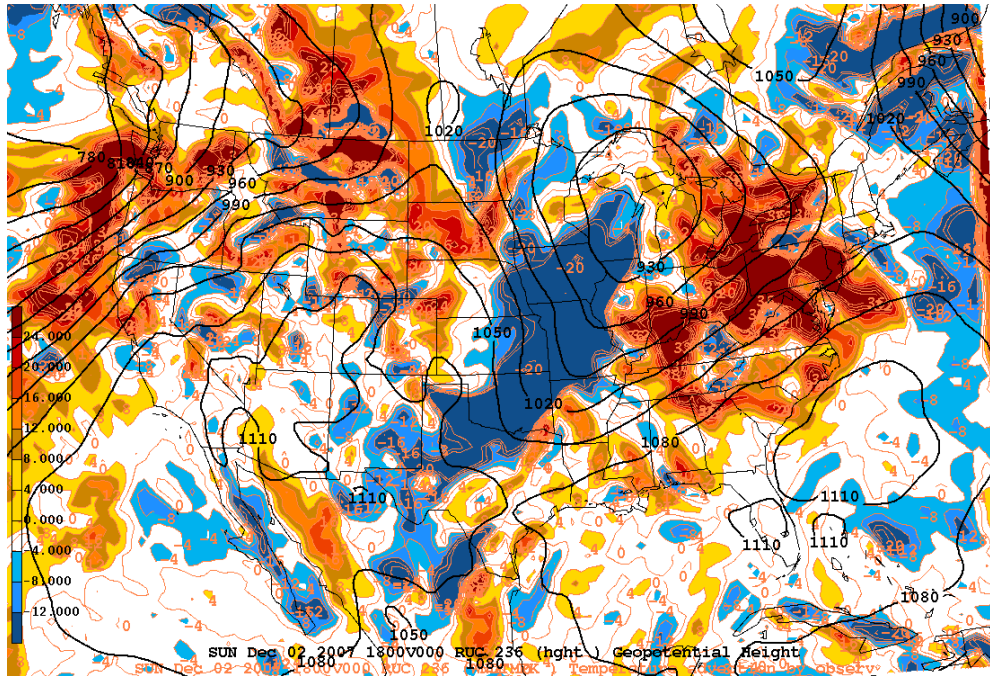


Figure 6.32 RUC initial analysis at 900 mb valid at 1800 UTC 02 December 2007. Geopotential height contoured in black every 30 gpm and temperature advection contoured every $4 \times 10^{-5} \text{ K s}^{-1}$. Positive values of temperature advection are shaded in warm colors and negative values of temperature advection are shaded in cool colors.

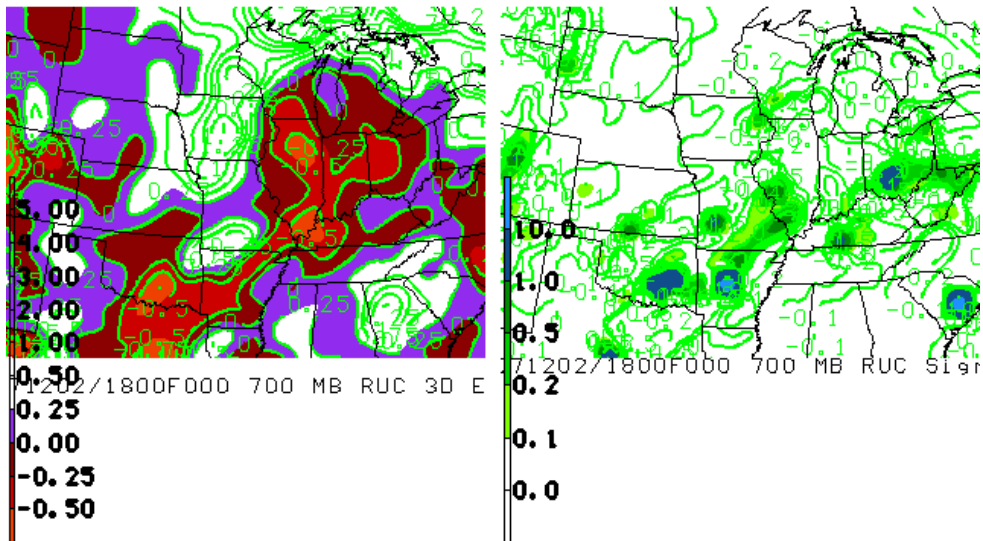


Figure 6.33 Stability profile valid at 1800 UTC 02 December 2007. Left panel is 3-dimensional equivalent potential vorticity. Shaded contours represent values of 0.25 PVU and less. The right panel is the σ^2 growth-rate parameter shaded for values above 0.1 h^{-2} .

in this case (Fig. 6.24), occurs slightly in the cooling air, but close to a thermal gradient.

Figure 6.33 shows a discernable EPV reduction zone located along the border of Illinois and Wisconsin. Values in this region are between -0.25 and -0.50 PVU. Values less than -0.50 PVU just to the south indicate an even greater EPV reduction zone directly to the south of this location in warmer air. The growth rate parameter in this instance is slightly positive again (between 0 and 0.1 h^{-2}). A band of values greater than 0.1 h^{-2} appears just to the west in a region immediately downstream of the best forcing for this location.

The sounding profile in Figure 6.34 for this location is the most unstable compared to the other soundings for lightning in this event. The winds at this time are steadily from the west to northwest and not off the lake shores, thus, removing the influence of the Great Lakes during a mostly synoptic system. However, this profile shows that temperatures were above 0°C from the surface up to just below 700 mb. The profile, though, resembles those of the NW composite. The frontal inversion extends from near the surface at 950 mb to 800 mb with a MULPL at 750 mb. This MULPL is closer to the surface than any of the NE composites and the NW composite. The stability parameters represent a region that is more unstable than the previous times. The profile begins to dry out near 500 mb. CAPE is found in this profile, near 99 J kg^{-1} , in a potentially

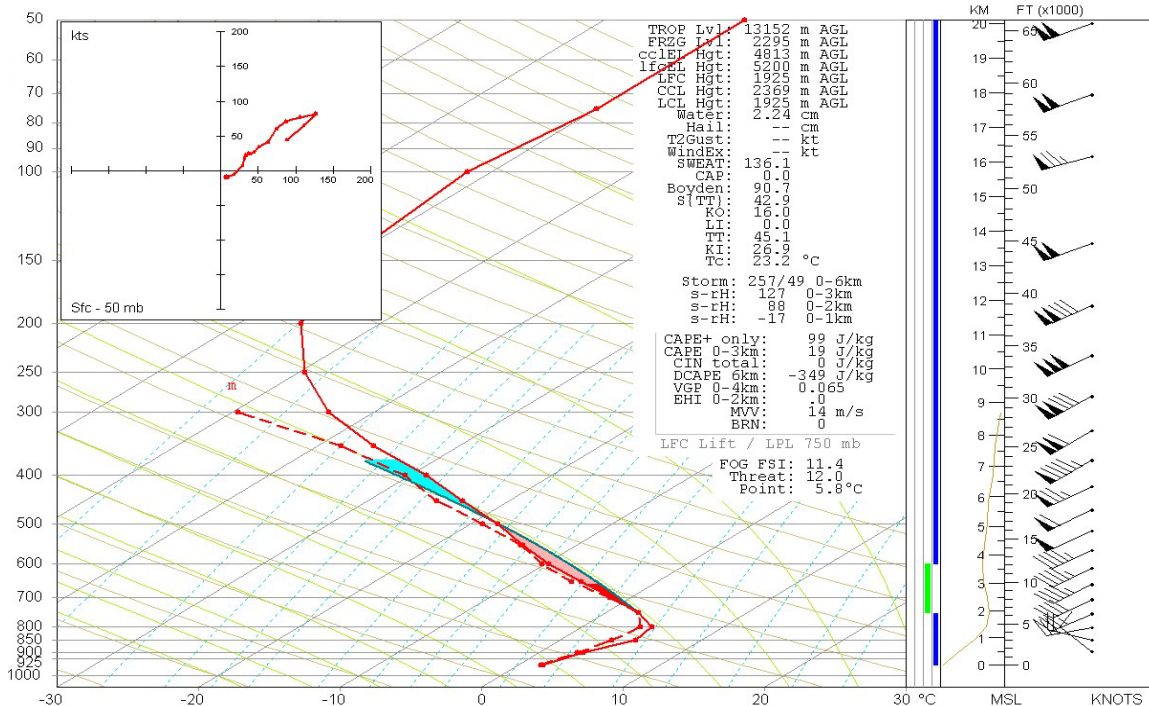


Figure 6.34 1800 UTC December 2, 2007 sounding. CAPE is shaded in color. Solid red line is temperature, dashed red line is dewpoint, and wind bars represent wind speeds in kts and wind direction. Vertical Θ_e in yellow to the left of wind bars.

unstable layer from 750 mb to 550 mb, represented by shading in Figure 6.34.

Furthermore, observe the slight decrease in Θ_e in Figure 6.34. The TT and KI values are also 45.1 and 26.9 respectively with an LI value of 0.0. The winds,

unlike the previous cases, are backing in the lowest 100 mb, showing cold air advection near the surface. It backs in direction from 317° at 950 mb to 240° at 800 mb. Also, the speed increases from 12 kts at 950 mb to near 37 kts at 800 mb.

In terms of the vertical thermal structure, the -10°C isotherm is located at 4.1 km, which is slightly above the 3.8 km altitude found in the NE composite and the 3.9 km altitude found in the NW composite. This time frame is most like a NW

event, and so would seem more reasonable for the -10°C isotherm to be slightly more elevated than those in the NE composites. Also, the -10°C isotherm is found above the MULPL, which would be expected in an environment conducive to lightning generation. A little higher, the -20°C isotherm is found at 5.6 km, at about 500 mb. This is fairly well correlated to the NE and NW composites as well, as those tended to occur around 490 mb and at 5.7 km above the ground.

In summary, this case produced three separate times where lightning occurred in winter precipitation. The first two times covered were at 0100 and 0800 UTC on 02 December. These were both events occurring NE of the surface low. While these events occurred in proximity to the Great Lakes, the events that transpired were dynamically driven on a synoptic scale masking any enhanced effects of the sea and land interface. Radar echoes at these times were both greater than 30 dBZ while cloud top temperatures from GOES-12 IR imagery were colder than -40°C . This temperature will be further compared to warm precipitation elevated convection in the following chapter. The synoptic and mesoscale environments for these two times were also very similar with the occurrence of an intense jet core and vorticity circulations. On the mesoscale, these times were dominated by warm air advection at both 700 and 900 mb while located in $\text{RH} > 80\%$ at 850 mb. These lightning events were in close proximity to

dry air intrusions being within 50 to 200 km of $RH < 70\%$ at 850 mb and 300 to 400 km of $RH < 70\%$ at 700 mb. Following Martin et al. (1998 a,b), this dry conveyor belt is part of cyclone development and dissipation in the mid-latitudes in winter time cyclonic events. The lightning at 0100 UTC 02 December occurred in $RH > 90\%$ at both 850 and 700 mb while being within 50 km and between 300 and 325 km of $RH < 70\%$ at 850 mb and 700 mb respectively. At 0800 UTC 02 December lightning was within 200 km and between 400 and 450 km of $RH < 70\%$ at 850 and 700 mb respectively. And finally at 1800 UTC 02 December, the lightning was within 100 km and 200 km of $RH < 70\%$ at 850 and 700 mb respectively. By 1800 UTC, the lightning is occurring NW of the surface low with radar echoes between 25-30 dBZ. Cloud top temperatures, however, are their coldest for this event reaching between -50° and -60°C . While jet dynamics and vorticity circulations are still present, the mesoscale shows a tendency to gain instability from local baroclinic development demonstrated by a strong thermal advection gradient at 700 and 900 mb as cold air advection from the west begins to dominate. Proximity to dry air at 850 and 700 mb remains with $RH < 70\%$ within 100 km of winter lightning and 200 km from $RH < 70\%$ respectively. The soundings fit the form of the composite soundings created in chapter 5. This most unstable time at 1800 UTC, however, develops close to 100 J/kg of CAPE, which has been uncharacteristic of the composite soundings. But the lower

MULPL allowed for more lifting into the slightly more elevated mixed phase region in order to obtain charge separation for lightning generation.

Chapter 7 Warm Precipitation Analysis

7.1 Introduction

Given the nature of the convection found in thundersnow, a second event of elevated convection was analyzed. This event, however, consists of only warm, liquid precipitation and no occurrence of frozen precipitation. A case study of thundersnow was presented outside of the primary dataset to show a comparison in lightning characteristics and the synoptic and mesoscale environments associated. Further, the local environment using RUC initial soundings were compared to composite soundings created from lightning analysis in chapter 4. A warm precipitation case will be presented in the following chapter to compare the lightning characteristics between an elevated convective event involving frozen precipitation and an elevated convective event only involving warm precipitation. Further, the synoptic and mesoscale

environment will be analyzed with these lightning characteristics along with the local environment where lightning is at its maximum. It is expected that lightning characteristics should be similar in terms of diurnal maximums, but may be different in terms of lightning types and percentage of occurrence. Also, the synoptic and mesoscale environment should present some differences when compared to a winter precipitation event. For the following section on lightning, the same terminology and storm timeline will be used as chapter 4. This section will describe a warm precipitation event and the physical characteristics surrounding it. This event consisted of a mesoscale convective system (MCS) that moved across Nebraska, Kansas and Missouri during 12 and 13 October 2007. While this event falls into our definition of the cool season (October through April), it is fully associated with warm precipitation, meaning it was an elevated convective system generating lightning and precipitation that fell only as rain without mixed phase precipitation.

7.2 Lightning Characteristics

The lightning in this event began at 0400 UTC on 12 October and lasted through 2000 UTC on 13 October. Through the 40 hours of this event, there were 156,135 observed lightning events. Of this total for the event, 20.2% were cloud

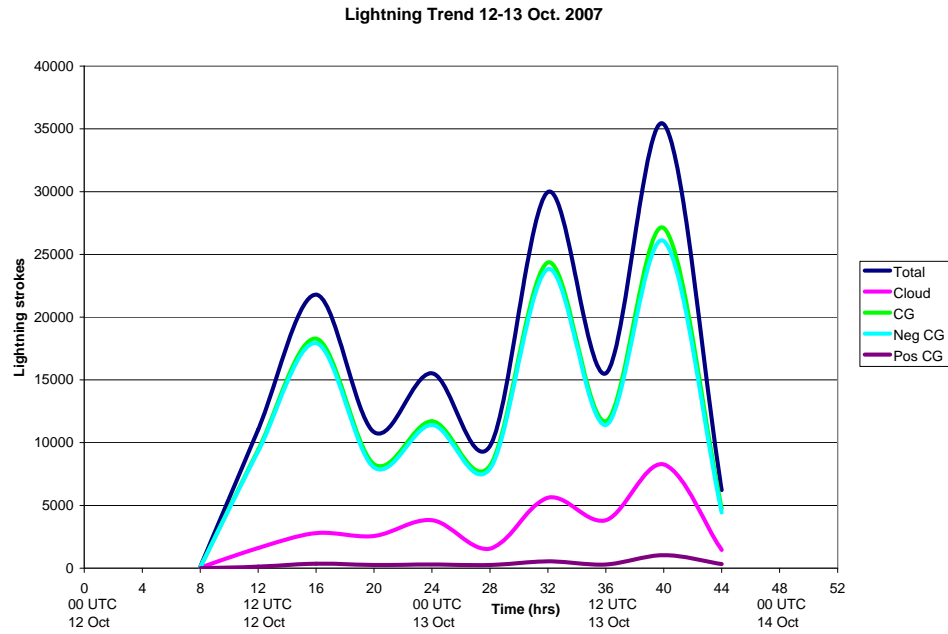


Figure 7.1 Storm total lightning trend for 12-13 October 2007. Time given in hours from the onset of lightning detected. Date labeled every 12 hours in UTC.

flashes and 79.8% were CG strokes. Of those CG strokes, 97.2% were negative CG strokes. The overall storm average stroke rate was 0.27 min⁻¹.

Figure 7.1 shows no single lightning maximum during this event. The first maximum occurred between 1200 and 1600 UTC (0600 and 1000 CST) on 12 October with a total of 21,803 observed lightning events at a rate of 90.8 min⁻¹. Only 12.8% of these were cloud flashes with 87.2% being CG strokes. 98.0% were negative CG strokes. The next maximum in lightning activity occurred between 0400 and 0800 UTC (0200 and 0600 CST) with a total of 29,972 observed lightning events, of which 18.7% were cloud flashes and 80.3% were CG strokes. Of the CG strokes, 97.7% were negative CG strokes. Lightning events were observed

during this time period at a rate of 124.8 min^{-1} . The final maximum in lightning occurred between 1200 and 1600 UTC (0600 and 1000 CST) with 35,373 observed lightning events. Of the lightning total in this maximum, 23.4% were cloud flashes and 76.6% were CG strokes, of which 96.2% were negative CG strokes.

In terms of lightning trends, this warm-season storm has several differences compared to those elevated events with winter precipitation. In this case, the peak lightning times were during the hours of 1200 to 1600 UTC whereas the dominant time was late afternoon (0000 to 0400 UTC) in the winter precipitation events. Further differences were the percentage of cloud flashes. The average percentage of cloud flashes for a winter precipitation event was 35.0% while the average percentage for this warm season case was 20.2%. This leads to a difference in the cloud:CG ratio. On average in the winter precipitation events, the ratio was 0.53 where this event produced a ratio of 0.25. There was also a difference in the percentage of negative lightning strokes. In the warm precipitation event, CG strokes consisted of 97.2% negative CG strokes compared to 92.0% negative CG strokes in winter lightning. Also, the rate for lightning associated with winter precipitation occurred at a rate of 76.6 min^{-1} , while the average rate for this warm precipitation event was about 65.0 min^{-1} .

7.3 Case Study

A synoptic and mesoscale case study including model initial soundings of the most active lightning times and locations for this event were analyzed for a comparison to the convective snow event. There are two maximum times for lightning analyzed in this section. The first time (1200 UTC 12 October) represents the first maximum in lightning (Fig. 7.1) and the second time (1200 UTC 13 October) represents the overall maximum in lightning for this event. Each time will be introduced by radar and satellite imagery of the observed precipitation followed by a synoptic and mesoscale analysis of the event. The subsequent sounding will be presented following the synoptic analysis and then compared back to composite soundings observed in chapter 5.

7.3.1 Case Overview

7.3.1.1 1200 UTC 12 October 2007

Two of the most active hours for lightning occurrence, according to Figure 7.1, were at 1200 UTC on 12 October and at 1200 UTC on 13 October. The most active lightning at 1200 UTC 12 October was located at 39.3° north and -98.6° west over north central Kansas (Fig. 7.2). Base reflectivity radar mosaic, provided by the National Climatic Data Center (NCDC) for 1200 UTC 12 October

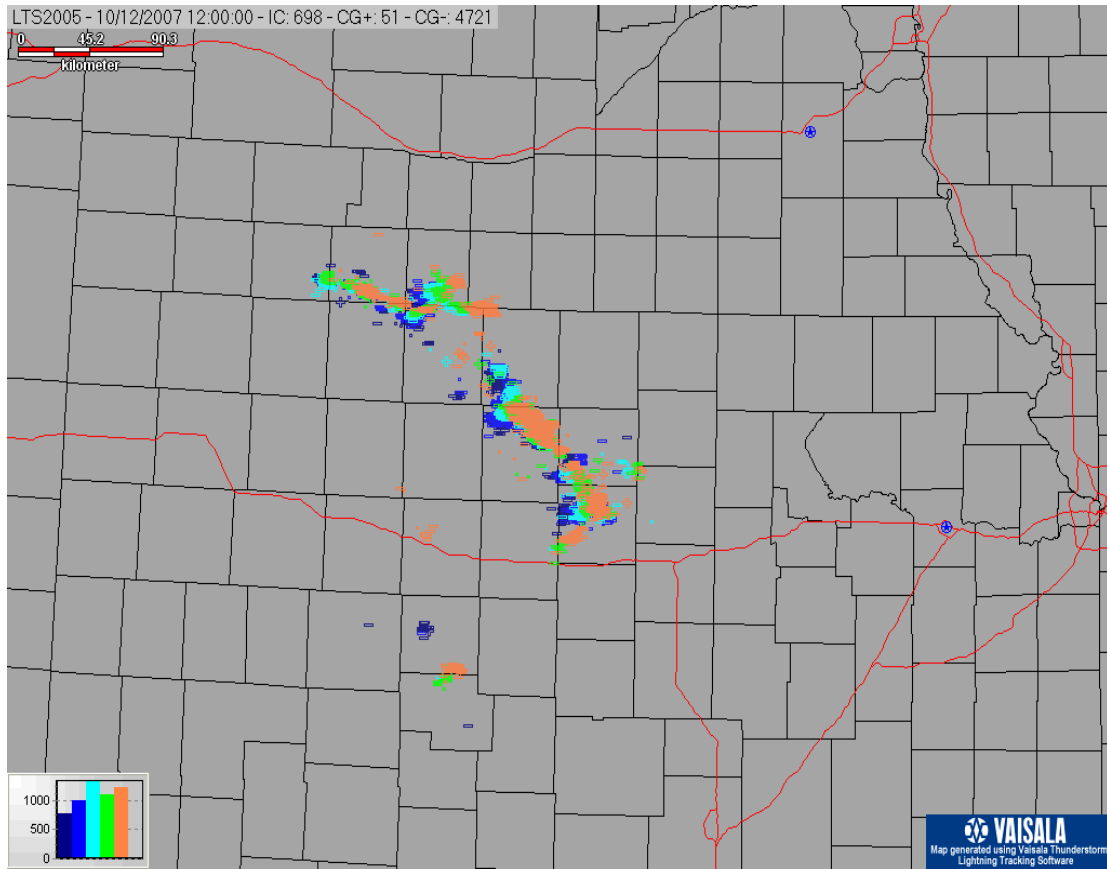


Figure 7.2 Lightning map indicating negative and positive CG strokes and cloud flashes for one hour ending at 1200 UTC 12 October 2007.

(Fig. 7.3), shows a small convective complex begin to develop over the same location.

Similar to the analysis performed in chapter 6, GOES-12 satellite IR imagery is used as a possible measure of lightning potential. Figure 7.4 shows GOES-12 IR imagery enhanced to show cloud top temperature valid at 1215 UTC on 12 October, which is approximately equivalent to the most active period of lightning on this day. According to Figure 7.2, the region of most active lightning occurs over north central Kansas where convection is further visible in

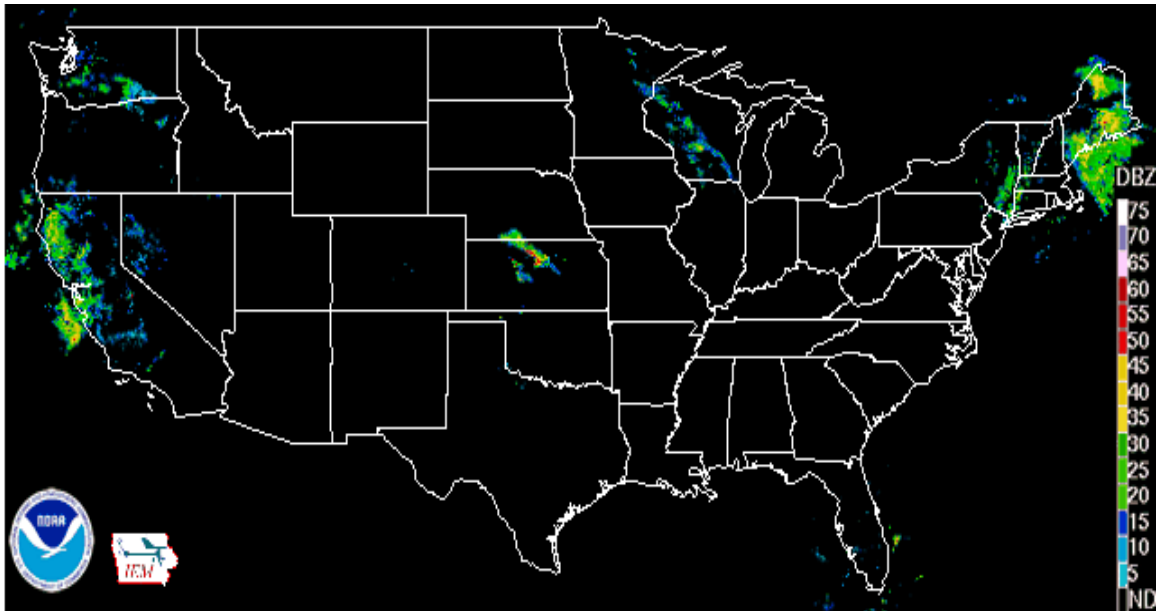


Figure 7.3 National Climate Data Center national base reflectivity radar mosaic valid at 1200 UTC on 12 October 2007.

Figure 7.3. The coldest cloud top temperature is below -60°C . Colder cloud top temperatures represent clouds reaching higher into the atmosphere. Further, cloud top temperatures have not been quantified with regards to lightning generation.

A synoptic and mesoscale analysis is provided here for the valid time when lightning occurrence was most active (Fig. 7.2). These maps are plotted using the RUC initial field, which, according to section 3.2, has been shown to be near truth. Starting at the surface at 1200 UTC 12 October (Fig. 7.5), there is a fairly weak surface low (1003 mb mean sea level) centered over southern Nevada and southern Utah. This low extends into an inverted trough axis aligned from the Colorado front range through northwest Kansas and into central Nebraska.

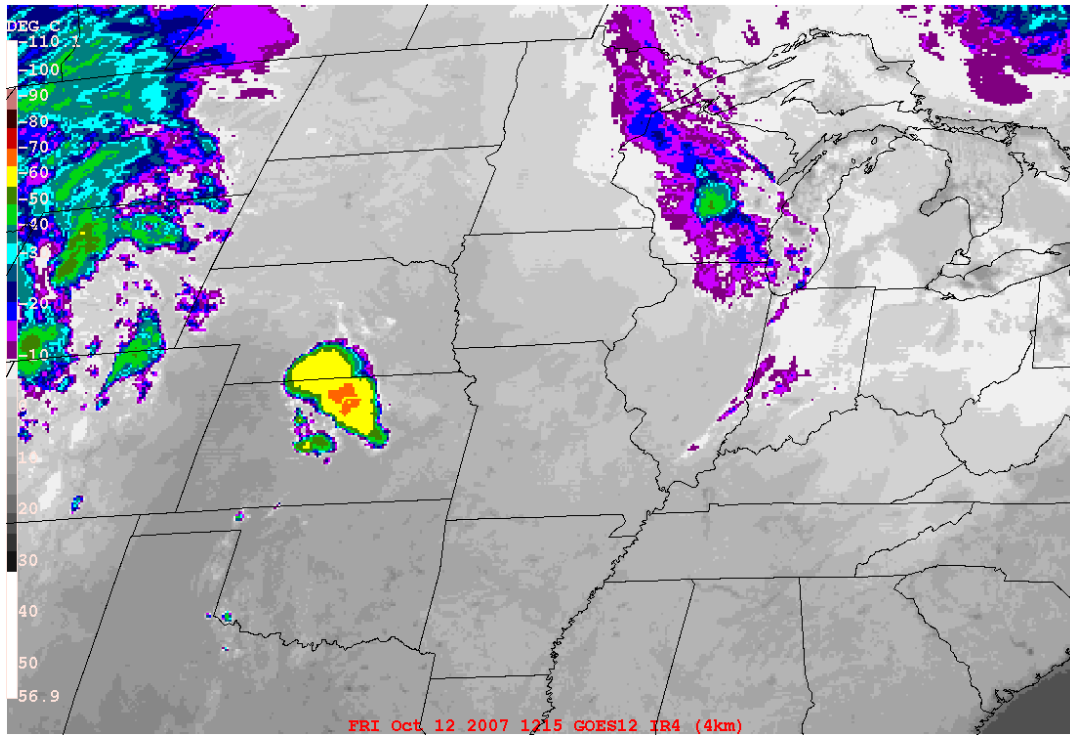


Figure 7.4 GOES-12 IR imagery valid at 1215 UTC 12 October 2007. Cloud top temperatures are shaded in color with color scale representing every 10°C. Colder temperatures are represented by warmer colors.

It is during this time that convection begins over north central Kansas along and slightly ahead of the inverted trough axis. The convection is supported by the surface observations in Figure 7.5 showing complete sky coverage along and ahead of this inverted trough axis extending from Kansas to Lake Superior. Concurrently, at 300 mb, there is a 50-kt jet streak oriented from northwest to southeast extending from the Canadian province of Alberta through North and South Dakota and into Minnesota and Iowa (Figure 7.6). A more tightly centered jet core of about 70 kts is located over the border between Minnesota and Iowa. This broader streak is located downstream of a 300-mb ridge. A deep longwave

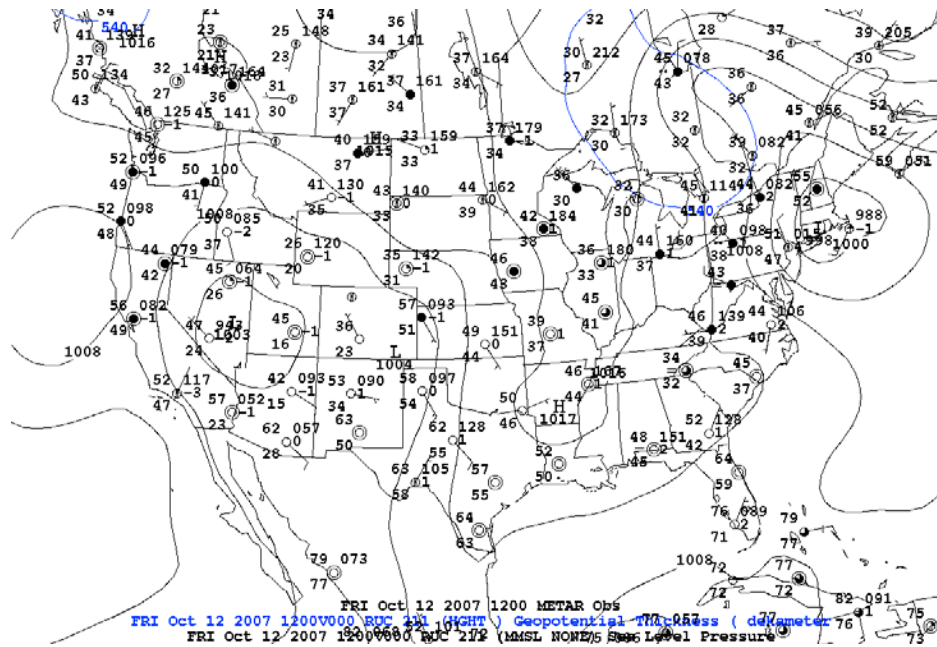


Figure 7.5 RUC initial analysis at mean sea level pressure valid at 1200 UTC 12 October 2007. Sea level pressure contoured in black every 2 mb with 5400 gpm thickness line (500:1000-mb layer) plotted in blue. METAR decoded surface observations are plotted valid at the same time.

trough axis is located along the Pacific coastline with a 70-kt jet streak rounding the base of the trough in southern California and into Arizona. A broader 50-kt contour extends along the Rio Grande River through New Mexico and into Texas. These jet stream features are not in the vicinity of the onset of convection at this time, nor the onset of lightning. In linear jet stream theory, one would expect to find significant weather in regions of mass divergence found in either the left exit region or right entrance region of the jet. Indeed this is the case with divergence values of $2 \times 10^{-5} \text{ s}^{-1}$ over the active lightning at this time (not shown).

A wave perturbation is found at 500 mb aligned with the inverted trough at the surface downstream of the ridge axis (Fig. 7.7). A weak circulation of

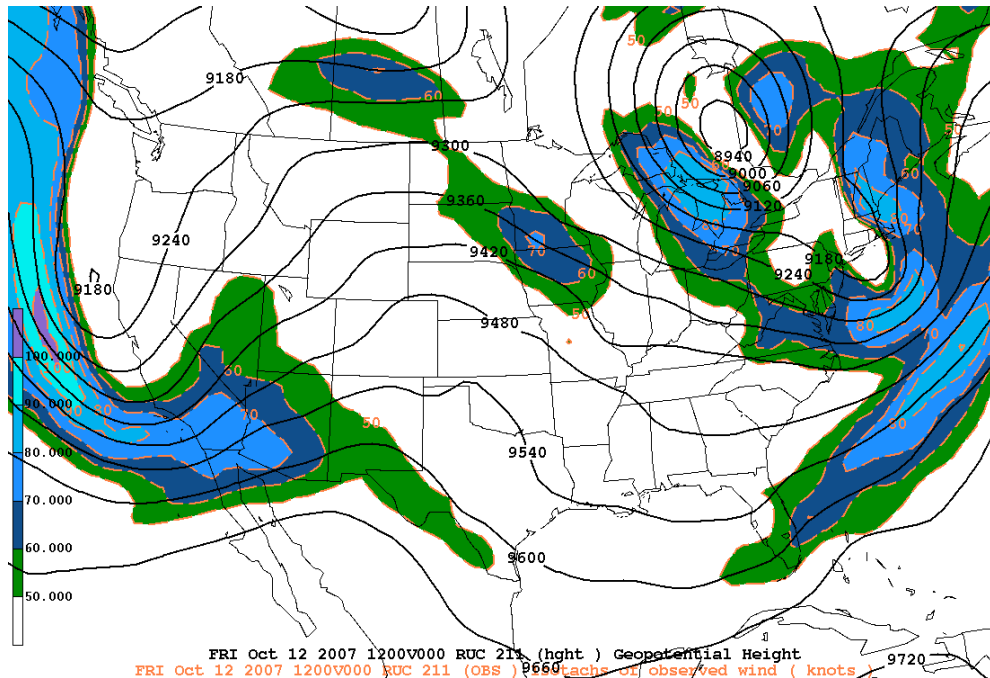


Figure 7.6 RUC initial analysis at 300 mb valid at 1200 UTC 12 October 2007. Geopotential height contoured every 60 gpm and isotachs in kts contoured every 10 kts above 50 kts and shaded.

absolute vorticity ($9 \times 10^{-5} \text{ s}^{-1}$) is contoured in Figure 7.7 in Kansas near the onset of convection and lightning at this time. There are also further vorticity maximums of the same magnitude immediately to the southwest. Further vorticity maximums are found north in Minnesota associated with the region of mass divergence aloft in the left exit region of the jet and off the coast of California at the base of the closed-off 500-mb low and along the longwave trough axis.

Figure 7.8 presents more of a mesoscale analysis showing regions of warm and cold air convection along with Θ_e at 700 mb. Looking at the contours of Θ_e ,

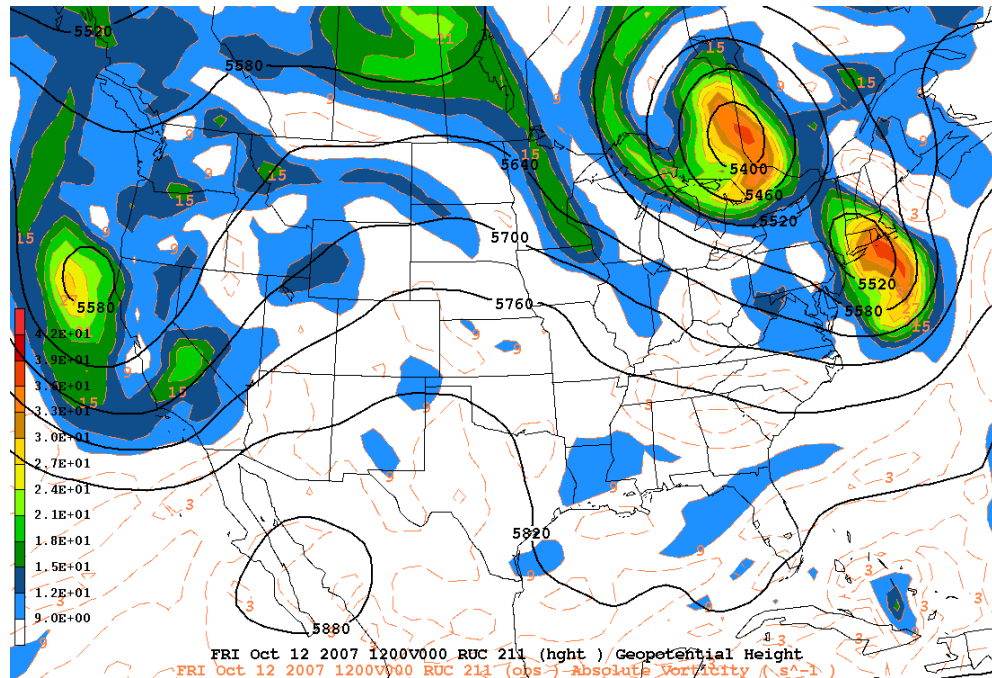


Figure 7.7 RUC initial analysis at 500 mb valid at 1200 UTC 12 October 2007. Geopotential height contoured every 60 gpm and absolute vorticity contoured every $3 \times 10^{-5} \text{ s}^{-1}$ and shaded above $9 \times 10^{-5} \text{ s}^{-1}$.

there is a tight gradient in central Nebraska representing a stationary boundary associated with the inverted trough in Figure 7.7. Further, there is a Θ_e maximum located over a region of model diagnosed warm air advection where the onset of lightning and convection took place with this event.

The inverted trough through Kansas and Nebraska is further observed at 850 mb (Fig. 7.9). Saturated air extends along this trough axis from the front range of Colorado into Kansas. Convection begins to occur along this gradient of moisture under a 700-mb Θ_e ridge (Fig. 7.8) representative of moist instability.

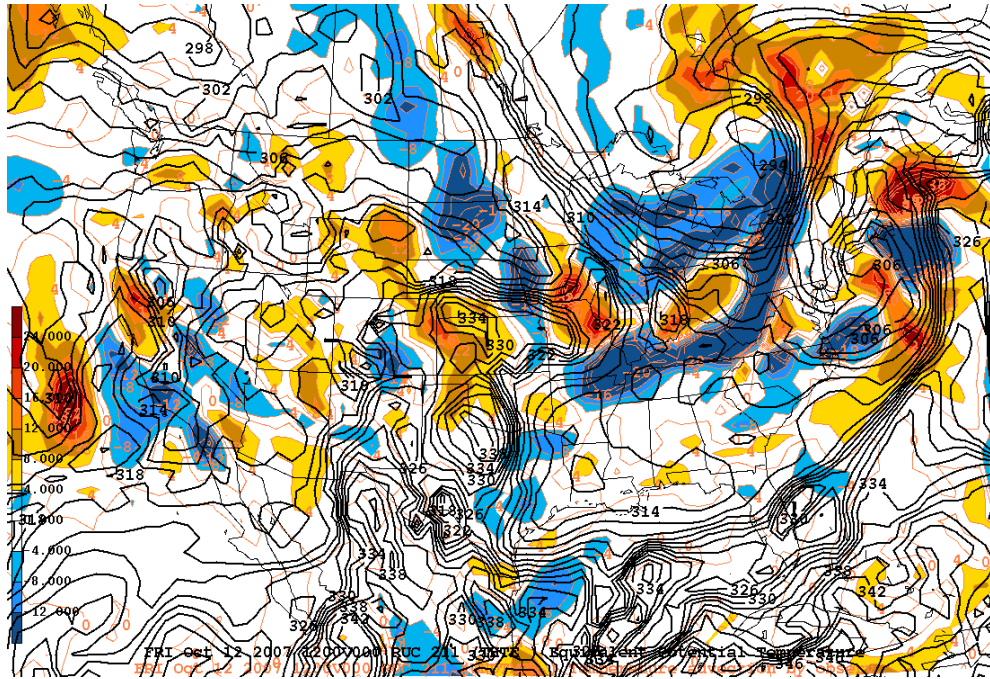


Figure 7.8 RUC initial analysis at 700 mb valid at 1200 UTC 12 October 2007. Equivalent potential temperature contoured every 2 K and temperature advection contoured every $4 \times 10^{-5} \text{ K s}^{-1}$. Positive values of temperature advection are shaded in warm colors and negative values of temperature advection are shaded in cool colors.

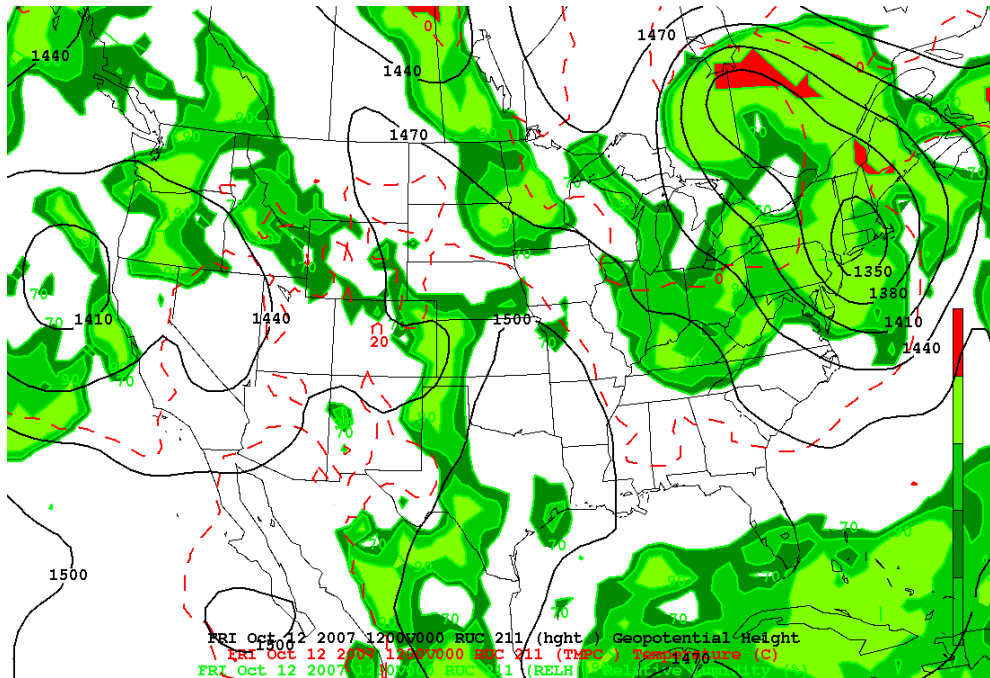


Figure 7.9 RUC initial analysis at 850 mb valid at 1200 UTC 12 October 2007. Geopotential height contoured in black every 30 gpm and temperatures contoured in red dashed every 10°C . Relative humidity contoured and shaded every 10% above 70%.

The heights at 900 mb (Fig. 7.10) continue to show the presence of the inverted trough extending into Kansas and Nebraska. Also, very prevalent at this level is the dominance of warm air advection giving the appearance of warm air advection near the surface and cooling aloft in a moist, unstable layer with support from a mid-tropospheric disturbance, all present in the onset of convection.

The subsequent sounding for this time and location as shown by RUC initial data (Fig. 7.11) shows a relatively dry layer below 750 mb with the most unstable parcel being lifted from a saturated layer from 750 mb to 700 mb and then drying out above. A steep frontal inversion layer is observed from 950 mb up to the top of the inversion at 850 mb. This is similar to the NE composite (Fig. 5.1) where the top of the frontal inversion is at the top of a nearly isothermal layer to around 850 mb. The difference in this warm case is that there is dry air directly above and below the frontal inversion. The layer between 850 and 700 mb shows a lapse rate steeper than the moist adiabatic lapse rate indicative of a moist, unstable layer. Above the inversion, the profile becomes gradually less moist, although the temperature profile follows the moist adiabat up the column, making this a nearly moist-neutral profile. Due to this very shallow layer of moist air between 700 and 750 mb, a large amount of convective energy and instabilities are present in the profile. Lifting a parcel from the bottom of this

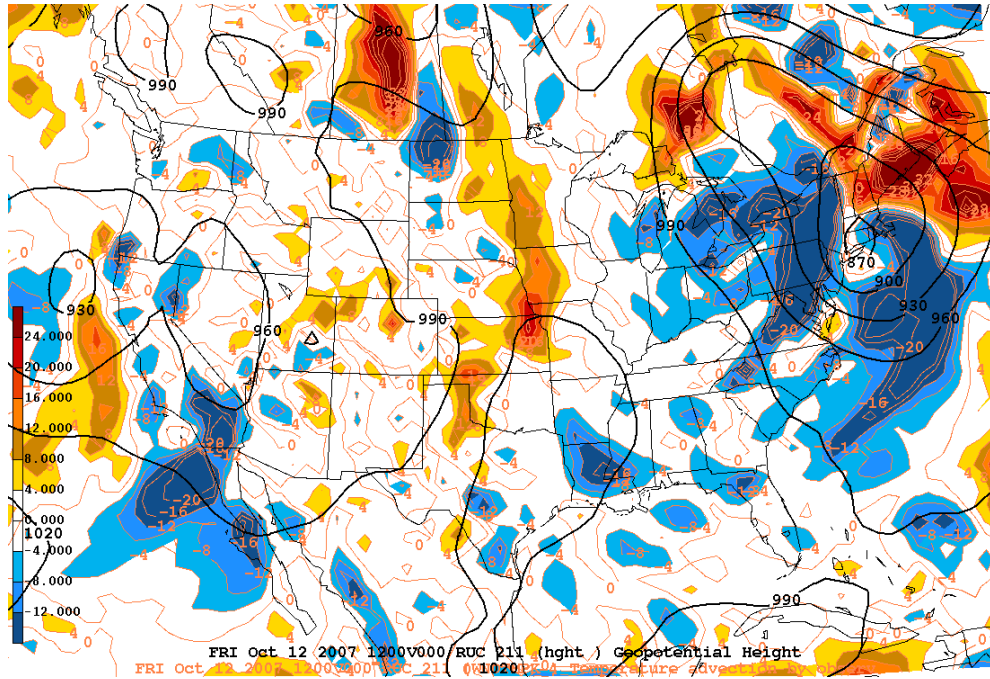


Figure 7.10 RUC initial analysis at 900 mb valid at 1200 UTC 12 October 2007. Geopotential height contoured in black every 30 gpm and temperature advection contoured every $4 \times 10^{-5} \text{ K s}^{-1}$. Positive values of temperature advection are shaded in warm colors and negative values of temperature advection are shaded in cool colors.

very shallow moist layer produces a CAPE of 138 J kg^{-1} with very little CIN (-13 J kg^{-1}) to contain the convection. Opposed to the winter lightning composites, though, the TT and KI are both substantially higher for the warm precipitation event, which is consistent with the warmer temperatures, at 47.3 and 34.4 respectively. Further the LI for this sounding is slightly negative at -1.3 as opposed to the slightly positive values for the winter composite. The winds are weak throughout the column, yet veering below the inversion indicating weak warm air advection. However, wind speeds do not exceed 25 kts

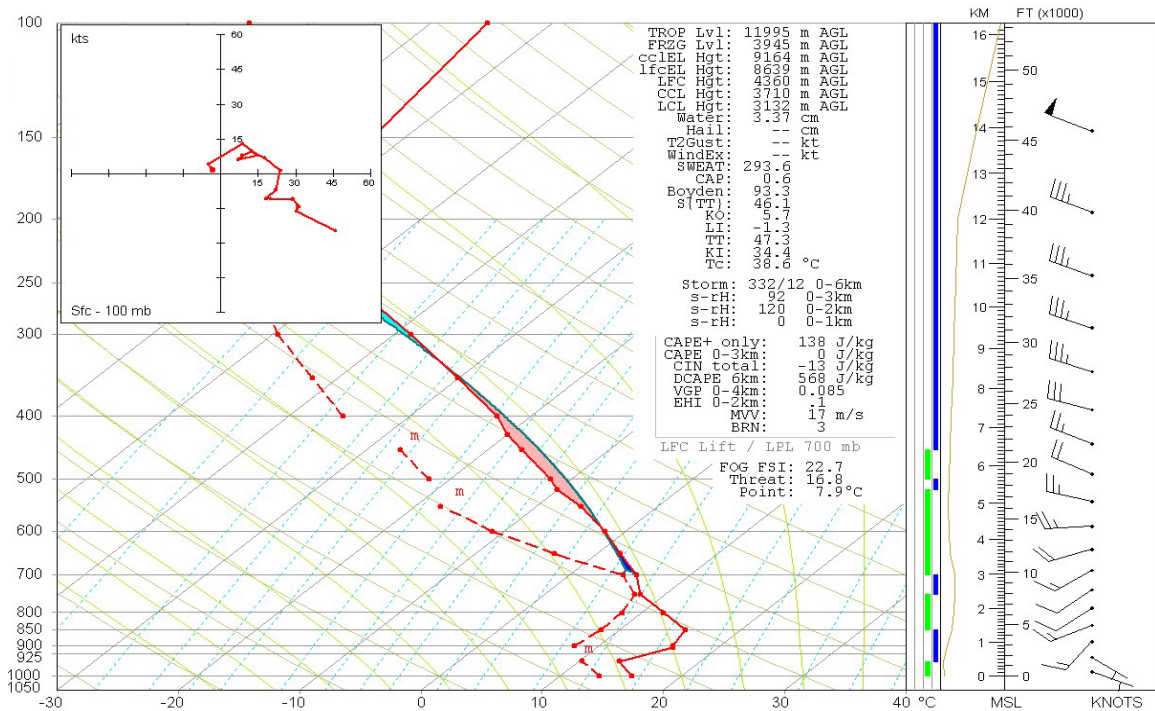


Figure 7.11 1200 UTC October 12, 2007 sounding. Solid red line is temperature, dashed red line is dewpoint, and wind bars represent wind speeds in kts and wind direction. CAPE is shaded. Vertical Θ_e in yellow to the left of wind bars.

anywhere below 500 mb. In terms of thermal structure for the generation of lightning, the -10°C isotherm is located just below 500 mb at 519 mb at a height of 5.5 km. This is significantly higher than the 3.9 km found in the winter precipitation composites and the 4.1 km altitude in soundings from the thundersnow case study (Fig. 6.34). The 5.5 km level in the winter composites was found to be typically the height at the top of the mixed-phase layer, or the -20°C isotherm. In this instance, the -20°C isotherm is located at 427 mb, or 6.9 km.

In summary, the synoptic situation was representative of MCS development. A dynamic pattern was fixed over the central U.S. with a trough over the east and a ridge in the High Plains. There was synoptic influences with the development of a surface low over the southwest U.S. (Fig 7.5) and weak vorticity circulations present, but mesoscale thermal patterns (warm/cold air advections) represented the bulk of the instability with a shallow layer of elevated moisture. A lifting mechanism was present with the mid-level perturbation and downstream inverted trough. A convectively unstable sounding profile revealed a region of favorable convective growth. The presence of moisture, lift, and instability favored a more vertical updraft as well, shown by high cold cloud tops (Fig. 7.4), generating favorable charge separation for lightning production.

7.3.1.2 1200 UTC 13 October 2007

The next most active time associated with this warm season event was at 1200 UTC 13 October 2007. This time is the most active time overall in terms of lightning occurrence according to Figure 7.1. The location for this time was 39.3° north and -95.5° west. Figure 7.12 shows the active lightning at this time. According to the NCDC base reflectivity mosaic (Fig. 7.13), this location

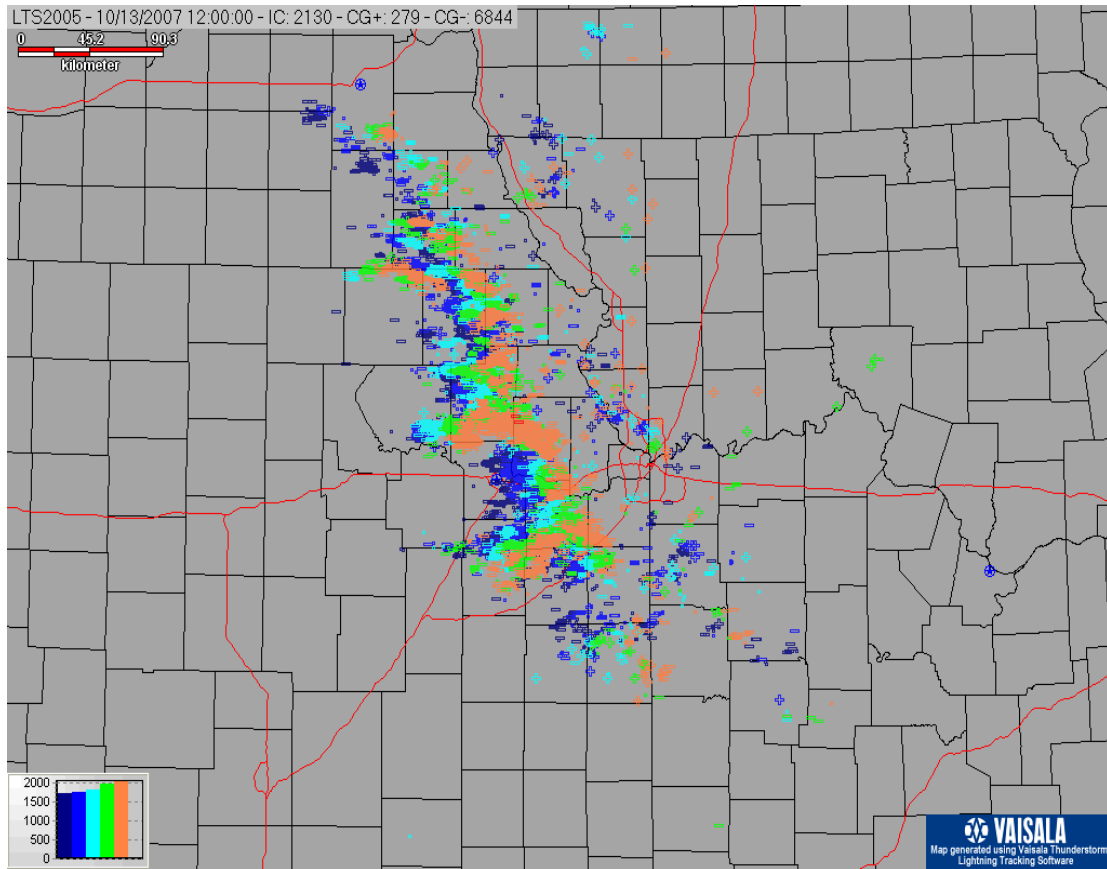


Figure 7.12 Lightning map indicating negative and positive CG strokes and cloud flashes for one hour ending at 1200 UTC 13 October 2007.

corresponds to convective development on the backside of the mesoscale convective system near Topeka, KS.

The IR imagery in Figure 7.14 indicates the most active convection over northwest Missouri and northeast Kansas, under the same area of most active lightning (Fig. 7.12). Compared with the convection 24 hours earlier, the cloud top temperatures are colder, extending to below -70°C . In this case, the cloud top extends well beyond -40°C , but this is most likely due to the warm nature of the

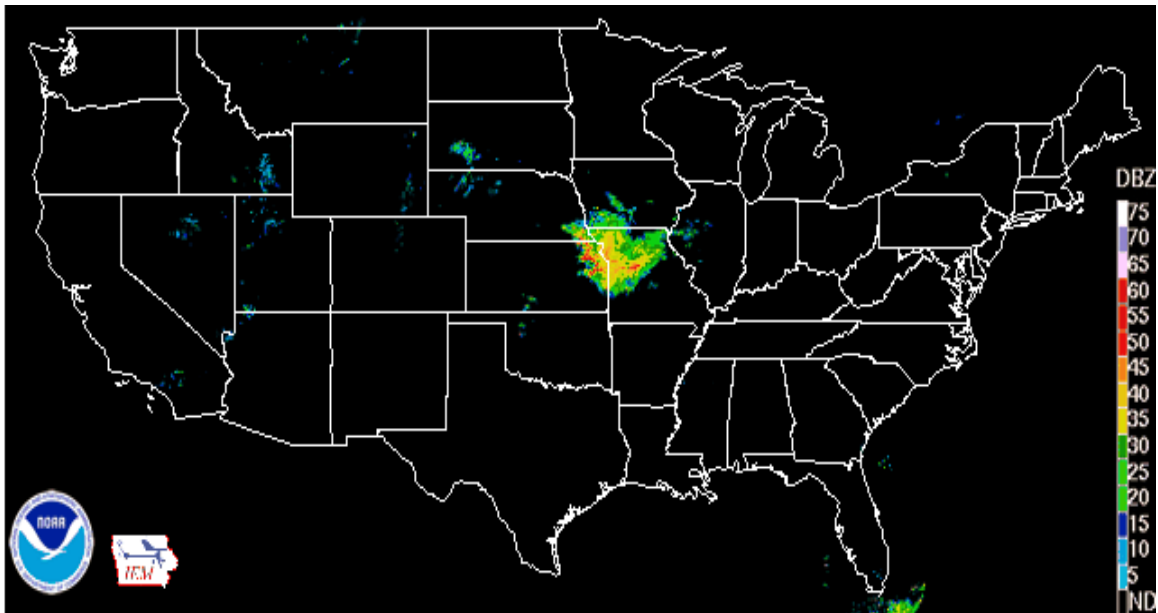


Figure 7.13 National Climate Data Center national base reflectivity radar mosaic valid at 1200 UTC on 13 October 2007.

storm, which would lead to greater atmospheric buoyancy and, in response, stronger, more upright, vertical motions.

The synoptic environment is much more active during this period. 24 hours earlier, the onset of convection was driven more by the mesoscale thermodynamics with forcing provided by a near surface inverted trough. A surface analysis for 1200 UTC 13 October (Fig. 7.15) shows a more prevalent low pressure system moving across the Continental Divide and centered in northeast New Mexico, near the panhandles of Texas and Oklahoma. The lowest observed pressure in the surface analysis in Figure 7.15 is 1002.8 mb over central New Mexico. The location of the MCS at this time is over northeast Kansas and northwest Missouri, northeast of the parent low. There is also a shortwave

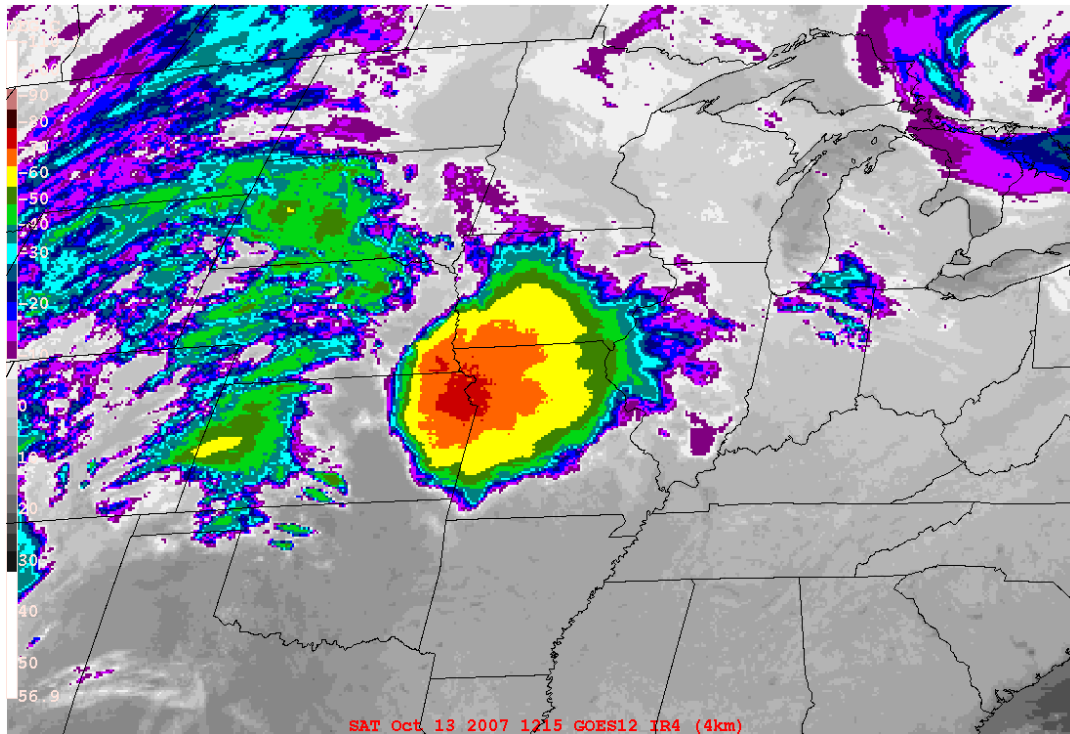


Figure 7.14 GOES-12 IR imagery valid at 1215 UTC 13 October 2007. Cloud top temperatures are shaded in color with color scale representing every 10°C. Colder temperatures are represented by warmer colors.

trough axis at the surface extending from the center of the low in Colorado into west-central Nebraska and into the Dakotas.

The 300-mb longwave trough (Fig. 7.16) previously located off the Pacific coast has closed off and pushed inland and is located over the Great Basin between Nevada and Utah. There is a 100-kt jet streak over western Arizona with 70 kts coming around the base of the trough into central Colorado. There are isolated regions of 50-kt jet cores associated with the MCS in the vicinity of a decaying upper air ridge. The lower-tropospheric and boundary layer shortwave axis resides under the apex of the upper-tropospheric ridge axis.

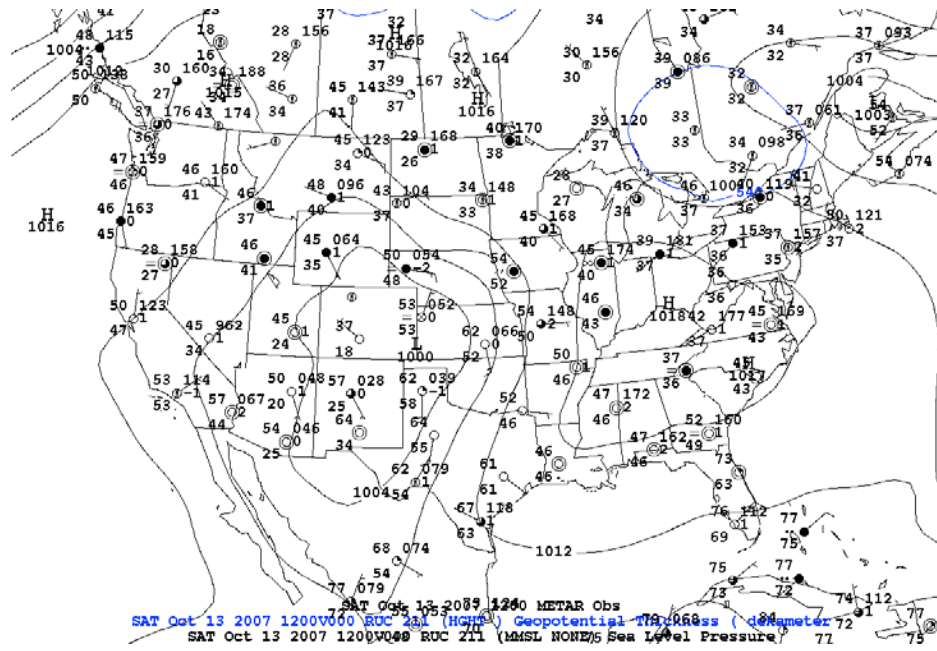


Figure 7.15 RUC initial analysis at mean sea level pressure valid at 1200 UTC 13 October 2007. Sea level pressure contoured in black every 2 mb with 5400 gpm thickness line (500:1000-mb layer) plotted in blue. METAR decoded surface observations are plotted valid at the same time.

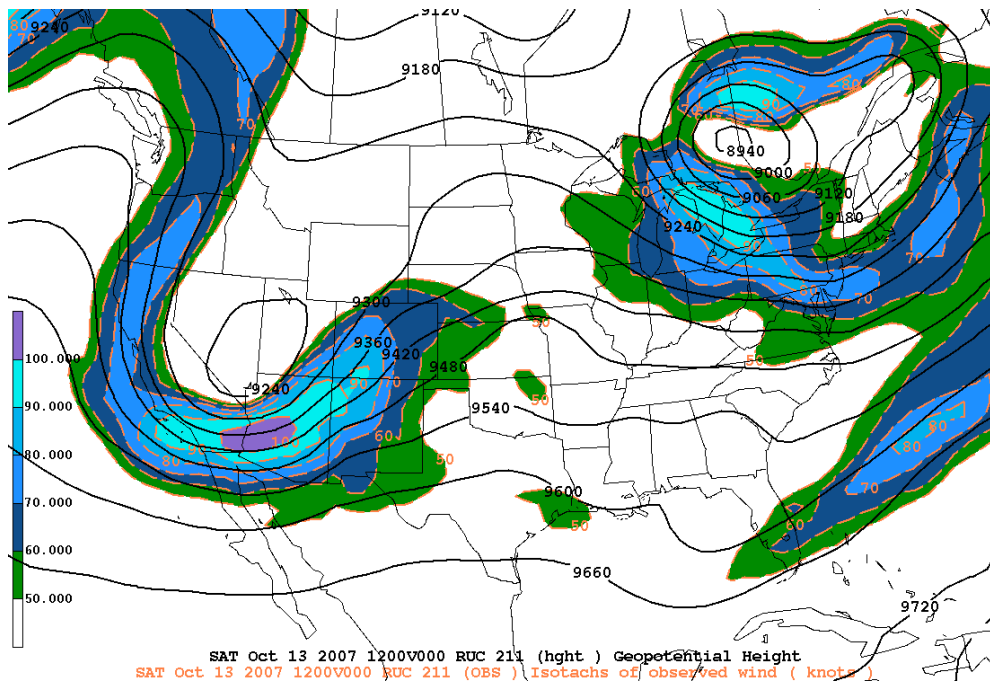


Figure 7.16 RUC initial analysis at 300 mb valid at 1200 UTC 13 October 2007. Geopotential height contoured every 60 gpm and isotachs in kts contoured every 10 kts above 50 kts and shaded.

Upper level divergence ($\geq 3 \times 10^{-5} \text{ s}^{-1}$; not shown) is present associated with the intensified jet.

This same longwave trough is located at 500 mb (Fig. 7.17), but is still an open wave allowing for warm air advection downstream of the trough axis along with the best region of potential vorticity advection, coinciding with the location of the analyzed surface low. Figure 7.17 shows increased vorticity ($15 \times 10^{-5} \text{ s}^{-1}$) at the top of the decaying 500 mb ridge over northeast Kansas and southwest Iowa aiding in the convection and lightning in this MCS. Further, the top of the downstream ridge extends into central Nebraska above the boundary layer shortwave.

The stationary boundary at 700 mb (Fig. 7.18), represented by the tightened Θ_e gradients, has lifted northward into central Nebraska and central Iowa along the boundary layer shortwave axis with a ridge extending along the Kansas and Missouri border. A closed off Θ_e maximum is present in eastern Kansas more closely associated with the average location of the maximum lightning activity (Fig. 7.12) and according to Figure 7.13, a new line of convection on the back side of the MCS. This new convection along with increased lightning is more than likely a result of decreasing Θ_e . Decreasing Θ_e is indicative of convective instability. This region of convection is no longer located along a gradient of warm and cold air advection, but is dominated by warm air

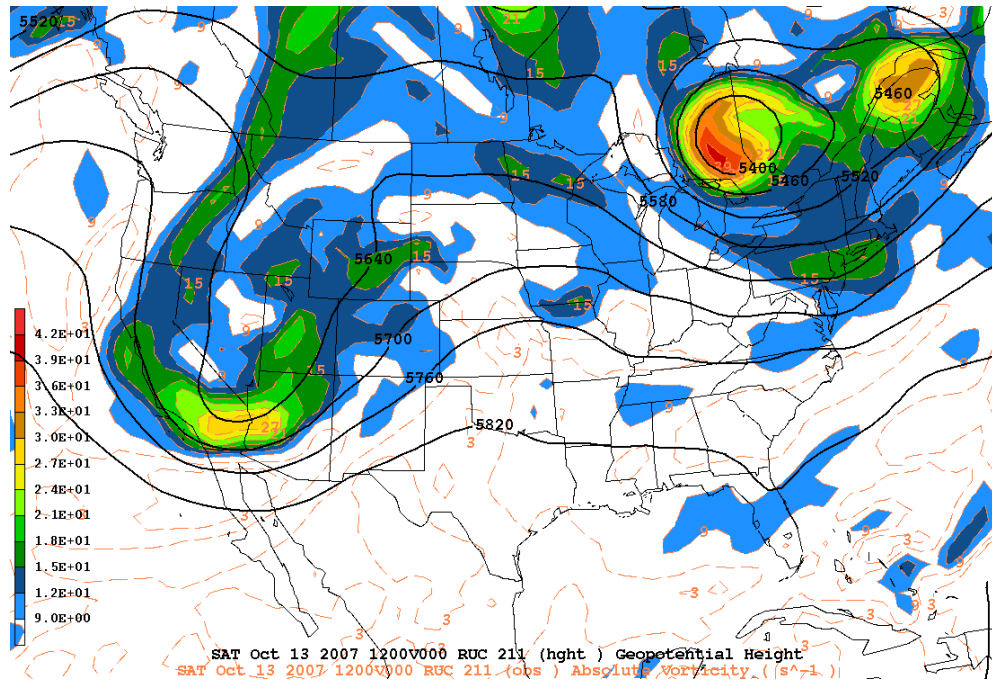


Figure 7.17 RUC initial analysis at 500 mb valid at 1200 UTC 13 October 2007. Geopotential height contoured every 60 gpm and absolute vorticity contoured every $3 \times 10^{-5} \text{ s}^{-1}$ and shaded above $9 \times 10^{-5} \text{ s}^{-1}$.

advection extending into eastern Missouri supported by the broader 850-mb low and open wave downstream.

This 850-mb low (Fig. 7.19) is centered over western Colorado and eastern Utah with a sharpening ridge aligned from southern Illinois into Iowa and Minnesota, allowing for stronger flow from the warm air in the south and the current warm air advection. The relative humidity at 850 mb is relatively low (less than 80%) in the region of greatest lightning activity. The highest relative humidity is north of this region located in central Nebraska along an 850-mb shortwave axis.

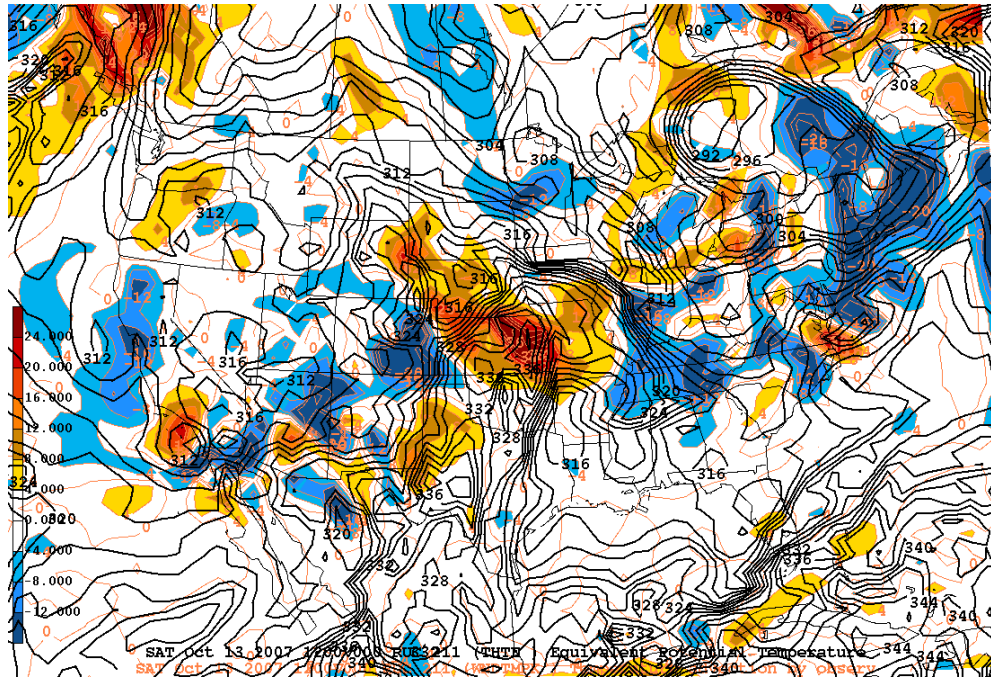


Figure 7.18 RUC initial analysis at 700 mb valid at 1200 UTC 13 October 2007. Equivalent potential temperature contoured every 2 K and temperature advection contoured every $4 \times 10^{-5} \text{ K s}^{-1}$. Positive values of temperature advection are shaded in warm colors and negative values of temperature advection are shaded in cool colors occurring at this time.

This same shortwave is present in the 900-mb height analysis (Figure 7.20) extending from the center of the low in Colorado through western Nebraska and the Dakotas and into Canada. Nebraska, Iowa, Kansas, and Missouri are dominated by warm air advection downstream of this shortwave axis. At this point, the convection and lightning originates from the inflection point of the mid-tropospheric low and downstream energy from a lower tropospheric shortwave. Notice the hole located over northwest Missouri where there is no warm air advection. This is more than likely due to the rain-cooled boundary

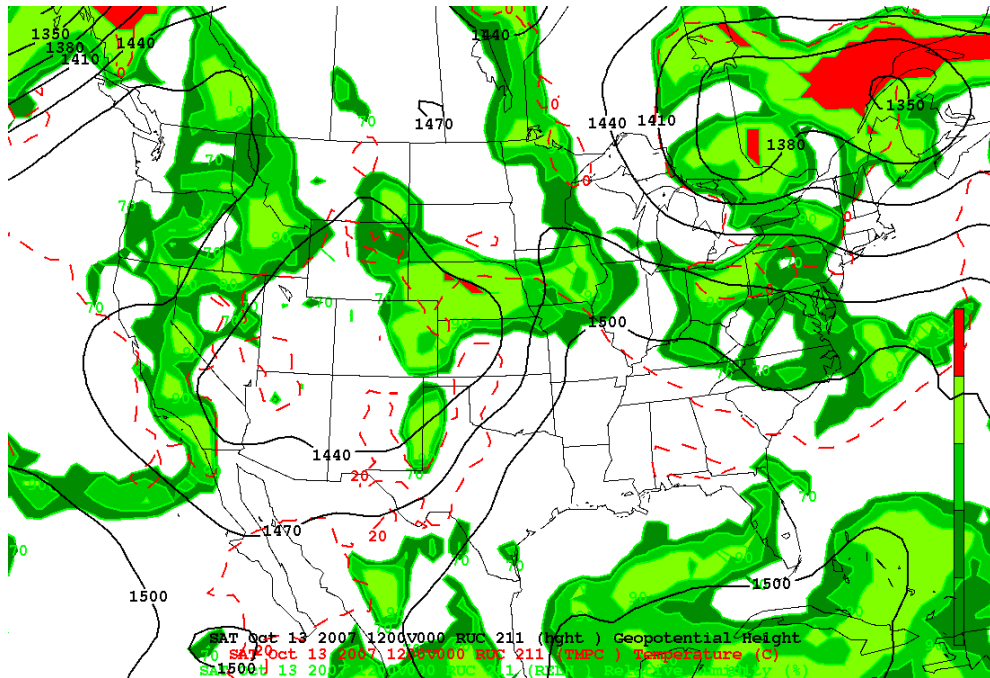


Figure 7.19 RUC initial analysis at 850 mb valid at 1200 UTC 13 October 2007. Geopotential height contoured in black every 30 gpm and temperatures contoured in red dashed every 10°C. Relative humidity contoured and shaded every 10% above 70%.

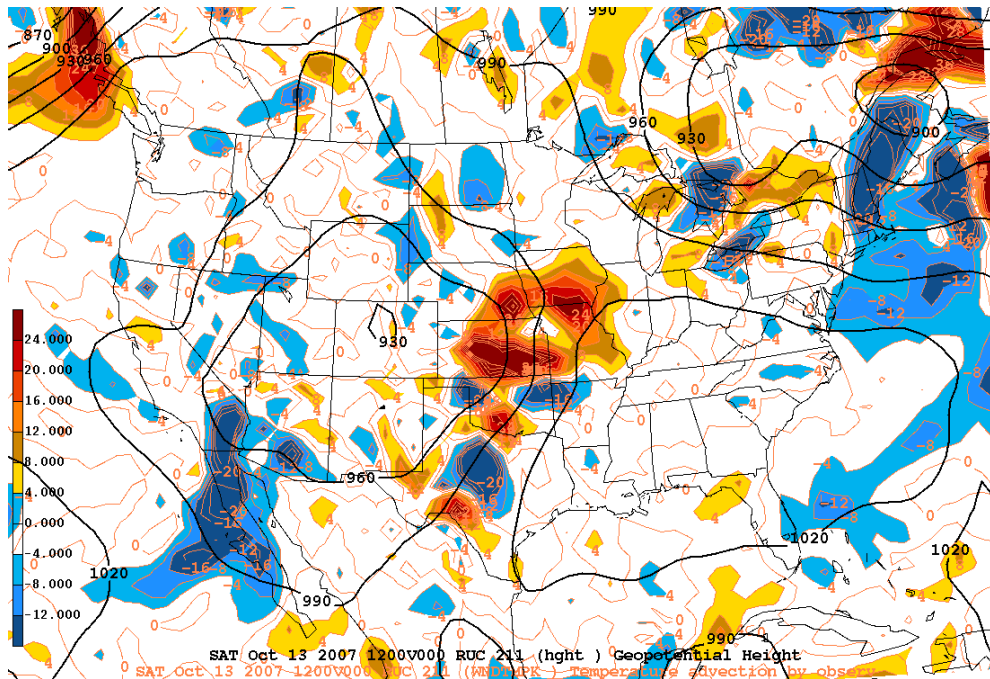


Figure 7.20 RUC initial analysis at 900 mb valid at 1200 UTC 13 October 2007. Geopotential height contoured in black every 30 gpm and temperature advection contoured every $4 \times 10^{-5} \text{ K s}^{-1}$. Positive values of temperature advection are shaded in warm colors and negative values of temperature advection are shaded in cool colors.

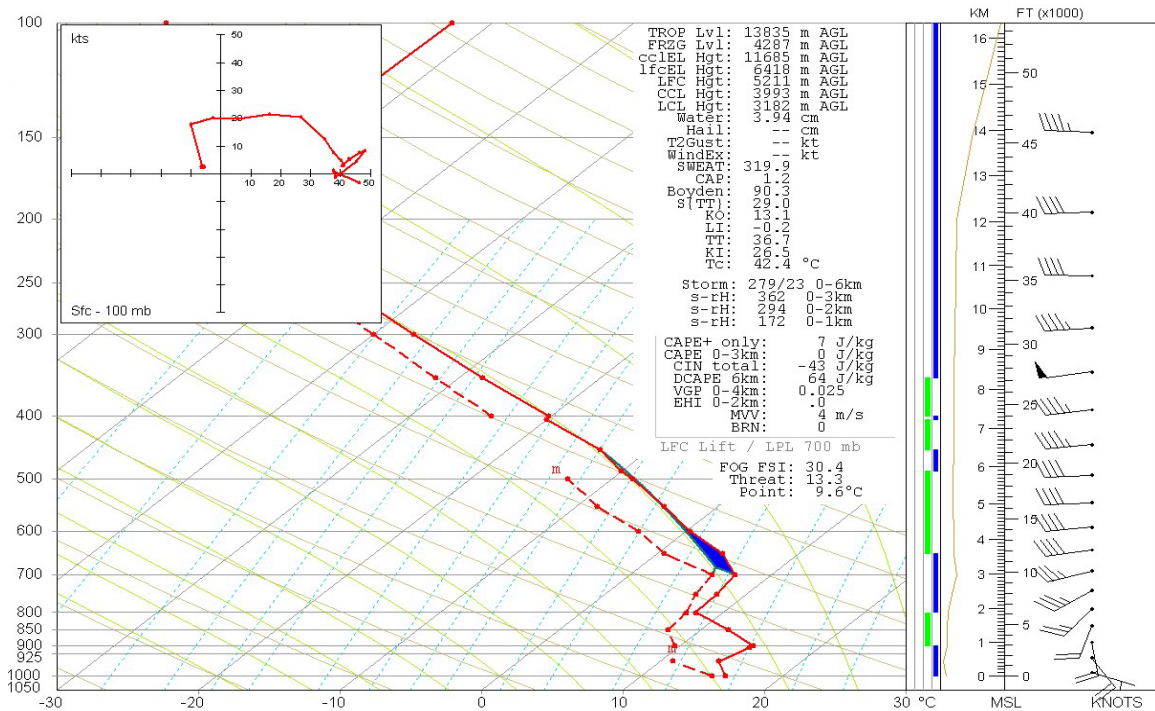


Figure 7.21 RUC initial sounding valid at 1200 UTC October 13, 2007 near Topeka, KS. Solid red line is temperature, dashed red line is dewpoint, and wind barbs represent wind speeds in kts and wind direction. CIN shaded in blue. Vertical Θ_e in yellow to the left of wind barbs.

layer. A similar minimum in advections is seen 24 hours previous at the onset of the MCS activity.

The resultant sounding profile for this time and location (Fig. 7.21) is considerably different from the sounding profile from 24 hours earlier. This profile maintains two inversion layers in the bottom layers of the atmosphere. The first is an isothermal layer from 1000 mb to 900 mb and the second is from 800 mb to 700 mb. The bottom 100 mb layer is defined by a dry atmosphere and winds veering from 112° at 6.5 kts at 1000 mb to 172° at 20.3 kts at 900 mb, indicative of continual warm air advection in the troposphere. The dewpoint

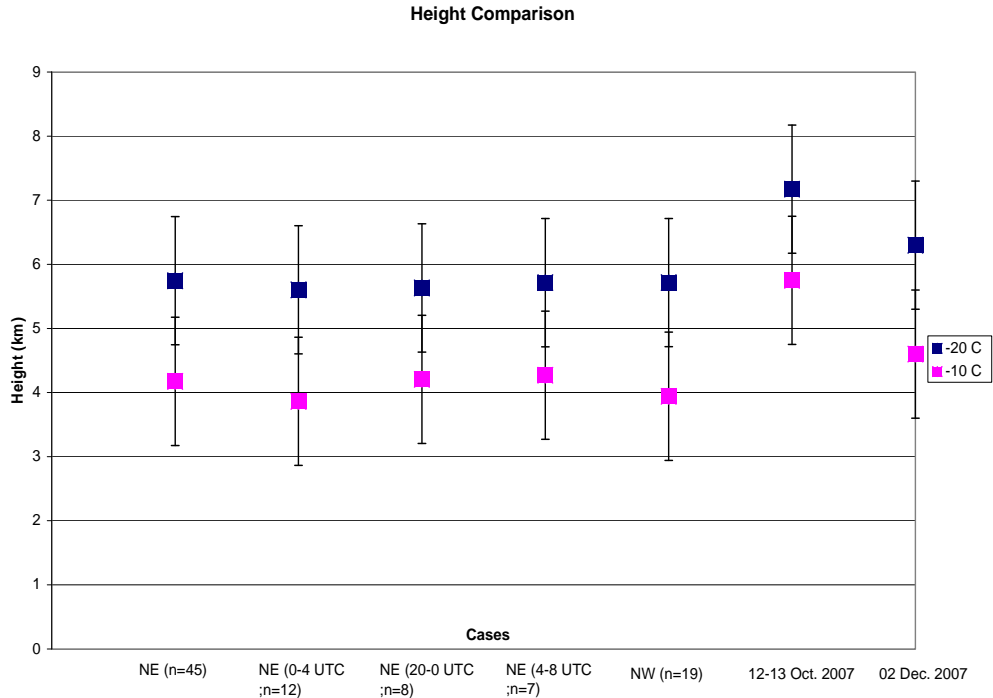


Figure 7.22 Comparison of height of -10° and -20°C isotherms for all derived northeast (NE) composites and the northwest (NW) composite along with the thundersnow and warm precipitation case study. Events are listed along the x-axis and height in km are along the y-axis.

depression in this layer decreases from $< 1^{\circ}\text{C}$ at the surface to 5.6°C at 900 mb showing increased drying. Between 900 mb and 800 mb, the atmosphere begins to moisten as the profile becomes potentially stable with decreasing lapse rates. However, the dewpoint depression returns to about 0.5°C by 800 mb. Winds in this layer continue to veer to 217° at 26.8 kts by 800 mb. The speed shear component is considerably less in this layer. Between 800 mb and 700 mb, the profile returns to isothermal in the presence of an elevated frontal zone. The most unstable lifted parcel originates in this sounding from the top of this

elevated frontal zone at 700 mb. In the 100 mb layer below it, the winds continue to veer further from 217° to 250° (near southwesterly) at 36.9 kts. The thermal profile above this inversion returns to near moist-neutral and potentially stable. The dewpoint depression does not vary much to the top of the tropopause in this sounding near 3° to 4°C, and winds are consistently from near 270° at 40 kts. Despite the two inversion layers, the wind indicates constant warm air advection up to the most unstable parcel at which the wind profile becomes neutral and does not change. In terms of stability parameters, there is very little CAPE (7 J/kg); most is due to the slight drying trend above this second inversion layer with 43 J/kg of Convective Inhibition (CIN). The -10°C isotherm is elevated further than the winter lightning composites and the composite from the same storm 24 hours earlier. In this case, the -10°C isotherm is near 500 mb at 6.0 km, higher than the 5.5 km and 519 mb in the 1200 UTC 12 October sounding and higher than the 3.9 km in the winter lightning composites. Further, the -20°C isotherm is located at 405 mb and 7.4 km, higher than the 427 mb and 6.9 km in the 1200 UTC 12 October sounding. Figure 7.22 shows an isothermal height comparison of all sounding composites in addition to the isothermal heights of both the thundersnow case study and the warm precipitation case study. Further stability parameters in this sounding are more elevated than its freezing precipitation counterparts with TT and KI of 36.7 and 26.5 respectively. The LI

for this sounding is comparable to the winter lightning composites with a value near 0. In this case, it is -0.2 as opposed to the slightly positive LI values found in the winter lightning composites. The result of this sounding is a stabilizing atmosphere. CAPE has decreased along with other stability parameters. The vertical Θ_e profile in Figure 7.21 indicates the existence of remaining potential instability. While the stability parameters would infer some weakening, conditions are still favorable for lightning generation with the continued presence moisture, albeit a shallow layer, lift and instability.

The profile for this time showed decrease in convective energies (i.e. CAPE) as convection and lightning was at its maximum. The synoptic and mesoscale environment is supportive of the maximized convection with the increased presence of a jet stream and upper level divergence along with the intensification of a mid-level shortwave trough. Moist, thermal energy at 700-mb (Fig. 7.18) supports convective development on the back side of the MCS where lightning more frequently occurred (Fig. 7.12).

In summary, this event was an MCS event that impacted parts of Kansas, Nebraska and Missouri. Convection was isolated to start and by 1200 UTC 13 October, it developed into a full MCS. Lightning characteristics for this elevated convection were dissimilar to the lightning characteristics found in elevated convection involving winter precipitation. Maximum lightning occurrence in

this event occurred near 1200 UTC on both 12 and 13 October. Trends for elevated convection involving winter precipitation however showed a tendency to occur between 0000 and 0400 UTC. Also, the percent occurrence of cloud flashes was dissimilar in that only 20.2% of lightning in this event were cloud flashes. Lightning in winter precipitation consisted of at least 35.0% cloud flashes. It can be inferred that cloud flash data is more useful when identifying lightning in winter convection. Further, the synoptic and mesoscale situation was also different between elevated convection types. These differences in lightning characteristics could also be a function of the differences in the synoptic and mesoscale conditions. Of further interest was the occurrence of lightning in close proximity to dry air. During this MCS event at 1200 UTC 12 October the maximum lightning occurred in regions of RH >90% at 700 mb while located about 150 km from RH >90% at 850 mb. Maximum lightning at 1200 UTC 13 October was again located in RH >90% at 700 mb while being between 100 and 125 km from RH < 70% and about 150 km from RH >90% at 850 mb.

Chapter 8 Conclusions

The primary objective of this study was to create a storm-based climatology of lightning occurring in winter precipitation. In this case, the climatology was started with events where thundersnow was observed in the Midwest. Further objectives were to observe the atmosphere where lightning did occur so as to create a representative profile of the environment for operational purposes and to assist in the analysis of the low frequency lightning detection used by Vaisala, Inc. in the NLDN. Representative profiles were established using data from one year of information and compared to soundings taken in different environments for comparison. This was indeed performed in this paper. Further, statistics on lightning detection during the 2006-2007 winter season consisting of thundersnow events were calculated and will hopefully lend understanding to other researchers using similar products.

To summarize, a storm relative climatology of lightning in winter precipitation was taken for the winter season of 2006 and 2007. The findings showed that during this winter season, lightning that was found associated with winter precipitation, particularly in events that were identified as thundersnow events, tended to occur in the time frame 0000 to 0400 UTC in a 24-hour day. During these events over the central U.S., there were over 3 million observed lightning events from Vaisala's NLDN. Of these 3 million lightning events, only 1.4% were found to occur in winter precipitation. Furthermore, 31% of observed lightning in winter precipitation were cloud flashes, which is less than the percentage of cloud flashes in the storm total lightning dataset. During the 0000 and 0400 UTC time frame, the percentages increased, specifically the percentage of lightning that was found associated with winter precipitation, 2.2% (Fig. 4.28). More importantly, the average percent that were positive lightning strokes in these storms was only 5.5%; 8.0% of all observed CG strokes were positive CG strokes.

The majority of lightning observed in these cases, with exception of cloud flashes, were low amplitude negative CG strokes. Additional data found in this work was the cloud to CG ratio, which served as more of a measure of the NLDN performance during these events. Again, this ratio was calculated using stroke data and not flash data, so values may not compare to other literature using this

ratio as a diagnostic tool. For the season, the ratio stood at 0.53. The ratio is the number of cloud flashes compared to the number of CG strokes (negative and positive). For this season there was about 1 cloud flash for every 2 CG strokes that were observed. This value fluctuated during the different times of day as well, matching each time's intensity in terms of lightning (Fig. 4.29). Not all events fit this profile. Also observed was the distance between cloud flashes and CG strokes in these events, which were found to be separated by an average of 0.74 km. Few events during this winter season exhibited two diurnal maximum of lightning occurring at 0000 UTC and at 1200 UTC. These events were deemed anomalous due to their rarity. Most prior publications had little to say about precipitation maximums occurring around 1200 UTC and offered only suggestions to its cause. One suggestion was the occurrence of cloud top evaporative cooling from cold cloud tops. This would help create additional instability aloft. While cloud top temperatures can be observed, this result is particularly difficult to quantify. Cloud top temperatures are indeed observed in further events described in this paper.

A seasonal trend was also determined despite the small dataset. This trend, however, appeared ideal when compared to results from previous research, in particular, the trend of thundersnow events. This trend showed a maximum occurrence of lightning associated with winter precipitation during

November and December, the early months of the 2006-2007 winter season. From late December through January and most of February, there were fewer occurrences of winter lightning. A second maximum occurred in late February through March and early April.

From this statistical analysis, latitude and longitude points from observed lightning were taken and a vertical profile was observed for the RUC initial model gridpoint encompassing this location. Similar sounding profiles were found for both lightning events that were found northeast and northwest of the parent cyclone. In these profiles, there was an evident frontal inversion with no CAPE. When looking at other vertical stability features, the height of the -10°C isotherm was observed for each of the profiles. In most instances, it is preferred to have the most unstable lifted parcel level below a temperature warmer than the -10°C isotherm such that parcels are being lifted into the best mixed phase region of the cloud. For northwest profiles, the -10°C isotherm was found to be slightly lower than those in the northeast cases. These profiles were used further to analyze locations of lightning in observed events.

Two case studies were performed outside of the statistical dataset in order to make comparisons of lightning characteristics and synoptic and mesoscale environments of individual elevated convective events, both with winter precipitation and without winter precipitation. One case represented a warm

precipitation event and the other a thundersnow event occurring in the following winter season outside of the statistical analysis. The warm precipitation event looked at elevated convection in an MCS occurring over Kansas and Missouri in October 2007. The cold season event analyzed was a thundersnow event from an extratropical cyclone event occurring through the Midwest in early December of 2007.

Using RUC initial analysis, it could be determined that while the warm precipitation event followed the conceptual model for MCS development, there were also some synoptic and mesoscale similarities to wintertime elevated convective events. When comparing sounding profiles, there were observed similarities, but the primary difference was the lack of a defined frontal inversion with regions of drier air in the lower levels for those soundings in warm elevated convection. Also, the heights of the -10°C and -20°C isotherms were significantly higher while most unstable lifted parcel levels were not.

Three maximum times were observed for the out-of-season thundersnow event. The soundings at these times resembled the composite soundings more closely with a defined frontal inversion and mixed phase regions of a similar height. In fact, the heights of the isotherms were more reminiscent of the heights found in the NE composites. Indeed, the first two maximum times were NE of the cyclone in this event. In both events, a low was defined with perturbations

present at 500 mb. They both also exhibited maximum Θ_e values at 700 mb with lightning tending to occur near thermal gradients, just inside the region of best warm advection. This is confirmed in the soundings where the veering in the lower levels represented warm air advection. For the thundersnow event, this could be similarly correlated to the warm conveyor belt and the trough of warm air aloft (TROWAL) producing additional instability aloft.

Of further interest in both events was the location of the lightning in relation to the gradient of moisture at 850 mb. In both cases and at all the analyzed times of these events, the preferred location for lightning occurred just on the moist side of the gradient where RH values rapidly changed from greater than 90% to less than 70% quickly. An attempt to quantify these distances was made. The horizontal extent of the moisture gradient was greater in the thundersnow producing winter cyclone as opposed to the warm precipitation MCS event.

Further analysis revealed similarities in cold cloud top temperatures occurring in the region of lightning occurrence. GOES-12 IR imagery was examined with enhanced cloud top temperatures. For the warm precipitation event, it was expected that the tops would reach a higher level, and thus, the cloud top temperatures would be colder. Indeed this was the case when the lightning maximized the convection was under cold cloud tops of -60°C to -70°C .

Convection during the thundersnow event did not reach temperatures this cold given the orientation of the convection, but were very close, and at its maximum, the cloud top temperature reached colder than -50°C .

This research is envisioned to gain a greater understanding of the physical characteristics associated with lightning in winter convection. Future work on this research will be to construct a more extensive climatology of the lightning in winter precipitating convection. A more extensive dataset will help to define a mean state associated with lightning in winter precipitation. A more robust dataset would also help to refine the composite soundings. Given the release date of the cloud flash detection (April 2006), more lightning data was not used for this project, but more lightning data is being added all the time. Other possible studies defined by this work would be to create ideal model simulations of such an event to further validate any physical mechanisms associated with lightning generation in thundersnow events. Also of interest would be to compile a dataset of observed soundings as opposed to model initial soundings to create composite soundings in a lightning producing environment. This sounding analysis could be further extended into a time series to obtain a more detailed view of stability characteristics.

References

Barnes, F. Caracena, and A. Marroquin, 1996: Extracting Synoptic-Scale Diagnostic Information from Mesoscale Models: The Eta model, gravity waves, and quasigeostrophic diagnostics. *Bull. Amer. Meteor. Soc.*, **77**, 519-528.

Benjamin, S. G., J. M. Brown, K. J. Brundage, B. E. Schwartz, T. G. Smirnova, T. L. Smith and L. L. Morone, 1998: RUC-2 - The Rapid Update Cycle Version 2. NWS Technical Procedures Bulletin No. 448. NOAA/NWS, 18 pp.

-----, S.G., G.A. Grell, J.M. Brown, T.G. Smirnova, and R. Bleck, 2004a: Mesoscale weather prediction with the RUC hybrid isentropic–terrain-following coordinate model. *Mon. Wea. Rev.*, **132**, 473–494.

-----, D. Dévényi, S.S. Weygandt, K.J. Brundage, J.M. Brown, G.A. Grell, D. Kim, B.E. Schwartz, T.G. Smirnova, T.L. Smith, and G.S. Manikin, 2004b: An hourly assimilation–forecast cycle: The RUC. *Mon. Wea. Rev.*, **132**, 495–518.

Bennetts, D. A., and B. J. Hoskins, 1979: Conditional symmetric instability--A possible explanation for frontal rainbands. *Quart. J. Roy. Meteor. Soc.*, **105**, 945-962.

-----, and J. C. Sharp, 1982: The relevance of conditional symmetric instability to the prediction of mesoscale frontal rainbands. *Quart. J. Roy. Meteor. Soc.*, **108**, 595-602.

Berger, K., 1977: The Earth Flash. In *Lightning, Vol. 1, Physics of Lightning*, ed. R.H. Golde, pp. 119-190. New York: Academic Press.

- Biagi, C. J., K. L. Cummins, K. E. Kehoe, and E. P. Krider, 2007: National Lightning Detection Network (NLDN) performance In southern Arizona, Texas, and Oklahoma in 2003–2004. *J. Geophys. Res.*, **112**, D05208, doi:10.1029/2006JD007341
- Brook, M., M. Nakano, P. Krehbiel, and T. Takeuti, 1982: The electrical structure of the Hokuriku winter thunderstorms. *J. Geophys. Res.*, **87**, 1207-1215.
- Brown, R. A., 1993: A compositing approach for preserving significant features in atmospheric profiles. *Mon. Wea. Rev.*, **121**, 874-880.
- Carpenter, D. M., 1993: The lake effect of the Great Salt Lake: Overview and forecast problems. *Wea. Forecasting*, **8**, 181-193.
- Carey, C.D., S.A. Rutledge, 2003: Characteristics of cloud-to-ground lightning in severe and nonsevere storms over the central United States from 1989-1998, *J. Geophys. Res.*, **108**, NO. D15, 4483, doi:1029/2002JD002951.
- Colman, B.R., 1990: Thunderstorms above frontal surfaces in environments without positive CAPE. Part I: A Climatology. *Mon. Wea. Rev.*, **118**, 1103-1121.
- Crowe, C., P. S. Market, B. Pettegrew, C. Melick, and J. Podzimek, 2006: An investigation of thundersnow and deep snow accumulations. *Geophys. Res. Lett.*, **33**, L24812, doi:10.1029/2006GL028214.
- Cummins, K. L., M. J. Murphy, E. A. Bardo, W. L. Hiscox, R. B. Pyle, and A.E. Pifer, 1998: A combined TOA/MDF technology upgrade of the U.S. National Lightning Detection Network. *J. Geophys. Res.*, **103**, 9035-9044.
- , J. A. Cramer, C. J. Biagi, E. P. Krider, J. Jerauld, M. A. Uman, V. A. Rakov, 2006: The U. S. National Lightning Detection Network: Post-Upgrade Status. *Preprints, 86th Annual Meeting*, Atlanta, GA, Amer. Meteor. Soc.
- Curran, J.T., and A.D. Pearson, 1971: Proximity soundings for thunderstorms with snow. *Preprints, 7th Conf. on Severe Local Storms*, Kansas City, MO, Amer. Meteor. Soc., 118-119.
- Fuquay, D.M., 1982: Positive cloud-to-ground lightning in summer thunderstorms. *J. Geophys. Res.*, **87**, 7131-7140.

Goodman, S. J., D. E. Buechler, and P. J. Meyer, 1988: Convective Tendency Images Derived from a Combination of Lightning and Satellite Data. *Wea. Forecasting*, **3**, 173–188.

Grell, G. A., 1993: Prognostic evaluation of assumptions used by cumulus parameterizations. *Mon. Wea. Rev.*, **121**, 764-787.

-----, G. A., J. Dudhia, and D. R. Stauffer, 1994: A description of the fifth-generation Penn State/NCAR Mesoscale Model (MM5). NCAR Technical Note, NCAR/TN-398 + STR, 138 pp.

-----, G. A., and D. Devenyi, 2002: A generalized approach to parameterizing convection combining ensemble and data assimilation techniques. *Geoph. Res. Letters*, **29**, 38-1-4.

Hanna, J. W., D. M. Schultz, and A. R. Irving, 2008: Cloud-Top Temperatures for Precipitating Winter Clouds. *J. Appl. Meteor. Climatol.*, **47**, 351–359.

Hobbs, P. V., 1974: *Ice Physics*, Clarendon Press, Oxford, 836pp.

Holle, R. L. and R. E. Lopez, 1993, Overview of Real-Time Lightning Detection Systems and their Meteorological Uses, NOAA Technical Memorandum, ERL NSSL- 102, National Severe Storms Laboratory, Norman, Oklahoma, 73 pp.

-----, R. L., J. V. Cortinas Jr., and C. C. Robbins, 1998: Winter Thunderstorms in the United States. *Preprints, 16th Conf. on Weather Analysis and Forecasting*, Phoenix, AZ, Amer. Meteor. Soc., 298-300.

-----, R. L., and A. I. Watson, 1996: Lightning during two central U. S. winter precipitation events. *Wea. Forecasting*, **11**, 599-614.

Iskenderian, H., 1988: Three-Dimensional Airflow and Precipitation Structure in a Nondeepening Cyclone. *Wea. Forecasting*, **3**, 18-32.

Kim, D., and S. G. Benjamin, 2001: Cloud/hydrometeor initialization for the 20-km RUC using satellite and radar data. *14th Conf. on Numerical Weather Prediction*, Fort Lauderdale, FL, Amer. Meteor. Soc., J113-J115.

Krider, E. P., R. C. Noggle, and M. A. Uman, 1976: A gated, wideband magnetic direction finder for lightning return strokes. *J. Appl. Meteor.*, **15**, 301-306.

Krider, E. P., R. C. Noggle, A. E. Pifer and D. L. Vance, 1980: Lightning direction-finding systems for forest fire detection. *Bull. Amer. Meteor. Soc.*, **61**, 980-986.

Kuo, H. L., 1965: On formation and intensification of tropical cyclones through latent heat release by cumulus convection. *J. Atmos. Sci.*, **22**, 40-63.

-----, H. L., 1974: Further studies of the parameterization of the effect of cumulus convection on large scale flow. *J. Atmos. Sci.*, **31**, 1232-1240.

MacGorman, D. R., and W. D. Rust, 1998: *The Electrical Nature of Storms*. Oxford University Press, 422 pp.

Magono, C. and C. W. Lee, 1966: Meteorological classification of natural snow crystals. *J. Fac. Sci., Hokkaido Univ., Ser. VII*, **2**, 321-335.

Market, P. S., C. E. Halcomb, and R. L. Ebert, 2002: A climatology of thundersnow events over the contiguous United States. *Wea. Forecasting*, **17**, 1290-1295.

-----, A. M. Oravetz, D. Gaede, E. Bookbinder, R. Ebert, and C. Melick, 2004: Upper air constant pressure composites of Midwestern thundersnow events. *20th Conference on Weather Analysis and Forecasting*, Amer. Meteor. Soc., Seattle, WA.

-----, A. M. Oravetz, D. Gaede, E. Bookbinder, A. R. Lupo, C. J. Melick, L. L. Smith, R. Thomas, R. Redburn, B. P. Pettegrew, and A. E. Becker, 2006: Proximity soundings of thundersnow in the central United States. *J. Geophys. Res.*, **111**, D19208, doi:10.1029/2006JD007061.

Marshall, T. C., and W. D. Rust, 1991: Electric field soundings through thunderstorms. *J. Geophys. Res.*, **96**, 22 297-22 306.

Marshall, T. C. and W. P. Winn, 1982: Measurements of charged precipitation in a New Mexico Thunderstorm: Lower positive charge centers. *J. Geophys. Res.*, **87**, 7141-7157.

- Martin, J. E., 1998a: The structure and evolution of a continental winter cyclone. Part I: Frontal structure and the occlusion process. *Mon. Wea. Rev.*, **126**, 303-328.
- , 1998b: The structure and evolution of a continental winter cyclone. Part II: Frontal forcing for an extreme snow event. *Mon. Wea. Rev.*, **126**, 329-348.
- McCann, D. W., 1995: Three-dimensional computations of equivalent potential vorticity. *Wea. Forecasting*, **10**, 798-802.
- Michimoto, K. 1993: A study of radar echoes and their relation to lightning discharges of thunderclouds in the Hokuriku district, Part II: Observation and Analysis of "single-flash" thunderclouds in midwinter. *J. Meteor. Soc. Japan*, **71**, 195-203.
- Moore, P. K. and V. P. Idone, 1999: Cloud-to-ground lightning at low surface temperatures. *Proc. 11th Int. Conf. on Atmospheric Electricity*, Guntersville, AL, NASA Marshall Space Flight Center, 472-475.
- Murphy, M. J., N. W. S. Demetriades, K. L. Cummins, and R. L. Holle, 2007: Cloud lightning from the U. S. National Lightning Detection Network (NLDN). *13th Int. Conf. on Atmospheric Electricity, Beijing, China*.
- Orville, R. E., 1991: Lightning ground flash density in the contiguous United States-1989. *Mon. Wea. Rev.*, **119**, 573-577.
- , R. W. Henderson, and L. F. Bosart, 1983: An East Coast lightning detection network. *Bull. Amer. Meteor. Soc.*, **64**, 1029-1037.
- , 1994: Cloud-to-ground lightning flash characteristics in the contiguous United States: 1989-1991. *J. Geophys. Res.*, **99** (D5), 10 833-10 841.
- and G. R. Huffines, 2001: Cloud-to-Ground Lightning in the United States: NLDN Results in the First Decade, 1989-98. *Mon. Wea. Rev.*, **129**, 1179-1193.
- , G. R. Huffines, W. R. Burrows, R. L. Holle and K. L. Cummins, 2002: The North American Lightning Detection Network (NALDN)—First Results: 1998-2000. *Mon. Wea. Rev.*, **130**, 2098-2109.

Peterson, W. A., S. A. Rutledge and R. E. Orville, 1996: Cloud-to-ground lightning observations from TOGA COARE: Selected results and lightning location algorithms. *Mon. Wea. Rev.*, **124**, 602-620.

Reap, R. M., and D. R. MacGorman, 1989: Clout-to-ground lightning: Climatological characteristics and relationships to model fields, radar observations, and severe local storms. *Mon. Wea. Rev.*, **117**, 518-535.

Reisner, J., R. M. Rasmussen, and R. T. Bruintjes, 1998: Explicit forecasting of supercooled liquid water in winter storms using the MM5 mesoscale Model. *Quart. J. Roy. Meteor. Soc.*, **142**, 1071-1107.

Rust, W. D., 1986: Positive cloud-to-ground lightning. *The Earth's Electrical Environment*, National Academy Press, 41-51.

Rutledge, S. A., and D. R. MacGorman, 1988: Cloud-to ground lightning activity in the 10-11 June 1985 mesoscale convective system observed during the Oklahoma-Kansas PRE-STORM Project. *Mon. Wea. Rev.*, **116**, 1393-1408.

Schultz, D.M., 1999: Lake-effect snowstorms in northern Utah and western New York with and without lightning. *Wea. Forecasting*, **14**, 1023-1031.

Simpson, G. C., and G. D. Robinson, 1941: The distribution of electricity in thunderclouds II. *Proc. Roy. Soc. London A*, **177**, 281-329.

Smith, L. L., Pettegrew, B. P., C. J. Melick, and P. S. Market, 2005: Investigating stability evolution of two winter storms using mobile GAUS data. *21st Conference on Weather Analysis and Forecasting*, Amer. Meteor. Soc., Washington D.C.

Steenburgh, W. J., S. F. Halvorson, and D. J. Onton, 2000: Climatology of lake-effect snowstorms of the Great Salt Lake. *Mon. Wea. Rev.* , **128**, 709-727.

Taniguchi, T., C. Magona, and T. Endoh, 1982: Charge distribution in active winter clouds. *Research Letters on Atmospheric Electricity*, **2**, 35-38.

Trapp, R. J., D. M. Schultz, A. V. Ryzhkov, and R. L. Holle, 2001: Multiscale structure and evolution of an Oklahoma winter precipitation event. *Mon. Wea. Rev.*, **129**, 486-501.

Uman, M. A., 2001: *The Lightning Discharge*. Dover Publications, Inc., 377 pp.

Van Den Broeke, M. S., D. M. Schultz, R. H. Johns, J. S. Evans, and J. E. Hales, 2005: Cloud-to-ground lightning production in strongly forced, low-instability convective lines associated with damaging wind. *Wea. Forecasting*, **20**, 517-530.

Ward, J. G., K. L. Cummins, and E. P. Krider, 2008: Comparison of the KSC-ER cloud-to-ground lightning surveillance system (CGLSS) and the U.S. National Lightning Detection Network (NLDN). *13th Conference on Aviation, Range and Aerospace Meteorology*, Amer. Meteor. Soc., New Orleans, Louisiana.

Watson-Watt, R. A., and J. F. Herd, 1926: An instantaneous direct-reading radio goniometer. *J. Inst. Elec. Engrs.*, **64**, 611-622.

Wilson, C. T. R., 1916: On some determinations of the sign and magnitude of electric discharges in lightning flashes. *Proc. R. Soc. London Ser. A*, **92**, 555-574.

-----, 1920: Investigations on lightning discharges and on the electric field of thunderstorms. *Philos. Trans. R. Soc. London Ser. A*, **221**, 73-115.

-----, 1929: Some thundercloud problems. *J. Franklin Inst.*, **208**, 1-12.

Zajac, B. A., and S. A. Rutledge, 2001: Cloud-to-ground lightning activity in the contiguous United States from 1995 to 1999. *Mon. Wea. Rev.*, **129**, 999-1019.

Vita Auctoris

Brian Patric Pettegrew was born on December 4, 1979 in Merrillville, Indiana, to Patric Lee and Martha Ruth (Showers) Pettegrew. Along with an older sister, Megan Carrie, and a younger sister, Lela Mary, the family moved to Aurora, Missouri, where the author's parents still live.

A strong educational background and willingness to learn combined with the intrigue of a constantly changing sky provided motivation to learn more about weather and pursue a life of studying it. Becoming a meteorologist was a strong ambition for the author following his graduation from Aurora High School, in Aurora, Missouri, in May of 1998. Keeping with his ambition to learn, the author enrolled at Central Methodist College in the fall of 1998 to study chemistry. The author obtained his Bachelor of Science degree in chemistry four years later, in May 2002. Following this, he obtained his Master of Science degree in Atmospheric Science in August of 2004.

While studying at the University of Missouri, the author gained much experience and travels working with the National Weather Service and performing field research with the National Center for Atmospheric Research. Following summers of traveling and researching combined with years of effort and writing, the author will transition into life as a professional researcher after obtaining his Ph.D. in May of 2008 at the University of Missouri.